Scientific Papers 2019

University
of Pardubice
Faculty of Transport Engineering

Collection of Academic Precis

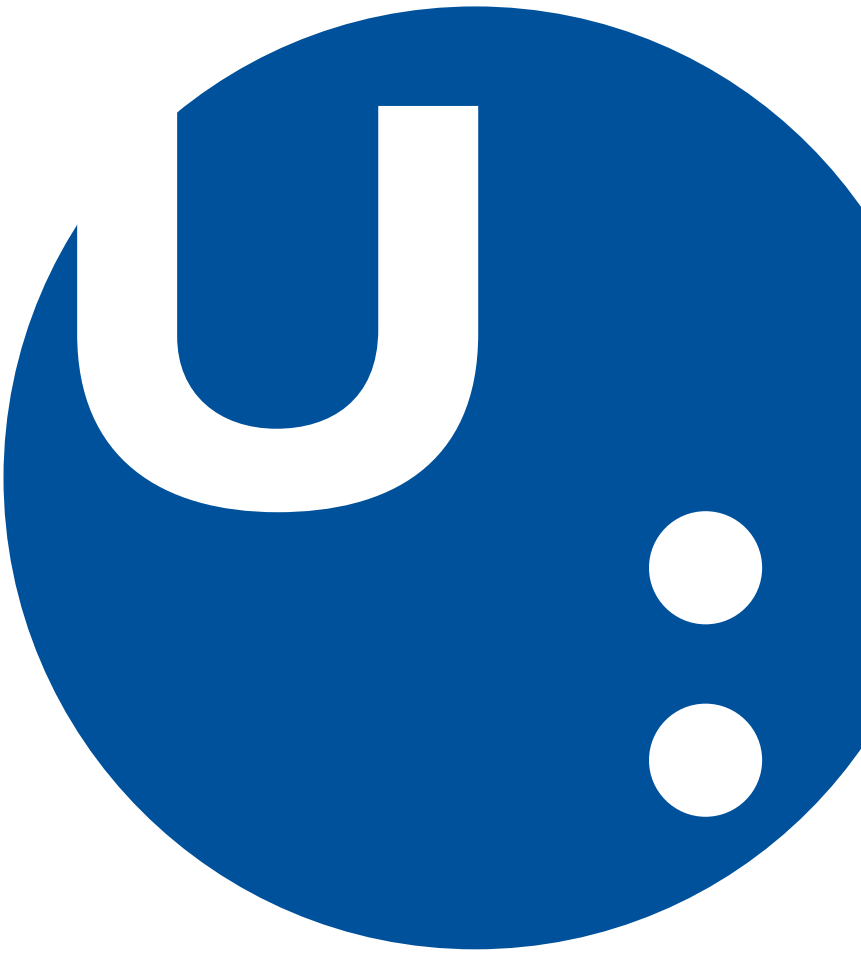

Scientific Papers of the University of Pardubice

Series B
Jan Perner Transport Faculty
10 (2004)

Ediční středisko Univerzity Pardubice
PARDUBICE 2005

University of Pardubice
Faculty of Transport Engineering

Collection of Academic Precis 2019

Content:

List of current grants - 2019

Technology Agency of the Czech Republic	
National Center of Competence for Josef Božek (JOBNAC)	Národní centrum kompetence Josefa Božka (NCKJB)
Improving efficiency of rail transport within energy optimization of the multimodal mobility systém	Zvyšování efektivity železniční dopravy v rámci energetické optimalizace systému multimodální mobility
System design to align education with labor market needs in the transport and communications sector	Nastavení nových vzdělávacích a výchovných priorit reflektujících měnící se potřeby trhu práce v sektoru dopravy a spojů
The impacts after low emission mobility implementation on the enviromental effects reduction in urban aglomerations	Dopady zavádění nízkoemisní mobility na snižování environmentálních vlivů městských aglomerací
Human Dimension of Sustainable Urban and Regional Mobility Plans.	Humanitní rozměr plánů udržitelné městské a regionální mobility
Design of new shape of prestressed reinforced concrete beam	Návrh nového tvaru předpjatého železobetonového nosníku
Elimination of the rail vehicles axles operational failures	Eliminace provozních poruch náprav kolejových vozidel
Competence Center of Railway Vehicles	Centrum kompetence drážních vozidel
Ministry of Industry and Trade	
Development of the Technology for Intelligent Traffic Flow Management	Vývoj technologie pro inteligentní řízení přepravních toků zboží
3D Printing of Computationally Optimized Metal Parts using DMLS Technology	3D tisk výpočtově optimalizovaných kovových součástí s využitím technologie DMLS
Hybrid Locomotive and Electronic Energy Optimization of its Operation	Hybridní lokomotiva a elektronická optimalizace energetiky jejího provozu

Ministry of Interior	
Intervention Simulations in the Airplane Accidents	Simulace zásahů u leteckých nehod
Development of an Innovative Method for Detecting Road Traffic Offenses Using Electronic Accident Data	Vývoj inovativní metody k odhalování trestných činů v silniční dopravě s využitím elektronických nehodových dat
EU	
Switch and Crossing Optimal Design and Evaluation (S-CODE)	Switch and Crossing Optimal Design and Evaluation (S-CODE)
Ministry of Education Youth and Sports	
Cooperation of the University of Pardubice and the application sphere in application-oriented research of location, detection and simulation systems for transport and transport processes (PosiTrans)	Spolupráce Univerzity Pardubice a aplikační sféry v aplikačně orientovaném výzkumu lokačních, detekčních a simulačních systémů pro dopravní a přepravní procesy (PosiTrans)
University of Pardubice (SGS)	
Selected aspects of contemporary transport technique, technology and management	Vybrané aspekty soudobé dopravní techniky, technologie a řízení
University of Pardubice (IRS)	
Innovation of geodesy,Total Stations	Inovace praktické výuky předmětů se zaměřením na geodézii
Zkvalitnění vzdělávacího procesu na DFJP v souladu s požadovaným profilem absolventů studijních programů v rámci předmětů Logistika II a Zelená logistika	Improving the educational process at FoTE in accordance with the required profile of the graduates of the study programs within the subjects Logistics II and Green logistics through the interaction of theory and practice
Special testing equipment for technical education	Speciální zkušební zařízení pro výuku technických předmětů DFJP

University of Pardubice (IRS)	
Air transport branch founding on the Faculty of Transport Engineering	Zavedení letectví na Dopravní fakultě Jana Pernera
Support and Innovation of the subject E- Commerce at Faculty of Transport Engineering	Podpora a inovace výuky odborného předmětu Elektronický obchod na Dopravní fakultě Jana Pernera

Analysis of Mechanically Stabilized Earth Wall, Reinforced Earth Structure

Author: Ing. Eren BALABAN

Doctoral study programme:
P3710 Technique and Technology in Transport and Communications

Field of study:
3706V005 Transport Means and Infrastructure

Supervisor:
Ing. Aleš Šmejda, Ph.D.

Supervisor specialist:
Assist. Prof. Dr. Mehmet İnanç Onur

Doctoral thesis has arisen at the supervising:
Department of Transport Structures

ABSTRACT

There is an increasing interest on environmental concern all around the world. Waste management or storage of wastes takes attention of civil engineers to design environment friendly structures. Developing world increased mobility of people all around world and transportation of goods. Tires are, used on vehicles which are, used transportation of goods and people. When tires comes to end of their life cycle, storage of them becomes huge problem. They are cutted into small pieces to use in civil engineering applications such as production of asphalt concrete, concrete. Another usage area of scrap tires is a fill material in geotechnical engineering structures, such as retaining walls and embankment. In this study, tire chips are mixed with sand and clay and their mixtures at a range of 10%, 20% and 30% by weight in order to produce lightweight backfill. In order to determine strenght parameters of mixed soils, direct shear tests are performed. Results of direct shear test is modelled on finite element code. Reinforced earth walls are designed using federal highway administration (FHWA) method using direct shear test results for sand, clay, sand tire crumb mixture and clay tire crumb mixture backfills. Designed walls are constructed at laboratory and tested with a loading plate. Another aspect of design of reinforced earth structures consist of effect of foundation layers, because design codes do not consider foundation layers' effect into consideration. Finite element analysis is conducted for a different foundation layer properties for reinforced earth wall with different backfills. Results of this study showed that, tire crumbs can be considered as a backfill material and performance of reinforced earth wall depends on properties of foundation soils'.

KEYWORDS

Sand, clay, tire crumb, reinforced earth wall, geosynthetic, foundation, direct shear test

1. INTRODUCTION

Reinforcement of concrete by steel rods has been a well known by civil engineers. Therefore, strengthening structures with other materials is not a new idea for civil engineers. French engineers adopted this idea to geotechnical engineering nearly five decades ago. Their idea was simple enough, could we strengthen the soil by using steel rods like in concrete structures. They performed some experiments and showed that the idea of reinforcing the soil could be applied in the design step of geotechnical structures. Since that time, a lot of research has been done to understand behaviour of reinforced earth structures.Reinforced earth could be used under the foundations where bearing capacity of the soil is under desired value. Another application of reinforcing soil is retaining walls. Reinforced earth walls can be used to retain railway and road embankments, bridge abutments. They are also used to retain contaminated wastes in valleys under some special conditions.Reinforced earth walls are constructed by inserting reinforcement material into backfill soil, placing facing elements (example: concrete blocks, steel facings, wooden facings), adding another backfill soil again. Construction of reinforced soil can be considered as staged construction because, first of all levelling pad is laid through foundation soil and then backfill soil must be placed, compacted, after that, reinforcement rods must be placed. This process continues until the desired height of the wall is reached. Since the day that reinforced earth walls are introduced, they are widely used in practical engineering. It is easier to construct reinforced earth wall than conventional retaining wall. Reinforced earth walls also have economical advantage than conventional retaining walls because it is cheaper to construct. Another advantage of reinforced earth wall is their aesthetic appearance. Reinforced earth walls are considered as flexible walls because they tolerate lateral and vertical deformation more than conventional retaining walls. They provide faster construction speed than traditional retaining walls.

1.1 Aim of Thesis

This thesis concerns about following topics

(i) Mixing sand and clay on different ratios to find out change in shear strenght parameters under low vertical stress.

(ii) Finite elemenet modelling of conducted direct shear tests.

(iii) Adding tyre crumbs into soil mixtures to determine new shear strenght parameters.

(iv) Construction of scaled reinforced earth walls at laboratory with sand and clay backfills and sand-tire crumb mixtures, clay tire crumb mixtures in order to clarify effect of tire crumb into performance of reinforced earth walls.

(v) Finite element modelling of the small scale reinforced earth walls tested at laboratory.

(vi) Finite element analysis of reinforced earth wall in order to determine the effect of foundation layers' properties into performance of reinforced earth walls.

2. BACKGROUND

Behaviour of reinforced earth wall is highly dependent on properties of reinforced backfill. Therefore, all design codes defines some restrictions on properties of reinforced backfill. Therefore, effect of backfill is discussed by various articles at the literature [11, 16, 41, 27, 29, 31, 44, 58 and 64].

M. Riccio et al. [11] found that cohesion tends to increase reinforcement strains. M. Pinho-Lopes [16] et al. conducted flume tests over reinforced earth wall with fine backfill. Results are compared with traditional walls which are used at region. Traditional walls are found to be more suitable than reinforced earth wall. Guangqing Yang et al. [41] measured behaviour of 12m height reinforced earth

wall with sand backfill from 0 to 6 meter and clay backfill from 6 meter to 12 meter. Highest foundation pressure is measure at the middle. Reinforcements in sand backfill showed two peaks in case of maximum strains. Huabei Liu [27] investigated short term and long term behaviour of reinforced earth wall with four different sands. It is seen that, stiffness of reinforced soil, lateral earth pressure behind the wall are affected from type of backfill. Huabei Liu et al. [29] studied long-term behaviour of reinforced earth wall with marginal soil by modelling 8 meter height wall on Abaqus. They concluded that, keeping soil creep rate constant, increasing reinforcement creep yields increased wall deformation. Abdelkader Abdelouhab [31] analysed reinforced earth wall with different backfills with finite element method. It is found out that as cohesion of backfill increases, lower displacement of wall is observed. Abdolhosein Haddad and Gholamali Shafabakhsh [44] investigated possible failure reason of a failed reinforced earth wall is investigated. It is found out that, backfill used during construction has a considerable fine content. High fine content yielded low permeability and low factor of safety against pull-out capacity. D. M. Carlos and Margarida Pinho-Lopes [58] conducted external stability analysis for a reinforced earth walls with sand and sand-fine particle mixtures with two different design methods. Results provided that, in case of short term behaviour walls might have a problem regarding sliding. Robert M. Koerner and George R. Koerner [64] suggested several solutions for a reinforced earth walls with a fine backfill regarding low drainage systems.

Several studies can be found in literature which are considered effect of foundation to behaviour of mechanically stabilized earth wall [24, 26, 34, 38, 43, 48]. Jian-Feng Chen et al. [24] studied behaviour of reinforced earth wall constructed over soft soil. Foundation layers consisted of preliminary fill, silty clay, mucky silty clay, clay and silty clay. Prefabricated vertical drains are installed till silty clay layer. Researchers concluded that, construction duration should be prolonged in order to construct more stable wall. This is due to dissipation of pore water pressure. Weaker sub-soil requires extension of reinforcement layers can be stated as another outcome of this study. Dev Leshchinsky et al. [26] studied difference between theoretical and actual failure of reinforced earth wall due to bearing capacity. It is concluded that, failure mechanism is different than failure mechanism assumed by Meyerhoff's method which is used in some design codes. I. P. Damians et al. [34] modelled a reinforced earth wall with respect to different foundation stiffnesses. Foundations are modelled by changing only stiffness. It is stated that as the stiffness of foundation and reinforcement stiffness are reduced, facing deformations increase. It is also stated that, if reinforcement with lower stiffness is used over the low stiff foundation soil, higher stresses are observed over reinforcement. Graeme D. Skinner and R. Kerry Rowe [38] studied design of reinforced earth wall on a one layer yielding foundation. Researchers concluded that, horizontal and vertical deformations of wall are increased after consolidation. Jian-Feng Xue et al. [43] investigated failure of reinforced earth wall constructed on soft clay foundation. They concluded that, prefabricated vertical drains are damaged during construction and excess pore water pressures can not be dissipated properly which caused failure of wall. A. Sengupta [48] investigated reasons of failure of failed reinforced earth wall constructed over multi-layered foundation soil. Researcher found the failure reason as underestimated unit weight of backfill and overestimation of bearing capacity of foundation soil. This yielded to high amount of consolidation which caused failure.

In order to design more reliable reinforced earth walls, researchers have been looking for several methods. Reinforcing backfill is one of those methods. Some of those studies can be found in the literature [10, 15, 18, 20, 22]. Taesoon Parka and Siew Ann Tanb [10] investigated behaviour of reinforced earth wall with sandy silt and polypropylene fibers. The mixture ratio of polypropylene and soil is chosen as 0.2%. Researchers concluded that, best results are obtained by reinforcing sand with geogrid and polypropylene. Sutapa Hazra Æ Nihar Ranjan Patra [15] studied counterfort retaining wall using sand-fly ash mixture as backfill and geogrid as reinforcement. They concluded that wall with sand-fly ash mixture with geogrid as backfill produced more stable results. S. Bali Reddy and A. Muradi

Krishna used recycled tyre chips mixed with sand. The wall performed better when 30% tyre chip is added to sand. Guangqing Yang et al. studied the behaviour of lime treated cohesive soil backfilled soil. Researchers concluded that, lateral earth pressure decreased with time due to increasing strenght of lime treated sand and horizontal deformation of wall face. Sompote Youwai and Dennes T. Bergado studied behaviour of reinforced earth wall with a backfill which consists of tire chips using finite difference method. Researchers concluded that, lateral movement of wall and tensile force in reinforcement increased as the ratio of chip tire increased.

It can be seen from the literature that, effect of reinforced backfill is generally evaluated using clay backfill and measuring or computing displacements. However, behaviour of reinforced wall covers more extensive range such as change of maximum forces on geotextile, horizontal displacements and settlements. In this work, different backfills are created by mixing sand and clay. Mechanical properties of backfills are determined in laboratory and used in finite element analysis in order fully evaluate behaviour of reinforced earth walls with different backfill regarding, horizontal displacements of wall face and retained soil, settlements and forces acting on reinforcements.

Another important aspect which determines behaviour of reinforced earth wall is condition of foundation beneath it. However, very little study is available on the literature for this phenomena. The related studies related to effect of foundation is generally case studies which are conducted after failure of reinforced earth wall. In order to prevent from failures, change of horizontal displacements of wall face, retained soil, settlement of wall and forces acting on reinforcement evaluated with respect to foundation conditions in this study.

There is a contradiction in the literature in case of using tyre chips to obtain light weight backfill. It is also unclear to effect of tyre crumbs which have smaller grains to behaviour of reinforced earth wall. In order to clarify its effects reinforced earthwalls constructed at laboratory with various tyre crumb contents. Effect of tyre crumbs to clay backfill is also evaluated at the laboratory.

3. METHODS AND METHODOLOGY

Backfills are created by mixing sand and clay. In each mixture, clay content is increased by 10%. Grain size disribution of sand and clay is determined. Maximum dry unit weights and optimum water content are evaluated. Direct shear tests are conducted to determine shear strenght parameters of mixtures. Direct shear tests are conducted under 9.81 kPa, 19.62 kPa, 40.81 kPa and 58.86 kPa. After that, direct shear tests are modelled on Abaqus. Then, tyre crumb is added to each mixture to determine effect of tyre crumbs. Tyre crumb is also added 10% of mixture and increased by 10% for increment of tyre crumbs in mixtures. Maximum dry unit weights of all mixture with tyre crumbs are also determined. Direct shear tests are also conducted for soil-tyre crumb mixtures. Then small scale reinforced earth walls are constructed at laboratory and tested in order to study effect of tyre crumbs to performance of reinforced earth walls. Finite element analysis are conducted in order to determine effect of backfill and foundation. Tested soil in laboratory are used during finite element analysis.

3.1 Experimental Setup

Standard proctor tests are conducted in order to determine maximum dry unit weight and optimum water content. Standard proctor test is chosen, because it is required during construction of reinforced earth walls construction by some codes.

Direct shear tests conducted at rate of 0.25 mm/min when sand content is above 50% of the mixture. When sand content in the mixture is below 50%, shear rate is decreased to 0.065 mm/min in order not to produce excess pore water pressure inside samples during shear test. Mixtures with tyre crumbs are also tested at same shear rates.

Small scale reinforced earth walls are constructed in Research and Educational Center (VVCD) at transport structures laboratory. Walls are constructed inside a steel frame which is placed inside the laboratory. This steel frame is given on Figure 3.1 below.

Figure 3.1 Steel Frame Used during Construction and Testing

Constructed walls tested with a loading plate which has a 300 mm diameter. Loading plate is placed 2 cm behind the wall face so that, entire load in applied to reinforced backfill. Loading is applied step by step. Initial load step is chose as 0.06 MPa and increased 0.06 MPa at each increment. Increment is applied when settlement of loading plate is stabilized.

Deformation of wall face is measured at three different points, while settlement of loading plate is measured from load application point. Loading system can be seen from Figure 3.2 below.

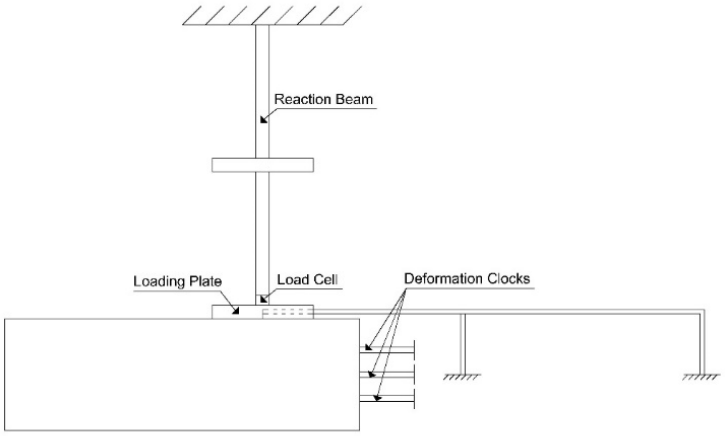

Figure 3.2 Schema of loading system

3.2 Analytical Design of Reinforced Earth Walls

Analytical design of reinforced earth wall is conducted for two different chapter of this study. In the first chapter, analytical design for laboratory. Wall height is chosen as 45 cm and length of reinforcement chosen as 0.7H to comply with minimum requirement of FHWA method. In the second chapter, reinforced earth wall is designed with height of 6 meter and reinforcement length is chosen as 1H.

Analytical design of the walls are done according to Federal Highway Administration (FHWA) design code. External analysis is conducted initially and safety of walls are determined for overturning and sliding. After external design is completed internal design is conducted. Forces on reinforcement and pull – out capacity are determined for each reinforcement layers.

3.3 Finite Element Modelling

Abaqus and Plaxis finite element codes are used in this study. Abaqus is used to model direct shear tests. Geometry and mesh structure is given on Figure 3.3. Mohr-Coulomb material model is used during analysis. Mohr – Coulomb material model properties are given on Table 3.1 below.

Small scale walls without tyre crumb content are modelled on Plaxis. Plane-Strain modelling technique is applied. Mohr-Coulomb material model is used during analysis. Geometry and mesh structure of paxis model for small scale wall is given on Figure 3.4. Material parameters for small – scale wall is provided on Table 3.2 below.

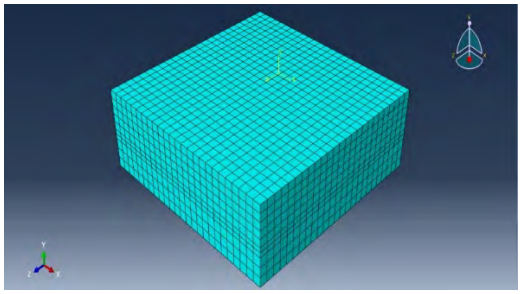

Figure 3.3 Geometry and mesh of finite element model for direct shear test

Table 3.1 Mohr – Coulom Material Model Parameters for Finite Element Analysis for Abaqus

							9,81 kPa	**19,2 kPa**	**40,81 kPa**	**58,86 kPa**
	γ_{sat} (kN/m^3)	γ_{unsat} (kN/m^3)	**Φ (º)**	**C (kPa)**	**φ (º)**	**ν**	**G** (MPa)	**G** (MPa)	**G** (MPa)	**G** (MPa)
100% Sand	19,50	1,74	47,38	0,456	17,38	0,3	4.04	7.20	13.5	14.41
80% Sand + 20% Fine	22,31	2,07	42,35	11,61	12,35	0,3	4.74	6.58	11.88	13.22
60% Sand + 40% Fine	22,10	2,05	41,19	24,01	11,19	0,3	7.76	11.04	13.77	24.08
40% Sand + 60% Fine	22,53	2,06	38,84	25,84	8,84	0,3	10.44	12.58	11.36	18.84
20% Sand + 80% Fine	22,10	2,00	36,51	34,36	6,51	0,3	13.30	15.59	22.5	22.93
100% Fine	20,80	1,85	32,44	37,66	2,44	0,3	15.73	17.77	21.05	25.39

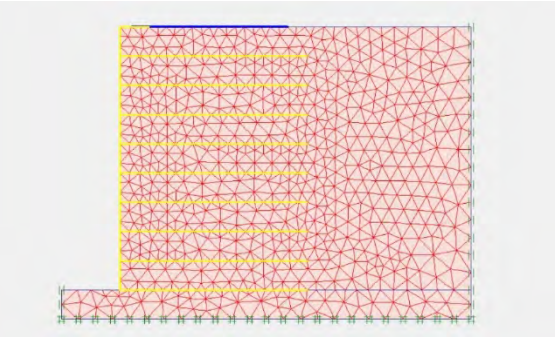

Figure 3.4 Geometry and Mesh Structure of Wall

Table 3.2 Material Parameters for Soil's Used During Analysis

Soil Type	γ (kN/m^3)	E (kPa)	ν	φ	c (kPa)	ψ
Sand	17.4	64020	0.3	47.4	1	17.4
Clay	18.5	85670	0.3	32.4	37.7	2.4

As it is told earlier, finite element analysis was conducted in order to determine effect of foundation layers. Created finite element model is given on Figure 3.5 below.

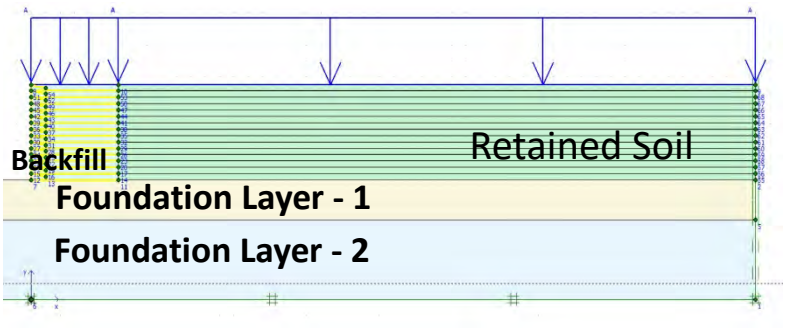

Material properties used to model reinforced backfill, retained backfill, and foundation layers are provided in Table 3.3, Table 3.4 and Table 3.5 respectively.

Table 3.3 Material Parameters of Reinforced Backfill

	Reinforced Backfill			
	φ	γ (kN/m^3)	c (kPa)	E (GPa)
100% Sand	47.4	17.4	0.5	64.02
80% Sand + 20% Fine	42.4	20.7	11.6	55.72
60% Sand + 40% Fine	41.2	20.5	24	90.22
40% Sand + 60% Fine	38.8	20.6	25.8	59.48
20% Sand + 80% Fine	36.5	20	34.4	85.54
Fine Soil	32.4	18.5	37.7	85.67

Table 3.4 Material Parameters of Retained Backfill

Retained Backfill			
φ	γ (kN/m^3)	c (kPa)	E (GPa)
20	15	1	15
30	17	20	50

Foundation Soil 1					Foundation Soil 2				
φ°	γ (kN/m^3)	c (kPa)	E (GPa)	D (m)	φ°	γ (kN/m^3)	c (kPa)	E (GPa)	D (m)
20	15	1	15	2.5	20	18	35	60	5.0
20	15	1	15	2.5	20	18	35	60	5.0
20	15	1	15	2.5	20	18	35	60	5.0
20	15	1	15	2.5	20	18	35	60	5.0
20	15	1	15	2.5	20	18	35	60	5.0
20	15	1	15	2.5	20	18	35	60	5.0
20	15	1	15	2.5	20	18	35	60	5.0
20	15	1	15	2.5	20	18	35	60	5.0
20	15	1	15	2.5	20	18	35	60	5.0
20	15	1	15	2.5	20	18	35	60	5.0
20	15	1	15	2.5	20	18	35	60	5.0
20	15	1	15	2.5	20	18	35	60	5.0
20	15	1	15	5.0	20	18	35	60	5.0
20	15	1	15	5.0	20	18	35	60	5.0
20	15	1	15	5.0	20	18	35	60	5.0
20	15	1	15	5.0	20	18	35	60	5.0
20	15	1	15	5.0	20	18	35	60	5.0
20	15	1	15	5.0	20	18	35	60	5.0
20	15	1	15	5.0	20	18	35	60	2.5
20	15	1	15	5.0	20	18	35	60	2.5
20	15	1	15	5.0	20	18	35	60	2.5
20	15	1	15	5.0	20	18	35	60	2.5

20	15	1	15	5.0	20	18	35	60	2.5
20	15	1	15	5.0	20	18	35	60	2.5
35	17	20	55	2.5	20	18	35	60	5.0
35	17	20	55	2.5	20	18	35	60	5.0
35	17	20	55	2.5	20	18	35	60	5.0
35	17	20	55	2.5	20	18	35	60	5.0
35	17	20	55	2.5	20	18	35	60	5.0
35	17	20	55	2.5	20	18	35	60	5.0
35	17	20	55	5.0	20	18	35	60	5.0
35	17	20	55	5.0	20	18	35	60	5.0
35	17	20	55	5.0	20	18	35	60	5.0
35	17	20	55	5.0	20	18	35	60	5.0
35	17	20	55	5.0	20	18	35	60	5.0
35	17	20	55	5.0	20	18	35	60	5.0
35	17	20	55	5.0	20	18	35	60	2.5
35	17	20	55	5.0	20	18	35	60	2.5
35	17	20	55	5.0	20	18	35	60	2.5
35	17	20	55	5.0	20	18	35	60	2.5
35	17	20	55	5.0	20	18	35	60	2.5
35	17	20	55	5.0	20	18	35	60	2.5
35	17	20	55	5.0	20	16	1	15	2.5
35	17	20	55	5.0	20	16	1	15	2.5
35	17	20	55	5.0	20	16	1	15	2.5
35	17	20	55	5.0	20	16	1	15	2.5
35	17	20	55	5.0	20	16	1	15	2.5
35	17	20	55	5.0	20	16	1	15	2.5
35	17	20	55	5.0	20	16	1	15	5.0
35	17	20	55	5.0	20	16	1	15	5.0
35	17	20	55	5.0	20	16	1	15	5.0
35	17	20	55	5.0	20	16	1	15	5.0
35	17	20	55	5.0	20	16	1	15	5.0
35	17	20	55	5.0	20	16	1	15	5.0

20	15	1	15	2.5	20	16	1	15	2.5
20	15	1	15	2.5	20	16	1	15	2.5
20	15	1	15	2.5	20	16	1	15	2.5
20	15	1	15	2.5	20	16	1	15	2.5
20	15	1	15	2.5	20	16	1	15	2.5
20	15	1	15	2.5	20	16	1	15	2.5
20	15	1	15	2.5	20	16	1	15	5.0
20	15	1	15	2.5	20	16	1	15	5.0
20	15	1	15	2.5	20	16	1	15	5.0
20	15	1	15	2.5	20	16	1	15	5.0
20	15	1	15	2.5	20	16	1	15	5.0
20	15	1	15	2.5	20	16	1	15	5.0
20	15	1	15	5.0	20	16	1	15	2.5
20	15	1	15	5.0	20	16	1	15	2.5
20	15	1	15	5.0	20	16	1	15	2.5
20	15	1	15	5.0	20	16	1	15	2.5
20	15	1	15	5.0	20	16	1	15	2.5
20	15	1	15	5.0	20	16	1	15	2.5
20	15	1	15	5.0	20	16	1	15	5.0
20	15	1	15	5.0	20	16	1	15	5.0
20	15	1	15	5.0	20	16	1	15	5.0
20	15	1	15	5.0	20	16	1	15	5.0
20	15	1	15	5.0	20	16	1	15	5.0
20	15	1	15	5.0	20	16	1	15	5.0

4. RESULTS

4.1 Determination of Soil Properties

As it is told before, sand, clay and their mixtures and tyre crumbs are used in this study. The grain size distribution of sand and tyre crumbs are given on Figure 4.1.

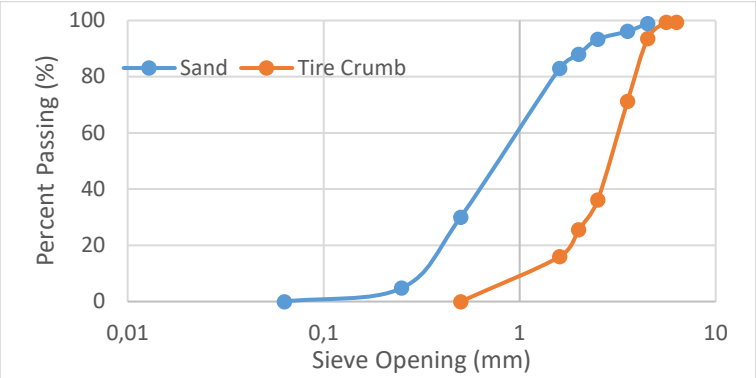

Figure 4.1 Grain Size Distribution of Sand and Tyre Crumb

Specific gravity of sand is given as 2.9. Coefficient of uniformity and coefficient of gradation is calculated as 3.3 and 0.84 respectively. Sand is classified as poorly graded (SP) sand according to unified classification system.

Hydrometer analysis results of clay is provided on Figure 4.2 below.

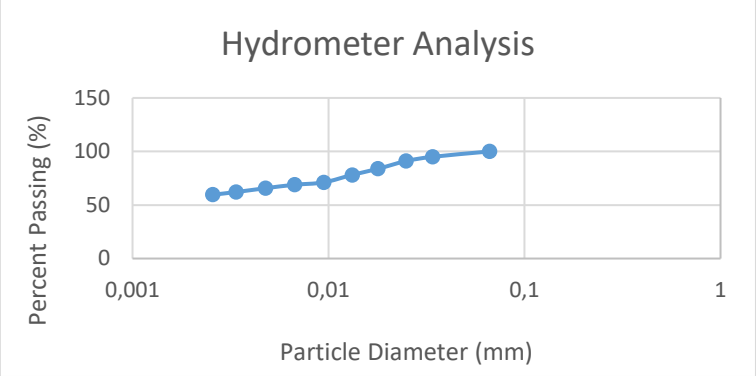

Figure 4.2 Grain Size Distribution of Clay

Specific gravity of clay is found as 2.69. Plastic limit and liquid limit is found as 20.18% and 35.86%. Clay is classified as CL according to unified classification system.

Maximum dry unit weight and corresponding optimum water content of sand clay and its mixtures are provided below.

Table 4.1 Maximum Dry Unit Weight and Optimum Water Content of Samples

Mixture	**Maximum Dry Unit Weight (g/cm^3)**	**Optimum Water Content (%)**
100% Sand	1,74	11,5
90% Sand + 10% Fine	1,80	9,5
80% Sand + 20% Fine	2,07	8,0
70% Sand + 30% Fine	2,13	6,8
60% Sand + 40% Fine	2,05	8,0
50% Sand + 50% Fine	2,12	8,6
40% Sand + 60% Fine	2,06	9,1

30% Sand + 70% Fine	2,02	10,0
20% Sand + 80% Fine	2,00	11,0
10% Sand + 90% Fine	1,99	10,0
100% Fine	1,85	12,5

When these mixtures are mixed with tyre crumbs with different ratios, maximum dry unit weights changes as follows on Table 4.2. It should be noted here that, water content is kept same to find out unit weight change.

Table 4.2 Unit Weight of Soil Tyre Crumb Mixtures

Tyre Chip Content				
Mixture	**10%**	**20%**	**30%**	**40%**
100% Sand	1,55	1,47	1,22	1,20
90% Sand + 10% Fine	1,75	1,56	1,33	1,27
80% Sand + 20% Fine	1,84	1,62	1,42	1,40
70% Sand + 30% Fine	1,91	1,69	1,46	1,42
60% Sand + 40% Fine	1,78	1,72	1,50	1,44
50% Sand + 50% Fine	1,90	1,69	1,50	1,42
40% Sand + 60% Fine	1,91	1,70	1,59	1,45
30% Sand + 70% Fine	1,85	1,74	1,58	1,44
20% Sand + 80% Fine	1,65	1,67	1,55	1,43
10% Sand + 90% Fine	1,79	1,64	1,52	1,40
100% Fine	1,79	1,64	1,50	1,39

Direct shear tests are conducted to these samples. Results showed that, as the sand content decreases, angle of friction decreases and cohesion increases. When tyre crumbs are added to mixture, angle of friction slightly decreases for 10% tyre crumb content. Addition of 20% tyre crumb content into soil mixtures, the highest values of angle of friction is measured. Adding 30% tyre crumb caused reduction in angle of friction. All tyre crumb inclusions caused increase on cohesion only for pure sand and 90% sand. In other soil mixtures, addition of tyre crumb reduced cohesion. Measured values of angle of friction and cohesion is given on Table 4.3.

Table 4.3 Measured angle of friction and cohesions from direct shear tests

	0 % Tyre Chip		**10% Tyre Chip**		**20% Tyre Chip**		**30% Tyre Chip**	
	ϕ	**c (kPa)**	**ϕ**	**c (kPa)**	**ϕ**	**c (kPa)**	**ϕ**	**c (kPa)**
100% Sand	47,38	0,46	45,39	7,39	47,74	5,86	41,16	6,64

90% Sand + 10% Fine	44,19	3,07	43,84	13,36	46,23	9,73	41,01	7,09
80% Sand + 20% Fine	42,35	11,61	42,17	17,46	46,02	11,56	39,89	8,88
70% Sand + 30% Fine	41,36	21,51	41,04	21,93	44,80	12,50	38,35	11,61
60% Sand + 40% Fine	41,19	24,01	40,70	23,09	43,30	17,11	38,06	17,86
50% Sand + 50% Fine	41,04	26,68	39,86	24,63	42,08	20,26	37,09	19,88
40% Sand + 60% Fine	38,84	25,84	37,78	25,74	41,72	20,63	36,69	20,02
30% Sand + 70% Fine	38,05	26,10	37,45	25,66	41,14	22,58	36,27	23,52
20% Sand + 80% Fine	36,51	34,36	35,61	25,76	40,62	22,64	36,07	26,56
10% Sand + 90% Fine	36,37	37,48	35,54	25,76	38,62	23,69	35,41	26,71
100% Fine	32,44	37,66	33,37	30,19	37,47	28,14	34,60	28,63

When direct shear tests of pure soils are modelled with Abaqus, less then 10% error is computed with respect to shear strenght of soils. The measured and computed results are given on Table 4.4.

Table 4.4 Maximum Shear Stress Values from Experiment and Finite Element Model and Difference

Content	**Confining Pressure**	**Experiment**	**Abaqus**	**Difference (%)**
100% Sand	**9,81 kPa**	11	10,8	1.82
	19,62 kPa	22,7	24,8	9.25
	40,81 kPa	43,1	44,9	4.18
	58,86 kPa	65,3	64,9	0.61
80% Sand + 20% Fine	**9,81 kPa**	19,2	17,7	7.81
	19,62 kPa	30,4	27,4	9.87
	40,81 kPa	50,5	46,8	7.33
	58,86 kPa	64	63,3	1.09
60% Sand + 40% Fine	**9,81 kPa**	34,7	34,8	0.29
	19,62 kPa	40,3	41	1.74
	40,81 kPa	55,9	59,5	6.44

	58,86 kPa	78,1	80,2	2.69
40% Sand + 60% Fine	**9,81 kPa**	31,6	32,6	3.16
	19,62 kPa	43,2	42,1	2.55
	40,81 kPa	61,1	60,1	1.64
	58,86 kPa	71,4	72,7	1.82
20% Sand + 80% Fine	**9,81 kPa**	40,7	39,1	3.93
	19,62 kPa	49,1	45,9	6.52
	40,81 kPa	66,6	74,1	11.26
	58,86 kPa	76,6	73,7	3.76
100% Clay	**9,81 kPa**	44,6	45,3	1.57
	19,62 kPa	50,4	49,7	1.39
	40,81 kPa	61,1	61,2	0.16
	58,86 kPa	76,6	79,5	3.79

When angle of friction and cohesion values are calculated from finite element analysis, less then 10% error occurred between results. Those values are provided on Table 4.5 below.

Table 4.5 Shear Strenght Parameters from Experiment and Finite Element Model and Difference

	Experiment		**Abaqus**		**Difference (%)**	
Content	**φ (º)**	**c (kPa)**	**φ (º)**	**c (kPa)**	**φ (º)**	**c (kPa)**
100% Sand	47.4	0.46	48.2	0	1.7	100,00
80% Sand + 20% Clay	42.4	11.61	43.0	8.80	1.5	24.20
60% Sand + 40% Clay	41.2	24.01	43.0	23.90	4.4	0.46
40% Sand + 60% Clay	38.9	25.84	39.4	25.40	1.5	1.69
20% Sand + 80% Clay	36.1	34.36	37.5	32.60	3.9	5.12
100% Clay	32.4	37.66	34.5	36.80	6.4	2.28

4.2 Results From Small Scale Wall Tests

When small scale walls are tested at the laboratory, it is seen that the lowest settlements of loading platemeasure for pure sand, while the highest settlements are measured for sand 20% tyre crumb mixtures. Change of settlement with respect to load and tyre crumb content is given on Figure 4.3 below.

When measured horizontal displacements are compared with each other, it is seen that, lower or almost equal horizontal displacements are measured for sand and 10% tyre crumb mixtures up to 0.42 MPa.

Then measured horizontal displacements gets higher than pure sand. This behaviour is given on Figure 4.4 for.

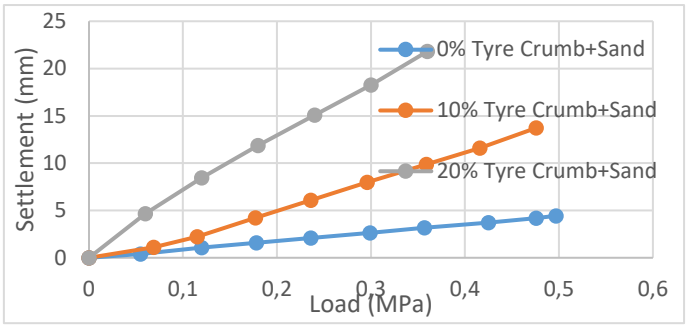

Figure 4.3 Settlement of Loading Plate for sand and tyre crumb mixtures

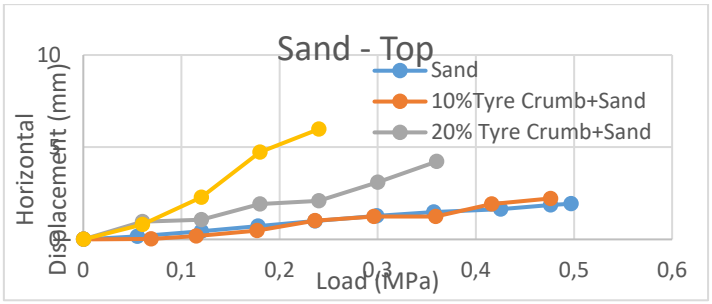

Figure 4.4 Measured horizontal displacements for sand and tyre crumb mixtures at top measurement point

When behaviour of small scale walls investigated, the lowest settlement is measured for pure clay. The change settlement with respect to tyre crumb content and load is given on Figure 4.5.

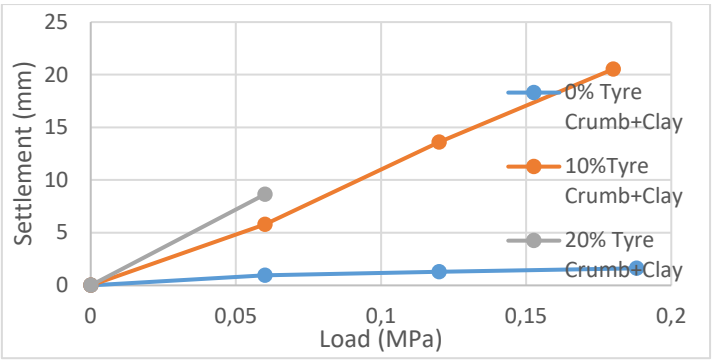

Figure 4.5 Settlement of Loading Plate for clay and tyre crumb mixtures

When horizontal displacements are compared with respect to different clay-tyre crumb mixtures, it is seen that the lowest horizontal displacements computed for a wall with a pure clay backfill. Figure 4.6 shows measured horizontal diplacement on top of wall for clay backfills and tyre crumb mixtures.

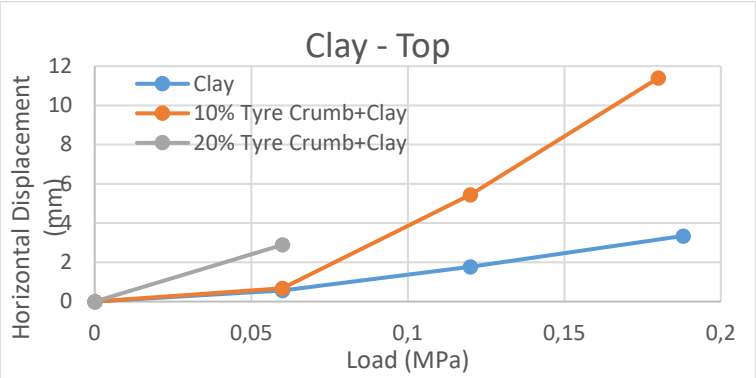

Figure 4.6 Measured horizontal displacements for clay and tyre crumb mixtures at top measurement point

4.3 Finite Element Model of Small Scale Walls

When tested walls are modelled in finite element software Plaxis, it is seen that walls with sand backfill approximates to real results better than walls with clay backfill. Measured and computed settlement values of loading plate are given on Figure 4.7 for sand backfill.

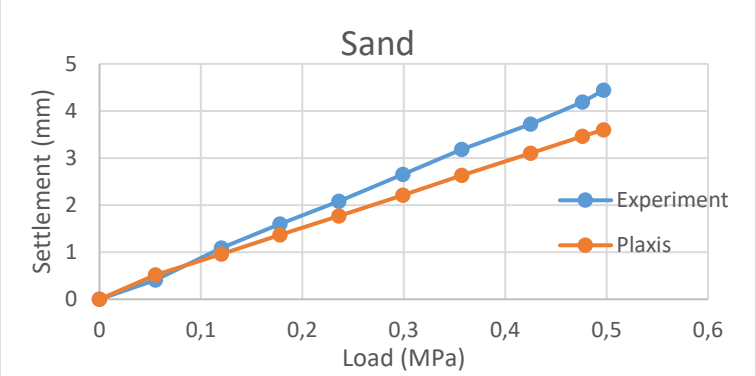

Figure 4.7 Measured and computed settlement of loading plate for sand backfill.

The measured and computed settlement of loading for clay backfill is given on Table 4.6 below.

Table 4.6 Measure and computed settlement values of loading plate for clay backfill

Load (MPa)	Test Settlement (mm)	Plaxis Settlement (mm)
0	0	0
0.06	0.97	0.36
0.12	1.28	0.63
0.188	1.62	0.99

4.4 Effect of Backfill Foundation Soil to Behaviour of Reinforced Earth Wall

The lowest horizontal displacements are computed for sand backfill while the highest displacements are computed for 80% sand + 20% clay backfill. The change of horizontal displacement at reinforced earth wall face is given on Figure 4.8.

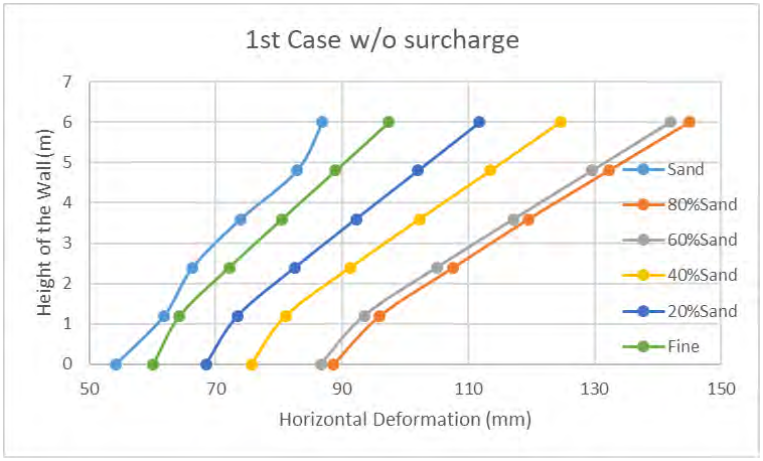

Figure 4.8 Computed horizontal displacements on wall face for different type of backfills.

If the settlement of reinforced earth wall with different backfills are considered, the highest settlements are computed for 80% Sand-20% clay backfill. Figure 4.9 shows change of computed displacements for different backfill.

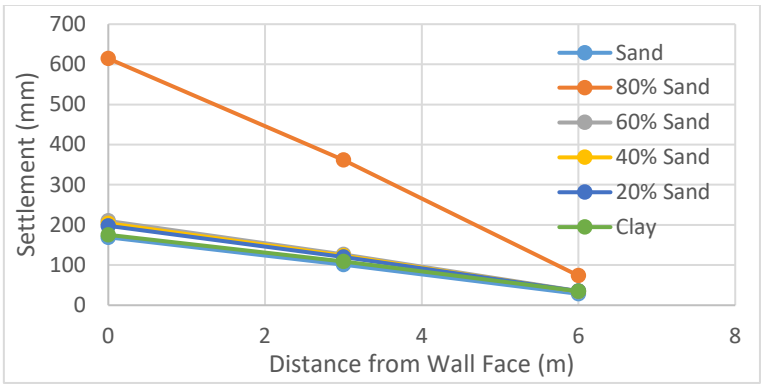

Figure 4.9 Computed settlement values for different type of backfill

Computed forces on reinforcements is shown on Figure 4.10. According to figure 4.10, the highest forces are computed for sand backfill except for the last layer. The highest force is computed for 80% sand – 20% clay mixture at last layer. The highest resultant force is computed for sand backfill.

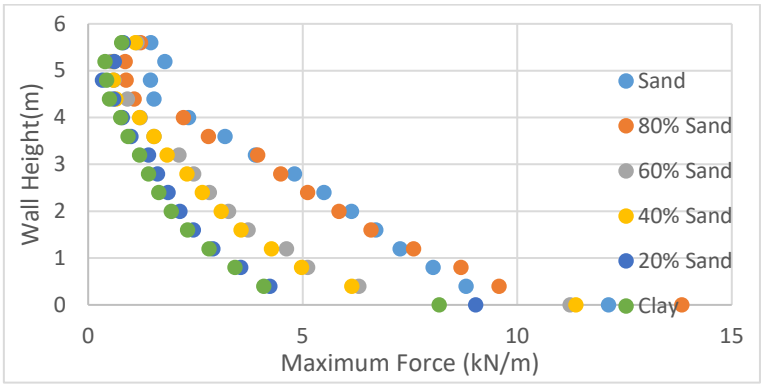

Figure 4.10 Computed maximum forces on geosynthetic layers

When the effect of foundation conditions to horizontal displacement of wall face is investigated, it is seen that, horizontal displacements are highly dependent on foundation conditions. Computed horizontal displacements for different foundation conditions are given on Table 4.7 below.

Table 4.7 Computed horizontal displacements with respect different foundation conditions

H (m)	1st Case	2nd Case	3rd Case	4st Case	5th Case	6th Case	7th Case	8th Case	9th Case	10th Case	11th Case	12th Case	13th Case
6.0	86.92	33.92	96.73	92.10	8.61	7.60	8.52	6.35	2.89	97.40	106.35	97.25	111.65
4.8	82.86	32.79	90.46	85.86	8.80	8.01	8.72	7.04	4.26	90.64	98.35	90.34	103.60
3.6	73.94	30.73	83.59	78.89	8.41	7.87	8.36	7.18	5.13	83.16	89.63	82.73	94.98
2.4	66.34	27.56	75.64	70.93	7.33	7.05	7.30	6.70	5.36	74.64	79.92	74.16	85.37
1.2	61.81	23.28	66.36	62.22	5.47	5.56	5.47	5.47	4.50	65.19	69.32	64.85	74.73
0	54.23	22.42	61.78	60.02	2.38	2.49	2.41	2.84	2.83	60.34	63.59	62.01	68.19

When the computed settlements are investigated with respect to different foundation conditions, it is seen that the magnitude and pattern of the settlements changes with respect to foundation conditions. Those changes are given on Figure 4.11 below for sand backfill.

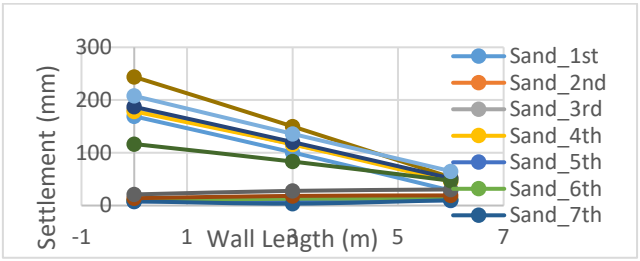

Figure 4.11 Computed settlements with respect to different foundation conditions for sand backfill

If the forces computed at different geosynthetic layers are investigated, it is seen that, computed forces on each geosynthetic layers are highly dependent on foundation conditions. Computed forces are given on Table 4.10 below for sand backfill.

Z (m)	1st Case	2nd Case	3rd Case	4th Case	5th Case	6th Case	7th Case	8th Case	9th Case	10th Case	11th Case	12th Case	13th Case
0	4.79	1.69	5.10	4.76	0.75	0.73	0.74	0.75	0.72	5.08	4.58	3.31	5.14
0.4	2.64	2.30	1.66	2.12	1.07	1.02	1.06	1.07	1.02	2.47	2.33	2.33	1.70
0.8	2.39	2.95	1.83	2.18	1.38	1.32	1.37	1.38	1.32	2.50	2.16	1.98	1.78
1.2	2.62	3.55	2.19	2.42	1.69	1.62	1.68	1.68	1.60	2.70	2.45	2.34	2.17
1.6	2.98	4.11	2.86	2.84	1.98	1.90	1.97	2.01	1.88	3.02	2.89	2.81	2.87
2.0	3.61	4.56	3.78	3.68	2.27	2.20	2.26	2.27	2.18	3.91	3.85	3.58	4.00
2.4	4.55	5.03	4.90	4.75	2.50	2.45	2.49	2.51	2.45	4.63	4.90	4.71	4.94
2.8	5.70	5.50	5.80	5.63	2.65	2.62	2.63	2.65	2.64	5.63	5.78	5.60	5.80
3.2	6.50	5.95	6.57	6.40	2.68	2.67	2.66	2.65	2.64	6.39	6.48	6.26	6.61
3.6	7.16	6.39	7.29	7.02	2.81	2.67	2.81	2.77	2.68	6.96	7.21	7.00	7.27

4.0	7.78	6.84	7.94	7.66	3.09	2.93	3.08	2.96	2.91	7.59	7.82	7.53	7.88
4.4	8.51	7.40	8.64	8.61	3.26	3.03	3.25	3.28	3.02	8.40	8.53	8.17	8.55
4.8	9.67	7.90	9.51	9.84	3.15	3.14	3.13	3.17	3.13	9.39	9.63	9.20	9.45
5.2	11.11	8.41	10.56	11.37	3.14	3.76	3.20	3.28	3.85	10.80	10.95	10.37	10.44
5.6	18.62	11.06	17.34	26.34	0.25	0.22	0.26	0.18	0.22	17.58	16.21	22.47	16.76
Resultant	98.63	83.64	95.97	105.63	32.69	32.28	32.59	32.62	32.25	97.06	95.77	97.66	95.36

5. CONCLUSION

Behaviour of reinforced earth wall is investigated under following conditions in this study.

- Addition of tyre crumbs in different ratios to sand and clay backfill in order to measure change of behaviour of reinforced eath walls.
- Effect of different backfill materials to behaviour of reinforced earth structures
- Effect of different foundation conditions to behaviour of reinforced earth structures.

According to results of this study, it is seen that, in case of sand backfill, lower horizontal displacements are observed for 10% tyre crumb inclusion. It should be noted that, settlement measured for this tyre crumb content is slightly higher than pure sand case. In case of clay backfill, addition of tyre crumbs resulted higher displacement and settlement than pure clay backfill case.

It seen that, behaviour of reinforced earth wall is highly dependent on used backfill soil. Different backfill soils react to surcharge load differently which may yield change of behaviour of reinforced earth wall.

Computed horizontal displacements, settlements and geosynthetic forces are highly dependent on foundation conditions. It should be also noted that, thickness of soil layer also affects computed deformations.

Following contributions to literature are made by the results of this study.

- Tyre crumbs can be used as a backfill material with sand up to 10% tyre crumb content. Several researchers found contradicting results about usage of tyre chips in reinforced earth wall, however, experimental part of study proved that, tyre crumbs can be used.
- Effect of backfill materials are generally considered by working condtions of reinforced earth wall. This study proved that, not only working conditions, but also change of working conditions of reinforced eath wall should be considered during design of reinforced earth walls, especially for the walls which contains fine particles.
- Foundation conditions are important property of the design stage. Changing foundation conditions may yield to totally different behaviour of the wall. Amount of change is revealed by this study.

The outcome of this study can be used for a furher research in the following areas.

- Investigation of decreasing settlement of loading plate when tyre crumbs are used with sand backfill.

- Implementing a coefficient to analytical design of reinforced earth walls in order to account foundation conditions. It is clear that, checking for a bearing capacity of foundation is not enough to design a reinforced earth wall.

REFERENCES

E. Bourgeois, L. Soyez, A. Le Kouby “Experimental and numerical study of the behaviour of a reinforced-earth wall subjected to a local load" Computers and Geotechnics, 2011, 38, 515-525

Suliman B.A. Mohamed, Kuo-Hsin Yang, Wen-Yi Hung “Finite element analyses of two-tier geosynthetic-reinforced soil walls: Comparison involving centrifuge tests and limit equilibrium results”, Computers and Geotechnics 2014, 61, 67 – 84

Myoung – Soo Won, You – Seong Kim “Internal deformation behavior of geosynthetic-reinforced soil walls” Geotextiles and Geomembranes, 2007, 25, 10 – 22

Guangqing Yang, Baojian Zhang, Peng Lv, Qiaoyong Zhou “Behaviour of geogrid reinforced soil retaining wall with concrete-rigid facing”, Geotextiles and Geomembranes, 2009, 27, 350 – 356

Ching – Chuan Huang, Woei – Ming Luo "Behavior of cantilever and geosynthetic-reinforced walls on deformable foundations" Geotextiles and Geomembranes, 2010, 28, 448 – 459

Eder C.G. Santos, Ennio M. Palmeira, Richard J. Bathurst "Behaviour of a geogrid reinforced wall built with recycled constructionand demolition waste backfill on a collapsible foundation", Geotextiles and Geomembranes, 2013, 39, 9 –19

Chengzhi Xiao, Jie Han, Zhen Zhang "Experimental study on performance of geosynthetic-reinforced soil model walls on rigid foundations subjected to static footing loading", Geotextiles and Geomembranes, 2016, 44, 81 – 94

M.Ehrlich, S.H. Mirmoradi , R.P. Saramago "Evaluation of the effect of compaction on the behavior of geosynthetic-reinforced soil walls", Geotextiles and Geomembranes, 2012, 34, 108 – 115

Chungsik Yoo, Hyuck – Sang Jung "Measured behavior of a geosynthetic-reinforced segmental retaining wall in a tiered configuration", Geotextiles and Geomembranes, 2004, 22, 359 – 376

Taesoon Parka, Siew Ann Tan "Enhanced performance of reinforced soil walls by the inclusion of short fiber" Geotextiles and Geomembranes, 2005, 23, 348-361

Mario Riccio, Mauricio Ehrlich, Daniel Dias "Field monitoring and analyses of the response of a block-faced geogrid wall using fine-grained tropical soils", Geotextiles and Geomembranes, 2014, 42, 127 – 138

Chungsik Yoo, Sun – Bin Kim "Performance of a two-tier geosynthetic reinforced segmental retaining wall under a surcharge load: Full-scale load test and 3D finite element analysis", Geotextiles and Geomembranes, 2008, 26, 460 – 472

Carina Maia Lins Costa, Jorge Gabriel Zornberg, Benedito de Souza Bueno Yuri Daniel Jatob a Costa "Centrifuge evaluation of the time-dependent behavior of geotextile-reinforced soil walls", Geotextiles and Geomembranes, 2016, 44, 188 – 2007

A. L. Shinde Æ J. N. Mandal "Behavior of Reinforced Soil Retaining Wall With Limited Fill Zone", Geotech Geol Eng, 2007, 25, 657 – 672

Sutapa Hazra Æ Nihar Ranjan Patra "Performance of Counterfort Walls with Reinforced Granular and Fly Ash Backfills: Experimental Investigation", Geotech Geol Eng, 2008, 26, 259 – 267

M. Pinho-Lopes, D. M. Carlos, M. L. Lopes "Flume Tests on Fine Soil Reinforced with Geosynthetics: Walls of the Salt Pans (Aveiro Lagoon, Portugal)", Int. J. of Geosynth. and Ground Eng, 2015, 1 – 12

H. Ahmadi, M. Hajialilue-Bonab "Experimental and analytical investigations on bearing capacity of strip footing in reinforced sand backfills and flexible retaining wall", Acta Geotechnica, 2012, 7, 357 – 373

S. Bali Reddy, A. Murali Krishna "Recycled Tyre Chips Mixed with Sand as Lightweight Backfill Material in Retaining Wall Applications: An Experimental Investigation", Int. J. of Geosynth. and Ground Eng, 2015, 1 – 31

Richard J. Bathurst, Sebastian Althoff, and Peter Linnenbaum "Influence of Test Method on Direct Shear Behavior of Segmental Retaining Wall Units", Geotechnical Testing Journal, 31, 1 – 9

Guangqing Yang, Huabei Liu, Peng Lv, Baojian Zhang "Geogrid-reinforced lime-treated cohesive soil retaining wall: Case study and implications", Geotextiles and Geomembranes, 2012, 35, 112 – 118

Guang – Qing Yang, Huabei Liu, Yi-Tao Zhou, Bao – Lin Xiong "Post-construction performance of a two – tiered geogrid reinforced soil wall backfilled with soil – rock mixture", Geotextiles and Geomembranes, 2014, 42, 91 – 97

Sompote Youwai, Dennes T. Bergado "Numerical analysis of reinforced wall using rubber tyre chips–sand mixtures as backfill material", Computers and Geotechnics, 2004, 31, 103 – 114

Chia – Cheng Fan "Three-dimensional behaviour of a reinforced earth-retaining structure within a valley", Computers and Geotechnics, 2006, 33, 69 – 85

Jian – Feng Chen, Jun – Xiu Liu, Jian – Feng Xue, Zhen – Ming Shi "Stability analyses of a reinforced soil wall on soft soils using strength reduction method", Engineering Geology, 2014, 177, 83 – 92

M. Ehrlich, S.H. Mirmoradi "Evaluation of the effects of facing stiffness and toe resistance on the behavior of GRS walls", Geotextiles and Geomembranes, 2013, 40, 28 – 36

Dov Leshchinsky, Farshid Vahedifard, Ben A. Leshchinsky “Revisiting bearing capacity analysis of MSE walls”, Geotextiles and Geomembranes, 2012, 34, 100 – 107

Huabei Liu "Long-term lateral displacement of geosynthetic-reinforced soil segmental retaining walls", Geotextiles and Geomembranes, 2012, 32, 18 – 27

Yan Yu, Ivan P. Damians, Richard J. Bathurst "Influence of choice of FLAC and PLAXIS interface models on reinforced soil–structure interactions", Computers and Geotechnics, 2015, 65, 164 – 174

Huabei Liu, Xiangyu Wang, Erxiang Song “Long-term behavior of GRS retaining walls with marginal backfill soils”, Geotextiles and Geomembranes, 2009, 27, 295 – 307

Jie Han, Dov Leshchinsky “Analysis of back-to-back mechanically stabilized earth walls”, Geotextiles and Geomembranes, 2010, 28, 262 – 267

Abdelkader Abdelouhab, Daniel Dias, Nicolas Freitag "Numerical analysis of the behaviour of mechanically stabilized earth walls reinforced with different types of strips", Geotextiles and Geomembranes, 2011, 29, 116 – 129

Hoe I. Ling *Æ*, Huabei Liu "Deformation analysis of reinforced soil retaining walls—simplistic versus sophisticated finite element analyses", Acta Geotechnica, 2009, 4, 203 – 2013

Yonggui Xie, Ben Leshchinsky “MSE walls as bridge abutments: Optimal reinforcement density”, Geotextiles and Geomembranes, 2015, 43, 128 – 138

I. P. Damians, R. J. Bathurst, A. Josa and A. Lloret "Numerical study of the influence of foundation compressibility and reinforcement stiffness on the behavior of reinforced soil walls", International Journal of Geotechnical Engineering", 2014, 8, 247 – 259

Lazhar Belabed, Hacene Benyaghla,Jarir Yahiaoui "Internal Stability Analysis of Reinforced Earth Retaining Walls", Geotech Geol Eng, 2011, 29, 443 – 452

Ben Leshchinsky "Limit Analysis Optimization of Design Factors for Mechanically Stabilized Earth Wall-Supported Footings" , Transp. Infrastruct. Geotech., 2014, 1, 111 – 128

XUE Jian – Feng, CHEN Jian – Feng "Reinforcement strength reduction in FEM for mechanically stabilized earth structures", J. Cent. South Univ., 2015, 22, 2691 – 2698

Graeme D. Skinnera, R. Kerry Roweb "Design and behaviour of a geosynthetic reinforced retaining wall and bridge abutment on a yielding foundation", Geotextiles and Geomembranes, 2005, 23, 234 – 260

Jie Huang, Robert L. Parsons, Jie Han, Matthew Pierson “Numerical analysis of a laterally loaded shaft constructed within an MSE wall”, Geotextiles and Geomembranes, 2011, 29, 233 – 241

Jie Huang, Jie Han, Robert L. Parsons, Matthew C. Pierson "Refined numerical modeling of a laterally-loaded drilled shaft in an MSE wall", Geotextiles and Geomembranes, 2013, 37, 61 – 73

Guangqing Yang, Junxia Ding, Qiaoyong Zhou, and Baojian Zhang "Field Behavior of a Geogrid Reinforced Soil Retaining Wall with a Wrap-Around Facing" Geotechnical Testing Journal, 2010, 33, 1 – 6

Krystyna Kazimierowicz-Frankowska "A case study of a geosynthetic reinforced wall with wrap-around facing", Geotextiles and Geomembranes, 2005, 23, 107 – 115

Jian – Feng Xue, Jian – Feng Chen, Jun – Xiu Liu, Zhen – Ming Shi "Instability of a geogrid reinforced soil wall on thick soft Shanghai clay with prefabricated vertical drains: A case study", Geotextiles and Geomembranes, 2014, 42, 302 – 311

Abdolhosein Haddad and Gholamali Shafabakhsh "FAILURE OF SEGMENTAL RETAINING WALLS DUE TO THE INSUFFICIENCY OF BACKFILL PERMEABILITY", Proceedings of the 4th Asian Regional Conference on Geosynthetics, June 17 - 20, 2008 852 – 856

Chungsik Yoo "Performance of a 6-year-old geosynthetic reinforced segmental retaining wall", Geotextiles and Geomembranes, 2004, 22, 377 – 397

R. Kerry Rowe and Allen Lunzhu Li "INSIGHTS FROM CASE HISTORIES: REINFORCED EMBANKMENTS AND RETAINING WALLS"

James G. Collin "Lessons learned from a segmental retaining wall failure", Geotextiles and Geomembranes, 2001, 19, 445 – 454

A. Sengupta "Numerical Study of a Failure of a Reinforced Earth Retaining Wall", Geotech Geol Eng, 2012, 30, 1025 – 1034

Assaf Klar, Tal Sas "The KC method: Numerical investigation of a new analysis method for reinforced soil walls", Computers and Geotechnics, 2010, 37, 351 – 358

Thai Son Quang, Hassen Ghazi, Buhan de Patrick "A multiphase approach to the stability analysis of reinforced earth structures accounting for a soil–strip failure condition", Computers and Geotechnics, 2009, 36, 454 – 462

Suliman B.A. Mohamed, Kuo-Hsin Yang, Wen-Yi Hung "Limit equilibrium analyses of geosynthetic-reinforced two-tiered walls: Calibration from centrifuge tests", Geotextiles and Geomembranes, 2013, 41, 1 – 16

V. A. Barvashov and I. M. Iovlev "METHOD OF ANALYSIS FOR REINFORCED SOIL MASSES", Soil Mechanics and Foundation Engineering, 2010, 47, 189 – 196

Jonathan T. H. Wu, Jean-Baptiste Payeur "Connection Stability Analysis of Segmental Geosynthetic Reinforced Soil (GRS) Walls", Transp. Infrastruct. Geotech., 2015, 2, 1 – 17

SATYENDRA MITTAL, K. G. GARG and SWAMI SARAN "Analysis and design of retaining wall having reinforced cohesive frictional backfill" Geotechnical and Geological Engineering, 2006, 24, 499 – 522

Richard J. Bathursta, Tony M. Allenb, Dave L. Waltersc"Reinforcement loads in geosynthetic walls and the case for a new working stress design method", Geotextiles and Geomembranes, 2005, 23, 287 – 322

Dov Leshchinsky, Beongjoon Kang, Jie Han, Hoe Ling "Framework for Limit State Design of Geosynthetic-Reinforced Walls and Slopes", Transp. Infrastruct. Geotech., 2014, 1, 129 – 164

R. Baker, Y. Klein "An integrated limiting equilibrium approach for design of reinforced soil retaining structures: Part I—formulation", Geotextiles and Geomembranes, 2004, 22, 119 – 150

D. M. Carlos, Margarida Pinho-Lopes "Reinforcement with Geosynthetics of Walls of the Saltpans of the Aveiro Lagoon", Geotech Geol Eng, 2011, 29, 519 – 536

R. Baker, Y. Klein "An integrated limiting equilibrium approach for design of reinforced soil retaining structures: Part II—design examples", Geotextiles and Geomembranes, 2004, 22, 151 – 177

Dov Leshchinskya, Yuhui Hua, Jie Hanb "Limited reinforced space in segmental retaining walls", Geotextiles and Geomembranes, 2004, 22, 543 – 553

B. Munwar Basha, G. L. Sivakumar Babu "Reliability Based LRFD Approach for External Stability of Reinforced Soil Walls" Indian Geotech J, 2013, 43 (4) 292 – 302

Ömer Bilgin "Failure mechanisms governing reinforcement length of geogrid reinforced soil retaining walls", Engineering Structures, 2009, 31, 1967 – 1975

O. Al Hattamleha, B. Muhunthanb "Numerical procedures for deformation calculations in the reinforced soil walls", Geotextiles and Geomembranes 2006, 24, 52 – 57

Robert M. Koerner and George R. Koerner "THE IMPORTANCE OF DRAINAGE CONTROL FOR GEOSYNTHETIC REINFORCED MECHANICALLY STABILIZED EARTH WALLS", Journal of GeoEngineering, 2011, 6, 3 – 13

Robert M. Koernera, Te-Yang Soong "Geosynthetic reinforced segmental retaining walls", Geotextiles and Geomembranes, 2001, 19, 359 – 386

P.K. Basudhar, Amol Vashistha, Kousik Deb, Arindam Dey “Cost Optimization of Reinforced Earth Walls”, Geotech Geol Eng, 2008, 26, 1 – 12

F. Tatsuokaa, M. Tateyamab, Y. Mohric, K. Matsushimac "Remedial treatment of soil structures using geosynthetic – reinforcing technology", Geotextiles and Geomembranes, 2007, 25, 204 – 220

Sajna Sayed , G.R. Dodagoudar, K. Rajagopal "Finite element reliability analysis of reinforced retaining walls" Geomechanics and Geoengineering, 2010, 5, 3, 187-197

Kalehiwot Nega Manahiloh, Mohammad Motalleb Nejad, Mohammad Sadegh Momeni "Optimization of Design Parameters and Cost of Geosynthetic – Reinforced Earth Walls Using Harmony Search Algorithm", Int. J. of Geosynth. and Ground Eng, 2015, 1 – 15

Maintenance Management of Rolling Stock for Dependability Optimalization

Author: Ing. Martin ELSTNER

Doctoral study programme:
P3710 Technique and Technology in Transport and Communications

Field of study:
3706V005 Transport Means and Infrastructure

Supervisor:

Prof. Ing. Jaroslav Menčík, CSc.

Supervisor specialist:

--

Doctoral thesis has arisen at the supervising:

Department of Mechanics, Materials and Machine Parts

ABSTRACT

This self-summary describes the dissertation, which focuses on the collection and analysis of data to evaluate the dependability of passenger transport railway vehicles. The starting point for its composition is customer expectations regarding railway transport dependability. The research involved in the analysis showed that the significant indicators are transportation accuracy and adherence to train unit order. Basic descriptions of the methods of analysing the relation of these indicators to vehicle dependability are presented here. The results of the performed research can be applied to the proposals for alterations of information systems used by carriers and subjects responsible for maintenance. The application of the described insights in the area of data collection and evaluation can result in acquiring the tools for improving the railway vehicle maintenance process to achieve the corresponding degree of their dependability.

1. The Current Situation in the Study Subject

The railway transportation system in the Czech Republic territory has been going through several changes during the recent years. Consequently, a major impact has the transport policy of the European Union [1] , which enforces a unified European market for the railway transportation of both cargo and personnel. Nowadays there are directives in place which decree the liberalisation of the interstate railway transportation of personnel. Starting in 2034 at the latest, railway transportation is supposed to be fully provided through public market competitions. The attempt to unify the security levels within the entire European Union is a second aspect of the efforts towards a unified railway market and transport infrastructure.

Therefore of the utmost importance to carriers are the attributes of the rolling stocks, which can be offered to their customers (respectively directly to the passengers, in the case of non-subsidiary transport routes).

As a general rule, the competitive environment increases the push towards increasing the internal process performance and the demand for the quality of the offered product. Transportation time is a decisive factor for most passengers and customers in public transport [2].

1.1 Dependability Standardisation

The latest edition of the International Electrotechnical Commission came into effect in 2015 [3]. The definitions in this document are further adopted by other norms. For the temporal attributes of the quality of the given object, the unified term dependability is used, which is why the dependability of rolling stocks is of crucial importance regarding the quality of railway transportation as perceived by the customers.

In general, the dependability of a given object can be either inherent or operational. Inherent dependability is the result of the quality of the project and vehicle manufacture and it does not change over time. Operational dependability is partially influenced by the magnitude of inherent dependability, although it is dependent on a large number of other factors, which can be influenced mainly by maintenance and its provision.

In the railway industry, the EN 50126 norm (first issued in 1998) can be considered as the first international norm regarding the dependability on our territory. For vehicles of different modes of transport, there have been branch norms for quality and dependability in place for about 50 years already. As stated by Michal Vintr, in the railway industry, dependability is understood as something slightly different than in other industrial branches[4].

The prevailing model in passenger railway transportation in the Czech Republic is the following - the railway carrier owns the vehicles and directly provides the basic maintenance through their own employees, a higher degree of maintenance is then provided by external suppliers in some cases. Until recently, the carriers have not been required to track and evaluate the dependability of rolling stocks through standardised indicators and attributes, thus the importance of the standardised indicators has been growing over the recent past years. Due to the global changes regarding the field of company management, the model of Integrated Management System has been growing in popularity since standardised indicators have a much larger importance within this model. The regulatory decrees concerning safety now determine new requirements for the evaluation of safety in cases of alterations and modifications of vehicles already approved for operation. The vehicle construction alteration approval process is more rigorous and it can be assumed that with the employment of standardised indicators, the implementation of the required construction alterations can be markedly less difficult.

1.2 The Changes in the Management of the České Dráhy, a.s. Company

The České dráhy, a.s. (ČD) company has provided the data sources necessary for the composition of the dissertation. The research objective which has been reached using this data has thus been influenced by the current environment in the ČD company.

The maintenance of rolling stocks is directed by the internal V25 norm within the ČD company. The current issue of this norm is in effect since 2000. It sets down the dependability requirements only in a general manner and it does not determine any specific indicators through which the vehicle dependability would be systematically evaluated.

In July 2018, the original ČD management units have been abolished, i.e. the Rolling stock depots, which provided the operation and maintenance of the rolling stocks in a complex manner. The management changes in the ČD company resulted in the management units ensuring the operation of vehicles and the Regional maintenance centres (facilitating the management and maintenance of rolling stocks) to be expressly separated.

A new reinvented edition of the V25 norm is currently in preparation, which is supposed to not only take into account the inter-management alterations in vehicle maintenance but also to fulfil some of the legislative requirements regarding the provision of maintenance including all of the required documentation.

Although general standards and norms for dependability have already existed in the past, railway carriers have thus far not been required to evaluate vehicle dependability directly through the indicators gathered from the data regarding operation and maintenance.

1.3 Vehicle Management and Maintenance Information Systems

Following the technological advances, the requirements for the usage and evaluation of data and information are also increasing, which is concurrently a direct requirement of the quality management norms.

The Enterprise Asset Management (EAM) information systems are used to facilitate the maintenance and management of technical devices.

Related to the „Industry 4.0“ initiative, the integration and factual interoperability of information between individual systems and devices is taking place, the devices communicate with each other without any human involvement, and thus, the Internet of Things (IoT) phenomenon emerges. The coming of Industry 4.0 is associated with alterations to the maintenance of devices by some authors. With the term "preventive maintenance 4.0" they are referring to the maintenance strategy, which employs an extensive data and information analysis to direct the maintenance interventions, the data is gathered from the continuous data flow coming from the sensors of the maintained objects and the environment in which they operate.

The current EAM system inventors are attempting to integrate these resources directly into their products, and concurrently they create modules which adhere to the specific requirements for the management and maintenance of devices in the given industrial branch. All of the foremost EAM system invention enterprises provide extensions specifically for the management and maintenance of transportation vehicles, respectively specifically for railway vehicles, while at the same time providing the IoT functionality and other technologies. Thus, a single system can integrate the management and maintenance of rolling stocks with the workplace safety during maintenance and qualification plans of the maintenance personnel today.

1.4 Working with the Vehicle Maintenance Data

The Current Situation at ČD

The SAP company information system is integrated within the ČD environment. The Plant Maintenance module has been implemented in 2005. Currently, only the information about the daily mileage in kilometers is automatically loaded into the module, all of the other data (operation hours of certain combustion engines, the data gathered by the measurements intended for vehicle technical inspection etc.) is entered into the system manually. Even the contracts for vehicle maintenance and completed work reports are entered manually. The information system primarily serves the purpose of tracking the company finances and keeping records of the documents required by the legislative, including some of the values gathered by the measurements intended for vehicle technical inspection.

The ČD is preparing the upgrade of the system database to a new technology, the SAP HANA. This technology will make it possible to process large volumes of data and to immediately analyse it, thus in the future it will be possible to use new technologies from the data mining field concerning the technical condition of vehicles and their analysis. These tasks are currently performed by maintenance engineers separately from a unified information system.

Data Collection and Evaluation Abroad

The degree of evaluation and collection of data regarding the dependability of rolling stocks differs a lot abroad, one example in the field of transport vehicles is that the European Commission decreed the "holders of transport vehicles" to uphold several duties ensuring safety. Based on this decree Poland has implemented the methodology which implements the evaluation of dependability attributes stated in the 50126 European norm. This methodology is described in detail by the collective of authors led by professor Sitarz [5].

Several foreign enterprises, which operate with rolling stocks and which the author was able to gather the necessary information about, evaluate availability based on the tracking of the time intervals needed for maintenance and time periods over which the vehicles can fulfil the desired transportation functions. Further attributes, such as reliability, maintainability or maintenance support performance, are however not tracked by them. Furthermore, the enterprises do not track the causes of failures (which cause train delays) in much detail, neither do they track the reliability or maintenance support performance.

The degree of tracking and evaluation of partial attributes of dependability, the record keeping and evaluation of causes which diminish it, are seemingly all dependent on the size of the company and its resources regarding the ability to afford the corresponding information systems.

Large enterprises employ advanced systems which transfer the measured diagnostic values directly into EAM systems, in their vehicle diagnostics. The Mainnovation and PwC companies have performed a research effort aimed at the application of the Preventive maintenance 4.0 technology and the results show the companies in the railway industrial branch in Germany, Belgium and Netherlands are at the forefront in terms of implementing these new technologies [6].

2. Dissertation Objectives

Due to the changes in the market environment, the main motive behind the determination of the dissertation objective was the relation between the customer expectations and the conduction of rolling stock maintenance, and thus the formulation of the dissertation objectives and the procedures of the conducted research can be characterised with the following formula:

Customer expectations → QUALITY → DEPENDABILITY → MAINTENANCE of rolling stocks.

The first partial objective of the composed dissertation is thus to identify the customer expectations and to describe their requirements regarding the quality and dependability of rolling stocks. Processing this methodology was the starting point for further stages of research.

2.1 Evaluation of Vehicle Dependability Based on the Available Data

Through the fulfilment of the research objective (to describe customer requirements) were identified the primary attributes based on which the contractors of public railway transport evaluate its quality and dependability. Thus, the expected dependability of rolling stocks is de facto also determined.

The next objective of the dissertation was to create the indicators for the evaluation of vehicle dependability, which use routinely collected data by the carrier (ČD) and through which the degree of attribute fulfilment (which is of customer interest) can be periodically tracked. The basic requirement for the data usable for fulfiling this objective is its credibility.

2.2 Using Dependability Data to Manage Vehicle Maintenance

The indicators which were created based on the previous objective directly reflect the customer expectations through reliable data, however, they do not necessarily lead towards the determination of causes preventing the increase of vehicle dependability, and thus they cannot contribute to the changes in vehicle maintenance and the overall increase of the degree of railway transport quality.

Therefore, another objective of the dissertation was to determine the usable data structures and to propose indicators which can serve the maintenance managers and engineers in deciding for measures and changes in vehicle maintenance. The credibility of data necessary for fulfiling this objective is however no longer guaranteed. An important step in this stage of research was to verify whether there are suitable data fields in the information systems, which would be usable after changing the data collection methodology along with certain other alterations, and the bridging of the inertial systems.

Determining the methodology which could be used to evaluate some of the dependability attributes from an operationally-economic perspective, was a specific objective in this stage of research.

3. Processing Methods and Manner of Solution

To perform a marketing research among the passengers, which could describe their expectations in transportation quality and dependability, would be above the scope of the dissertation - the identification of customer expectations has been performed in the form of research of the contracts between public transportation personnel clients and the carriers. Since the clients are either self-regulatory bodies or state authorities, and transportation for public benefit is financed by public budgets, thus also the contracts facilitating such transportation are publicly available. In total, 5 contracts and 1 transportation provision supply competition documentation have been analysed.

3.1 Train Delay and Kilometre Mileage Data Analysis

There are three perspectives from which transport clients evaluate vehicle dependability from:

- train delays,
- adhering to the planned ordering of train units (adhering to planned quality norms for train units),
- the dependability of onboard devices in train units.

The third perspective employs evaluation using spot checks; however, the data regarding them was not available to be processed in the dissertation.

Train Delays

Investigations into train delays within the ČD environment used to exist in the form of dispatcher orders and admonitions. To make the routine analysis of the data from these documents possible, the dissertation author created his own software using the Visual Basic programming language functionality in the Microsoft Word software - the data collection was standardised using this custom software. Based on this the author created his own methodology for data collection and train delay evaluation. The train delay data research method was the conduction of a range of analyses which differ in their purpose and usage of specific values, which have been gathered for the purpose of train delay evaluation.

The Evaluation of Vehicle Deployment Based on Kilometre Mileage

It is not possible to obtain data that would be immediately usable for the evaluation of the adherence to the planned ordering of train units from the current information systems used for vehicle maintenance - this is caused by the absence of an information link between the operation and maintenance systems. One of the credible quantitative data sources regarding vehicle operation is their mileage, which is entered into the system daily.

For the evaluation of vehicle dependability based on kilometre mileage, the comparison of the statistic files representing different vehicles or vehicle groups is included in the dissertation. For such comparisons, "box plots" can be used for our advantage.

The method of comparison between the empirical mileage of vehicle fleets designated for the given transport route and the created theoretical operation model is included in the dissertation for the purpose of periodical evaluation of the adherence to the deployment of vehicles in trains. From this comparison of daily values, time series have been prepared. As one out of the available methods for their analysis, the application of the Box-Jenkins methodology "ARIMA models“ is included in the dissertation.

Then, from their application coupled with the analysis of the time series, several conclusions can be reached regarding the fulfilment of the anticipated operation concept at the given route and the actual operation security attained by the given vehicle groups.

3.2 Investigations of Data Structures for Dependability Management

Due to the fact that from the evaluation of kilometre mileage no conclusions can be drawn within the ČD environment regarding the causes of operation failures for specific vehicles, it is necessary to specify other indicators for the management of maintenance and de facto also the dependability of vehicles. In order to create the possibility of determining the causes of the decrease in the degree of vehicle availability, it is appropriate to evaluate the following attributes - reliability, maintainability and maintenance support performance.

The usage of standardised indicators for dependability evaluation carries many advantages, however, for them to be applied, it is necessary to identify the individual time periods and intervals in which the rolling stock can find itself in.

As a part of composing the dissertation, the time intervals in which a given rolling stock can find itself in over the duration of its operational and maintenance life cycle have been identified. They have been identified through the general period description (stated in [3]), for some of these intervals the

description of their current records in the ČD environment is included in the attachment of the dissertation.

For the purposes of analysing the usability of the data which has been determined by the previous study, we have merged the data from the databases: Operation performance data archive (using the PARIS task) and the SAP Plant Maintenance module information system.

The data usability analysis itself was conducted according to an unified methodology through experiments. The experiment has been evaluated as successful if for the randomly chosen attributes, Weibull distribution parameters have been found that would not necessitate the refusal of the data distribution approximation hypothesis based on a $\chi 2$ Pearson's chi-squared test. 8 experiments using different statistical files are presented in the dissertation, the files are mutually related and they have been created using the maintenance and operation data regarding vehicles designated for specific transport routes in both regional and long-distance transport.

To demonstrate the importance of tracking the time intervals, the dissertation includes the application of the multivariate random variable. It is possible to determine the need for a backup vehicle using a random attribute determined by the previous step using the method published in [7] with minor alterations.

4. Achieved Results

The contract research shows that the expectations of the majority of transport clients regarding vehicle dependability can be described through two main attributes: accuracy indicator and adherence to the ordering plan (Figuere 1).

The accuracy indicator is a form of a certain expression of the relation of train delays to the total ordered transport performance. The threshold value for train delays which the clients are normally willing to tolerate is approximately between 5 to 10 minutes, and the threshold value for delays in case of which the clients are no longer willing to compensate for the train operation expenses is approximately between 30 to 60 minutes.

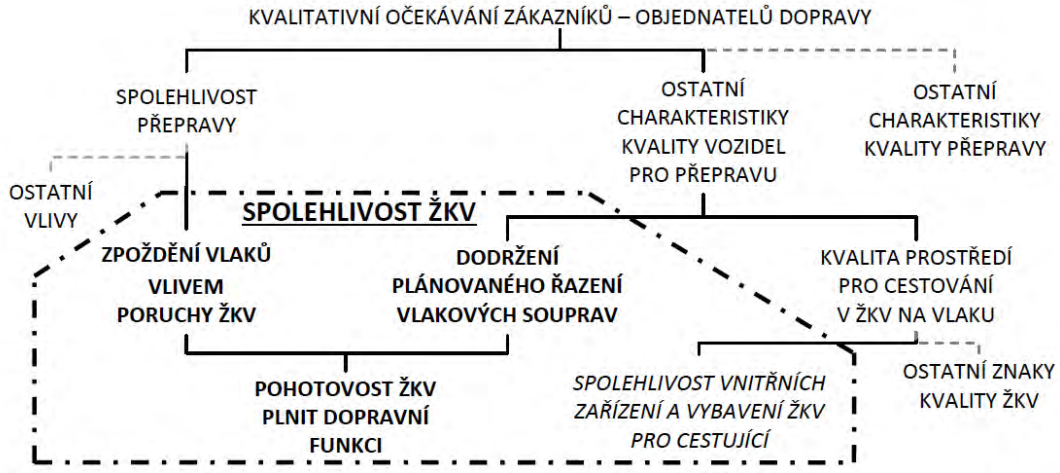

Figure 1. Dependence of the public transport customers' expectations and the dependability of rolling stock

The indicator of the adherence to the ordering plan is an expression of the relation between the number of trains which are formed by planned vehicles, to the amount of all ordered transport performances. For clients, the acceptable value of this attribute is approximately between 90 to 98 %.

4.1 The Possibilities Regarding Train Delay Analysis

As a part of the research necessary for the composition of the dissertation, a new comprehensive methodology for collecting data regarding train delays has been employed. The data which was successfully gathered over the duration of the application of this methodology can be processed into analyses and indicators, which can then be used to identify the real causes of vehicle malfunctions that cause the delays. An example of the analysis is depicted in Figure 2.

To achieve a blanket application of the stated methodology, it is appropriate to integrate the information and to minimise manual data entry - a proposal for the integration of information through the linking of several data sources is described in the dissertation.

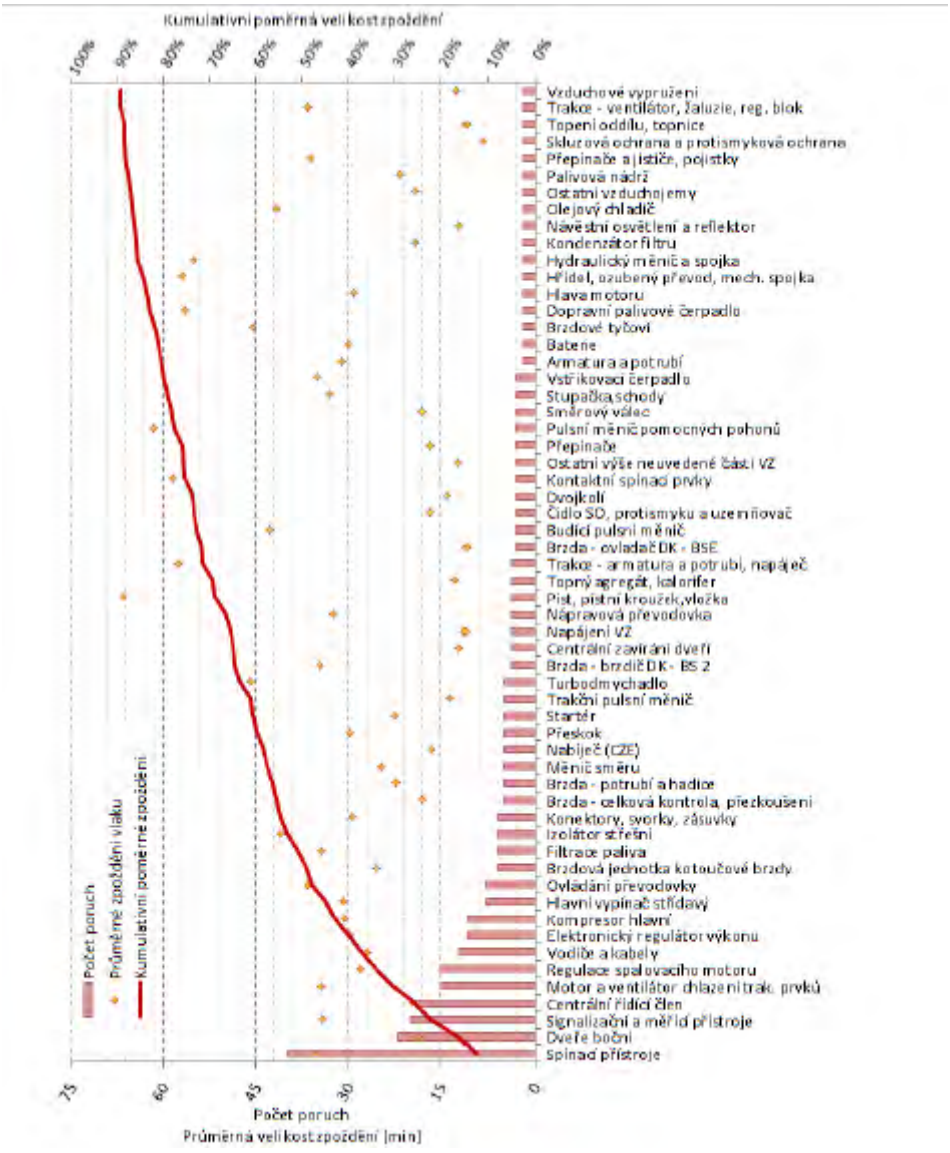

Figure 2. Pareto analysis of the causes of train delays due to vehicle failure

4.2 The Evaluation of Rolling Stock Availability

Even though no exact statements regarding the standard dependability attributes can be found in the contracts between the clients and the carriers, it is clear that one of the dominant vehicle attributes in relation to the customers is its availability.

The dissertation includes a description of the indirect evaluation of the degree of availability of a vehicle fleet using the kilometre mileage data. With the aid of the comparison between empirical values and the planned operation theoretical model, it is possible to evaluate the degree of customer

expectation fulfilment at specific transport routes. In the ČD environment, an advantage of the described method is that it is not necessary to collect new data, or more specifically, to alter the methodology for collecting the used data. However, its disadvantage is the limited ability to identify the causes of diminishing availability of specific vehicles, yet the basic information about the development of the vehicle group availability can be gathered using the method. (See Figure 3.)

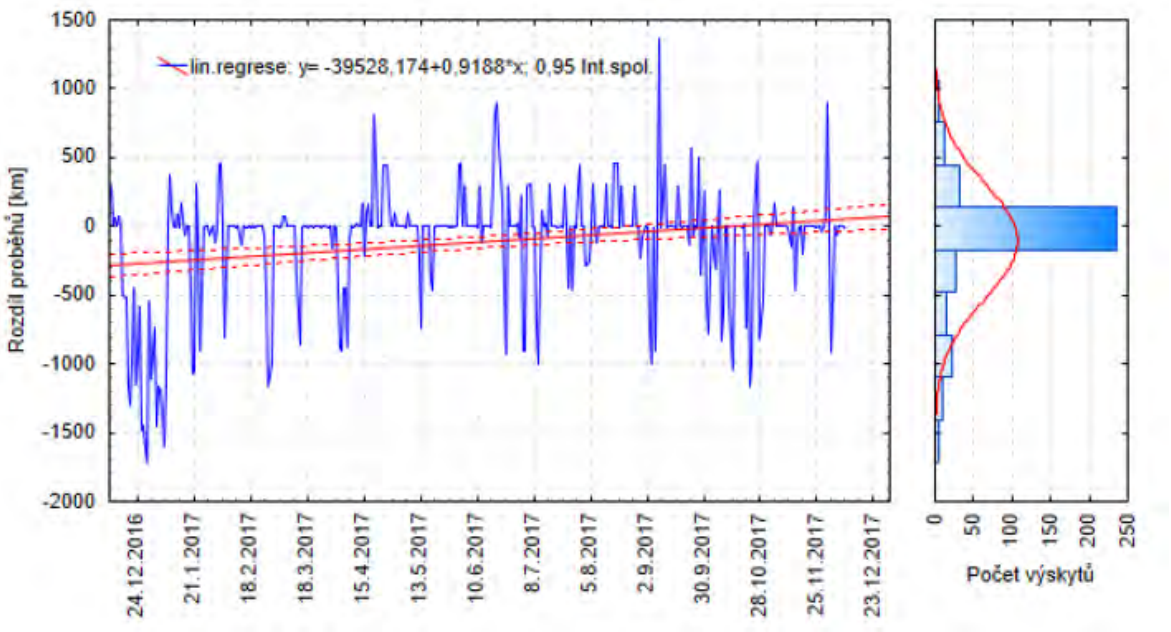

Figure 3. Time series of differences in empirical and planned runs of selected fleets of vehicles

Vehicle availability is dependent on attributes which need to be tracked and evaluated to enable the identification of causes which decrease vehicle availability [3]. An appropriate data source has been identified for maintainability and partially maintenance support performance through the research of current data structures, and the random attributes determined by this data can be approximated through known distribution. Thus, the result of this part of the research is the conclusion that current data structures provide the data appropriate for vehicle dependability evaluation using standardised indicators. The partial results are the conclusions drawn from the evaluation of individual attempts at approximating various random attributes. The results show that the corresponding evaluation of dependability attributes requires the analysis of data, which is specifically collected for the dependability evaluation, among other reasons.

The Operationally-Economic Perspective

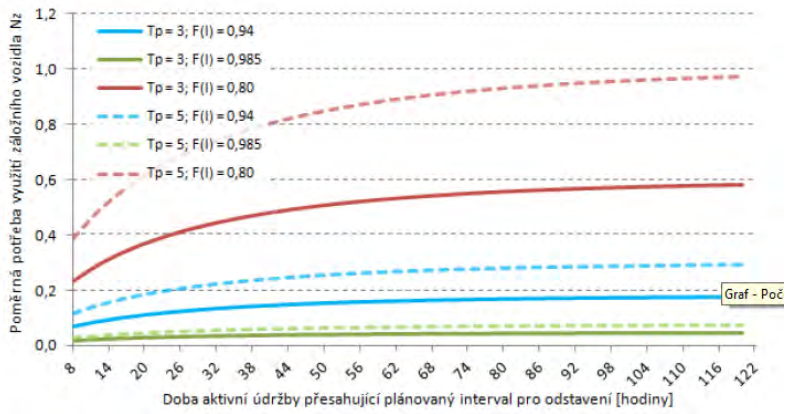

Figure 4. Need for backup vehicle depending on the maintenance time that exceeds the scheduled interval by a random vector

A partial result of the dissertation is the verification of the applicability of the multivariate random variable for determining the need for a backup vehicle. It is then possible to quantify the degree of need for a backup vehicle for various degrees of maintainability and availability (See Figure 4.). The method can generally be applied to random variables without any regard for their physical dimension, and it can also be beneficially applied to smaller vehicle fleets designated only for selected transport routes.

The possibility of investigating the impact of maintenance support performance and maintainability on the need for further backup vehicles can be significant in the consideration regarding the provision of alteration of individual vehicle dependability data collection systems.

5. Dissertation Contributions

The basic requirement for quality management systems is customer orientation. The dissertation includes a new description of the relation between customer expectations and vehicle dependability - it is apparent that individual transport clients have different requirements. Yet, based on the analysed public contracts, it is possible to determine two primary attributes which involve the total vehicle dependability, or more precisely the availability in fulfiling the desired transport role.

5.1 Using the Train Delay Data

For it to be possible to conduct a more detailed analysis of the causes behind train delays, the dissertation author created his own software for train delay data collection. Then, based on this data, he proposed a methodology for its evaluation which enables the analysis of the possible causes behind malfunctions and to consider measures for vehicle maintenance which would minimise the occurrence of train delays, thus generally it is possible to fulfil the requirements for quality management systems regarding the improvement of processes based on data evaluation thanks to the methodology and its application proposed by the author.

The dissertation includes several data analyses and examples of train delay studies, some of which can be generalised and applied to any given carrier. Some of them can also be applied for ČD when an appropriate data structure is used. The published examples are most often only general descriptions, but they can provide valuable information for workers involved in vehicle maintenance and operation when applied to a given vehicle group.

A description of the proposal of the integration of information from various information systems currently used in ČD is included in the dissertation. The advantage of such integration would be the routine collection of data regarding the occurrence of train delays, which is only slightly intensive in terms of manual data entry by the workers at the given units. The implementation of the described proposal would enable the creation of an objective summary of the train delay issue, based on which the considerations regarding the alterations needed to minimise the negative impact on customers could take place.

5.2 Dependability Attributes and their Evaluation

The dissertation includes a description of a method of indirect evaluation of availability based on the data regarding the daily vehicle mileage. Since there is no link between information systems which would enable the tracking of the functional conditions of vehicles, as well as their transport performance, in the ČD environment, the usage of kilometre mileage analyses is one of the few options in terms of quantitative evaluation of the dependability degree.

The method of comparison between the real mileage of vehicle fleets and the vehicle fleet theoretical operation model can be used without any large requirements for information system alterations.

Since the causes behind the decrease of dependability in specific vehicles cannot be determined using the methodology of fleet dependability degree evaluation, the author also focused on the options regarding the evaluation of availability and other standard vehicle attributes. For the purpose of their tracking, the current options regarding the usage of data in the ČD environment are published in the dissertation. Furthermore, a new delimitation of time intervals according to the responsibility of vehicle operation and maintenance units is also published in the dissertation. This delimitation is a key factor in further analyses of risks attached to vehicle dependability, precisely in the manner specified with the current quality management systems norm.

The dissertation describes the research of the applicability of the indicators for maintainability and maintenance support performance, based on which it is possible to acquire a real perspective on the current condition of the data in the ČD environment. Due to the developments in the areas of legislation and railway transport market, it can be presumed that in the future it will be necessary to track and evaluate the dependability using the standardised comparable attributes. The published research of data evaluation for such dependability attributes shows that the quality of the data has crucial influence over the results. A key factor for the researched issue is also the collection of data with the purpose of dependability evaluation. A large contribution of the conducted research is the gathered insight regarding the significance of the collection of specific data, which is credible and usable for the evaluation of dependability in railway transportation. This applies generally for all carriers and subjects operating in the passenger rail transport industry.

The dissertation includes a description of a method for determining the need for a backup vehicle using the multivariate random variable. This method can be used to appropriately interpret the impact of the alteration of attributes such as availability, maintainability or maintenance support performance, on the operationally-economic planning and other internal processes of carriers. Its inclusion in the dissertation has primarily the purpose of demonstrating the significance of dependability evaluation in maintenance management. The basic requirement for the procedural access of the organisation includes the application of the PLAN-DO-CHECK-ACT cycle to attain process improvement. If the degree of dependability required by the customer is to be safely attained, it is necessary to also continually improve the railway vehicle maintenance and management process. Without the information entered in the CHECK phase, the systemic increase in vehicle dependability cannot be ensured.

In the present day, a large number of technically-technologic assets (e.g. IoT, Preventive maintenance 4.0) are available, which enable the collection and analysis of significantly larger volumes of data, than there were in the recent past years. The usage and implementation of these assets can currently (and in the future) provide the carriers with significant advantages compared to their competitors. The author of this publication attempted to contribute to the general insights regarding the facts about which data is worthy to be collected and evaluated to attain the improvement of railway vehicle dependability and maintenance

REFERENCES

EVROPSKÁ KOMISE. Politiky Evropské unie: Doprava: Spojení pro evropské občany i podniky. 1. Lucemburk: Úřad pro publikace Evropské unie, 2014, 20 s. ISBN 978-92-79-42773-2. DOI: 10.2775/12584. Dostupné také z: http://europa.eu/pol/pdf/flipbook/cs/transport_cs.pdf

BRONS, Martijn a Piet RIETVELD. BETROUWBAARHEID EN KLANTTEVREDENHEID IN DE OV-KETEN: EEN STATISTISCHE ANALYSE: Internal research report for the Transumo project

Betrouwbaarheid van transportketens [online]. Amsterdam: Vrije Universiteit Amsterdam, 2007, 104 s. [cit. 2018-08-04]. Dostupné z: http://www.transumofootprint.nl/upload/documents/03%20Projecten/Betrouwbaarheid%20Transportketens/03%20Output/05%20Rapporten,%20notities,%20verslagen/Rapport%20Betrouwbaarheid%20en%20klanttevredenheid%20OV-keten.pdf

ČSN IEC 60050-192. Mezinárodní elektrotechnický slovník - Část 192: Spolehlivost. Katalogové č. 98237. Praha: Úřad pro technickou normalizaci, metrologii a státní zkušebnictví, 2016.

VINTR, Michal. Systém managementu spolehlivosti v železničním průmyslu. In: Management spolehlivosti v průmyslových aplikacích: Materiály z 55. semináře odborné skupiny pro spolehlivost. 1. Brno: Česká společnost pro jakost, 2014, s. 11-20, 36 s. ISBN 978-80-7231-965-7.

SITARZ, Marek, Katarzyna CHRUZIK a Rafał WACHNIK. Aplication of Rams and FMEA Methods in Safety Management System of Railway Transport / ZASTOSOWANIE METOD RAMS I FMEA W SYSTEMACH ZARZĄDZANIA BEZPIECZEŃSTWEM W TRANSPORCIE KOLEJOWYM. In: Journal of KONBiN. Warszawa: Wydawnictwo Instytutu Technicznego Wojsk Lotniczych, 2012, 24(1), s. 149-160. DOI: 10.2478/jok-2013-0061. ISSN 2083-4608. Dostupné také z: http://content.sciendo.com/view/journals/jok/24/1/article-p149.xml

GARLO-MELKAS, Nina. Predict the Unpredictable with Predictive maintenance 4.0. Maintworld: maintenance & asset management. Helsinki: Omnipress Oy, 2017, (4), 28-30, 52 s. ISSN 1798-7024.

FAMFULÍK, Jan, Jana MÍKOVÁ a Rudolf KRZYŽANEK. Mission completion probability of cycle rate system. In: BRIŠ, Radim, ed., C.Guedes SOAREL, ed. a Sebastián MARTORELL, ed. Reliability, Risk and Safety: Theory and Appliations. 1. London: Taylor & Francis Group, 2010, s. 1603-1606. ISBN 978-0-415-55509-8.

Author's publications

[I] ELSTNER, Martin a Jaroslav MENČÍK. Reliability evaluation of vehicles after modernization. In: Deterioration, Dependability, Diagnostics. 1. Brno: Univerzita Obrany, 2012, s. 147-154. ISBN 978-80-7231-886-5.

[II] ELSTNER, Martin. Změny údržby po modernizaci kolejového vozidla. In: ÚDRŽBA 2012: sborník mezinárodní odborné konference. 1. Liblice: Česká společnost pro údržbu, 2012, s. 176-182, 210 s. ISBN 978-80-213-2312-4.

[III] ELSTNER, Martin. Provoz a údržba vozidel po modernizaci. In: Současné problémy v kolejových vozidlech: XXI. konference s mezinárodní účastí. Vydání I. Česká Třebová: Univerzita Pardubice, 2013, s. 169-176, 268 s. ISBN 978-80-7395-676-9.

[IV] ELSTNER, Martin. Vliv modernizace vozidel na jejich údržbu. In: ÚDRŽBA 2013: Sborník mezinárodní odborné konference. 1. Liblice: Česká společnost pro údržbu, 2013, s. 193-200. ISBN 978-80-213-2410-7.

[V] ELSTNER, Martin. Ukazatele změn kvality po modernizaci kolejových vozidel. In: KVALITA 2014: 23. ročník konference s mezinárodní účastí. 1. Ostrava: DTO CZ, s.r.o., 2014, s. 45-53. ISBN 978-80-02-02532-0.

[VI] ELSTNER, Martin and Alois KOTRBA. Zpoždění vlaku jako zdroj informací pro řízení kvality. In: Súčasné problémy v koľajových vozidlách: XX. Medzinárodná konferencia - Prorail 2015. Prvé vyd. Žilina: Vedeckotechnická spoločnosť při Žilinskej univerzite v Žilině, 2015, s. 109-116. ISBN 978-80-89276-48-6.

[VII] ELSTNER, Martin. Řízení kvality pomocí údajů o zpoždění vlaku. In: KVALITA 2016: 25. ročník konference s mezinárodní účastí. 1. Ostrava: DTO CZ, s.r.o., 2016, s. 7. ISBN 978-80-02-02660-0.

[VIII] ELSTNER, Martin. Současné možnosti kvalitativních ukazatelů pro údržbu kolejových vozidel. In: ÚDRŽBA 2016: sborník mezinárodní odborné konference. 1. Liblice: Česká společnost pro údržbu, 2016, s. 176-182, 196 s. ISBN 978-80-213-2668-2.

[IX] ELSTNER, Martin. Sledování a hodnocení spolehlivosti kolejových vozidel v osobní železniční dopravě. In: Současné problémy v kolejových vozidlech 2017: XXIII. konference s mezinárodní účastí, sborník příspěvků. Vydání 1. Česká Třebová: Univerzita Pardubice, Dopravní fakulta Jana Pernera, 2017, s. 59-66, 460 s. ISBN 978-80-7560-085-1.

[X] KOTRBA, Alois, Petr FIALA a Martin ELSTNER. Současný provoz železničních osobních vozů v Depu kolejových vozidel Brno. Nová železniční trendy, doprava - telematika: Recenzovaný neimpaktovaný časopis. Brno: KMP Consult, a.s., 2012, 20(5), 13-17. ISSN 1210 – 3942.

Specifics of the Rail and Road Transport in Terms of Positive Externalities and Their Valuation Methods

Author: Ing. Jakub HAŠEK

Doctoral study programme:
P3710 Technique and Technology in Transport and Communications

Field of study:
3708V024 Technology and Management in Transport and Telecommunications

Supervisor:

doc. Ing. Ivo Drahotský, Ph.D.

Supervisor specialist:

Ing. Roman Hruška, Ph.D.

Doctoral thesis has arisen at the supervising:

Department of Transport Management, Marketing and Logistics

INTRODUCTION

This work is focused on the issue of external transport effects focusing on the positive externalities of transport and their complex analysis in context of economic evaluation of transport projects. Based on the analysis of the economic evaluation of negative externalities in transport and methods that are used to their evaluation, selected methods are used to evaluate the positive externalities in transport using case studies. Based on case studies, the road and rail specifics are interpreted and suitability of the selected methods for the evaluation of positive externalities in transport is assessed.

The first case study deals with the area of time savings valuation based on traffic-economic behavior of the population combined with the methods of willingness to pay and willingness to accept. Next case study examines the impact of the proximity of the transport infrastructure on the cost of apartments, where the hedonic price method is applied. This method most often determines how environmental factors are reflected in the market price of real estate. Next case study evaluates the benefits of the construction of transport infrastructure and its impact on changes in the business environment considering passenger road and rail transport. The latest case study looks at the benefits of improving the quality of public transport using Level-of-service rating method.

1. ANALYSIS OF THE CONTEMPORARY STATE IN THE FIELD OF THE THEME DISSERTATION

The term positive externality refers to a situation where one entity's business benefits another entity and does not have to bear the costs associated with it. From the economic point of view, positive externalities are market failures and allocation inefficiencies resulting from inaccurate ownership rights. State authorities can respond to these externalities by explicitly defining ownership rights or promoting internalization of externalities, as described by Hořejší et al. (2012).

As with rail transport, the development of road transport is linked to historical trend and development of the transport policy. At present, the greatest benefits of the road sector can generally be seen at these points (Zelený, 2007):

- door-to-door transport system,

- dense network of road infrastructure,

- high variability of means of transport,

- speed, operability and almost unlimited accessibility,

- adaptability to changes in demand,

- public transport systems in combination with rail transport,

- an irreplaceable role in multimodal transport for shorter distances.

On the other hand, the increase in popular road transport brings a number of problems to users, which are reflected in the negative cost-benefit analysis in the negative externalities. Geographically a demographically dense network of road infrastructure is often a criticized for its poor quality and neglected maintenance. In terms of positive externalities, the benefits of this mode of transport can be considered in the assessment of transport projects compared to the considered alternative modes, eg different travel speeds, availability of infrastructure and level and quality of service.

The specificities of rail transport come largely from the historical context of transport development. Tracks could lose importance over a decade, change purpose (eg, transformation of industry, strategic

military requirements), or completely disappear from the point of view of economic inefficiency. Therefore, the dense railway network can be perceived by one as positive and others as dearly maintained inefficient luxury. Zelený (2007) sees the largest benefits of the railway sector in the following points:

- very low accident rates and a rare incidence of emergencies,

- elevation profile of railway track is more energy-efficient than the elevation of roads,

- high transport capacity of trains, high load capacity of trucks,

- lower susceptibility of transport infrastructure to damage due to frequent inspections,

- less dependence on weather conditions,

- traffic safety through dispatcher control,

- fast forwarding (corridor lines),

- comfort of traveling high-end trains is comparable to air travel,

- lower environmental impact (electrical traction, converted to performance),

- an important role in multimodal transport in long-distance transport.

Prentice and Mazurek (2010) divide the hierarchical framework to classify the benefits of transport to direct benefits, conditional (or mitigating) benefits, incidental benefits and tertiary benefits. These benefits are presented with a verbal evaluation or subjectively ranked according to a particular criterion. The economic assessment of intangible benefits is usually based on the best estimate or the evaluator's experience, when the so called shadow price principle is applied. Rodrigue (2017) classifies the benefits of direct, indirect, and derived.

Valuation can be divided into a pricing approach according to Blum (2008), where the value of externality is defined by the corresponding price in the private market, which in most cases is related to the costs of repair or damage, a substitution approach where the external value is defined by the possibility of replacing the source, technology or farm, while preserving its original quality and attributes, a risk approach where the value of externality is defined by a discounted expected monetary value based on risk assessment and a utility approach where the value of externality is defined by willingness to pay to reduce negative effects.

Špalek (2005) sets out two basic ways of regulating externalities, namely public solutions that focus on bringing private costs associated with the production or consumption of a farm that negatively or positively externalize the cost of social private solutions that are related to the operation and functioning of the market.

Analysis of the issue of evaluation of positive externalities in the Czech Republic

In the Czech Republic Ing. Mgr. Hana Brůhová-Foltýnová, Ph.D deals with issues of externalities and their influence on the environment. She focuses mainly on the environmental issues of negative externalities and their internalization, both in their own publications and in publications projects of the Ministry of Transport. The problem of positive externalities is briefly discussed in "Transport and Society" by Brůhová-Foltýnová (2009). The field of external transport effects and their quantification is also discussed by Mgr. Vojtěch Máca, Ph.D. (2013) and Ing. Jan Melichar, Ph.D. (2005, 2013), both currently working for Center for Environmental Issues of Charles University.

In 2016, the Central Committee of the Ministry of Transport approved the material "Prováděcí pokyny k Metodice pro hodnocení ekonomické efektivnosti a ex-post posuzování nákladů a výnosů projektů železniční infrastruktury, pozemních komunikací a dopravně významných vodních cest", which is a binding document for assessing the economic efficiency of projects that are co - financed by OPD funds in the 2014-2020 programming period, and projects exclusively financed by SFDI fund and projects by private non-state investors co-financed from their own resources. On 15 November 2017, the "Prováděcí pokyny pro hodnocení efektivnosti projektů dopravní infrastruktury" came into force, the integral part of which is the "Rezortní metodika pro hodnocení ekonomické efektivnosti projektů dopravních staveb".

The evaluation of the economic efficiency of projects in the Czech Republic is based on the HDM-4, which has been developed since 1993 by the University of Birmingham, and its support and funding, including the World Bank, the British Ministry for Foreign Cooperation and other institutions. HDM-4 compares different investment options.

Efficiency assessment of road and motorway constructions is carried out on the basis of CBA analysis, using net present value (NPV), internal rate of return (IRR) and return on investment costs (BCR).

Current status analysis in abroad

Goodwin and Persson (2001) summarize the most appropriate approaches in the evaluation of positive externalities in “Assessing the Benefits of Transport”, but it is only a certain methodological guide, which also contains suggestions for expert discussion.

The issue of transport benefits is one of the main field area of the founder of the independent Canadian organization Victoria Transport Policy Institute, Mr Todd Litman, who is often quoted in thematic studies. For example Litman (2001) is the author of the publication "Evaluating Public Transit Benefits and Costs , Best Practices Guide".

An interesting publication is also the "Guidebook for Assessing the Social and Economic Effects of Transportation Projects" by Forskenbrock and Weisbrode (2001), which provides a handbook for US authorities dealing with the social and economic impacts of transport projects on surrounding communities.

The assessment of impacts on land prices depends on the point of view. This is demonstrated, for example, by the studies of Iacon and Levinson (2011) or Cao and Hough (2007), who present different findings and results in this field area.

In terms of use Cost- Benefit Analysis, according to OECD / ITF (2008) the Cost- Benefit Analysis - in terms of a comprehensive economic evaluation of public benefit projects – is not used so much to evaluate infrastructure-investment infrastructure projects. And if CBA assessment methods are used, they are used to evaluate smaller projects in road transport and mostly in rural areas. In these cases, the benefits of, for example, increased traffic safety are higher than travel time savings. And since funding is dependent on the nature of the project (laying new surfaces, increasing capacity, increasing safety), the focus is mainly on the cost effectiveness. The OECD / ITF publication (2008) further notes that Cost- Benefit Analysis is systematically applied in northern European countries, although they are mostly the only input of the decision-making process. In the UK, the CBA is used systematically, which together with the document the environmental impact of the project and the multi-criteria analysis presented to those who ultimately decide on the future of the project. At the same time, however, factors that are difficult to evaluate, are taken into account.

Some experts also point to the diversity of short-term and long-term objectives, underlining that policy decisions are often motivated only by short-term goals. According to Hallsworth et al. (1998) or Seidenglanz (2006) it is just a typical example of a sector in which attempts at political regulation to create unintended consequences are very vulnerable.

The dissertation thesis presents several case studies from abroad dealing with the appreciation of benefits, respectively positive externalities in transport.

Model Example 1 - Transit Improvement Economic Evaluation Model

Study "Benefit / Cost Analysis Of Converting A Lane For Bus Rapid Transit " from the National Academy of Sciences , Engineering , and Medicine (2009) outlines the costs and benefits of valuing transport projects in the USA, which addresses the allocation of one lane for public transport. This study provides relatively complete an idea of what benefits costs can generate transport projects focused primarily on road transport.

Model Example 2 - Benefits of Public Transport in Montreal

Study "Public Transit: A Powerful Engine For The Economic Development Of The Metropolitan Montreal Area " by Board of Trade of Metropolitan Montreal (2004) sought to quantify the benefits of public transport in Montreal, Canada. This study investigated the links between public transport, economic development and quality of life. The study also mentions a relatively strong relationship between rising urban public transport and increasing competitiveness and urban metropolitan agglomerations, as well as factors influencing the growing popularity of public transport.

Model example 3 - New railway line in the region

This study addresses the new railway line project, which would cost US $ 250 million, annual operating costs would be US $ 5 million, daily would attract 10 thousand new passengers, or equivalent would be 2.2 million rail journeys per year, half of which would was a substitute for automotive transport. Contrary to the rules used to assessing rail projects in the Czech Republic, the study also calculates a series of direct and indirect positive benefits that have the character of so-called wider economic benefits for the micro-region or larger territorial unit. Study of the high-speed rail project in Great Britain by The Department for Transport (2011) also includes wider economic benefits.

Model example 4 - CrossRail high-capacity rail

Crossrail is a high-capacity railroad project within the London agglomeration, characterized by a high frequency of connections. Materials by DfT (2011) and GVA (2017) report as the main benefits of the rail network decrease of congestions in London, creating reliable backbone connections, better access to investment opportunities and the generation of job opportunities.

Interesting is the interpretation of benefits that do not fall under the conventional assessment of Transport Infrastructure Projects (CBA). According to estimates, Crossrail should also raise the total cost of residential and commercial real estate near the Crossrail network. Residential object values should increase in central London by 25% and in suburban areas by 20%, as reported by the British Ministry of Transport (DfT , 2005).

The issue of positive externalities, or the benefits of transport, has not been widely resolved in EU legislation. Greater attention is therefore still being given to negative externalities, as harmonized conditions and a methodical procedure for the internalisation of external costs in EU (HEATCO) were published. The world's most widely used HDM-4 methodology in the world basically takes into account time valuation (passenger or cargo), savings from accident, noise and noise reduction emissions as benefit considerations.

The disadvantage of CBA is that it gives space to interest groups to manipulate inputs and outputs. Often, the relevance of inputs or the exclusion of important cost aspects is also questioned. Conversely, well-thought-out, meaningful and sustainable transport projects may come up with incomplete or incorrectly-designed analysis of the benefits of projects that might otherwise have a positive influence on the decision-making process.

2. AIMS OF THE DOCTORAL THESIS

There are a number of studies dealing with negative transport externality, but only a few studies available that deal with the economic evaluation of positive externalities in conditions of the Czech Republic. The question is how methods for evaluating negative externalities in transport can be used for valuation of positive externalities and what the areas of practical application of these methods are. The following objectives were set for the dissertation:

Synthesize knowledge related to the evaluation of negative external effects associated with transport and assess the possibilities of using these methods to evaluate positive externalities.

Create suggestions for using selected methods of evaluating negative externalities to evaluate positive externalities using case studies.

3. LIST OF USED METHODS

Here are the most common methods used for assessing transport externality. These methods mainly relate to measurement of negative transport externalities. There are a number of studies and materials dealing with the assessment of the negative impacts of transport such as CE DELFT (2008), INFRAS / IWW (2004), including later updates, ExternE (2005) or HEATCO (2006); on the contrary, only a limited number of studies or expert articles dealing with positive externalities.

Hedonic price model

This is one of the oldest approaches to determining the demand for non-market commodities. This method determines how much of the difference in property prices is due to a certain difference in the environmental properties of properties and how many people are willing to pay for improving environmental performance, Garrod and Willis (2000). In the case study presented in chapter 4.2., a hedonic pricing model is applied using correlation and regression analysis, such as Forrest et al. (1992), who in his study examined the influence of city railways on the property price in Manchester. Forrest et al. (1992) found the mildly negative influence of urban railways on the price of properties near them, which explains above all the increased noise burden, increased movement of the users around the station and frequent traffic congestion around the traffic junction. Haripriya (2014) states that the hedonic price method is very demanding in terms of input data. In order to estimate the hedonic price function for a particular market, it is necessary to have a large number of observations describing both sales prices and numerous property characteristics in a given market. The biggest advantage of this model is that it is based on real market observation. At the same time, however, it is assumed that respondents are fully aware not only of the actual noise burden, but also possible negative impacts in exposure to this noise load. This can often lead to distorted and unrealistic conclusions that differ from professional literature as well.

The travel cost method

This method is based on an expanded theory of consumer demand and is based on quantification of the environmental benefits of public goods or damages associated with the loss of these benefits, which are derived from travel costs. Just as the hedonic price method belongs to the methods of revealed preferences, as reported by Melichar (2005). The main idea is to determine the financial and time-

consuming nature of the visit to the recreational area. Analyzing how people respond to travel costs can be determined by awarding natural assets.

Random utility / discrete choice model

Špalek (2005) states that, unlike the travel cost method, random utility / discrete choice model to evaluate the properties of the sites under consideration. The principle consists in explaining the choice between two or more goods with variable levels of an attribute. This model can be applied as a superstructure in the case study presented in Chapter 4.1, which deals with time appraisal (WTP and WTA) depending on the mode of transport chosen for the given session based on the population's traffic-economic behavior.

Contingent valuation method (stated preference method)

According to Šauer (2007), it is a method of out-of-market valuation and valuation of natural goods, which by means of a questionnaire survey finds a hypothetical willingness to pay for an environmental item, a hypothetical willingness to accept compensation for damage. For a more detailed description of the application of the conditional assessment method, see Boyle (2003) or Melichar et al. (2008).

Willingness to pay (willingness-to-pay - WTP)

According to Kršková (2011) this method represents the maximum amount a subject is willing to pay to gain some benefit or, on the contrary, to avoid negative consequences. Blomquist (2003) criticizes the WTP model for being too much burdened by the budget options or limitations of the subject involved, ie it is directly dependent on the distribution of wealth in society. This leads to a relatively different WTP in countries that are relatively similar from other angles (for example, culturally or historically), as Kršková (2011) mentions.

Willingness to accept compensation (willingness To Accept - WTA)

The opposite of willingness to pay is the willingness to accept that Kršková (2011) defines as the minimum amount that the body is willing to accept to accept some unwanted or negative consequences. Kršková (2011) mentions the shortcomings of the WTA model in that when the subject decides only on the basis of how much he would accept, his valuation is too exaggerated, ie he will usually say more than the perceived value (benefit) of the farm. Both methods (WTP and WTA) are in the dissertation work was used in calculating the estimations of positive externalities of transport, especially in combination with method of preference.

Level-Of-Service

Level-of-service rating is a method used to assess the quality of transport and, unlike the above methods, Litman (2008) currently focuses on the evaluation of positive externalities, due to improved transport planning and decision-making based on a comprehensive quality assessment of the survey of the transport system. It was created to solve traffic flows, congestions and related traffic planning. Within the LOS ratings, the A (best) to F (worst) assesses travel conditions (use of the transport system) to identify problem areas and generally evaluate the quality of the examined transport system. The method of assessing the quality of the transport system using LOS ratings is applied in a case study to assess the change in the quality of urban transport in Pardubice city, presented in chapter 4.4.

Market price method

Špalek (2005) defines market price as a price that balances supply and demand in conditions of perfect competition. Distortions in the form of imperfect competition, incomplete use of resources, taxes, subsidies or externalities can be eliminated through adjustments to so-called shadow prices. This

method is used in the case study presented in Chapter 4.2. to investigate the impacts of the proximity of the transport infrastructure on property prices.

Scientific methods

The following scientific methods are used during the dissertation:

- analysis and synthesis ,
- deduction and induction ,
- case studies, system approach,
- multi-criteria analysis , Saaty's method,
- regression analysis and correlation,
- analysis of statistical data,
- questionnaire survey.

The description of the individual methods and the possibilities of their application can be found in relevant chapter of the dissertation.

4. PROBLEMS SOLVING

Four studies are presented in this chapter, which includes the application of selected valuation methods used for valuation of externalities.

Case study - Time savings valuation based on WTP and WTA

This chapter deals with application of the WTP and WTA methods. Application of both methods is presented on conditions of the Czech Republic. At the same time, data from questionnaire survey where a WTP method with dichotomical choice format was used for the purposes of this case study when respondents were asked whether they were willing to pay the price for the surveyed entity or not. It has always been a choice between road and rail transport, more precisely between the use of car and train on the submitted cases of four selected sessions.

Input data to technical-economic analysis of this case study are tariff conditions available for both road and rail transport, the current price of petrol and diesel, technical data about the consumption model car and valid timetables. Questionnaire survey was attended by 398 respondents from all 14 regions of the Czech Republic.

In the expert part of the questionnaire survey, certain questions were asked, of which the relevant ones are further analyzed in relevant chapter of the dissertation. To quantify the willingness to accept or willingness to pay, derived equations for the calculation of WTP and WTA are used for selected scenarios.

At sessions 1 (Trutnov - Pardubice), the narrow majority of respondents chooses the train transfer option over car. There is a saving of 110 CZK, but also increase the travel time by 40 minutes. The Preference Coefficient (Preference Weight) is 0.52.

Scenario: I'll pay less, I'll be there later.

WTAR1 = 1,43 CZK/min – the cost of higher travel time

Positive value is the financial cost of a freely chosen transport mode selection higher travel time for that session.

At session 2 (Prague - Pardubice), a clear majority chooses train. There is a saving of CZK 160 and also less travel time by 25 minutes. The cost paid for a motorway usage can hardly be recognized for selected session, so it has not been counted in. The preference coefficient is 0.82.

Scenario: I'll pay less, I'll be there earlier.

WTP R2 = -5.25 CZK / min - savings for less travel time

A negative value indicates cost saving while saving travel time at the session.

At session 3 (Liberec - Pardubice), three quarters of the respondents choose a passenger car option over train. There is time saving of 67 minutes, but also a cost increase of 100 CZK. The preference coefficient is 0.77.

Scenario: I'll pay more, I'll be there earlier.

WTP R3 = 1.15 CZK / min - cost saving time

On the considered session, the rail link is similar to that of the rail link from session 1, a monorail line of regional character with speed limitation a large number of railway stations and stops.

At session 4 (Pardubice - Ostrava) the clear majority of respondents choose the option of transport by train. There is a saving of 15 minutes and saving of 270 CZK. The preference coefficient is 0.82.

Scenario: I'll pay less, I'll be there earlier.

WTP R4 = -14.76 CZK / min - savings for less travel time

A negative value indicates cost savings while saving travel time for the session.

Since September 2018 discounts on fares were introduced, involving passengers from 6 to 18 years, students 18 to 26 years and passengers older than 65 years. This would, in a new questionnaire survey, influence the transport and economic behavior of passengers, in particular the age groups of public transport users concerned.

The resulting complete case study data, including the limiting conditions and the evaluation of the results, are presented in relevant chapter of the dissertation.

Case study - Influence of the proximity of transport infrastructure on property prices

Pardubice city study was selected for a case study investigating the impact of the proximity of the transport infrastructure (public transport stops) on the property price. Data source is real estate portal Reality.cz. The aim of the correlation analysis is to find out which of the of these variables affects the price of the property. The focus is on the proximity of public transport stops, namely three modes: urban public transport, rail and bus services. Software Statistica 12 was used for statistical analysis. Within this analysis, it is necessary to define a set of factors and the conditions under which the given method is applied to the model case of Pardubice city.

The subject of statistical analysis is to determine the strength and type of observed variables. Force and dependence (correlation) is expressed through various degrees of statistical dependence including correlation coefficients. The absolute value of the degree of statistical dependence should be in closed interval from zero to one.

After the first calculation step, the case of the undesirable multicollinearity between the train stop distance and the bus station occured. After the elimination of the variable "Distance to Bus" multi-collinearity does no longer occur.

As expected, a very strong dependence between the apartment's price and the size (living area) of the flat has been demonstrated. At the same time, the weak and negative dependence of the apartment price on the given sample was proved in relation to proximity to nearest urban transport stop and to the main railway station.

Regression model can be used to determine the equation, including the individual factors that affect the price of the apartment near to the transport infrastructure. The regression is thus:

cena bytu=629547,4+17060,9*vel.bytu-53,3*vzd.MHD-27,1*vzd.žel. (1)

where: vel.bytu surface area of the flat [m2]

vzd.MHD is the distance from flat to nearest urban transport stop [m]

vzd.žel is the distance from flat to the main railway station [m]

Pozn.: absolute value of the regression model [CZK]

Based on verification calculations made in the dissertation thesis , the resulting regression equation can be interpreted in such a way that the apartment price increases with the growing residential area of the flat, decreasing with increasing distance to the nearest public transport stop and the decreasing distance to the railway station. The resulting complete data of the case study, including the conditions and the evaluation of the results, are presented in the relevant chapter of the dissertation.

Case study - Benefits from the construction of transport infrastructure

This case study explores the benefits of the construction of transport infrastructure and its impact on changes in the business environment in the field of passenger road (bus) and rail transport. The benefits of commercially operating traffic on the section under consideration or through a transparent tender for the transport serviceability of a particular session is to save government subsidies for ordered transport services in sessions that are currently private carriers willing to operate without subsidies or with lower subsidies than is the case with national carrier. However, this concept is not applicable to the entire railway network but only to commercially interesting sessions.

The aim is to estimate the potential of the completed D11 motorway for bus carriers, which can be expressed by the aggregate coefficient using Saaty's method. For evaluating the potential for bus carriers following procedure shall apply using Saaty method (Olivková, 2011; Friebelová 2008).

The first step is to establish the evaluation criteria and their description. Criteria determination was carried out by the research team together with the supervisor and supervisor by a specialist based on the Delphic method, a prognostic method of group finding a solution. For clarity, the criteria and their description are given in the relevant chapter of the dissertation.

Using the pairwise comparison method, you need to verify the consistency of pairing each criterion with a consistency test (Saaty , 1987). The consistency test calculation according to Hasse and Meixner (2009) follows in five steps. The calculated consistency rate is:

CR=0,1103/1,24=0,089 (2)

The CR consistency rate is considered acceptable at 0.10 (10 %). Consistency is therefore acceptable. Next steps of the calculation can follow. For the needs of the model, it is necessary to define the various

scenario scenarios and the verbal description of the criteria in the next step. On the basis of expert estimates, an optimistic variant, a pessimistic variant and a realistic variant are set.

The last step of the calculated model of calculation is the evaluation of the potential of the considered relationship for the bus carrier itself. A comparison of the individual data of both scenarios is given in Table 23 of the respective chapter in the dissertation.

The resulting coefficient of 0.73 for the expected option means that the completion of the remaining section of the D11 motorway opens up a considerable potential for bus carriers in this session. At the same time, there would be a greater competitive potential against rail transport, and this session would become more attractive to car users, as travel time would be shortened.

The resulting complete case study data, including the specification of factors affecting road and rail transport, are set out in the relevant chapter of the dissertation. .

Case study - benefits from improving the quality of public transport

According to Litman (2008), it is generally the tendency to value qualitative factors such as comfort, comfort, safety and prestige with higher values. However, practice often focuses on quantitative factors and impacts in transport planning and economic assessment and underestimates qualitative factors and impacts. This chapter of the dissertation thesis aims to estimate the economic quality factors in public transport, which have the positive benefits of transport, by applying the method of the so-called Level-of-Service rating. For the conditions of the Czech Republic, author applies a method of determining suitable factors divided into the following five phases, according to Litman (2008):

- Defining quantifiable factors
- Determination of appropriate methods of quantification of selected factors
- Data collection
- Integrating calculations into aggregate index
- Include results in the planning process

For the needs of the method, it is necessary in the first step to determine the factors and the way of their evaluation, on the basis of which a table of intervals of individual LOS ratings expressing the level of public transport quality is constructed. On the basis of the theoretical knowledge, a questionnaire was drawn up, which included selected factors and their score: The author chose a model example of the urban transport in Pardubice city. The selected cases are being solved in follow-up chapters in dissertation, expert assessments were carried out in cooperation with supervisors.

The first step is to calculate the sum of the best variants (a), where the best options are summed, ie. the ideal scenario. This gives the upper limit of the entire evaluation interval. The sum of the worst variants (c) is summed up by the worst options, ie. worst case scenario. The sum of the middle variants (b) summed up the mean values of the options, with the calculated fare factor being taken as the mean value between 1 and 0. The calculated values a, b, c are further used to calculate the evaluation intervals between the individual LOS stages. Then, the entire evaluation interval is divided into LOS A-C and LOS D-F, the split value being b. The final distribution of LOS ratings according to the model questionnaire is entered in Table 26 in the relevant chapter of the dissertation.

In this chapter a calculation methodology of Litman (2008) is used. It calculates the savings through LOS ratings. For the model example of application of the LOS rating method for Czech conditions, the author chose Pardubice city. In the case study there is considered change in the quality of public transport rating LOS E to LOS C. This change is by Litman (2008) interpreted as a change from poor

quality of the space waiting to good one, such as a covered waiting area, possibly with benches, increase perceived quality of the vehicle, such as new interior upholstery, elimination of unwanted noise, deploying vehicles of the newer production year or with more seats, minor adjustments to the platforms, adjustment of the stopping environment or new ways of paying the fare, installing additional ticket machines, etc. For the case study, the following two sessions were selected.

Session 1: Session with transfer: Dubina, center - Airport

In the first step input data need to be defined. For the urban transportation it is considered walking for 5 minutes, waiting is 10 minutes. The driving time is 9 minutes. In the transit hub there is a waiting time of 5 minutes. Then travel to the finish stop is 13 minutes. Walking time from the destination stop to the destination is 5 minutes. For individual car transport, the distance from Dubina to the Airport is approximately 7.2 km and the passenger car will overcome this distance under normal city traffic conditions in 13 minutes. Walking time to vehicle and from vehicle is always considered for 2 minutes.

The next step is to calculate the partial travel costs of time for individual time factors, such as walking, waiting, time spent in the vehicle or time to switch. The calculations are presented in Table 29 in the respective chapter of the dissertation, which also sums up the cost reduction resulting from the increased comfort of waiting and increasing the comfort and comfort of public transport from LOS E rating to LOS C. Driving time, the timetable has also remained unchanged. This is the upper limit of cost savings when there is an improvement in the perception of the quality of public transport by its users.

Session 2: Session without transfer : Dukla, carriage - Globus

For the urban transportation it is considered walking to the stop for 5 minutes. Then waiting is 10 minutes. Travel time to the finish stop is 20 minutes. Walking time to the destination is 5 minutes. For car there is the shortest distance from Dukla (carriage) to Globus about 5 km. If a driver travels the same route as a bus, it will take 10 minutes considering usual city traffic. Walking time to vehicle and from vehicle is always considered for 2 minutes.

Even though Litman (2008) calculates savings only for public transport users who have to transfer, there are experimentally calculated savings for a user who uses a direct link without transfer. Comparison is carried out again with alternative individual car traffic. From Table 30 in the relevant chapter of the dissertation is seen that due to the increased comfort of waiting and increasing the convenience and comfort of traveling by public transport (from rating LOS E at LOS C) decreased travel expenses in proportion to the IAD from 123% to 84%.

This case study describes a practical approach how the LOS ratings can economically evaluate a qualitative level and change the perceived quality of services within the considered public transport system. The result is the transformation of qualitative factors into the monetary value of time.

5. RESULTS AND DISCUSSION

Practical part of the thesis dealt with four areas of appreciation of positive externalities in transport. The selected methods of evaluating predominantly negative externalities were applied to case studies and the results obtained are summarized and interpreted in the following paragraphs.

Time savings valuation based on WTP and WTA

On the basis of the processed data and the results of the computation of the willingness to pay and the willingness to accept, using the dichotomical choice format in the questionnaire survey on the WTP

application, a case study was prepared in the Czech Republic. By applying the WTP method, the advantages over conventional valuation can be seen in the following points:

- compared to conventional methodology it is not an estimate of macroeconomic indicators,
- this method is based on current tariff and fuel prices, takes into account direct competition between IAD and rail passenger interregional transport,
- this method takes into account the so-called European approach, ie the WTP approach in foreign studies on this topic, eg Eboli and Mazzolla (2008).

The application of the WTP method to a case study shows how to obtain the bases for calculating user time savings in the economic evaluation of traffic projects in a given session (especially the assessment of positive externalities of the project) as well as the preference coefficient that determines preferential user choice in relation to travel costs and driving time based on WTA and WTP methods. If the total time of transport was considered, it is necessary to add to the train the time needed to transport from the starting point to the railway station, the waiting time and the time to move from the destination railway station to the destination. Due to the individual differences of the individual times and times transport costs are therefore considered only for the net travel times of the given means of transport for selected sessions.

UNITE (2003) uses value 21 EUR per hour for work time and 4 EUR per hour (private and leisure time) for road traffic value. Other studies, such as INFRAS / IWW (2004), use higher values that also take into account possible indirect costs from the risk of congestion affecting employees, customers and other transport users.

HEATCO study (2006) recommends using time values based on vehicle-kilometer instead of person-kilometer. Differences are, for example, when assessing commuting time (8,48-10,89 EUR / car) and private journeys (7,11 - 9,13 EUR / car), for example used to estimate delays or congestion in congestions. For congestion in private passenger transport, it is recommended to multiply the standard time value by 1.5, in freight 1.9 and in passenger transport by 2.5. Values of time savings estimates, as recommended by the HEATCO and the differentiated by country, mode of transport, purpose of journey and length of journey, are based on WTP based surveys.

Alternatively, the application of the method may be combined or supplemented by the above-mentioned coefficients, depending on the processors of the economic study, as to which other variables may lead to more accurate results, to extend this basic model accordingly.

The hedonic price and the impact of the proximity of the transport infrastructure on the property price

A case study was prepared on the chosen example of Pardubice city and its aim was to express the influence of the proximity of the transport infrastructure on the prices of apartments in Pardubice city using the application of the hedonic price method. There is dependence between the price of apartments and distances of the transport infrastructure in Pardubice city. The case study shows that the proximity factor of the public transport stops at an average of 0.46% at the price of apartments in Pardubice, and the factor near to the main railway station accounts for an average of 2.92% for the price of apartments in Pardubice city. Negative correlation in both cases means that the greater the distance of the transport infrastructure is, the lower the flat rate is. Proven dependence is mild.

The principle of evaluating positive externalities by the hedonic pricing method can thus be one of the imaginary counterparts to the negative externalities assessed in the studies of transport projects. Based on the results of a case study, for example, price maps in the given locations can be revised. The results generated by this case study may vary depending on the quality of the data being processed or the

property parameters under consideration, to which Haripriya (2008) or Forrest (1992) also draws attention.

However, the possible extension of the study with transport at rest on the price of real estate is subject to several restrictive conditions. It is necessary to carry out a thorough analysis of the transport at rest in the city, to consider only real estate with comparable parking conditions, as distorted results can be made clear and cluttered by often confusing the assignment of particular parking spaces and their number to apartment buildings and other properties, attendance distance from parking spaces and last but not least, it is necessary to take into account other individual factors that affect the transport at rest in connection with the price attractiveness of residential locations.

For the above reasons, due to the complexity of the data collection and analysis of the parking areas in Pardubice city, the transport at rest was not included in the model case, but if the above mentioned conditions are fulfilled, this factor can be put into the evaluation method appropriately, as transport at rest has a significant impact on the real estate price.

At the same time, it should be mentioned that this method is not used so much in the Czech Republic because, using the hedonic method, it is assumed that the real estate market represents a market of perfect competition, as Melichar and Honigová (2005) say . Similarly, different conclusions are reached with the application of this method, as evidenced, for example, by Forrest et al. (1992) who found the city's rail transport negative impact on the property price in Manchester, and Bajic (1983), which found the positive effect of a metro proximity on the property price in Toronto. Not only from these cases can be deduced that the results of the hedonic price model differ from case to case, it is always necessary to describe the input data, the specifics of the given location, including the historical and urban development, the specifics of the transport behavior of the population and, last but not least, the restrictive conditions of the case study, which also influence the interpretation of the results and conclusion of the study.

By using correlation and regression analysis combined with real estate data, the dependence between property prices and distance to traffic junctions can be determined. When applying this analysis, there may be a multicollinearity problem that has arisen in this practical study so the variable needs to be eliminated. When assessing the environmental characteristics of Haripriya (2008), a frequent example of multi-collinearity is, for example, an increased concentration of harmful emissions and an increased noise level in the property near the road infrastructure. It also points out that the input data in the hedonic analysis should only come from one real estate market.

From a certain distance, it is also necessary to take into account negative externalities such as noise and vibrations that can be valued by the WTP method based on the hedonic valuation or expressed noise reduction preferences or the so-called Impact Pathway Approach in relation to the impacts of these negative externalities on human health.

Also technological and technical level of rail transport in the area needs to be taken under consideration and also the general level of these transport systems. Reference can be made to Chapter 4.4., where the impact of changing the quality of the transport system in the case of urban public transport in Pardubice city was examined in the case study. The perceived quality of bus and rail transport, expressed through LOS ratings, can thus help to improve transport planning while reducing the time travel cost, and secondly to increase the competitiveness of bus and rail transport towards individual car traffic, thereby increasing the interest in these modes of transport in the intended location, increasing real estate prices near transport hubs.

Benefits from the construction of transport infrastructure – motorway D11 case

This case study is aimed at evaluating the benefits of building a new transport infrastructure. Criteria were defined by Saaty's method of quantitative pair comparison, their description and weight, and the outcome of scenario 1, which foresees the completion of D11 motorway. The result is the attractiveness coefficient for initiating or expanding business in bus traffic on a model session.

When pairing occurs, there is always a certain inconsistency of the pairwise comparisons, the goal being not to exceed the stated consistency level. Otherwise, the study would lose its predictive value and the results would be distorted.

The resulting coefficient of 0.73 for the expected variation "Model Case - D11" means that the completion of the remaining new section of the D11 motorway presents a relatively high potential for bus carriers in this session.

Completion of D11 motorway would increase the competitive potential for rail transport and at the same time make this session more attractive to IAD users, as travel time would be shortened. This deduction was confirmed in 2016 by the entry of the Student Agency (RegioJet) to this session where from May 2016 it started to operate one pair of connections a day, although the D11 motorway is currently completed to Hradec Králové only.

Thus, the case study can serve as one of the inputs in the preparatory phase of the project to process the economic analysis based on determining the attractiveness of the relationship for the carrier. Differential factors for evaluating the attractiveness of the projected session for carriers in the road and the railway transport are level of market liberalization, construction and modernization of road infrastructure, minimum attractive sessions for expansion existing private carriers, or even for the entry of new private railway carriers, high business risk in rail transport, different transport infrastructure charges, different tariff conditions, unless there is a uniform tariff of the integrated regional transport system (eg IREDO) and, last but not least, the limited capacity of rail transport.

Analogously, Saaty's method and the same procedure for assessing the commercial potential of a railway taking into account the current situation, which the processor must undergo a thorough technical-economic analysis in the preparatory phase. In case of rail transport there is an ideal condition if a case study can count on a fully open transport market for rail carriers. The resulting coefficient can thus be defined as the degree of attractiveness of a given session for initializing or expanding a business in the area of public passenger transport, in particular when comparing travel times and fares for variants without and with project.

The use of Saaty's method assumes the existence of a team of experts who determine the most appropriate criteria that have the greatest impact on the project scenario compared to the current state, ie without a project. The research team also participates in the point evaluation of the individual pairs of criteria. This team is usually made up of experts who have to meet requirements such as education or length of practice in the field. The use of this method is sensitive to the subjective views and perspectives of the individual problem solver, which is reflected, for example, in defining the optimistic, pessimistic and realistic variant of the scenario. Each of the scenarios should be based on trends estimated based on available statistical data in context with the analysis of the current status. Similarly, the factors influencing the modes of transport to be compared must be taken into account, such as the commercial potential of the route in relation to the current and potential traffic flows of the passengers, the level of competitive environment, for example by the number of carriers operating regular connections to the sessions under consideration, the number of connections between the carriers, the financial background of the carriers, modes of transport on the session, economic and temporal terms railroad and individual automobile traffic on the session, administrative burden with respect to the comparison of transport modes, level of transport market liberalization, or barriers for

entry, contractual obligations in the context of transport services and the last but not least, the potential for qualitative improvement of the provided transport services in the given relation, for example on the quality of the available transport infrastructure, the attractiveness of the region being assessed, etc. Analogous factors can be considered in the same way from the point of view of rail transport.

Assessing the benefits of improving the quality of public transport

The last case study in the practical part of the thesis deals with the evaluation of the benefits of improving the quality of public transport. The results show that, as a result of increased waiting comfort and increased comfort and comfort of public transport (from the LOS E rating to the LOS C), the travel cost in relation to the IAD was 123% to 84%. For the model case, two sessions were selected by the author in the public transport network in Pardubice city, with the first session being Dubina, Centrum - Letiště and the second session is Dubina, Centrum - Globus. Inputs are expert estimates.

Improving the quality of public transport services can be, by analogy, implemented into other influential aspects such as increased travel speeds, transit rates, reduced fares, or parking fees. When introducing programs for the qualitative improvement of transport systems, individual strategies should create a synergistic effect that results in an increase or even a multiplier effect on the overall benefits of transport for its users.

Similarly, the LOS rating method can be applied to rail passenger transport. Most transport operations in the Czech Republic are carried out by a state-owned carrier ČD as (MDČR, 2016), while the owner of the infrastructure is the state, through the SŽDC. For programs to improve infrastructure for increased competitiveness and greater use of rail transport, owners can, in turn, request the infrastructure manager (eg SŽDC) to apply for subsidies. One of the supported activities is, for example, to increase the comfort and facilities of the station and stop infrastructure in the management of the railway infrastructure manager, or to modernize and reconstruct the lines and other infrastructure related to upgrading within the railway hubs.

Case study in Chapter 4.4. shows how comfort and comfort can substantially reduce the travel costs of time. Moreover, these benefits are virtually invisible for most current models for the economic evaluation of transport projects.

Conventional methods of economic evaluation tend to concentrate mainly on travel times (driving speed) and give little weight to comfort and comfort factors when traveling. Consequently, the results of conventional valuation are based on a planning process that does not take into account all the factors and thus they can not achieve full optimization of the transport system compared to what would maximize the efficiency of the transport system and social well-being. Litman (2008) also notes that conventional methods also often underestimate alternative modes of transport, as they are generally judged to be slower and as well as service options because they overlook the value offered by multiple levels of service and also the quality of service because quality improvements are often underestimated. If investment in improving the quality of public transport is neglected, public transport is less attractive than individual car traffic, resulting in higher travel time compared to travel costs of car travel. Motorists have the possibility to have comfort and comfort directly influenced by investments in a better car or guaranteed or better parking space. However, an individual user of public transport in the city does not have this option. If public transport does not meet the user's quality requirements, the user switches to alternative modes of transport.

Improving the quality of services in alternative modes should take into account the benefits for existing users, the benefits for new users of the improved transport system, the benefits for other road users by reducing the risk of accidents and the occurrence of congestions, benefits for society by optimizing

existing infrastructure and transport capacities, cost savings (time), benefits in energy savings and reduction of pollutant emissions, or the benefits of higher sales of transport companies from increased passenger interest. The use of the LOS rating method is foreseen in case studies or preparatory phases of new projects focusing on improving transport standards in public transport. In USA, UK or Australia, this evaluation method is used to optimize the traffic planning process and the evaluation of transport projects.

6. AUTHOR'S OWN CONTRIBUTION

The dissertation deals with issues of positive externalities in transport and methods of their valuation. In the practical part of the dissertation there were presented four case studies, using methods used primarily for the evaluation of negative externalities. Based on the results of studies, it is then possible to include this evaluation of positive externalities in the overall assessment of the economic efficiency of transport projects.

Main benefits of the dissertation:

- elaboration of the analysis of the present state of the issue of evaluation of positive externalities in transport,
- application of WTP and WTA methods for the evaluation of time, time savings,
- application of the hedonic price method to assess the impact of transport infrastructure proximity on property prices,
- application of Saaty's method for determining the aggregate coefficient for assessing the benefits of the construction of a new transport infrastructure, including the specification of the different aspects of road and rail transport,
- application of the LOS rating method for assessing the quality of public transport services, expressing time savings in improving the quality of the transport system,
- usability of case study methods and backgrounds for further research on the issue of assessing positive externalities in transport,
- applicability of the presented methods for expanding the basis of the transport projects economic evaluation in terms of both negative and positive externalities.

CONCLUSION

The importance of positive externalities in relation to transport policy is currently unquestionable, and in the coming years this trend will continue as a result of the need for more and more accurate and relevant economic evaluation of transport projects. From the analysis of the current state of the given issue it follows that the topic of dissertation is very topical, which results also from the analysis of domestic and foreign sources where the problem is solved by the most frequent case studies. Even so, less attention is paid to positive externalities than negative externalities, which are still ahead of transport policy, mainly due to programs to reduce emissions and generally mitigate the impact of negative externalities on the environment.

The analysis shows that the transport projects in road and rail transport are mostly assessed in terms of negative externalities and positive externalities are mentioned only in a qualitative and not quantitative way. Examples of unconventional economic assessments of selected transport projects from Great Britain, the USA, or Canada show that evaluating positive externalities can contribute to the positive economic balance of the evaluated project, its adoption by competent authorities and subsequent implementation.

For example, frequent arguments against the economic efficiency of high-speed rail projects in the Czech Republic appear to be odd in analyzing materials in the UK high-speed rail project where a group

of experts defines so-called wider economic benefits that assess the positive impact of the project on the region and in terms of business activities, job opportunities, agglomeration benefits, foreign investments and their multiplier effects, etc. However, this assessment method is demanding for data collection and some statistical data required for the application of this model are not available in the Czech Republic.

For application of WTP and WTA, sessions with different road and rail transport segments were deliberately chosen, with two sessions having the advantage of rail transport in the form of a corridor with high travel speed for the user, with two sessions having the advantage of road transport in the form of motorways. The most logical option is when the user pays less and will be in the destination earlier. This is an example of the Prague - Pardubice session, when compared to car, it is a user's point of view to save less travel time. The opposite case is the Trutnov - Pardubice session, where users choose the option to pay less, but they will be in the destination later. Methods WTA and WTP can be used to economically assess the behavioral and economic behavior of the population in relation to the willingness to pay and to receive compensation for lower and / higher travel time.

When assessing the impact of the proximity of transport infrastructure on real estate prices, the findings of the above mentioned studies were already found in the research. The theory of the hedonic price method thus faces paradoxical situations and often contradictory conclusions that are influenced by many geographical, environmental, economic or psychological aspects where the property price positively affects the proximity of transport infrastructure or agglomerations with good transport accessibility and environmental aspects such as proximity to parks, forests or a no-noise environment. Some studies, on the other hand, found that in certain cases the negative externalities predominate in the assessment of the real estate price in the areas under consideration, for which there are also specifics, which are also an explanation of these negative trends. For a case study on the impact of the proximity of the transport infrastructure on property prices, a model example of Pardubice city was chosen, where it was determined how much the factor near the public transport stops and the factor near to the railway station is at the price of apartments in Pardubice. Negative correlation in both cases means that the greater the distance between the transport infrastructure and the home, the lower the apartment price, and vice versa, with the observed dependence being mild. Within limiting conditions and described specifics of the location under consideration, the link to transport at rest, which also affects the price of real estate, is mentioned. However, should a case study be extended to the effect of this aspect, several conditions would have to be considered, in which compliance could be included in the input data for correlation and regression analysis.

In a case study to measure the benefits of building a new transport infrastructure, the Saaty's method was used to determine the cumulative coefficient for the scenarios that is expected to complete the D11 motorway. This study works with the multi-criterion decision method and results in a coefficient of attractiveness for initializing or expanding a business in bus transport to a chosen session that takes into account the criteria that characterize the change in the transport market. The result of the case study can then be interpreted in such a way that the realization of the remaining section of the D11 motorway opens up a great potential for bus carriers in this session. At the same time, there would be greater competition potential for rail transport and at the same time, this session would become more attractive to car users, as travel time would be reduced in the case of bus traffic. This deduction was confirmed in 2016, among other things, by the entry of Student Agency (RegioJet) to this session, where from May it started to operate one pair of connections a day, although the D11 motorway is only completed to Hradec Králové. From the tariff point of view, the bus service is the most advantageous and, with the entry of another competitor, there is no prerequisite for rising fare prices, except for the usual price adjustments in relation to the macroeconomic indicators and the performance of the domestic economy.

An analogous procedure can be chosen for assessing commercial potential for rail carriers, in the case of rail transport, it is an ideal condition if the case study can count on a fully open transport market for rail carriers.

The latest case study analyzes the benefits associated with improving the level of public transport services. The method and so-called LOS ratings were applied to the conditions of the Czech Republic, namely the model case of public transport in Pardubice city. Sessions were selected from the Dubina, Centrum stop to Letiště stop and the non-transfer session from the Dukla, Centrum stop to Globus stop. Based on the results of both model sessions, it can be deduced how comfort and comfort can substantially reduce the travel costs of time. Moreover, these benefits are virtually invisible for most current models for the economic evaluation of transport projects. Conventional assessment methods often focus only on the cruising speed parameter and attach little weight to the comfort and comfort of traveling. The case study shows how qualitative factors can be translated into the quantitative expression of travel time value.

The author sees the potential of using the method of determining LOS ratings also in rail passenger transport, where the level of comfort and comfort is generally very variable and depends on the fleet renewal and scale, the level of information provided by the carrier and the quality of the infrastructure or the levels of modernization of the tracks and stops / stations on the side of the rail operator. The use of the LOS rating method is foreseen in case studies or preparatory phases of new projects focusing on improving transport standards in public transport and optimizing the decision-making process in line with the requirements of the users of the transport system.

REFERENCES

BAJIC, V. 1983. The Effects of a New Subway Line on Housing Prices in Metropolitan Toronto. Urban Studies.

BATEMAN, I.J. et al. 2002. Economic valuation with stated preference techniques: A manual. [online]. Cheltenham, UK. [cit. 2017-10-20] Dostupný z: https://webarchive.nationalarchives.gov.uk/20120919162306/http://www.communities.gov.uk/documents/corporate/pdf/146871.pdf

BLOMQUIST, G. C. 2003. Self Protection and Averting Behavior, Values of Statistical Lives, and Benefit Cost Analysis of Environmental Policy, [online]. University of Kentucky. [2018-10-17]. Dostupné z https://pdfs.semanticscholar.org/84ed/3a7107c326f06faeb1d2666a558571720751.pdf

BLUM, Ulrich, 2008. Positive Externalities and the Public Provision of Transportation Infrastructure: An Evolutionary Perspective [online]. Dresden University of Technology [cit. 2018-10-17]. Dostupný z: https://rosap.ntl.bts.gov/view/dot/4714/dot_4714_DS1.pdf

BOARD OF TRADE OF METROPOLITAN MONTREAL, 2004. Public Transit: A Powerful Engine For The Economic Development Of The Metropolitan Montreal Area [online]. Montreal, BTMM [cit. 2013-11-25]. Dostupný z: http://www.ccmm.qc.ca/documents/memoires/2004_2005/BTMM_PublicTransit_study.pdf

BOYLE, K. J. 2003. The Contingent Valuation in Practice. in A Primer on Nonmarket Valuation [online]. London, Kluwer Academic Publishers. [cit. 2017-09-12] DOI: 10.1007/978-94-007-7104-8_4

BRIŠ Radim a Martina LITSCHMANNOVÁ, 2007. Statistika II [online]. VŠB, Ostrava [cit. 2018-04-27]. Dostupný z: http://homel.vsb.cz/~bri10/Teaching/Statistika%20II/skriptum/1_Modely_a_modelovani.PDF

BROWN, G. M. Jr. et al. 1977. Economic valuation of shoreline. The Review of Economics and Statistics 59, MIT Press, s. 272-278.

BRŮHOVÁ-FOLTÝNOVÁ, Hana, 2004. Aplikace mikrosimulačních modelů v osobní dopravě: zkušenosti z ČR a zahraničí [online]. VŠE [cit. 2014-04-08]. Dostupný z: http://www.vse.cz/polek/download.php?jnl=polek&pdf=681.pdf

BRŮHOVÁ-FOLTÝNOVÁ, Hana, 2012. Analýza každodenního dopravního chování dospělého městského obyvatelstva a nástroje regulace dopravy [online].. Univerzita Karlova [cit. 2016-04-08]. Dostupný z: https://www.czp.cuni.cz/urbantransport/deliverables/Aktivita_2_1_reserse_ekonomicka.pdf

BRŮHOVÁ-FOLTÝNOVÁ, Hana. 2008. Vytvoření a empirická verifikace ekonomického modelu dopravního chování [online]. Univerzita Karlova [cit. 2016-04-08]. Dostupný z: https://www.czp.cuni.cz/urbantransport/deliverables/Aktivita_2_5_Model.pdf

BRUYELLE, P. a Peter THOMAS. 1994 The impact of the Channel Tunnel on Nord-Pas-de-Calais. Applied Geography, 14 (1). pp. 87-104. ISSN 0143-6228.

BusinessInfo.cz, 2007 Ekonomicko-statistický slovník A až K [online]. BusinessInfo.cz [cit. 2013-11-25]. Dostupný z: http://www.businessinfo.cz/cs/clanky/ekonomicko-statisticky-slovnik-a-k-3098.html

CAO, Jason a Jill HOUGH. 2007. Hedonic Value of Transit Accessibility: An Empirical Analysis in a Small Urban Area. [online]. ResearchGate. [cit. 2018-11-30]. Dostupný z: https://www.researchgate.net/publication/238726280_Hedonic_Value_of_Transit_Accessibility_An_Empirical_Analysis_in_a_Small_Urban_Area

CDV, 2005. Analýza trendů silniční nákladní dopravy I. část. [online]. Brno. [cit. 2018-12-29]. Dostupný z WWW: http://www.zelenykruh.cz/wp-content/uploads/2015/01/Studie-CDV.pdf

CE DELFT, 2008. Handbook on estimation of external costs in the transport sector [online]. Brusel: Evropská komise [cit. 2014-10-19]. Dostupný z WWW: http://ec.europa.eu/transport/sustainable/doc/2008_costs_handbook.pdf

CONFIMA, 2007. Hodnocení efektivnosti projektu výstavby vodního koridoru DUNAJ-ODRA-LABE [online]. ČR [cit. 2018-03-19]. Dostupný z WWW: www.d-o-l.cz/index.php/cs/kestazeni/category/7-?download=15%3A

ČSÚ. 2017. Statistická ročenka České republiky [online]. ČSÚ [cit. 2017-08-04]. Dostupné z: https://www.czso.cz/csu/czso/statisticka-rocenka-ceske-republiky

Department for Transport, 2005. Transport, Wider Economic Benefits, and Impacts on GDP. DfT [cit. 2014-04-04]. Dostupné z: http://webarchive.nationalarchives.gov.uk/+/http:/www.dft.gov.uk/pgr/economics/rdg/webia/webmethodology/sportwidereconomicbenefi3137.pdf

Department for Transport, 2011. Crossrail Business Case Update - Summary Report, July 2011. DfT. [cit. 2018-04-04]. Dostupné z: http://74f85f59f39b887b696f-ab656259048fb93837ecc0ecbcf0c557.r23.cf3.rackcdn.com/assets/library/document/c/original/crossrail_business_case_update-summary_report_july_2011.pdf

DVOŘÁK, Antonín a kol. 2007. Kapitoly z ekonomie přírodních zdrojů a oceňování životního prostředí. Praha, VŠE. 195 s. ISBN 978-80-245-1253-2.

EBOLI, Laura a G. MAZZULLA. 2008. Willingness-to-pay of public transport users for improvement in service quality. [online]. University of Calabria – Faculty of Engineering. [cit. 2017-09-12]. Dostupný z: http://www.istiee.org/te/papers/N38/38_EboliMazzulla.pdf

ExternE, 2005. Externalities of Energy – Methodology 2005 Update. European Commission [cit. 2017-11-12]. Dostupné z: http://www.externe.info/externe_d7/sites/default/files/methup05a.pdf

FOLTÝNOVÁ, Hana, 2009. Doprava a společnost: ekonomické aspekty udržitelné dopravy. Praha: Karolinum. ISBN 978-80-246-1610-0.

FORKENBROCK, D. J. et al. 2001. Guidebook for Assessing the Social and Economic Effects of Transportation Projects [online]. National Cooperative Highway Research Program [cit. 2018-11-18]. Dostupný z: http://onlinepubs.trb.org/onlinepubs/nchrp/nchrp_w31.pdf

FORREST, D., et al. 1992. Both sides of the track are wrong: a study of the effect of an urban railway system on the pattern of housing prices. University of Salford: Department of Economics.

FRIEBELOVÁ, Jana. 2008. Vícekriteriální rozhodování za jistoty. [online]. Ekonomická fakulta, Jihočeská univerzita v Českých Budějovicích. [cit. 2018.11-28]. Dostupné z: http://www2.ef.jcu.cz/~jfrieb/tspp/data/teorie/Vicekritko.pdf

GARROD, G. et al. 2000. Economic Valuation of the Environment: Methods and case studies. United Kingdom: Edward Elgar Publishing Limited, s. 365. ISBN 978-1-85898-684-5.

GAVORA, P. a kol,. 2010. Elektronická učebnica pedagogického výskumu. [online]. [cit. 2018-02-28]. Bratislava : Univerzita Komenského,. ISBN 978–80–223–2951–4. Dostupné z: http://www.e-metodologia.fedu.uniba.sk/

GOODWIN, Phil a Stefan PERSSON, 2001. Assessing the Benefits of Transport, European Conference of Ministers of Transport; OECD (www.oecd.org).

GOODWIN, Phil et al. 2004. Elasticities of Road Traffic and Fuel Consumption with Respect to Price and Income: A Review. Transport Reviews, 24 (3). s. 275-292. ISSN 01441647. 24. 10.1080/0144164042000181725.

Google Maps. 2018. [online]. Google. [cit. 2018-11-18]. Dostupné z: https://www.google.com/maps

GVA, 2017. Crossrail Property Impact&Regeneration Study. GVA [cit. 2018-04-04]. Dostupné z: http://www.gva.co.uk/uploadedfiles/GVA_UK_Research/Crossrail%20Report.pdf

HAGUE, Paul. 2003. Průzkum trhu. 1. vydání. Brno: Computer Press, 2003. 234 s. ISBN 80-7226-917-8.

HALLSWORTH, Alan et al. 1998. Transport policy-making: the curse of the uncomfortable consequence. Journal of Transport Geography. Volume 6, Issue 2, 1998, s. 159-166

HARIPRIYA, G. 2014. Hedonic price method: A concept note. [online]. ResearchGate, Chennai. [cit. 2018-11-08]. Dostupný z: https://www.researchgate.net/publication/241758177_Hedonic_price_method_-_A_Concept_Note

HASS, Rainer a Oliver MEIXNER, 2009. An Illustrated Guide to the Analytic Hierarchy Process [online]. Institute of Marketing & Innovation, University of Natural Resources and Applied Life Sciences, Vienna [cit. 2015-11-12]. Dostupné z: https://mi.boku.ac.at/ahp/ahptutorial.pdf

HEATCO, 2006. Developing Harmonised European Approaches for Transport Costing and Project Assessment [online]. European Commission. [cit. 2014-04-08]. Dostupný z: http://heatco.ier.uni-stuttgart.de/HEATCO_D5.pdf

HENSHER, David A. 2007. Bus Transport: Economics, Policy and Planning. [online]. Research in Transportation Economics Vol. 18, Elsevier. [cit. 2018-11-04]. Dostupné z: www.elsevier.com

HOŘEJŠÍ, Bronislava et al., 2012 Mikroekonomie. Praha: Management Press. 576 s. ISBN 978-80-7261-218-5

CHAN, Felix, Henry LAU a Ralph IP, 2006. An AHP approach in benchmarking logistics performance of the postal industry. Benchmarking: An International Journal [online]. Vol. 13, no. 6, s. 636-661 [cit. 2018-11-15]. Dostupné z: http://www.researchgate.net/profile/Ralph_Ip/publication/228355154_An_AHP_approach_in_benchmarking_logistics_performance_of_the_postal_industry/links/0c9605201b8727168c000000.pdf

IACONO, Michael a David LEVINSON. 2011. Accessibility Dynamics and Location Premia: Do Land Values Follow Accessibility Changes? [online]. ResearchGate. [cit. 2018-10-30]. Dostupný z: https://www.researchgate.net/publication/238601114_Accessibility_Dynamics_and_Location_Premia_Do_Land_Values_Follow_Accessibility_Changes

INFRAS/IWW, 2004. EXTERNAL COSTS OF TRANSPORT – Update Study [online]. INFRAS/IWW [cit. 2017-10-08]. Dostupný z: habitat.aq.upm.es/boletin/n28/ncost.en.pdf

KJAER, T. 2005. A review of the discrete choice experiment - with emphasis on its application in health care. [online]. Health Economics, University of Southern Denmark. [cit. 2017-10-20] Dostupné z: https://www.sdu.dk/~/media/52E4A6B76FF340C3900EB41CAB67D9EA.ashx.

KOSIOR, Jake. 2011. Benefits of Transportation. CTRF [cit. 2018-11-12]. Dostupný z: http://ctrf.ca/wp-content/uploads/2014/07/52KosiorPrenticeBenefitsofTransportation.pdf

KRŠKOVÁ, Martina, 2011. Stanovení hodnoty trhem neoceněných statků [online]. VŠE [cit. 2013-11-04]. Dostupný z: https://www.vse.cz/eam/14

KUTÁČEK, Stanislav, 2009. Aplikace teorie externalit na vybraný segment odvětví dopravy [online]. Masarykova Univerzita Brno [cit. 2018-05-04]. Dostupné z: https://is.muni.cz/th/11271/esf_d/DIZERTACE_Kutacek_velka-obhajoba.pdf

LANGR, Martin, 2010. Doprava v klidu [online]. ČVUT, DF [cit. 2017-12-04]. Dostupné z: http://www.lss.fd.cvut.cz/Members/langr/2010-drup/2010-drup-5-pdf/at_download/file

LITMAN, Todd, 2008. Build for Comfort, Not Just Speed Valuing Service Quality Impacts In Transport Planning [online]. Victoria Transport Policy Institute [cit. 2017-05-04]. Dostupné z: http://www.vtpi.org/quality.pdf

LITMAN, Todd, 2018. Evaluating Public Transit Benefits and Costs, Best Practices Guide [online]. Victoria Transport Policy Institute [cit. 2018-10-04]. Dostupné z: http://www.vtpi.org/tranben.pdf

M.O.Z. Consult. 2016. Koncepce řešení dopravy v klidu na území městské části Praha 11. [online]. M.O.Z. Consult, Praha. [cit. 2018-10-14]. Dostupné z: https://www.praha11.cz/cs/doprava/koncepce-dopravy/reseni-dopravy-v-klidu/koncepce-reseni-dopravy-v-klidu.html

MÁCA, Vojtěch a Jan MELICHAR, 2013. Metodika kvantifikace externalit z dopravy. [online]. Univerzita Karlova v Praze – Centrum pro otázky životního prostředí [cit. 2018-03-04]. Dostupné z: https://www.tacr.cz/dokums_raw/metodiky/TB010MD017_metodika.pdf

MARKANDYA, Anil, 2006. The Hedonic Pricing Method [online]. University of Bath [cit. 2013-10-20]. Dostupné z: http://www.bath.ac.uk/~hssam/Hedonicpricing.ppt

MELICHAR, Jan a Iva HONIGOVÁ, 2005. Oceňování životního prostředí: Letní škola pořádaná Centrem pro otázky životního prostředí Univerzity Karlovy v Praze ve dnech 25. – 31. července 2005 v Jizerských horách. Praha: Centrum pro otázky životního prostředí Univerzity Karlovy v Praze. ISBN 80-239-6295-7.

MELICHAR, Jan et al. 2008. Peněžní hodnocení rekreačních a estetických funkcí lesních ekosystémů v České republice, redakčně upravená závěrečná zpráva projektu výzkumu a vývoje č. 1R56014. [online]. Praha, Centrum pro otázky životního prostředí UK, str. 20 – 27. [cit. 2017-11-04]. Dostupné z: http://mze-vyzkum-infobanka.cz/DownloadFile/2441.aspx

MELICHAR, Jan, 2005. Představení výzkumu metody cestovních nákladů [online]. Centrum pro otázky životního prostředí UK [cit. 2016-08-02]. Dostupné z: https://www.czp.cuni.cz/czp/images/stories/Vystupy/Seminare/2005%20LS%20Ocenovani%20ZP/melichar_metoda_cestovnich_nakladu.pdf

MINISTERSTVO DOPRAVY ČR, 2012. Věcný záměr zákona o železničních dráhách a železniční dopravě [online]. MDČR [cit. 2015-09-25]. Dostupný z: http://www.mdcr.cz/NR/rdonlyres/A87D8F89-F012-4CFE-92AC-77DCCD0AD761/0/Vecnyzamer_16_10_2012.doc

MINISTERSTVO DOPRAVY ČR, 2013. Dopravní politika pro období 2014-2020: [online]. Ministerstvo dopravy ČR [cit. 2018-10-20]. Dostupné z: https://www.mdcr.cz/Dokumenty/Strategie/Dopravni-politika-CR-pro-obdobi-2014-2020-s-vyhled

MINISTERSTVO DOPRAVY ČR, 2013. Metodika hodnocení efektivnosti investic – železniční infrastruktura [online]. Ministerstvo dopravy ČR, Věstník dopravy č. 11/2013 [cit. 2015-10-20]. Dostupný z: http://www.mdcr.cz/NR/rdonlyres/1184767E-37D5-4111-BCA0-605F802FFB4B/0/130522_Vestnik_dopravy_11.pdf

MINISTERSTVO DOPRAVY ČR, 2018. Ročenka dopravy 2017 [online]. Ministerstvo dopravy ČR [cit. 2017-10-14]. Dostupné z: https://www.sydos.cz/cs/rocenka-2017/index.html

MOLNÁR, Zdeněk et al. 2012. Pokročilé metody vědecké práce. Praha, první vydání, 2012. ISBN 978-80-7259-064-3.

MORALES, D. J. 1980. The contribution of trees to residential property value. Journal of Arboriculture, 6, s. 305-308.

MPSV ČR. 2017. Nařízení vlády č. 567/2006 Sb., o minimální mzdě, o nejnižších úrovních zaručené mzdy, o vymezení ztíženého pracovního prostředí a o výši příplatku ke mzdě za práci ve ztíženém pracovním prostředí, ve znění pozdějších předpisů. In: ASPI. Praha.

MRZENA, Rudolf, 2011. Integrované systémy veřejné osobní dopravy a jejich vliv na životní prostředí [online]. Univerzita Pardubice [cit. 2018-04-04]. Dostupné z: https://dk.upce.cz/bitstream/handle/10195/39630/MrzenaR_IntegrovaneSystemy_JM_2011.pdf

MVA Consultancy, 2009. High-Speed Rail Development Programme 2008/9. Evaluation Methodology. Final Report for Workstream 3. MVA [cit. 2015-02-17].

Dostupný z: http://www.greengauge21.net/wp-content/uploads/Workstream-3-assessment-Methodology.pdf

NAESS, Petter, 2012. Critical view on cost-benefit analyses [online]. The 5th Concept Symposium on Project Governance. Aalborg University [cit. 2017-10-17].. Dostupný z: https://www.ntnu.edu/documents/1261865083/1263461278/1_1_Naess.pdf

NASH, Chris et al. 2003. UNIfication of accounts and marginal costs for Transport Efficiency [online]. 5th RTD Framework Programme. [cit. 2018-11-24]. Dostupný z: https://trimis.ec.europa.eu/sites/default/files/project/documents/20060821_164701_60888_UNITE%20Final%20Report.doc

NASH, Chris, 2003. Unification of accounts and marginal costs for transport efficiency (UNITE), Final report [online]. Leeds : ITS, University of Leeds [cit. 2018-01-17].. Dostupný z: http://www.its.leeds.ac.uk/projects/unite/downloads/Unite%20Final%20Report.pdf

NATIONAL ACADEMIES OF SCIENCES, ENGINEERING, AND MEDICINE. 2009. Benefit/Cost Analysis of Converting a Lane for Bus Rapid Transit. Washington, DC: The National Academies Press. Dostupné z: https://doi.org/10.17226/23025

NATIONAL COOPERATIVE HIGHWAY RESEARCH PROGRAM, 2009. Cost/Benefit Analysis of Converting a Lane for Bus Rapid Transit [online]. In Research Results Digest 336. NCHRP [cit. 2016-08-01]. Dostupný z: http://onlinepubs.trb.org/onlinepubs/nchrp/nchrp_rrd_336.pdf

NELSON, J. P. 1980. Airports and property values, a survey of recent evidence. Journal of Transport Economics and Policy, 14, s. 37-52.

OECD/ITF, 2008. The Wider Economic Benefits - Discussion Paper No. 2008-6, Boston, OECD/ITF [cit. 2014-02-15]. Dostupný z: http://www.internationaltransportforum.org/jtrc/discussionpapers/DP200806.pdf

OLIVKOVÁ, Ivana, 2011. Aplikace metod vícekriteriálního rozhodování při hodnocení kvality veřejné dopravy [online]. In Perner's Contacts, Ročník 6, číslo IV. UPCE [cit. 2016-02-15]. Dostupný z: http://pernerscontacts.upce.cz/23_2011/Olivkova.pdf

Operační program Doprava – OPD, 2013. Operační program Doprava - základní informace [online]. MDČR [cit. 2015-09-20]. Dostupný z: http://www.opd.cz/cz/Zakladni-informace

PHILLIPS, Rhonda, KARACHEPONE John an Bruce LANDIS. 2001. Multi-Modal Quality of Service Project. [online]. Florida DOT. [cit. 2018-11-24]. Dostupné z:www.dot.state.fl.us/Planning/systems/sm/los/FinalMultiModal.pdf

PRENTICE, Barry a L. MAZUREK, 2010. Benefits Generated by Transportation in Canada [online]. Monograph prepared for Transport Canada Full Cost Investigation [cit. 2018-10-07]. Dostupný z: http://ctrf.ca/wp-content/uploads/2014/07/52KosiorPrenticeBenefitsofTransportation.pdf

RODRIGUE, Jean-Paul, 2017. The Geography of Transport Systems, Fourth edition. New York: Routledge, 440 pages. ISBN 978-1138669574.

ROSENBERGER, Randall S. et al. 2012 Attitudes, willingness to pay, and stated values for recreation use fees at an urban proximate forest. In Journal of Forest Economics [online]. Elsevier. [cit. 2017-10-11] Dostupné z: http://nature.forestry.oregonstate.edu/sites/default/files/2012-3%20JFE%20-%20Rosenberger%20Needham%20Morzillo%20Moehrke%20(2012).pdf

ROTHENGATTER, Werner, 1994. Do external benefits compensate for external costs of transport?. Elsevier. Transportation Research Part A: Policy and Practice, Volume 28, Issue 4, s. 321-328.

Ředitelství silnic a dálnic ČR, 2012. Prováděcí pokyny pro hodnocení ekonomické efektivnosti projektů silničních a dálničních staveb. [online]. ŘSD [cit. 2015-10-10]. Dostupné z: http://www.rsd.cz/doc/Technicke-predpisy/HDM-4/provadeci-pokyny-pro-hodnoceni-ekonomicke-efektivnosti-projektu-silnicnich-a-dalnicnich-staveb

SAATY, Thomas, 1987. The Analytic Hierarchy Process. Mathematical Modelling [online]. Vol. 9, no. 3-5, s. 161-176 [cit. 2015-09-20]. Dostupné z: http://www.sciencedirect.com/science/article/pii/0270025587904738

SEIDENGLANZ, D, 2006. Železnice v Evropě a evropská dopravní politika. Masarykova univerzita. ISBN 80-210-4221-4.

SEJÁK, J. et al. 1999. Oceňování pozemků a přírodních zdrojů. 1. vyd. Praha: Grada Publishing, s. 256. ISBN 80-7169-393-6.

SFDI. 2017. Rezortní metodika pro hodnocení ekonomické efektivnosti projektů dopravních staveb. SFDI [cit. 2018-11-14]. Dostupný z: https://www.sfdi.cz/soubory/obrazky-clanky/metodiky/2017_02_rezortni_metodika-komplet.pdf

SCHILLER, Brad. R. 2004. Mikroekonomie dnes, 1. vyd. Brno: Computer Press. ISBN 80-251-0109-6.

SOUKOPOVÁ, Jana, 2012. Vícekriteriální metody hodnocení [online]. MUNI [cit. 2017-09-04]. Dostupný z: https://is.muni.cz/el/1456/jaro2014/MKV_VZVP/um/33149329/Studijni_text_metody_vicekriterialniho_rozhodovani.pdf

Správa železniční dopravní cesty, 2018. Ekonomické hodnocení [online]. SŽDC [cit. 2018-11-02]. Dostupný z: https://www.szdc.cz/modernizace-drahy/ekonomicke-hodnoceni.html

sReality.cz. 2018. Reality a nemovistosti z celé ČR. [online]. Seznam.cz, a.s. Dostupný z: https://www.sreality.cz/

STATSOFT, 2014. Úvod do regresní analýzy [online]. StatSoft [cit. 2017-05-12]. Dostupný z: http://www.statsoft.cz/file1/PDF/newsletter/2014_26_03_StatSoft_Uvod_do_regresni_analyzy.pdf

STIGLITZ, Joseph E, 1997. Ekonomie veřejného sektoru. Praha: Grada Publishing. ISBN 80-716-9454-1.

ŠALOVSKÁ, Božena, 2009. Makroekonomie a mikroekonomie. Praha: Česká technika – nakladatelství ČVUT. ISBN 978-80-01-04373-8.

ŠAUER, Petr, 2007. Kapitoly z environmentální ekonomie a politiky i pro neekonomy. Praha. Centrum pro otázky životního prostředí UK. ISBN: 978-80-87076-06-4.

ŠPALEK, Jiří. 2005. Oceňování nehmotných užitků a externalit. MUNI [cit. 2018-11-12]. Dostupný z: https://is.muni.cz/el/1456/jaro2005/PVHVP/um/

UPTON, Graham J. a Ian COOK, 2008. A dictionary of statistics. New York: Oxford University Press. ISBN 0199541450.

URBAN, Jan. 2005. Kroky při přípravě a realizaci dotazníkového šetření. [online]. Centrum pro otázky životního prostředí, UK Praha. [cit. 2018-11-13]. Dostupný z:

https://www.czp.cuni.cz/czp/images/stories/Vystupy/Seminare/2005%20LS%20Ocenovani%20ZP/urban_priprava_dotazniku.pdf

Victoria Transport Policy Institute, 2017. TDM Encyclopedia Multi-Modal Level-of-Service Indicators [online]. Victoria Transport Policy Institute [cit. 2017-08-04]. Dostupné z: http://www.vtpi.org/tdm/tdm129.htm

WISER, Ryan H. 2007. Using contingent valuation to explore willingness to pay for renewable energy: a comparison of collective and voluntary payment vehicles. In Ecological economics [online]. Elsevier. [cit. 2017-10-18] Dostupné z: http://www.sciencedirect.com/science/article/pii/S0921800906003375

ZELENÝ, Lubomír, 2007. Osobní přeprava. Praha: ASPI. ISBN 978-80-7357-266-2.

LIST OF AUTHOR'S PUBLICATIONS RELATED TO THE FIELD OF THE DOCTORAL THESIS

HAŠEK, J. – DRAHOTSKÝ, I. Aplikace komunitárního práva v silniční dopravě v ČR. In Recenzovaný sborník příspěvků vědecké interdisciplinární mezinárodní vědecké konference doktorandů a odborných asistentů – QUARE 2013. Hradec Králové: MAGNANIMITAS, 2013. s. 1054-1062. ISBN 978-80-905243-7-8.

HAŠEK, J. – DRAHOTSKÝ, I. Aplikace komunitárního práva v železniční dopravě v ČR. In Recenzovaný sborník příspěvků z mezinárodní vědecké konference – Právní rozpravy 2013. Hradec Králové: MAGNANIMITAS, 2013. s. 89-97. ISBN 978-80-905243-5-4.

HAŠEK, J. Mobility management jako nástroj změny postojů a chování směrem k udržitelné dopravě. In Sborník příspěvků mezinárodní vědecké konference MMK 2012. Hradec Králové: MAGNANIMITAS, 2012. s. 1325-1332. ISBN 978-80-905243-3-0.

HAŠEK, J. – DRAHOTSKÝ, I. Dopravní trh a jeho nerovnosti. In Proceedings of the 5th International scientific conference for Ph.D. students and young scientists. Karviná, Slezská univerzita v Opavě, 2012. s. 499-505. ISBN 978-80-7248-800-1.

HAŠEK, J. – DRAHOTSKÝ, I. Specifika železniční a silniční dopravy z hlediska pozitivních externalit. In Proceedings of the 6th International scientific conference for Ph.D. students and young scientists. Karviná, Slezská univerzita v Opavě, 2013. s. 735-741. ISBN 978-80-7248-901-5.

HAŠEK, J. – DRAHOTSKÝ, I. Metody pro ekonomické vyjádření pozitivních externalit v dopravě. In Sborník příspěvků z mezinárodní vědecké konference MMK 2013. Hradec Králové: MAGNANIMITAS, 2013. s. 665-672. ISBN 978-80-87952-00-9.

HAŠEK, J. – DRAHOTSKÝ, I. Výzvy a limity v oblasti elektromobilismu v ČR. In Aktuální trendy v dopravě a ekonomice 2013. s. 331-340. ISBN 978-80-86530-90-1.

HAŠEK, J. – KOZLOVSKÝ, J. – MYŠKOVÁ, I. Vývoj a trendy v bezpečnosti dopravy v kontextu dopravní politiky. In Aktuální trendy v dopravě a ekonomice 2013. s. 283-298. ISBN 978-80-86530-90-1.

HAŠEK, J. – DRAHOTSKÝ, I. Problematika externích nákladů dopravy v evropském právu. In Recenzovaný sborník příspěvků z mezinárodní vědecké konference Právní rozpravy 2014. Hradec Králové: MAGNANIMITAS, 2014. s. 17-24. ISBN 978-80-87952-02-3.

HAŠEK, J. – DRAHOTSKÝ, I. Assessing Wider Economic Benefits of the High-Speed Rail Project in the UK. In Reviewed Conference Proceedings CER 2014. London, SCIEMCEE, 2014. ISBN: 978-0-9928772-0-0

HAŠEK, J., HRUŠKA, R., VASILIAUSKAS, A. Potencial valuation of route Prague – Trutnov after D11 completion. LOGI – Scientific Journal on Transport and Logistics, 2017, roč. 8, č. 2, s. 33-40. ISSN: 2336-3037.

Implementation System of TSI for the Rolling Stocks

Author: Ing. Katarína MAGDECHOVÁ

Doctoral study programme:
P3710 Technique and Technology in Transport and Communications

Field of study:
3708V024 Technology and Management in Transport and Telecommunications

Supervisor:
doc. Ing. Jaromír Široký, Ph.D.

Supervisor specialist:
Ing. Petr Nachtigall, Ph.D.

Doctoral thesis has arisen at the supervising:
Department of Transport Technology and Control

ABSTRACT

A dissertation thesis deals with the analysis of existing situation on authorisation type of vehicles in Slovak Republic and foreign countries. It is concerned with the Commission Recommedation 2014/897/EU of 5th December 2014 on matters related to the placing in service and use of structural subsystems and vehicles under Directives 2008/57/EC and 2004/49/EC of the European Parliament and of Council which should be application guide for this area. A main goal of dissertation thesis is to ensure the interoperability (new directives, regulations, decisions, recommendations) and to create the methodology of authorisation type of vehicles especially SW model as a tool with using the EU legislation for speeding up the whole process. It contains the analysis of scientific methods which were used for the assurance of the main goals.

1. Current state in the field of doctorate thesis

The main task of the authorisation process of the type of vehicles is to attract wider interest of the public into production and import in the area of transport. It is regarded mainly to safety but also to ensure the quality, reliability and lifecycle of the rolling stocks at a required level. These requirements need to be assured and at the same time they should be a tool to satisfy transport needs. The vehicles should reflect the progress in science and technology and their construction should be in harmony with the development of transport.

Ensuring the aims of interoperation within the spectre of rail system in the European Union should result in setting up the optimal level of technical harmonization and mitigate, improve and further develop services that are offered within the international railway transport. The aim is to create an inner market with facilities and services targeting at building, innovation, modernization and operation of railway system in the Union. Within the fourth railway packet is suggested a new procedure of authorising a new type of rail vehicles and their allowance into operation. The aim is to move the competences of authorising and certifying the types of rail vehicles onto European Union Agency for Railways "EUAR". Individual activities should be carried out on the basis of dividing the competences between EUAR and National Safety Authority "NSA". Objective activities will be carried out on the basis of the legal relation of these two bodies. Fundamental is elimination of national regulations and direct exercisability of TSI as internal regulations for the whole railway network.

Analysis of the current state both home and abroad

Authorising the types of railway vehicles is an integral part of transport process. The main goal should be securing the safety of transport. The aim of every authorising body is to ensure that the authorising process was carried out in accordance with the European legislation and in a non-discriminating way.

Current state of authorising the types of railway vehicles within the conditions in the Slovak republic

Development of authorising the types of railway vehicles has gone through several changes since the establishment of the Slovak republic. Every development stage was aiming to make the process easier and ensure the continuity of particular activities in every area.

Authorising the types of railway vehicles has changed a lot since the Slovak republic was established in 1993. It is possible to divide this process into several development stages that are described in detail in this doctorate thesis. These are:

- authorising the types of railway vehicles in years 1993-1996,
- authorising the types of railway vehicles in years 1996-2009,
- authorising the types of railway vehicles in years 2009- 2014.
- authorising the types of railway vehicles in years after possible shift of competences onto EUAR (after year 2020).

Current state of authorising the types of railway vehicles abroad

Authorising the types of railway vehicles and putting them into operation are carried out in individual countries by the authorising bodies or NSA (National Safety Authority) in accordance with the directive (EU) 2016/797 of the European Parliament and of the Council on the interoperability of the rail system within the European Union and also in accordance with particular related regulations, decisions and recommendations, and upon its transposition into national legislation.

To analyse the current situation in the area of authorising the types of railway vehicles we have used the knowledge acquired at different conferences and also available literature as well as studies from universities and research institute. The analysis was carried out in six countries – Poland, Austria, Hungary, the Czech Republic, Spain and Germany.

Within the analysis we have also analysed the legislature in the area of authorising the types of railway vehicles and competencies of particular bodies. With the help of administrative outputs, we have made an overview of registered vehicles in individual member countries, notified people carried out in member countries and types of vehicles registered in the European Register of Authorised Types of Vehicles (ERATV).

Conclusion of the analysis

Commission Recommendation 2014/897/EU defines particular important parts in the area of authorising structural subsystems and vehicles into operation. It is a broad manual or rectification how to proceed in this area in such way as to follow clauses of directive 2008/57/ES. There is not a graphically shown procedure in the area of authorising the types of railway vehicles that are in accordance with technical specifications of the interperability (TSI) or are not in accordance with TSI and their consequent putting into operation. This will be a part of the suggested methodology.

Individual studies from scientific fields concentrate only on partial activities in the area of authorising the types of railway vehicles. They do not define the authorising process as a complex of activities, they do not say how to simplify or fasten it as a whole. To shorten the length of time of the authorising process, it was necessary to review and analyse particular problems that could emerge during the process. Because of this, it was inevitable to secure operative solutions of problems that can occur. Not to foresee these problems could lead into extending the length of time necessary for authorising. Creating a convenient methodology for authorising the types of railway vehicles is an appropriate solution of these drawbacks and prevention from extending the authorising process.

2. Defining the aim of the doctorate thesis

The aim of the doctorate thesis was to outline methodology in the area of authorising the types of railway vehicles with the emphasis on applying interoperability, new European regulations, directions and decisions. The methodology was graphically plotted with the help of a developing diagram. We have also created SW model of applying the European legislature aimed at authorising the types of railway vehicles and minimising the administrative difficulties.

The doctorate thesis includes verification of the outlined model on practical examples right at the execution of actions of the authorising body.

Setting up the hypothesis

On the basis of acquired experience we have set up the following hypothesis:

With the use of the outlined methodology the length of time of the authorising process of the types of railway vehicles will be shortened by 30%.

To verify the hypothesis, we have used the Gantt's graph. With its use is shown the length of particular actions during the process of authorisation with and without the use of SW model. Objective verification was carried out in the following three cases:

1. installing a mobile part ETCS L 1 into a vehicle – essential change of a railway vehicle,
2. authorising a type of railway vehicle – three system electric locomotive class 381 type 109 E2,
3. authorising a type of railway vehicle – diesel unit class 861, type VR – 24 – 2010 - DMJ.

Following the procedure of current authorising system on particular examples, it was possible to rate how much time can be saved when compared with the current authorising system. The aim was to lead to minimise the administration during the authorising or allowing the types of railway vehicles, in accordance with the new regulation of interoperability which should be transposed until June 16th2019, latest until year 2020.

3. Methods and solution way used

In the doctorate thesis is, based on the found differences and problems that could emerge during the process of authorising the types of railway vehicles, outlined methodology of authorising the types of railway vehicles as a supporting tool for setting up the SW model.

3.1 Chosen methods

Apart from the basic methods (analysis, synthesis, brainstorming etc.) we have used also other methods that are necessary for solving the stated problematics.

The theory of system modelling

The theory of modelling deals with particular areas of knowledge. Modelling itself is used within the research of social phenomena, psyche and cognitive phenomena. In relation to modelling is used also term model that could be characterised as an "imitation". It could be carried out with the relation to practical tasks or in relation with the research. And its parts are also working methods such as mathematical and experimental modelling. (55)

Usage: while creating the SW model.

Simulation

Simulation is an experimental method during which a real system is replaced by a computer model. Its basis is that the examined dynamic system is replaced by its simulator and this one is used to gain information about the original system. Simulation is carried out on a created model (simulator) which imitates simulated system and is limited on a physical object created for this particular use. (56)

Usage: verifying the model on particular examples

Visual Basic Application (VBA)

Visual Basic Application Excel macros allow saving time, optimising processes and also lowering the number of mistakes in particular calculations. Excel macro is a program that can take several actions instead of a person, worker. As an appropriate example, we can imagine that a person needs to copy several different tables daily from different Excels into one file and in every table also needs to make particular mathematical calculations, format the table, underline very other line etc. (58)

Usage: SW model as a support of the methodology

Gantt's graph

Gantt's graph is used to display particular actions and their length of time. It is then used for planning the project and displaying its stages. It can be used to display expected time consumption and also sequence of particular parts within the stated project. To manage and control the project it is necessary to have a detailed and realistic planning. Gantt's graph acts as an overview of the observed process only. (59, 60)

Usage: displaying the length of time of particular activities and verifying the hypothesis

3.2 Methodology of authorising the types of railway vehicles and a SW model as a supporting tool of authorising methodology

The aim of the outlined methodology in the area of authorising the types of railway vehicles with the emphasis on using the interoperability, new European regulations, rules and decisions, was to set up particular possible ways how the authorising itself can be carried out. The methodology is graphically shown with the help of development diagram and is afterwards reflected onto a SW model which is the main tool to minimise the administrative difficulties of the whole process.

SW model can also be called as a tool to minimise the administrative problems of the whole process. It was created by the VBA macros.

When creating the Form, we have used used one of the parts of Microsoft Office package – Microsoft Excel with VBA editor. I have based my decision to use this on several criteria:

1. MS Excel is a part of Microsoft Office package which is currently installed on most computers used in administration.
2. MS Excel includes VBA editor which is actually a programming language for Microsoft Office, and this opens a lot more other options.
3. It is possible to open also other files from MS Excel which allows us to have a database in a separate file.
4. Within the VBA it is possible to create files in program MS Word.
5. Possibility to create pleasant and user-friendly graphical environment.
6. To create keys and sheets in a standard that the user is familiar with from MS Windows.

Programming

Overall creating or generating the Form and final decision about authorising the type of railway vehicle was carried out by VBA macros – by the programming. Used were both global variables and functions.

Form (Exercise book)

The main exercise book that is used by the user was named as “Form”. It contains one page with the same name. The whole Form is named as “The Form about decision of authorising the railway vehicle”. It is pre-programmed and locked and the user can fill it in by the keys used for this purpose. In the first part are keys “Fill in” that are used to fill in information and “Delete” that is used to delete the filled in data. The latter is of course secured by the warning whether the Form should really be deleted. Filling in the Form can be postponed at any stage and particular steps can be filled in separately. For filling in the Form are always used sheets created in VBA. There are programmed functions and automatic filling in to make the work for the user as easy as possible, effective and without mistakes. The Form adapts itself according to filled in data so the original and the final one can look completely different. The outcome of the whole Form is a prescribed decision in MS Word. Another advantage of the Form is also that it is automatically saved into a file and so it is possible to go back to filling it in any time in the future.

VBA

Programming in VBA is divided in the following files:

1. Modules

It contains only one module (General) which includes global variables and functions that serve for work with programs Word and Outlook.

2. Microsoft Excel Objects

It contains one „Workbook“ which also has a function that starts right after opening the Form. This function should serve to find the way to the file. It is a key for next steps to make it possible to open the database and prescribed documents in Word.

It also contains one „Worksheet“ which includes:

1. function for opening the database,
2. function that controls whether the particular cells in the Form have not been changed and on the basis of these changes it saves the Form with a new name or it adapts the Form according to filled in data (shows and hides parts of the Form),

It also contains serving functions that are invoked by pressing particular keys. Note: these functions open further particular forms and functions according to the key pressed.

Forms

There are 15 forms that are used to fill in the Form. These forms invoke by themselves or after pressing a key.

Every form consists of two parts:

- „Object“ which is its graphic draft,
- „Code“ which includes source code for particular „Object “. „Code“ contains functions that invoke themselves when opening particular form (it serves for initial initialisation and filling in the form based on the data already stated in the form). It also includes functions that are opened while filling in particular cells (these serve mainly as an assurance that the data have been filled correctly or to make sure that data have been filled automatically). Functions that are shown after pushing a button serve mainly to open other forms or to close the form.

Parts in a graphic interface for Form have been set up with the help of „Properties“ for particular elements. All the functions and methods used when programming are described in the Help Excel – VBA (option to display after pressing key F1 when the cursor is on this command).

The whole filling in the Form leads to generating a complete decision that is filled in with the data from the database too.

As is shown below in pictures 1 -3, the basis is to submit a request for authorising the type of railway vehicle. At first it is necessary to state or decide whether it will be authorising of the type of railway vehicle, its modernisation or innovation. Sending the request in an electronic form will enable its faster submitting and authorising body can start the process of its evaluation sooner. Afterwards, the authorising body can find an applicant in a database of producers, or it can generate it for the next use. The database is or will be constantly updated according to the needs of the authorising body which will speed up the process of making the decision, where the date will be automatically reflected.

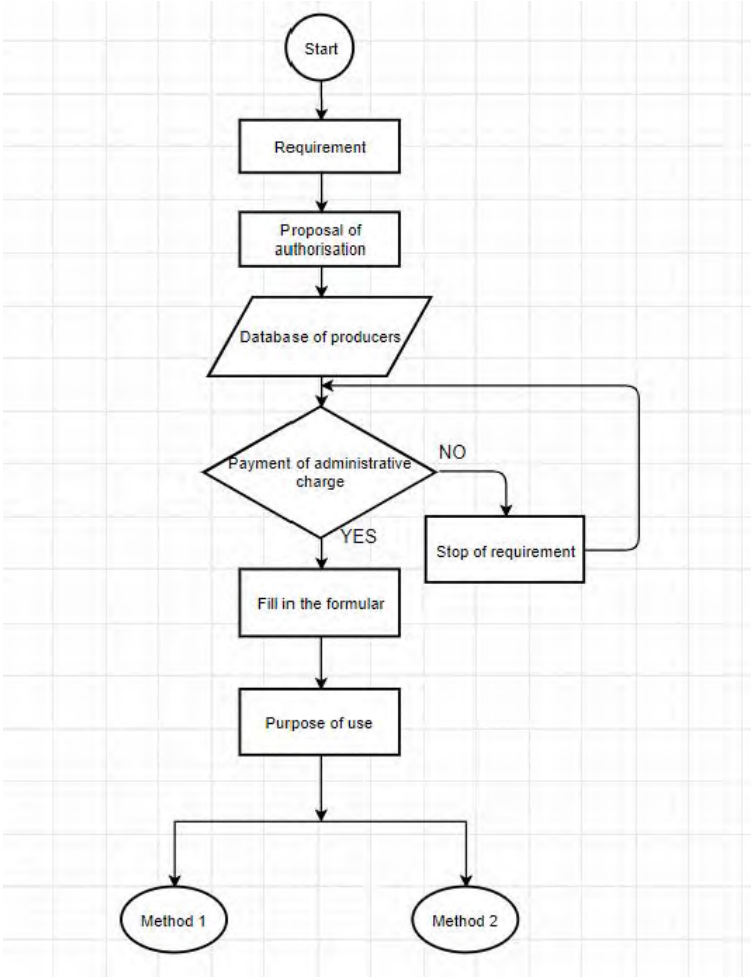

Picture 1. Basis for VBA I. Source: author

After setting the purpose of use it is possible to state which way the authorisation will go, or which method will be used**.**

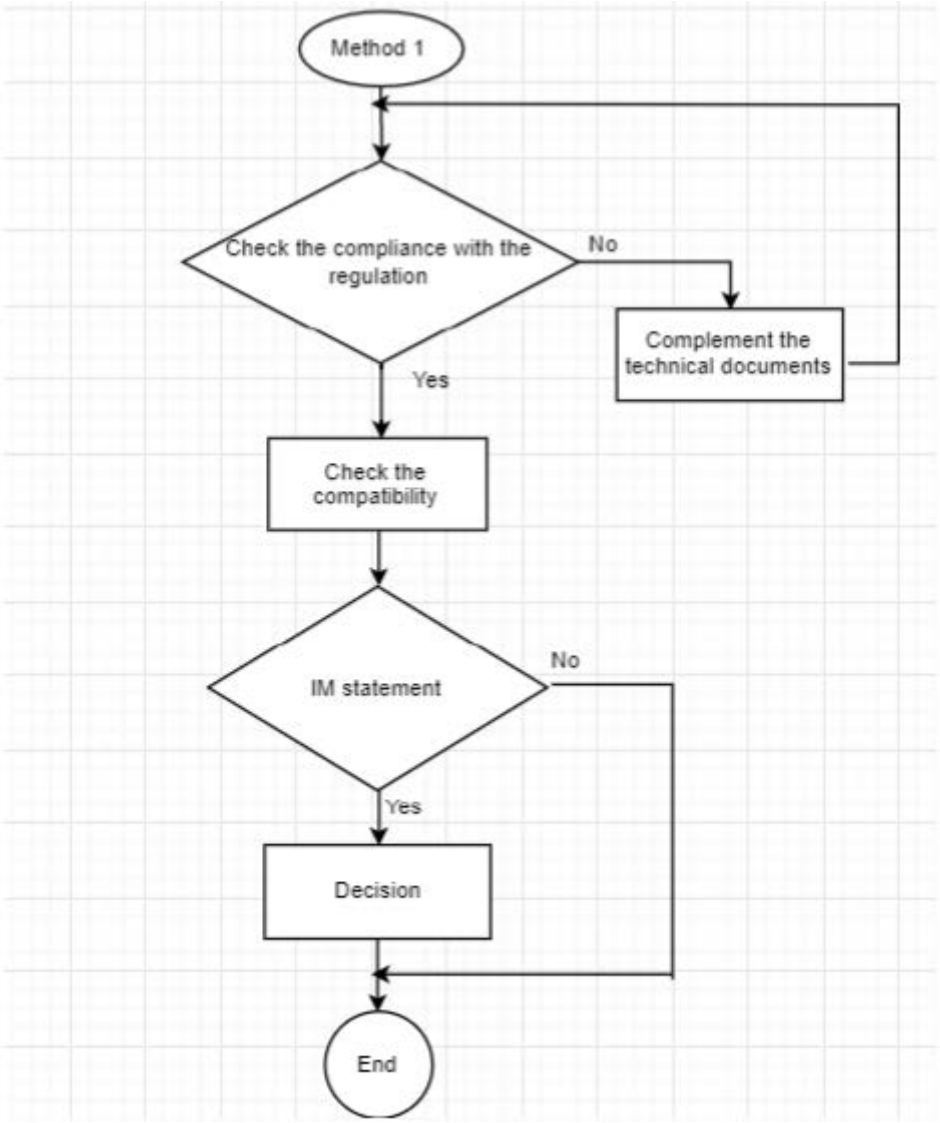

Picture 2. Basis for VBA II. Source: author

In method 1 we count with the authorisation according to specifications of regulative, mainly with the intestate legislature. That is the reason why we have already accounted in this methodology with the fact that the user will have an updated version of the regulation. After accomplishing the requirements, it is possible to proceed to generating the decision itself.

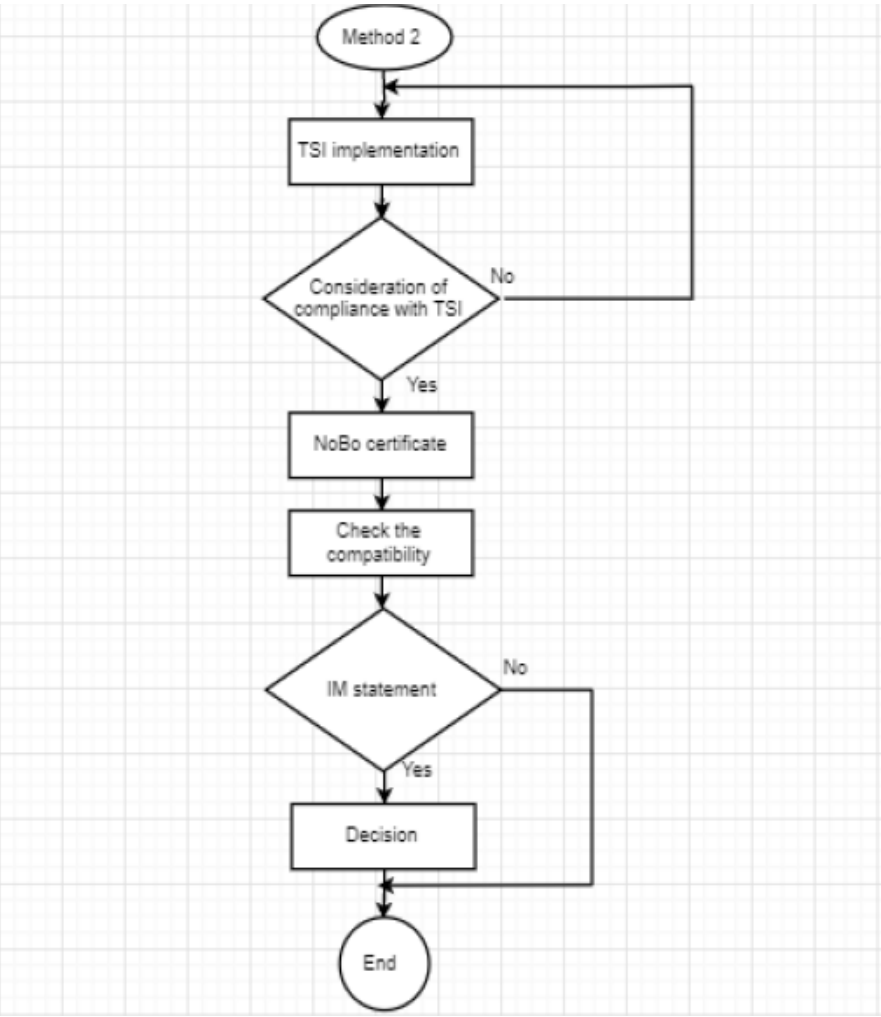

Picture 3. Basis for VBA III. Source: author

Second version of authorising is verifying the compliance with TSI. Here it is necessary to get a reviewing from Notified Body (NoBo). That is the reason why we have already accounted with the option of connecting to NoBo. The system also takes into account a possibility of submitting the information about the type of vehicle, range of vehicle, power etc.

4. Achieved results

Methodology of authorising the railway vehicles and its usage was verified by the use of simulation directly in MS Excel with the use of macros VBA (Visual Basic Application). The aim was to state an estimation or the length of time of the authorising process of the railway vehicles or different cases within this process. To show the length of particular activities we have used the Gantt's graph.

4.1 Installing a mobile part ETCS L1 into an electrical multiple unit class 671 type 214

Overall time of the process allowing the essential change dwelling in installing ETCS L1 into EPJ class 671 type 214 was 213 working days.

Overall time of the process allowing the essential change dwelling in installing EPJ class 671 type 214 into ETCS L1 into a vehicle with the use of SW was 164 working days.

Process of authorisation with the use of the system was shortened as followed:

213 – 164 = 49 working days

Process without the use of SW..... 213 working days

Process with the use of SW ..... 164 working days

Save (U) ..... 49 working days

U= 49/213×100

U=23 %

Percentual savings..... 23%

Hypothesis:

With the use of the outlined methodology the time of authorising process of the railway vehicles will be shorter by 30 %.

In this case the stated hypothesis was not fulfilled. Percentual saving is 23%. We have not accounted with creating a prototype board. Even with this, we can see a large percentage of shortening the length of the process. The time of the authorisation is therefore individual, case to case.

4.2 Authorising the three-system electrical locomotive class 381 type 109 E2

Overall time of the authorising process of the locomotive class 381 type 109 E2 was 122 working days.

Overall nett time of the authorising process with the use of SW system was 64 working days. To make this time even more effective, there was established a prototype commission which allowed solving several possible inconsistencies even before submitting the application for authorisation.

The process of authorisation with the use of the system was shortened as follows:

122 – 64 = 58 working days

Process without the use of SW..... 122 working days

Process with the use of SW (without the commission)..... 64 working days

Process with the use of SW (with the commission) ..... 85 working days

Savings (U1) ..... 58 working days

Savings (U2) ..... 37 working days

U_1= 58/122×100

U_1= 47 %

U_2= 37/122×100

U_2= 30,33 %

Percentual savings without the commission..... 47 %

Percentual savings with the commission..... 30, 33 %

Hypothesis:

With the use of outlined methodology, the authorisation process of the types of railways vehicles can be shortened by 30 %.

In this case the stated hypothesis was approved. Percentual saving of the authorisation process means, including the length of time of the prototype commission, 30, 33 %. The prototype commission

markedly influences the nett time of the authorisation process. As we have already mentioned, the saving of time is very individual. To improve or shorten this can be secured by establishing the prototype commission.

4.3 Authorising the diesel unit class 861 type VR – 24 – 2010 – DMJ

Overall time of the authorisation process of DMJ class 861 type VR – 24 – 2010 - DMJ was 153 working days.

Overall nett time of the authorisation process with the use SW was 40 working days. To make this time even more effective, there was established the prototype commission which enabled to solve some of the inconsistencies even before submitting the application for authorisation.

The process of authorising with the use of the system was shortened as follows:

153 – 40 = 113 working days

153 – 96 = 54 working days

Process without the use of SW..... 153 working days

Process with the use of SW (without the commission).....40 working days

Process with the use of SW (with the commission).....96 working days

Savings (U1) ..... 113 working days

Savings (U2) ..... 54 working days

U_1= 113/153×100

U_1= 73 %

U_2= 54/153×100

U_2= 35,29 %

Percentual savings without the commission..... 73 %

Percentual savings with the commission..... 35, 29 %

Hypothesis:

With the use of the outlined methodology the time of the authorisation process of the railway vehicles will be shortened by 35, 29 %.

In this case the hypothesis was approved. Percentual savings of the authorisation process is, including the length of time of the prototype commission, 35,29%. As we have mentioned before, the savings of time are very individual and change with each case. To improve or shorten the time is also possible by establishing the prototype commission which can influence the length of the authorisation process.

4.4 Concluding the acquired results

On the basis of the verification of the outlined methodology of the authorising the types of the railway vehicles with the use of SW system, we can conclude that the time of the authorisation process is very individual and changes with each case.

When verifying the stated hypothesis in practice in the first case – Implementing a mobile part ETCS L1 into an electric multiple unit class 671 type 214, the hypothesis was not approved. The saving of the authorisation time was by 23%. However, even this result is a significant shortening.

In the second case – authorising the three-system of an electric locomotive class 381 type 109 E2, there was a significant shortening of the authorisation time. It is very important to remark that there was established a prototype commission which can directly influence the nett time of the authorisation process. Because there was a 30,33% shortening of time, the hypothesis was approved.

The third case – approving the diesel unit class 861 type VR – 24 – 2010 – DMJ – have also approved the stated hypothesis. There was also established a prototype commission which influenced the overall authorisation time into such extent, that the shortening was by 35, 29 %

In the table 1 is shown comparison of the verified results in particular cases.

Table 1. Conclusion of verifications

Case	Without SW	Savings days with SW (Without commission)	Saving %
C1	213	49	23
C2	122	64	47
C3	153	113	73

Source: author

During the verification of the particular cases, we have used simulation, stated estimation of the length of particular stages (mostly when using the SW system), and also the method of brainstorming. The lengths of time were estimated on the basis of discussions with the representatives of the authorising bodies or related subjects.

5. Contributions of the graduant

The doctorate thesis contains complex mapping and summarising of the current situation in authorisation process of the types of railways vehicles both home and abroad. It gives information of the real legislature related to train railway vehicles. It also offers an overview of the stated problematics to both wide public and academic field.

Methodology, which is based on SW model, significantly makes the authorisation process easier and faster. It secures clear evidence and more effective cooperation. It also sets up a possibility of using new modern SW tools in the authorisation process. Most of the communication happens online, including the issuing the particular documents which are a basis for the decision of the authorisation. Therefore, it creates savings of postage costs as well as office material.

The outlined methodology can be used also internationally. It is possible to change it according to one's needs. After supplementing further functions, it can be adjusted for the needs of EUAR and can speed up the communication and exchanging of the information between the EUAR and interstate authorisation bodies. This can be secured by the contact treaty between the EUAR and NSA. The aim is to use the SW model in accordance with the European legislature. It will result in saving the time of the authorisation process, as well as saving the costs related to it.

The methodology is an asset also to producers and owners of the railway vehicles as well as wide public. Thanks to this methodology there will be a faster exchange of the information, time and cost saving and a possibility of operative solution of the possible problems.

References

MAGDECHOVÁ, K. Analýza vývoja schvaľovania typov dráhových vozidiel v podmienkach Slovenskej republiky, In: Zborník z medzinárodnej konferencie Horizonty železničnej dopravy 2014, str. 140 - 149, ISBN 978 – 80 – 554 – 0918 - 4

Zákon č. 51/1964 Zb. o dráhach vrátane jeho neskorších zmien

Zákon č. 104/1974, ktorým sa mení a dopĺňa zákon č. 51/1964 o dráhach

Vyhláška Ministerstva dopravy č. 52/1964 Zb., ktorou sa vykonáva zákon o dráhach

Vyhláška Federálneho ministerstva dopravy č. 18/1981 Zb. o schvaľovaní dráhových vozidiel a osobitných dráhových mechanizačných zariadení úloha

TOMČALA, I. Niektoré problémy uplatňovania vyhlášky MDPT SR č . 250/1997 Z . z . pri schvaľovaní typu dráhového vozidla, In: Zborník zo XIV. medzinárodnej konferencie- Súčasné problémy v koľajových vozidlách, PRORAIL 99, Žilinská univerzita v Žiline 1999, ISBN 978 – 80 – 7100 – 645 - 9

Zákon NR SR č. 164/1996 Z. z. o dráhach a o zmene zákona č. 455/1991 Zb. o živnostenskom podnikaní (živnostenský zákon) v znení neskorších predpisov

Vyhláška MDPT SR č. 250/1997 Z. z., ktorou sa vydáva dopravný poriadok dráh

Zákon NR SR č. 513/2009 Z. z. o dráhach a o zmene a doplnení niektorých zákonov (vrátane konsolidovaného znenia)

SMERNICA EP a RADY č. 2008/57/ES o interoperabilite systému železníc v Spoločenstve (vrátane konsolidovaného znenia)

SMERNICA EP a RADY č. 2004/49/ES o bezpečnosti železníc spoločenstva a o zmene a doplnení smernice Rady č. 95/18/ES o udeľovaní licencií železničným podnikom a smernici č. 2001/14/ES o prideľovaní kapacity železničnej infraštruktúry, vyberaní poplatkov za používanie železničnej infraštruktúry a bezpečnostnej certifikácii

Vyhláška MDPT SR č. 351/2010 Z. z. o dopravnom poriadku dráh (vrátane konsolidovaného znenia)

MAGDECHOVÁ, K., NACHTIGALL, P. Zmeny v schvaľovaní typov dráhových vozidiel, In: Zborník z medzinárodnej konferencie Horizonty železničnej dopravy 2013, str. 242 - 248, ISBN 978 – 80 – 554 – 0764 - 7

ROZHODNUTIE KOMISIE č. 2011/314/EÚ o technickej špecifikácii interoperability týkajúcej sa subsystému „prevádzka a riadenie dopravy“ (vrátane konsolidovaného znenia)

ROZHODNUTIE KOMISIE č. 2012/757/EÚ o technickej Specifikácii interoperability týkajúcej sa subsystému „ prevádzka a riadenie dopravy“ systému železníc v Európskej únii a o zmene a doplnení rozhodnutia Komisie č. 2007/756/ES s účinnosťou od 1. 1. 2014 (vrátane konsolidovaného znenia)

ROZHODNUTIE KOMISIE č. 2007/756/ES, ktorým sa prijíma spoločná špecifikácia národného registra vozidiel uvedená v čl. 14 ods. 4 a 5 smerníc 96/48/ES a 2001/16/ES (vrátane konsolidovaného znenia)

ROZHODNUTIE KOMISIE č. 2011/665/EÚ o Európskom registry povolených typov železničných vozidiel (vrátane konsolidovaného znenia)

LAVOGIEZ, H., DECHAMPS, J - M., ARDIACA, F. Type of Vehicle, ERA Workshop on Vehicle Authorisation, Lille 08. February 2012

ERA: Informácie o krížovej akceptácii, dostupné z: http://www.era.europa.eu/Core-Activities/Cross-Acceptance/Pages/home.aspx

ROZHODNUTIE KOMISIE č. 2009/965/ES z 30. novembra 2009 o referenčnom dokumente uvedenom v článku 27 ods. 4 smernice Európskeho parlamentu a Rady 2008/57/ES o interoperabilite systému železníc v Spoločenstve (vrátane konsolidovaného znenia)

Dopravný úrad SR: Informácie o krížovej akceptácii a referenčnom dokumente [online], dostupné z: http://drahy.nsat.sk/interoperabilita-zeleznicnych-drah/referencny-dokument-a-krizova-akceptacia/

ERA, SK NSA: National Reference Document: Slovak Republic; 31. May 2011, ERA/TD/2009-01/XA

Ministerio de Fomento España: Case Study: APIS for SW upgrade, november 2012

UTK: Informácie o poľských dopravných predpisoch a postupoch schvaľovania [online], dostupné z: http://www.utk.gov.pl/

NKH: Informácie o maďarských dopravných predpisoch a postupoch schvaľovania [online], dostupné z: http://www.nkh.gov.hu/a-hatosagrol

OBB: Informácie o rakúskych dopravných predpisoch a postupoch schvaľovania [online], dostupné z: http://www.ts.oebb.at/de/

OBB Infra: Informácie postupoch schvaľovania v Rakúsku [online], dostupné z: http://www.oebb.at/infrastruktur/de/

TOURNIER, NT., DRILLER, J. The National Legal Framework (DE), Technical Document (Reference Document Part 3)

EBA: Informácie o nemeckých dopravných predpisoch a postupoch schvaľovania [online], dostupné z: http://www.eba.bund.de/DE/Home/home_node.html

EBA, Schweizerische Eidgenossenschaft, ANSF, BMVIT, HETI: Cross Acceptance and Corridor Guideline, Control Command and Railway Communication Conference 2012, Lille, 6 - 7 November 2012

ERA. Progress with Railway Interoperability in the European Union, Biennial Report, 2013

ERA: Informácie o registri povolených typov vozidiel [online], dostupné z: https://eratv.era.europa.eu/eratv

IHNÁT, P. Interoperabilita železníc Spoločenstva, In: Železničná doprava a logistika, Žilinská univerzita v Žiline 2006, str. 103 - 109, ISSN 1336 - 7493

MAGDECHOVÁ, K. Telematické aplikácie v nákladnej a osobnej železničnej doprave, In: Zborník z medzinárodnej konferencie LOGI 2012, str. 252 - 256, ISBN 978 - 80 – 263 - 0336 - 7

MDVRR SR: Informácie o technických špecifikáciách interoperability [online], http://www.telecom.gov.sk/index/index.php?ids=60401

EUROPEAN COMMISSION, DG MOVE. Report on the work performed by the task force on railway vehicles authorisation, Brussel 09. July 2012

ERA, EK. Progress on the Vehicle Authorisation Task Force Recommendations, EC ERA Workshop on Vehicle Authorisation, Lille 08. February 2013

ODPORÚČANIE KOMISIE č . 2014/897/EÚ z 05. decembra 2014 o záležitostiach súvisiacich s uvedením do prevádzky a používaním štrukturálnych subsystémov a vozidiel podľa smerníc Európskeho parlamentu a Rady 2008/57/ES a 2004/49/ES (vrátane konsolidovaného znenia)

EK: Informácie o dopravnej legislatíve EÚ [online], dostupné z: http://ec.europa.eu/index_en.htm

ARDIACA, F. DV 29bis, Workshop DV 29 bis, Lille 14. November 2013

LOCKETT, R. The Vehicle Authorisation Process, ERTMS Conference, Lille 6. - 7. November 2012

ARDIACA, F., LO YACONO, L. Authorisation Type of Vehicles, Final Report, 30. April 2013

VÚD Žilina. Implementácia interoperability konvenčných železníc SR, Záverečná správa 2005

BAČIŠIN, M., FUSATÝ, M., PALUCH, J. Výpočtový nástroj obrysu koľajových vozidiel s dôrazom na interoperabilitu, Žilinská univerzita v Žiline 2012, str. 10 - 15, ISSN 1336 - 7943

REMING Consult, a. s., SUDOP Praha, a. s., AM Sudop spol. s. r. o.: Technicko- ekonomická štúdia pre prípravu a implementácia ERTMS na koridore E , jún 2010

GUIDO, P. Specifications for Interoperability, ERTMS Conference, Lille 6. -7. November 2012

ČECH, R.: Analýza nákladů a přínosů implementace TSI, disertační práce DFJP, 2012

JINDRA, P. Systémová implementace provozní interoperability železniční nákladní přepravy, disertační práce DFJP, 2010

Frid, A., Leth, S., Högström, C., Färm, J.: Noise control design of railway vehicles- Impact of new legislation, Journal of Sound and Vibration, 2006, Vol. 293 (3), pp. 910 - 920, ISSN 0022 - 460X

ROZHODNUTIE KOMISIE č . 2012/88/EÚ o technickej špecifikácii interoperability týkajúcej sa subsystémov riadenia- zabezpečenia a návestenia transeurópskeho železničného systému z 25. januára 2012 (vrátane konsolidovaného znenia)

MYDIA, S., THOTTAPPILLIL, R.: An overview of electromagnetic compatibility challenges in European Rail Traffic Management Systém, In: Transportation research Part C, 2008, Vol. 16(5), pp. 515 - 534, ISSN 0968 - 090X

GHAZEL, M. Formalizing a subset of ERTMS/ETCS specifications for verifications purposes, In: Transportation Research Part C, 2014, Vol. 42, pp. 60 - 75, ISSN 0968 - 090X

GUIDO, P. ERTMS Baselines, UIC ERTMS World Conference, Istanbul 2. Apríl 2014

BIERLEIN, H. Certification and placing in service, ERTMS Conference, Lille 6. - 7. November 2012

ŽU v Žiline – Fakulta špeciálneho inžinierstva: Úvod – všeobecné základy modelovania [online], dostupné z: http://www.fsi.uniza.sk/ktvi/leitner/2predmety/OA/00Vseobecne%20o%20modelovani.pdf

Strojnícka fakulta TU v Košiciach: Simulácia technologických procesov [online], dostupné z: http://www.sjf.tuke.sk/mmnv/UPLOAD/studentom/PS/2.pdf

Paholok, I.: Simulácia ako vedecká metóda, In: E – LOGOS (Electronic Journal for Philosophy/2008) [online], ISSN 1211 – 0442, dostupné z: http://nb.vse.cz/kfil/ elogos/student/paholok08.pdf

LMCTn: Informácie o práci s VBA makrami [online], dostupné z: http://www.lmctn.sk/makra_excel

Lorenc, M.: Ganttův diagram v Excelu [online], dostupné z: http://lorenc.info/3MA381/graf-ganttuv-diagram.htm

Ott, V.: Co je to Ganttův diagram a k čemu vám může být dobrý, In: Denník neziskovky [online], dostupné z: http://denikneziskovky.cz/co-je-to-ganttuv-diagram-a-k-cemu-vam-muze-byt-dobry/

Author´s publikations

Publikačná činnosť

Magdechová. K.: Telematické aplikácie v nákladnej a osobnej železničnej doprave; Logi 2012; Pardubice 22. 11. 2012; zborník str. 252- 256, ISBN 978-80-263-0336-7

Magdechová, K., Široký, J.: Telematic applications for freight and passengers in railway transport; Horizons of Railway Transport; str. 84 - 86; Vol.3 ; 2012

Magdechová, K.: Analýza vytvárania spoločného podniku Shift²Rail; Železničná doprava a logistika, str.61, X ., 2014, ISSN 1336 - 7943

Magdechová, K.: Analýza železničních priecestí v podmienkach Slovenskej republiky; Aktuální trendy v dopravě a ekonomice 2013 (virtuálna konferencia), Pardubice 2014, zborník str. 22 - 30, ISBN 978 – 80 – 86530 – 90 - 1

Magdechová, K., „Analýza technických špecifikácií interoperability železničného systému v Európskej únii“, poster na 12. fóre koľajovej dopravy, Bratislava 15. – 16. 03. 2016

Active participation at conferencies and publications in collections

Magdechová, K., Nachtigall, P.: Zmeny v schvaľovaní typov dráhových vozidiel; Horizonty železničnej dopravy 2013, 26.-27. september 2013, zborník str. 242 - 248, ISBN 978 – 80 – 554 – 0764 - 7

Magdechová, K.: Analýza vývoja schvaľovania typov dráhových vozidiel v podmienkach Slovenskej republiky, Horizonty železničnej dopravy 2014, 18.-19. September 2014, zborník str. 140 - 149, ISBN 978 – 80 – 554 – 0918 - 4

Výberová prednáška na zasadnutí TSI PRM poradného orgánu: „National Implementation Plan of the Slovak Republic“ (Brusel 05th November 2015)

Magdechová, K., Aktuálny stav implementácie interoperability konvečného systému železníc v SR, presentation at conference Horizonty železničnej dopravy 2016, Strečno 29. – 30. september 2016

Magdechová, K., Národné kontaktné miesto pre telematické aplikácie v osobnej a nákladnej doprave (TAF/TAP TSI), presentation at 5th regional meeting on telematics application for freight (TAF TSI), Bratislava 4th october 2016

Magdechová, K., 5th TAF TSI Workshop in Bratislava – solutions of the problems, presentation at TAF TSI working group, Lille 22nd March 2017

Magdechová, K., Slovak National Implementation Plan for TSI PRM, presentation at TSI PRM Advisory Committee, Brusel 5th apríl 2017

Magdechová, K., WAGON SERVICE travel – Special trains, prezentácia na konferencii Horizonty železničnej dopravy 2017, 21. -22. september 2017

Siroky, J., Sramek, P., Magdechova, K., Tischer, E., Siroka, P.: Capacity range calculation, Electronical technical journal of technology, engineering, and logistic in transport „Perner´s Contacts“, University of Pardubice, Jan Perner Transport faculty, Pardubice, Number IV, Volume XIX, December 2019, in print, ISSN 1801-674X, avaible: <http://pernerscontacts.upce.cz/>

Siroky, J., Sramek, P., Magdechova, K., Tischer, E., Hlavsova, P.: Timetable performance evaluation, Proceedings of 23rd International Scientific Conference. Transport Means 2019. Pp. 1427-1432. ,ISSN 1822-296X

Loss of Stability of Thin-Walled Conical Shells with Circumferential Ring Loaded by Axial Force

Author: Ing. Haluk YILMAZ

Doctoral study programme:
P3710 Technique and Technology in Transport and Communications

Field of study:
3708V024 Technology and Management in Transport and Telecommunications

Supervisor:

doc. Ing. Petr Tomek, Ph.D.

Supervisor specialist:

Prof. Ing. Petr Paščenko, Ph.D.

Doctoral thesis has arisen at the supervising:

Department of Mechanics, Materials and Machine Parts

ABSTRACT

This dissertation is devoted to the effects of the circumferential ring on the loss of stability of the conical shells loaded by an axial force. The truncated conical shell with different shell thicknesses and base angles at the lower edge are investigated in this thesis. The main aim is a proposal a new method to calculation of load carrying capacity of the conical shell structures with a base angle less than 25° loaded by axial force. The proposed method is applicable for different radial stiffness of the circumferential ring. Two dimensionless similarity parameters are used in this method. Numerical models are created in COSMOS/M package program. The numerical analyses were performed for different angles, shell thickness and radial stiffness of circumferential ring. Empirical relationships are established based on the results of the numerical analysis.

KEYWORDS

Conical shell, Circumferential ring, Load Carrying Capacity, Axial loading, FEM

1. INTRODUCTION

Thin-walled shells have a widespread application in aerospace, mechanical, civil and structural engineering concepts in different shapes and types such as robots, shelters, domes, tanks, silos, machinery and energy absorbers. They have also significant importance for carrying liquids, pressurized gasses, and hazardous substances in road haulage, railroad and water transports. The use of the curved skin of vehicles as a load bearing member has similarly revolutionized the construction of aircraft. In the construction of all kind of spacecraft, the idea of a thin but strong skin has been used from the beginning. The demands in the thin- walled shells are quite prevalent as stated above. However, the thin- walled shells are considerably prone to loss of stability. Therefore, there is a great concern for the designers achieving maximum strength with a cost-efficient solution in the shells.

In present days, updated standards and recommendations provide useful approaches. They solve stability of the conical shells with the base angle which is higher than 25° and clamped lower end [5,6]. Nevertheless, the standard methods are not applicable for the shells which have the base angle less than 25°. Besides, the rules which are included in the recommendations can be applied only to conical shells which have clamped edges or edge with the very stiff ring. In other words, if a conical shell has either base angle less than 25° or free/flexible radial stiffness at the edges, these rules cannot be applied.

Determining the load carrying capacity of the nonstandard structure might be infeasible by referring the procedures within the context of the standards and recommendations because it is difficult to estimate the nonlinearity of the structure. Likewise, the recommendations and standard methods are based on the linear theory of the shells.

This study focuses on the load carrying capacity of the conical shells with a base angle less than 25° which have flexible boundary ring under axial loading. This area has lack of knowledge in the literature. Therefore, the main goal of the study is assigned to propose of a new method to estimate load carrying capacity of the conical shell structure with a base angle less than 25° for different radial stiffnesses under axial loading. The influence of the geometrical initial imperfection is included in the proposed method. A new reduction coefficient that simulates the effect of the initial imperfection on the load carrying capacity is suggested different from the standard and recommendations [5,6]. Thus, the load carrying capacity of the conical shells which stay in the non-linear area, that is mentioned above, can be estimated without any need of numerical analysis.

The study also aims to derive two dimensionless similarity parameters. These parameters allow for evaluation of the load carrying capacity of the conical shell for numerous configuration of geometrical dimensions in a wide range. One of these parameters represents the general geometrical form of the conical shell in terms of base angle, shell thickness, and radius. The other one characterizes the radial stiffness of the circumferential ring which is located around the lower edge of the conical shell.

Effects of the circumferential ring on the load carrying capacity of a conical shell has an important role. Effectiveness depends on the radial stiffness of the circumferential ring. It is quite indispensable to determine the contribution of the ring only by itself. The study also mentions the influence of the circumferential ring stiffness on the loss of stability. The boundary conditions are assigned according to fixed supported (infinite radial stiffness), simply supported (zero radial stiffness) and flexible radial stiffness at the lower edge. Numerical models and simulations have been performed using FEM package program COSMOS/M [9].

2. CURRENT SITUATION OF THE PROBLEM

Stability of the thin-walled shell structures has been studied by many prominent authors. Results of their studies are embedded in standards, regulations, and recommendations. In this dissertation, two of

the most important documents of them are cited. These are “Recommendations for Design of Steel Shell Structures ECCS” [5] and the “European Standard for Design Steel Structures EN 1993- 1-6-2007 [6]. On the standards and recommendations, limit state of the shell structures is given in consequence of buckling. Some of the other studies which are concerned in this dissertation study are presented by, Seide P., Chryssanthopoulos MK, Spagnoli A., Gupta NK and more.

3. SCOPE OF THE STUDY

Design criteria of the standard shell structures are provided with some analytical approximations within the context of standards and regulations. Whereas, designing of the nonstandard structures requires to perform numerical analysis or experiment.

Additionally, effects of the circumferential ring on the load carrying capacity of a conical shell have a significant role depending on the radial stiffness of the ring. It is quite indispensable to determine the contribution of the ring on load carrying capacity. It is a robust process to optimize a structure by understanding the individual influence of each design parameter.

As mentioned before, the conical shells with a base angle less than 25° behave highly nonlinear. Unfortunately, the limit load of these type of nonstandard structures is not determined in the literature, adequately. In addition to this, the standards and recommendations are not bright enough for conical shells with the low base angle which have flexible radial stiffness at the lower edge. Therefore, the standard methods are not applicable for the selected base angle and assigned boundary conditions in the study.

The main goal of this study is to propose a new method to estimate load carrying capacity of the conical shell structure with a base angle less than 25° for different radial stiffnesses under axial loading. The influence of the initial geometrical imperfection is included in the proposed method. A new reduction coefficient that simulates the effect of the initial imperfection on the load carrying capacity is suggested different from the standard and recommendations [5,6]. Thus, the load carrying capacity of the conical shells, which stay in the mentioned nonlinear area, can be estimated using the new proposed method without any need of numerical analysis.

The study also aims to derive two dimensionless similarity parameters. These parameters allow evaluation load carrying capacity of the conical shell for numerous configuration of geometrical dimensions in a wide range. Derivation of nondimensional similarity parameters makes possible to simulate real applications with a simple model. This study also aims to clarify the effect of radial stiffness of circumferential ring on the load carrying capacity under axial loading. For this reason, the study includes some topics as follows,

- Determination of the load carrying capacity of the conical shells which have a base angle of less than 25°.
- Investigation of the influence of the radial stiffness on the limit load.
- Evaluation of the effect of the initial geometrical imperfection on the load carrying capacity.
- Derivation of the dimensionless similarity parameters to evaluate limit load in a wide range of the conical shell geometries.
- Suggestion of a new methodology to estimate load carrying capacity for conical shells with a base angle less than 25°.

4. PROBLEM DESCRIPTION

4.1 Analytical Study

An analytical solution is a procedure for determining the carrying capacity of the thin-walled conical shell structures which is described in the standards and recommendations. This method is based on the linear shell theory, and it is derived from the critical load under axial loading of the cylinder. Amount of this value is adjusted with counting some coefficients for simulation of the real applications. These coefficients can originate from the effect of boundary conditions, geometry, material model, initial imperfection, etc. In order to adapt the analytical approach to the conical shells for evaluating the critical load, the existing regulations are modified by finding out compatible correlation factors.

4.2 Definition of the Model

Upper radius rl and bottom radius r2 are defined 50 and 250 mm relatively for the simulations. The base angle is appointed as $10° \leq \propto c \leq 20°$. According to these values, the equivalent radius of the conical shell is set between 730 and 1440 mm. The width of the circumferential ring bring is chosen as a constant value which is 15 mm. Applying the load directly on the upper edge of the conical shell may cause convergence error in the numerical study. Stress gradients may occur on this line with the high amount of stress values. Therefore, a very stiff pipe is used on the upper edge to apply load. The load is distributed uniformly to the body of the structure by means of this stiff pipe (auxiliary surface). On the other hand, the conical shell, which is used as a connection component, is investigated in the study. In the present case, the stiff pipe also characterizes an adjacent part to simulate real condition more precisely. The height of the relatively stiff pipe *h* is assigned as 10 mm. Cross section area of the circumferential ring is evaluated between $6 \leq$ Aring ≤ 300 mm 2.

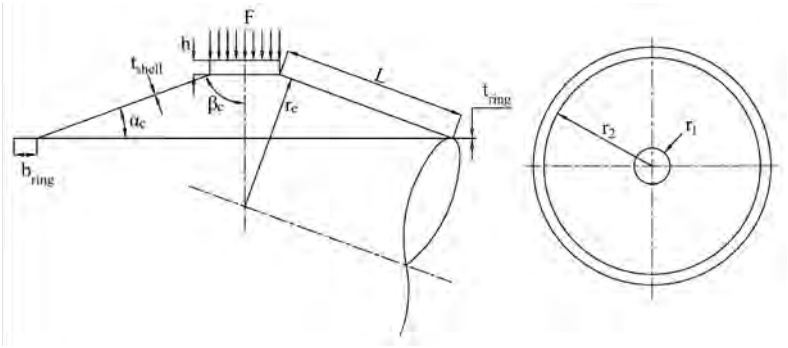

Figure 4.1 Front and top view of the conical shell (a) Front view (b) Top view

The thickness of the shell tshell is set $0.5 \leq$ tshell $\leq$ 4 mm

interval. re/tshell dimensionless parameter is assigned depending on the equivalent radius and the thickness of the shell between $240 \leq$ re /tshell ≤ 2880. Additionally, the model is performed without ring (no radial stiffness) and with infinite stiff ring (fixed supported) in order to find ring effect on the limit load. Equivalent radius is calculated in the study as stated below,

$$R_e = \frac{r_2}{cos\beta c} \qquad \text{eq. 4.1}$$

Where $cos\beta c$ is half-cone angle of conical shell in [Rad],

$$\beta_c = \frac{\pi}{2} - \alpha_c$$

Upper radius r1 has relatively small effect on the carryingcapacity of the conical shell structure under axial loading. It influences the capacity especially in the r1/r2 ratio is near to 1. These cases are not

common in practical applications. The aim of the study is derivation non-dimensional parameter for similarity. To achieve this goal, it is needed to be a simplification. Otherwise the behavior characteristic of structure under axial load can solely be expressed as a partial function. This situation makes the problem highly complicated. For this reason, the $r1/r2$ ratio excluding between 0.1 and 0.8 is neglected and it is assumed that upper radiusdoes not affect the limit load. The problem is simplified with a constant upper radius value ($r1$=50mm). On the other hand, the value of $r2$ is selected 250mm initially. But, it is used in similarity parameters as a variable that can be seen in further chapter of the study.

4.3 Numerical Study

Numerical models and simulations were performed using FEM programme COSMOS/M [9]. For the numerical analysis, large displacement module and Quadrilateral thick Shell element (SHELL4T) were assigned. Models were generated from three base angle ac (10°, 15° and 20°). Basic sketch of the structure is illustrated in Figure 4.1. with dimension parameters.

In this study, geometrically nonlinear analysis (GNA) is performed using COSMOS/M [9], and the elastic limit load is carried out. At the first step of the study; the two limit conditions, which are fixed and simple end supported conical shells, are evaluated (Figure 4.2). It is important to see the extremities of the load carrying capacity.

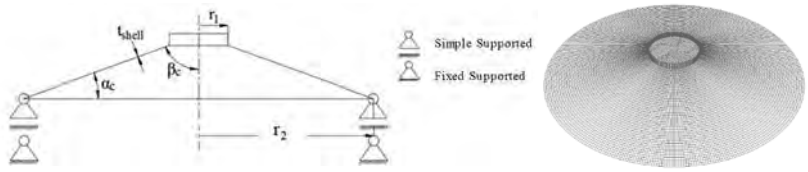

Figure 4.2 Schematic representation and numeric model of extreme cases.

In further studies, the limit load of the conical shell for various radial stiffnesses, which is represented by a circumferential ring, is investigated. The influence of the radial stiffness on the load carrying capacity is one of the central parts of this study. Schematic representation of the conical shell with the dimensions is illustrated in Figure 4.3 for this case. Models are axially loaded with $320\,N$ at the initiation of the analysis. Because the upper edge is divided into 320 nodes and the load is assigned as 1 N for each node to make post-processing easy. The arc-length algorithm controls the loading increment step by step during the solution process.

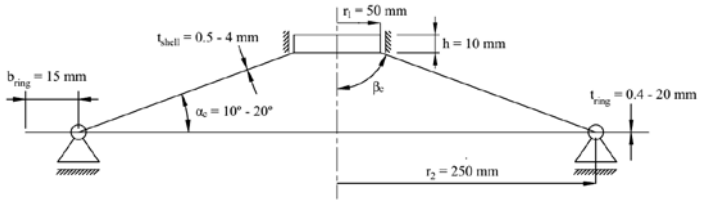

Figure 4.3 Schematic representation of the conical shell with the circumferential ring.

4.4 Mesh Study

A number of analyses are performed to evaluate dependency of the results to mesh structure. Thus, a conical shell which has current dimensions (Table 4.1) is modeled with different element sizes.

Table 4.1 Geometric dimensions and number of elements of the models (r1=50 mm and r2=250 mm).

Notation	$\propto_c$ [°]	t_{shell} $[mm]$	A_{ring} $[mm^2$	Γ	Number of element	F_{lim} $[kN]$	u $[mm]$
M_1	15	0.5	6	20.8	11002	6.778	3.72
M_2					20720	7.131	4.81
M_3					33308	7.101	4.18
M_4					49020	7.087	4.21

The load carrying capacity and the displacements in the vertical direction at the limit point can be seen in Figure 4.4 and Table 4.1. Displacement values are taken from same data point at which the top of the conical shell for all analysis.

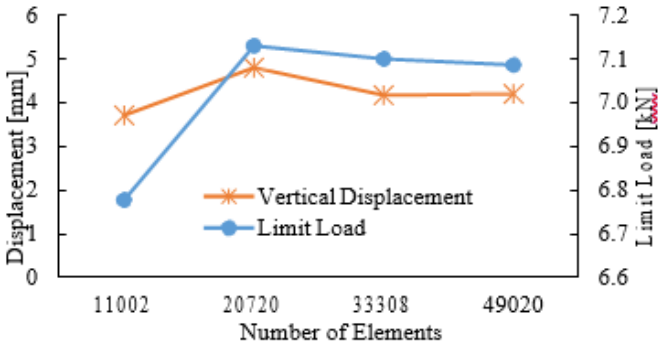

Figure 4.4 The results of the mesh study

The results do not change over 1% between the models created with 2.6 mm (M_3) and 2.1 mm (M_4) element sizes. Therefore, the element size is chosen 2.6 mm for the numerical study considering computer supplement and time-consuming.

4.5 Boundary Conditions

In this study, the conical shells which are used as a connection component for the structure are investigated. Simple cone–cylinder connections are the most common form of connections and a ring is often provided to strengthen it. Therefore, a typical practical usage of the conical shell structures which have a circumferential ring with a cylindrical shell is modeled in the study (Figure 4.5). Assignment of the boundary conditions is a critical step for the numerical solution.to simulate problem, properly.

Concerning the solution time and mesh structure, the full scaled numerical model is simplified in the numeric analysis (Figure 4.6). This simplification provides decreasing the solution time and getting better mesh structure quality with lower computational system requirement. For this purpose, a simplified numerical model and a full scaled numerical model are performed to be able to make comparison. This step is vital to ensure whether the simplified model is simulated the full scaled one accurately or not.

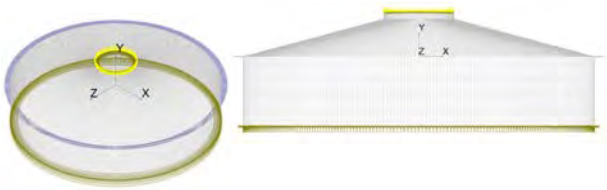

Figure 4.5 Full scaled numerical model.

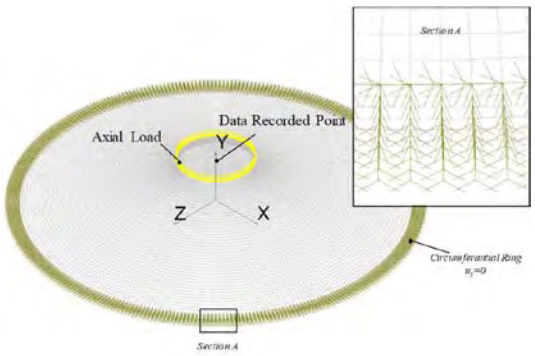

Figure 4.6 Simplified numerical model.

Four different models are generated, and they are illustrated with "*C_*" notation. The results show that the simplified models can simulate the full scaled model for various dimensionless parameters (r_e/t_{shell} and Γ. see Table 4.2).

Table 4.2 Geometric parameters and the limit load of the numerical models.

Notation	r_e/t_{shell}	Γ
C_1	1931.8	49.7
C_2	965.9	39.7
C_3	603.7	31.8
C_4	321.9	14.9

	$F_{lim}[N]$			
	C_1	*C_2*	*C_3*	*C_4*
Simplified. Model	7431.84	28498.88	72620.8	272617.6
Full Scaled Model	7494.72	29658.56	74268.8	272595.2

Limit loads of the conical shell structures are substantially same for different parameters. Thus, the simplified model is used instead of a full scaled model in the study hereinafter. This numerical model can be seen in Figure 4.6. The schematic representation of the conical shell with geometric parameters and boundary conditions are illustrated in Figure 4.3.

Where, the dimensionless Γ is the rigidity parameter of the circumferential ring. It depends on the radius of the lower edge of the conical shell, the thickness of the shell and the cross-sectional area of the ring. This parameter expresses the influence of the circumferential ring on load carrying capacity of the conical shells corresponding to the same base angle α_C. The parameter is

$$\Gamma = \frac{r_2 t_{shell}}{A_{ring}} \qquad \text{eq. 4.2}$$

5 RESULTS AND DISCUSSION

The primary purpose of this chapter is to determine the carrying capacity of the conical shells under axial loading within two limit boundary conditions. In addition to this, the effect of the circumferential ring on the carrying capacity of the conical shell is investigated. These limit conditions simulate the ring allows unlimited radial displacement or entirely prevents against the radial displacement of the lower edge of the structure.

5.1 Influence of Boundary Conditions

The results of the numerical analysis for the conical shells show the limit load of the structure. The limit load is substantially dependent on selected boundary conditions (Figure 5.1). Possible displacement of the circumferential ring at radial direction causes a reduction in buckling strength of the structure.

Significance of the boundary condition against the carrying capacity of the conical shell increases, especially at the lower re /tshell values. The results of the fixed supported conical shell (wholly restricted radial displacement) suggest that the circumferantial ring stiffness is quite efficacious on the limit load of the structure. The relation between the limit load and parameter:

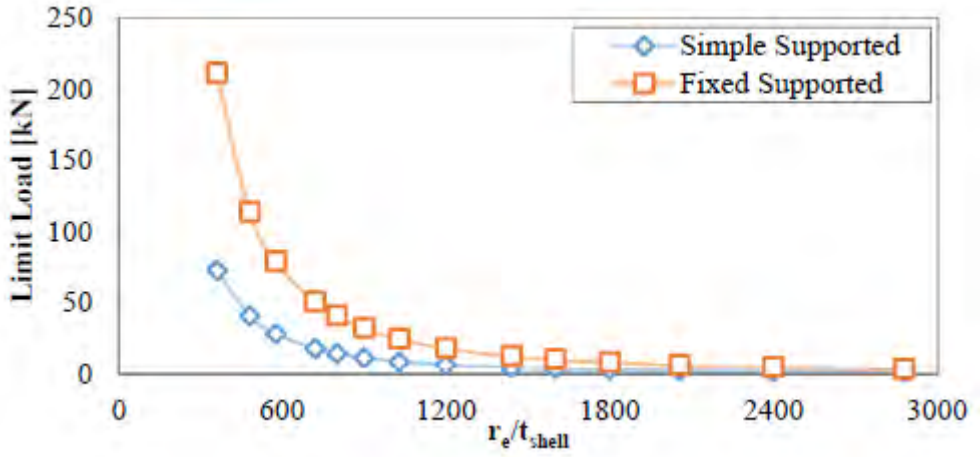

Figure 5.1 Influence of the boundary conditions on the carrying capacity of the conical shell base angle 10°.

It is possible to derive regression curve as a power function of this parameter using the data points (Eq. 5.1). The curve is relatively dependent on r_e/t_{shell} parameter.

$$F_{lim} = K'(\frac{r_e}{t_{shell}})^{m'} \qquad \text{eq. 5.1}$$

The Eq. 5.1 uses for creating the regression curves as a power function and data from GNA analyses are taken into consideration.

Coefficients K' and m are shown in Table 5.1 considering the linear elastic behaviour of the fixed supported conical shell.

The load carrying capacitiy of the simple supported conical shell (utterly allowable radial displacement) is relatively low when compared to the fixed one at the same r_e/t_{shell} value. These differences are caused by the radial stiffness of the structures. That means, the carrying capacity of the structure is relatively dependent on the radial stiffness.

Table 5.1. The coefficients of the regression curves of the fixed supported conical shell.

Base angle $\propto_c$ [°]	Range of dimensionless parameter r_e/t_{shell}	Coefficients	
		K' [kN]	m'
10	480 - 2880	$3x10^7$	1.995
15	320 - 1930	$3x10^7$	1.999
20	240 - 1460	$3x10^7$	1.992

5.2 Conical Shell with Circumferential Ring

In the previous chapter, relations and coefficients were mentioned to calculate the carrying capacity of the simple supported and fixed supported conical shells. These boundary conditions at the lower edge are the representations of the extremities. However, in the practical application, the conical shell is used with the boundary conditions which are located between these two cases (with a circumferential ring). The conical shell is evaluated for the base angle ∝c= 10,15,20°. Cross-sectional area of the circumferantial ring Aring is kept between 6 ÷ 300 m m 2.

The following figure is drawn depending on the limit load for different circumferential ring stiffnesses. As expected, the curves which belong to various ring cross-sectional areas (different radial stiffness) are positioned between the extrimities. It is interesting that the ring area Aring = 6m m 2 also contributes significantly positive effect to the carrying capacity of the conical shell. On the other hand, Aring = 300m m 2 provides nearly same contribution with fixed supported one. Graph for base angles 10° is seen below (Figure 5.2). In addition to these, the limit load values can be seen in the section of appendixes which is found at the end of the dissertation.

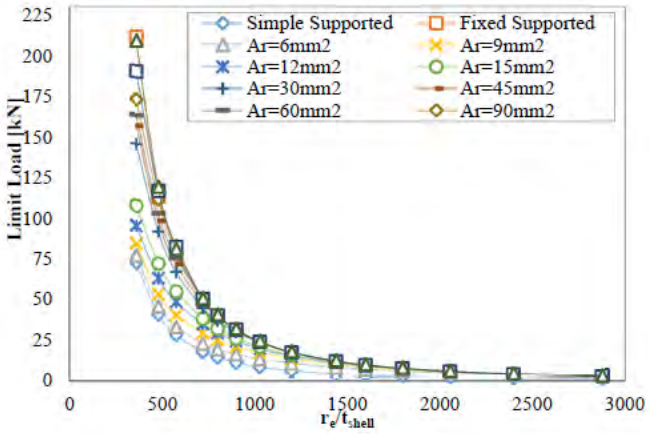

Figure 5.2 Limit loads for different radial stiffnesses.

It is apparently seen that the importance of the radial stiffness on the conical shell structures which have base angle lower than 25°, in Figure 5.2. The capability of load carrying can reach three times higher in comparison between the structures which have cross-sectional area of the circumferential ring of Aring = 300m m 2 and Aring = 6m m 2 in the lower re /tshell ratios. However, this difference decreases in higher re /tshell ratios. This situation is related to the slenderness of the structure. The expected limit load will be low in higher re /tshell ratios, therefore, even the circumferential ring with Aring = 6mm^2 behaves stiff enough against the radial displacement during the nonlinear collapse occurs. Hence, the limit loads of the structures with Aring = 6mm^2 and *Aring = 300mm^2* become nearly same.

5.3 Similarity criteria

The load carrying capacity of the conical shell which has rl=50 mm and r2=250 mm was investigated up to now in the present study. The influence of the geometrical parameters on the limit load of the structure was examined, separately. But, this section mentions about the derived similarity parameter which is the main aim of the thesis. Thus, the load carrying capacity of many different configurations of the conical shells can be estimated. For instance, a large conical shell which is used under operation can be simulated with a simple model using similarity parameters. In addition to this, the load carrying capacity of the structure can be calculated via Eq. 5.3 non-dimensionally without any need to a numerical analysis.

According to results, a similarity between load carrying capacities of the conical shells regarding geometrical parameters is tried to derive. Since distributed line load is applied to the structures, it is hard to express similarity in terms of limit load for different conical shell geometries. To achieve this purpose, the load is normalized by a constitutive relation with respect to the cross- section area of the lower edge. Therefore, normalized axial load (Eq. 5.2) is adapted to the results as exhibited in the literature before [44 and 45]. It is a function of limit load and geometrical parameters of the structure; besides, it represents the limit load in nondimensional form. The limit load of the structure can be calculated easily from this nondimensional form.

$$F_{normalized} = \frac{F_{lim}}{2\pi r_2 t_{shell} E} \qquad \text{eq. 5.2}$$

The function that is seen in Eq. 5.3 gives results in maximum 15% variation when it is compared to FEM. Normalized load can calculate with this equation using a and b from corresponding to base angle and rigidity parameter Γ.

$$F_{normalized} = a\left(\frac{r_e}{t_{shell}}\right)^{-b} \quad \text{eq. 5.3}$$

The aforementioned non-dimensional similarity parameters are re /tshell and Γ. Γ is calculated as seen below. If these parameters are identical for the same base angle, the normalized load of these structures is expected to be equal.

$$r = \frac{r_2 t_{shell}}{A_{ring}}$$

The numerical analyses results and obtained values from Eq. 5.3 for randomly selected conical shell structures are seen in Table 5.2. The structures which are expected to operate in real applications have different upper and bottom radii.

Table 5.2 FEM and analytical results for the conical shells with base angle 10°

	r_1 $[mm]$	r_2 $[mm]$	t_{shell} $[mm]$	r_e $/t_{shell}$	Γ	$F_{Normaliz}$ $*10^6$ [-] (FEM)	$F_{Normalized}$ $*10^6$ [-] (Analytical (Eq. 5.3))
A_1	100	500	5	575.88	20	83.54	85.8
A_2	250	500	5	575.88	20	82.80	85.8
A_3	300	2000	20	575.88	20	86.81	85.8
A_4	800	2000	20	575.88	20	87.53	85.8
A_5	700	5000	50	575.88	20	86.95	85.8
A_6	2000	5000	50	575.88	20	88.04	85.8

It is seen that Eq. 5.3 has good agreement with the FEM results. Besides, the similarity parameters are well matched. The structures with various geometrical dimensions but same similarity parameters have a similar normalized load. In addition to this, if the rigidity parameter of the structure is not found in the Table 5.3, linear interpolation is used to get coefficients.

Table 5.3 Coefficients of the conical shell for parameter Γ.

Base Angle α_c [°]	Range of r_e/t_{shell} parameter	Rigidity Parameter $\Gamma = \frac{r_2 t_{shell}}{A_{ring}}$	Coefficients	
			a	b
10	480 - 2880	Fixed Supported	0.0696	0.995
		Simple Supported	0.0190	1.001
		1	0.1652	1.067
		5	0.1173	1.066
		10	0.0569	0.987
		20	0.0286	0.913
		40	0.0371	0.957
		60	0.0508	1.015
		80	0.0546	1.044
		100	0.0417	1.015
15	320 - 1930	Fixed Supported	0.1141	0.999
		Simple Supported	0.0289	0.998
		1	0.1697	1.032
		5	0.1320	1.028
		10	0.0814	0.979
		20	0.0424	0.899
		40	0.0515	0.948
		60	0.0700	1.008
		80	0.0730	1.032
		100	0.0614	1.025
20	240 - 1460	Fixed Supported	0.1526	0.991
		Simple Supported	0.0375	0.996
		1	0.2634	1.038
		5	0.2036	1.033
		10	0.1230	0.984
		20	0.0566	0.880
		40	0.0730	0.946
		60	0.0936	1.006
		80	0.0937	1.023
		100	0.0650	0.992

5.4 Influence of Initial Imperfection

When researching thin-walled shell structures, the influence of initial imperfections on the loss of stability cannot be ignored. The membrane stiffness of the shells is much higher than the flexural stiffness. Initial imperfections may cause bringing the structure into bending state at the beginning of loading.

The bending state may also arise due to the nature of the structure (e.g. conical shells with a base angle less than 25°). Therefore, the sensitivity of initial imperfection is less pronounced in nonstandard structures than the structures with membrane stress dominantly (e.g. a cylindrical shell).

Initial imperfections may be seen in several types, for example, imperfections in shape, structural attachment, non-uniform loading on the structure, residual stresses, uneven distributions of mechanical properties of the material, etc. One of the most notable imperfection is called initial geometrical imperfection. Initial geometrical imperfections may be caused during manufacturing or transportation of equipment.

Only the influence of geometrical initial imperfections on the load carrying capacity is investigated in the present study. The recommendation ECCS evaluates the initial geometrical imperfections as follows.

- Out of roundness
- Eccentricities
- Local dimples

Size of the characteristic imperfection amplitude Δwk is measured using the ruler for measuring of initial geometric imperfections. The rulers are devised to relate to the size of buckles that are expected to form under each of the different basic load cases. The length of the ruler is determined by $Ig = \sqrt{4r_2 t_{shell}}$ in axial loading (Figure 5.3). The influence of other geometrical imperfections (out of roundness and eccentricity) is less pronounced therefore, they are not investigated in this study.

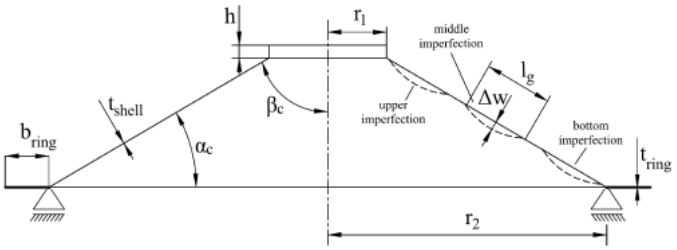

Figure 5.3. Characteristic imperfection amplitude (depth of dimple) and geometrical parameters symbolically.

The characteristic imperfection amplitude, Δw_k expresses the maximum permitted depth of the dimple. Its value depends on the quality of production and the geometrical dimensions of the conical shell.

$$\Delta W_k = \frac{1}{Q_{pr}} \sqrt{\frac{r_e}{t_{shell}}} t_{shell} \qquad \text{eq. 5.4}$$

where, Qpr is the influence of fabrication quality parameter from Table 5.4. The influence of the initial geometric imperfection on the load carrying capacity of the shell structure is expressed by the reduction coefficient α. In order to calculate the reduction coefficient, the ECCS [5] states the relationship as follows:

Table 5.4 Values of fabrication quality parameter Qpr [5].

Fabrication tolerance quality class	Description	Q_{pr}
Class A	Excellent	40
Class B	High	25
Class C	Normal	16

$$\alpha = \frac{0.62}{1+1.91(\Delta Wk/t_{shell})^{1.44}} \qquad \text{eq. 5.5}$$

Changing of the reduction coefficient α is shown in Figure 5.4 depending on re /tshell. The figure apparently shows that the structure with higher re /tshell parameter is more sensitive to initial geometrical imperfection where the reduction coefficient a decreases.

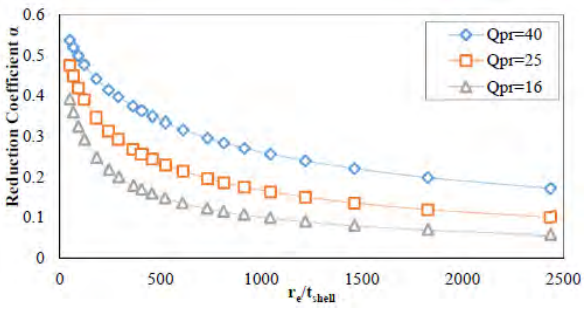

Figure 5.4 The change of the reduction coefficient.

The reduction coefficient is presented in the ECCS for a fixed supported conical shell (infinite radial stiffness) under axial loading. However, the bending effect is higher for simple supported conical shell than a fixed supported conical shell. Therefore, it can be assumed that the reduction coefficient specified in the ECCS is too conservative for the simple supported structure. For this reason, it is important to determine the dependence of the reduction coefficient on the radial stiffness of the conical shell. Figure 5.5 shows the dependence of reduction coefficient on the depth of imperfection Δw.

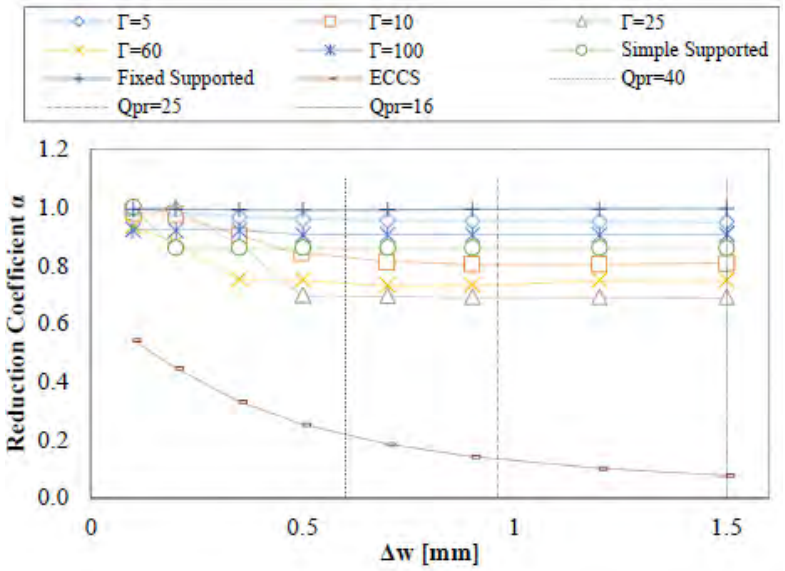

Figure 5.5 Reduction coefficient for different configuration of conical shells with a base angle 15° and tshell = 0.6 mm

The production quality classes (Table 5.4) and their respective reduction coefficients according to recommendation [5] are illustrated in the graphs (vertical lines nominated with Qpr). Those lines also show the maximum permissible depth of the imperfection. The reduction coefficient values that obtained from ECCS are too conservative for conical shells even for the quality class A. Hence, this value could be replaced by a = 0.70.

It is also interesting to see from the curves in Figure 5.5 that the increment in the depth of imperfection can result in a reduction of its effect on the load carrying capacity. The reduction coefficient may tend to increase after a point in some cases. In those cases, the dimple starts to act as a stiffener.

According to the European Recommendation, the value of the reduction coefficient for conical shells under axial loading is calculated using Eq. 5.5. The proposed calculation methodology by ECCS to estimate load carrying capacity of the conical shells is originated from the cylindrical shells. In contrast to the cylindrical shells, the conical shells have a significant bending stress. Therefore, the influence of initial imperfections, which represents an additional bending effect, is less significant in conical shells with base angle less than 25°. From this point of view, it can be assumed that the reduction coefficient that is determined based on the cylindrical shell is considerably conservative for conical shells. The reduction coefficient does not drop below a = 0.70 for different combinations of shell thickness and radial stiffness. Thus, the newvalue of the reduction coefficient is determined in this chapter as a constant value of a = 0.70.

6. COMPARISON OF CALCULATION METHODS

The load carrying capacity estimations for the conical shells are compared in this chapter. Obtained results from the ECCS recommendations, the proposed method in the present study and the numerical analyzes are examined. The load carrying capacity values of the conical shells with diverse types of boundary conditions are considered. Influence of the initial imperfections is taken into account using the reduction coefficient that is proposed as a=0.70 in previous section.

The dimensions of the fixed conical shell are shown in Table 6.1.The geometry of the cylinder, which originates from the geometry of the conical shell, falls within the area of medium length cylindrical shells. For this reason, the influence of boundary conditions, which is expressed by the Cx factor, assigned to 1. It is assumed that the loss of stability occurs in the elastic region for the randomly selected conical shells. Therefore, the effect of the elastic-plastic behavior of the material is not applied for the solutions. The reduction coefficient is determined according to the ECCS recommendation by ax in calculation of ECCS (Eq. 5.5). (for reasons of clarity, the reduction coefficients are indicated with the corresponding indices as $a_{NM}$and a_{ECCS} in the following sections).

Table 6.1 Fixed supported conical shell dimensions.

a_c[°]	r_1[mm]	r_2[mm]	t_{shell}[mm]	r_e[mm]	r_e/t_{shell}[-	C_x[-]
10	200	600	2	3455	1728	1

Calculation according to ECCS

Critical elastic stress for the conical shell is expressed by the relation,

$$\sigma_{xRcr} = 0.605EC_x\frac{t_{shell}}{r_e} = 0.605x2E5x1x\frac{2}{3455} = 70[MPa]$$

Characteristic imperfection depth for production quality class A and the reduction coefficient are determined as follows,

$$\Delta\text{Wk} = \frac{1}{Q_{pr}}\sqrt{\frac{r_e}{t_{shell}}}t_{shell} = \frac{1}{40}\sqrt{\frac{3455}{2}}2 = 2.08\ [mm]$$

$$\alpha_{ECCS} = \frac{0.62}{1 + 1.91(^{W_K}/_{t_{shell}})^{1.44}} = \frac{0.62}{1 + 1.91(2.08/2)^{1.44}} = 0.21$$

The factor Cx is determined using the relationship for a medium length cylindrical shell regarding to the dimensionless length parameter ω.

$$\omega = \frac{l_e}{\sqrt{r_e t_{shell}}}$$

It is assumed that the loss of stability will occur for this conical shell structure in the elastic area (i.e.$\lambda_x \leq \lambda_p$). The characteristic buckling stress is given by the relation,

$$\sigma_{xRk} = Xxf_{y,k} = \frac{\alpha}{\lambda_x^2}f_{y,k} = \alpha_{ECCS} = 0.21*70 = 14.7\ [MPa]$$

Limit load is calculated with the following equation for the conical shell,

$$F_{lim,ECCS} = 2\pi r_e t_{shell}\sigma_{xRk}cos^2{}_{\beta c} = 2\text{xrrx}3455\text{x}2\text{x}14.7\text{x}\cos^2(80) = 19245\ [\text{N}]$$

then the limit load is normalized using geometrical parameters and modulus of elasticity,

$$F_{normalized,ECCS} = \frac{F_{lim,ECCS}}{2\pi r_2 t_{shell}E} = \frac{19245}{2x\pi x600x2x2E5} = 12.76x10^{-6}$$

GNA type numerical analysis

Load carrying capacity of the conical shell (see Table 6.1) obtained using GNA type numerical analysis. The numerical result is seen below. The influence of initial imperfections is taken into account by means of the proposed reduction coefficient value α_{NM}= 0.70

$$F_{lim,GNA} = 68171.5\ [N]$$

when the effect of initial imperfections is considered the limit load decreases to $F_{lim,GNA}, \alpha,$

$F_{lim,GNA},\alpha = \alpha_{NM} F_{lim,GNA}$ = 0.70*x*68171.5 = 47720 [N]

and it is normalized

$F_{normalized,GNA,\alpha} = \frac{F_{lim,GNA,\alpha}}{2\pi r\_2\ t\_shell\ E} = \frac{47720}{2x\pi x600x2x2E5}$ = $31.64x10^{-6}$

Proposed method - The proposed method calculates the load carrying capacity by means of Eq. 5.3 as given below,

$$F_{normalized} = a\left(\frac{r_e}{t_{shell}}\right)^{-b}$$

The coefficients of the regression curve of the fixed supported conical shell are shown in Table 5.3.

Table 6.2 Regression curve coefficients

a	b
0.0696	0.995

$F_{normalized} = a\left(\frac{r_e}{t_{shell}}\right)^{-b}$ = $0.0696\left(\frac{3455}{2}\right)^{-0.995}$ = $41.82x10^{-6}$

and the effect of initial imperfections reduces the calculated value using reduction coefficient α_{NM}.

$F_{normalized,\alpha} = \alpha_{NM} F_{normalized} = 0.70x41.82\ x\ 10^{-6} = 29.28x10^{-6}$

Comparison of the results

A summary of the previous results is shown in Table 6.3.

Table 6.3 Comparison of results for the fixed supported conical shell.

Fixed Supported Conical Shell	ECCS	GNA Analysis	Proposed Method
$\boldsymbol{F_{normalized} * 10^6}$	12.76	31.64	29.28

The value of the reduction coefficient α_{ECCS} is relatively low in the calculation of ECCS. Thus, the calculation with respect to ECCS is quite conservative in the case of the fixed supported conical shell. On the other hand, the proposed method gives quite compatible value to numerical result.

7. CONCLUSION

In this study, the load carrying capacity of the conical shell structures which have different radial stiffnesses is examined. The base angle of the conical shell structures is kept less than 25° to contribute to filling the deficiency in the literature. A new method is proposed to estimate the load carrying capacity for mentioned conical shell structures. Results which are obtained from the nonlinear FEM analyses are stated below.

In order to predict load carrying capacity of the conical shell structures under the axial load with lower base angles (i.e. 10, 15 and 20º), non-dimensional design parameters (Γ and re /tshell) are derived. Based on these parameters, a similarity approach is proposed which estimates load carrying capacity of the shells of different shell geometry configurations at the same base angle. This similarity approach tells that the two different shell configurations having the same Γ, re /tshell and base angle have the same normalized loads. Practically, this provides an enormous advantage of estimating load carrying capacity of the conical shells from small to large structures. Therefore, there is no need to perform some series of the experiments to determine the load carrying capacity of the structures.

A simple expression is proposed to calculate the normalized load of the conical shell structure as a function of the dimensionless geometrical shell parameters and two constant coefficients of “a” and “b” which are selected considering the base angle, rigidity parameter. In this way, it enables an appropriate prediction of the load carrying capacity of the conical shell structures under the axial load for a variety of the shell configurations without performing some complex non-linear FEM analysis or numerical solutions. Furthermore, the discrepancy of the proposed new method and FEM results of the normalized load is found out to be the maximum 15% which can be considered in the acceptable limits for a highly nonlinear shell behavior of the lower base angles (10, 15 and 20º).

Implementation of the linear theory in the load carrying capacity calculations concludes with the high amount of deviations due to the presence of the circumferential ring and highly nonlinear shell response of the shell structures which is encountered at low base angles such as 10, 15 and 20º. The proposed expression for the normalized load minimizes this aforementioned deviation and keeps the results within the acceptable limits. Since particular equation coefficients of “a” and “b” are selected in order to characterize the non-linear response of the corresponded shell geometry.

In the scope of the thesis, the value of r1 is kept constant to be 50mm. Because the influence of the upper shell radius r1 on the load carrying capacity can be neglected for a wide range of upper-to-bottom shell radius ratios “r1/r2” as a result of performed FEM simulations. However, the influence of the upper shell radius on the load carrying capacity of the shell structure is observed to be more apparent as the upper-to-lower shell radius ratio “r1/r2” approaches its extremities which are r1/r2=0 and 1.

The influence of initial imperfections, which represents an additional bending effect, is less significant in conical shells with base angle is less than 25°. From this point of view, it can be assumed that the reduction coefficient that is determined based on the cylindrical shell is considerably conservative for conical shells.

The reduction coefficient does not drop below $\alpha = 0.70$ for different combinations of shell thickness and radial stiffness. Thus, the new value of the reduction coefficient is proposed as a constant value of $\alpha = 0.70$.

Circumferential ring implementation and its radial stiffness make a contribution to the load carrying capacity of the structure under the axial loading. The influence of the radial stiffness increases as re /tshell parameter decreases. The results show that application of circumferential ring in lower re /tshell dimensionless parameter value becomes more advantageously.

7.1 Scientific Contribution of the Doctoral Dissertation

The influence of the circumferential ring on the load carrying capacity of a conical shell under axial loading has not been involved fully in the European Recommendation ECCS [5]. Also, relationships in the recommendation are not applicable to the conical shells structures that have a base angle less than 25°.

Evaluation of the load carrying capacity of the fixed supported shell structures is outlined in the ECCS [5]. Nevertheless, this calculation may give higher values for the real application because of the flexible radial restrains. The results are presented in the study in order to complement the current state of knowledge of science and technology.

Determination of the limit load for the nonstandard conical shell structures with a circumferential ring has not been resolved yet. Validating the numerical results with the experimental study is necessary. After validation process, the study will be put on authorities display.

7.2 Implementation of the Results in Practice

This study proposes a new method to predict load carrying capacity of a conical shell structure and it suggests similarity parameters. By means of these parameters, experiments can be performed with small-scaled structures for simulation the real one. Additionally, the method allows estimation the load carrying capacity without any need of numerical analysis and avoids timeconsuming. Thus, efforts have been made to contribute to the design process in fields such as transport, machinery and civil engineering where thin-walled shells are widely used. For this purpose, further studies should be accomplished primarily.

7.3 Future Works

For the further parts of the current study, the following evaluations and statements are to be completed, respectively which are;

- A validation methodology will be conducted in order to ensure that how the numerical study approaches the experimental results. Hereby, a specimen will be manufactured, and it will be loaded by a hydraulic press. A load history concerning vertical deformation will be extracted to make a comparison of proximity.
- The influence of the material nonlinearity is described in the ECCS for cylindrical shells. It is suggested that the determination of the transition boundaries to the plastic and elastic-plastic region for the conical shells under axial loading should be investigated in further studies.

8. REFERENCES

Orion Spacecraft NASA https://www.nasa.gov/exploration/systems/orion/gallery/index.html?id=368774 Viertürmiger slowakischer Staubsilowagen vom Einsteller WAGONSERVIS spol.s.r.o. http://karow900.startbilder.de/bild/gueterwagen~slowakei~behalterwagen-mit-druckluftentladung-zbzementstaubsilowagen/91164/viertuermiger-slowakischerstaubsilowagen-vom-einsteller-wagonservis.html

Ars Technica and WIRED http://arstechnica.com/science/2013/04/how-nasa-brought-themonstrous-f-1-moon-rocket-back-to-life/ Meridian Manufacturing

http://www.meridianmfg.com/hopper-bottom-galvanized-bins/ ECCS TC8 TWG 8.4 Buckling of Steel Shells. European Design Recommendations. 5th Edition, ECCS, (2008), ISBN: 92-9147-000-92.

EN 1993-1-6 (2007) Eurocode 3: Design of Steel Structures - Part 1-6: Strength and Stability of Shell Structures, The European Union, ISBN: 978 0 580 50669 7

Středová D., Stabilitní Prolomení Kuželových Skořepin S Malým Vzepětím. Doctoral Thesis, Jan Perner Transport Faculty, 2012.

Teng J.G. and Rotter J.M., Buckling of Thin Metal Shells, Spon Press, London, 2004, ISBN 0–419–24190–6.

FEM Computer program COSMOS/M GeoStar 2010, SRAC (Structural Research and Analysis Corporation), Santa Monica, California.

Seide P., Axisymmetrical Buckling of Circular Cones Under Axial Compression, Journal of Applied Mechanics, 1956;78:625-628.

Donnell L. H., Stability of Thin-Walled Tubes Under Torsion, NACA, Technical Report, No. 479, Washington, 1933.

Batdorf S. B., A Simplified Method of Elastic-Stability Analysis fornThin Cylindrical Shell, NACA, Technical Report, No. 874, Washington, 1947.

Lackman L, Penzien J., Buckling of Circular Cones Under Axial Compression,

Seide P., Buckling of Circular Cones Under Axial Compression, Journal of Applied Mechanics, 1961.

Weingarten VI, Morgan EJ, Seide P., Elastic Stability of Thin-Walled Cylindrical and Conical Shells Under Axial Compression, AIAA J, 1965;3:500-05.

Weingarten VI, Morgan EJ, Seide P., Elastic Stability of Thin-Walled Cylindrical and Conical Shells Under Combined Internal Pressure and Axial Compression, AIAA J, 1965;3:1118-25.

Singer J., Buckling of Circular Conical Shells Under Uniform AxialTani J, Yamaki N., Buckling of Truncated Conical Shells Under Axial Compression, AIAA J, 1970;8:568-71.

Pariatmono N, Chryssanthopoulos MK., Asymmetric Elastic Buckling of Axially Compressed Conical Shells with Various End Conditions, AIAA J, 1995;33:2218-27.

Tavares SA., Thin Conical Shells with Constant Thickness and Under Axisymmetric Load, Computer & Structures, 1996;60:895-921.

Teng JG, Barbagallo M., Shell Restraint to Ring Buckling at Cone- Cylinder Intersections, Engineering Structures, 1997;19:425-31.

Chryssanthopoulos MK, Spagnoli A., The Influence of Radial EdgeConstraint on The Stability of Stiffened Conical Shells in Compression, Thin-Walled Structures, 1997;27:147-63.

Gupta NK, Easwara Prasad GL, Gupta SK., Plastic Collapse of Metallic Conical Frusta of Large Semi-Apical Angles. International Journal of Crashworthiness, 1997;2(4): 349-366.

Chryssanthopoulos MK, Poggi C, Spagnoli A., Buckling Design of Conical Shells Based on Validated Numerical Models, Thin-WallednStructures, 1998;31:257-270.

Spagnoli A, Chryssanthopoulos MK., Elastic Buckling and Postbuckling Behaviour of Widely-Stiffened Conical Shells Under Axial Compression, Engineering Structures, 1999;21: 845-55.

Chryssanthopoulos MK, Poggi C., Collapse Strength of Unstiffened Conical Shells Under Axial Compression, Journal of Constructional Steel Research, 2001;57:165-84.

Yu TX, Xue P, Tao XM., Flat-Topped Conical Shell Under Axial Compression, International Journal of Mechanical Sciences, 2001;43:2125-45.

Thinvongpituk C, El-Sobky H., The Effect of End Conditions on The Buckling Load Characteristic of Conical Shells Subjected to Axial Loading, ABAQUS Users' Conference, Munich, 4-6 June 2003.

Gupta NK, Sheriff NM, Velmurugan R., A Study on Buckling of Thin Conical Frusta Under Axial Loads, Thin-Walled Structures, 2006;44:986-996.

Błachut J, Ifayefunmi O, Corfa M., Collapse and Buckling of Conical Shells, Proceedings of the Twenty-first (2011) International Offshore and Polar Engineering Conference, Maui, Hawaii, USA, June 19-24, 2011.

Shakouri M, Kouchakzadehn MA., Stability Analysis of Joined Isotropic Conical Shells Under Axial Compression, Thin-Walled Structures, 2013;72:20-27.

Gere J.M. and Goodno B.J., Mechanics of Materials, Global Engineering, Stamford, 2012, ISBN: 978-1-111-13602-4

Caitríona de Paor, Buckling of Thin-Walled Cylinders: Experimental and Numerical Investigation, The Boolean, 2010.

Tomek P., Vliv Počátečních Imperfekcí Na Pevnost A Stabilitu Tenkostěnných Skořepinových Konstrukcí. Doctoral Thesis, Jan Perner Transport Faculty, 2012.

Brush, D.O. and Almorth, B.O., Buckling of Bars Plates and Shells, 1st Edition, McGraw Hill, New York, 1975, ISBN: 978-0-070-85028-6.

Timoshenko, S.P. and Gere, J.M., Theory of Elastic Stability, McGraw Hill, New York and London, 1961, ISBN: 978-0-486-42207-2.

Chajes, A., Principles of Structural Stability Theory, Prentice-Hall, Inc., Englewood Cliffs, New Jersey, 1974, ISBN: 978-0-137-09964-1.

COSMOS/M User's Guide. Structural Research and Analysis Corporation. 2001.

Lavasani A., Simple Solutions for Buckling of Conical Shells Composed of Functionally Graded Materials, Journal of Solid Mechanics, 2009;1:108-117.

Ifayefunmi O., A Survey of Buckling of Conical Shells Subjected to Axial Compression and External Pressure, Journal of Engineering Science and Technology Review, 2014;7:182-189.

Bushnell D., Computerized Buckling Analysis of Shells. Kluwer Academic Publishers, 1989, ISBN 90-247-3099-6. 38

Bushnell D., Computerized Analysis of Shells – Governing Equations, Computer & Structures, 1984;18:471-536.

Simulia, D. S., Abaqus 6.13, Getting Started with Abaqus Interactive Edition, Dassault Systems, Providence, RI, 2013.

EN ISO. 6892-1. metallic materials-tensile testing-part 1: Method of test at room temperature. International Organization for Standardization, 2009.

9 STUDENT PUBLICATIONS

1. Yilmaz H., Ozyurt E., Pascenko P., (2015) Elastic buckling of thin conical caps with edge ring constraint under uni-axial compression, International Journal of Scientific and Technological Research Vol 1, No.9, 1-9

2. Ozyurt E., Yilmaz H., Pascenko P., (2015) An investigation on dynamic response of truncated thick walled cones with edge ring under axial compressive impact load, International Journal of Scientific and Technological Research Vol 1, No.9, 21-30

3. Yilmaz, H., Ozyurt, E. Tomek, P, (2017) A Comparative study between numerical and analytical approaches to load carrying capacity of conical shells under axial loading, International Journal of Engineering Trends and Technology (IJETT), Vol 52, No.l

4. Yilmaz H., Kocabas I., Ozyurt E, (2017) Empirical equations to estimate non-linear collapse of medium-length cylindrical shells with circular cutouts, Thin-Walled Structures, Vol 119, 868-878.

5. Ozyurt, E.Yilmaz, H., Tomek, P, (2018) Prediction of the influence of geometrical imperfection to load carrying capacity of conical shells under axial loading. Sigma Journal of Engineering and Natural Sciences, Vol 36, 11-20.

Probabilistic Nonlinear Computer Simulations for Realistic Prediction of Structural Response

Author: Ing. Özgür YURDAKUL

Doctoral study programme:
P3710 Technique and Technology in Transport and Communications

Field of study:
3706V005 - Transport Means and Infrastructure

Supervisor:
Ing. Ladislav Řoutil, Ph.D.

Supervisor specialist:

Doctoral thesis has arisen at the supervising:
Department of Transport Structures

ABSTRACT

The effect of inherent uncertainties in material properties on the global response of substandard reinforced concrete (RC) structural members was investigated by the stochastic study. An experimentally validated finite element model (FEM) was, therefore, combined with a suitable stochastic sampling technique (Latin Hypercube Sampling (LHS)). Then, the effect of inherent uncertainties on the material mechanical properties was studied by uncertainty analysis, while the uneven distribution of concrete mechanical properties over the specimen was accurately characterized by random fields theory. The partial correlation coefficient between material parameters and response variables was also evaluated to outline the parameters which mainly contribute to the global response (i.e., sensitivity analysis). Such an advanced modelling strategy was implemented on three different testing programs comprising RC members designed with structural details and material properties non-conforming to current codes and guidelines. The first testing program deals with experimental performance of an over-reinforced and shear critical beams together with stochastic assessments of beam members via computational stochastic mechanics. The effect of uncertainties on the response of shear critical and carbon fiber reinforced polymer (CFRP) retrofitted beam-column joints, which were selected from available testing programs in the literature, was also discussed. The stochastic-based numerical prediction of beam-type RILEM bond specimens characterized variability in the identical tests satisfactorily. Owing to the more realistic assessment capability of the stochastic-based nonlinear finite element (FE) analysis, the global response of the substandard RC members (over-reinforced and shear critical beams; shear critical and CFRP retrofitted beam-column joints; beam-type RILEM bond specimens) was accurately reproduced.

Keywords: Reinforced Concrete, Substandard, Sensitivity; Stochastic Assessment; Finite Element Method, Nonlinear Analysis, Uncertainty, Random Fields

1 INTRODUCTION

According to the capacity design principles specified in most modern codes and guidelines, structural members should exhibit a ductile response. The requirements to meet the ductile behavior and design principles are carefully described in the relevant documents. However, a significant portion of RC buildings in the existing building inventory of both developed and developing countries have specific deficiencies at the local level, which usually cause premature failure of structural members. Severe damage at the member remarkably violates the integrity of the structural system. The obvious outcomes are poor energy dissipation and sudden degradation of strength and stiffness. As local damages also actuate the global failure mechanism, investigating the behavior of substandard members is essential. Based on field observations and laboratory tests, capacity design principles have earmarked deficient RC members as critical components in the moment-resisting frames. It is, therefore, important to pay enough attention to the assessment of RC members with local deficiencies.

Several attempts have been made to investigate the response of substandard RC members by using experimental and numerical methods. However, further developments are urgently needed due to the randomness in either material properties or strength distribution over specimen geometry. Therefore, a more advanced method, which combines the nonlinear FEM with the stochastic sampling technique, is required. Owing to the more realistic assessment capability of the stochastic-based nonlinear FE analysis, which is available in user-friendly computer tools, reproducing the structural response of substandard members using computational stochastic mechanics could yield more accurate results for assessment purposes. Therefore, a focus on the probabilistic nonlinear computer simulations should be given.

In this study, different kinds of failure modes in substandard RC members were assessed by using stochastic approaches. For this reason, the nonlinear FEM was combined with a suitable stochastic sampling technique for the realistic prediction of the structural response in substandard RC members. Overall, the effect of inherent uncertainties on the material mechanical properties was studied by using uncertainty analysis, which leads to obtaining the basic statistics of response variables. The sensitivity of material properties on the global response was also measured by evaluating the partial correlation coefficient between material parameters (i.e., input variables) and strength parameters (i.e., response variables). Moreover, the uneven distribution of concrete mechanical properties over the specimen was accurately characterized by random fields theory, which establishes weaker and stronger spots over the specimen. All of these provided a broad perspective in assessing the results.

The stochastic approach was implemented in three different testing programs. The first testing program deals with over-reinforced and shear critical beams. The experimental performance of two substandard beam specimens was first obtained and then accurately reproduced in the FE environment. The effect of inherent uncertainties at a material level for an over-reinforced and shear critical beam, and the uneven distribution of concrete mechanical properties over the shear critical beam were handled by an uncertainty analysis and random fields approach, respectively. The stochastic assessment of shear critical and CFRP retrofitted beam-column joints, which were selected from available testing programs in the literature, was also investigated. The experimental performance of shear failed joints, and CFRP fracture was closely estimated by using the stochastic approach. The relative impact of each material properties on the shear critical and CFRP retrofitted joints was then provided, which remarks the most critical material parameters affecting the global response. The third testing program focused on the stochastic-based numerical prediction of beam-type RILEM bond specimens. The proposed bond stress-slip relations, which were evaluated from the experimental data, were first implemented in the FE models. Thus, the deterministic numerical models accurately reproduced the experimental performance of confined and unconfined specimens under cyclic and monotonic loading. The variability in the identical tests was satisfactorily characterized by the stochastic assessment.

To conclude, the stochastic approach described in this study was implemented on three different testing programs. The performance of the advanced assessment method on different failure modes, which combines the nonlinear finite element method with the stochastic sampling technique, was evaluated.

2 MODELLING PARAMETERS

As the computer-aided nonlinear analysis is now available for RC members, refined numerical models allow for reproducing the response of substandard members with satisfactory accuracy. This chapter briefly presents the numerical modeling strategies in a user-friendly computer tool ATENA software [1], used for different RC members that have exhibited different failure types.

The concrete geometry was modeled using the hexahedral element *CCIsoBrick*. The constitutive models of tensile and compressive behaviors were combined in *CC3DNonLinCementitious2* (a fracture-plastic concrete model) in the software. Moreover, the *Reinforced Concrete* material model provides an opportunity to model the reinforcement in a smeared manner. An elliptical hardening and linear softening behavior were assumed in defining the uniaxial compressive behavior of the concrete [2]. Accordingly, a strain-based hardening response was followed by a displacement-based linear softening response in compressive. The relation in the form of the Gaussian curve was implemented to reduce the compressive strength in cracked concrete while its parameters were obtained from available literature [3,4]. Menetrey and Willam criteria [5] was implemented for the definition of the failure surface in the numerical model. The behavior of plain concrete under tension was assumed to be uncracked in the elastic region while an exponential softening response between the stress in the crack σ and crack width w was adopted in the post-elastic region [6]. The crack width at complete stress release w_c was evaluated by the relation between fracture energy G_f and displacement w [6]. The smeared crack concept in combination with crack band theory [7] was implemented in the software for the strain-displacement relation. The stress in the crack is not completely released in the heavily reinforced members due to the strength provided by the reinforcing bar. Therefore, tensile softening behavior was modified accordingly in the beam and column by using the relation proposed in CEB-FIP Model Code [8].

The longitudinal reinforcing bars were defined as truss elements with a bilinear elastoplastic model, considering the hardening behavior. It was modeled as a discrete reinforcement embedded in the concrete geometry. Menegotto and Pinto [9] model for the nonlinear cyclic material behavior of the reinforcing steel was employed. The reinforcing bar was fully connected to the surrounding concrete geometry with the limited bond strength, which is defined by a *CCBarWithBond* type element [1].

The CFPR sheets were modeled using membrane elements with composite material properties. Namely, the CFRP net was defined by the smeared reinforcement concept by the *Reinforced Concrete* material model, which combines the brittle material with reinforcement [10]. Therefore, the brittle response of epoxy resin was defined as that of a fracture/plastic material (i.e., *CC3DNonLinCementitious2*), while the CFRP was modeled as a smeared reinforcement. The bond between the concrete surface and CFRP sheet was characterized by inserting a supplementary surface (an interface) between the two materials. The interface material is based on Mohr-Coulomb criterion [11].

The efficiency of the numerical model is strongly related to the mesh size as it has vital importance on the accuracy of numerical results. The mesh size was optimized by trying different mesh size until the variation in the computed maximum load is minimized.

3 STOCHASTIC STUDY

3.1 Uncertainty Analysis

The randomness in the material properties can be simulated by computational stochastic fracture mechanics. Hence, the deterministic model was evolved to the stochastic level. Sets of input parameters were simulated by a stratified sampling technique (i.e., Latin Hypercube Sampling (LHS)) using defined distribution functions. The deterministic values with their distribution, and the correlation among the material parameters are presented in Table 1, and Table 2, respectively. Those are based on experimental observations, Pukl *et al.* [12], fib Bulletin No.22 [13], Gulbrandsen [14], Atadero and Karbhari [15], Baji *et al.* [16] and Joint Committee on Structural Safety (JCSS) [17].

A set of load-displacement curves was achieved as the outcome of the performed analyses with generated samples. The distribution of the ultimate load (i.e., response variable) corresponding to each cycle was obtained from that bundle. Moreover, basic statistics of the response variable (e.g., mean value, standard deviation, and PDFs of capacity) were provided. Finally, the Spearman rank-order correlation coefficient between the generated input and response variables was found. The major material parameters characterizing the overall behavior of the specimens were thus provided.

Table 1. Material properties as random parameters and their statistical distributions

Parameter	Mean Value, μ	COV	Distribution
	Concrete		
Elastic Modulus, E_c (MPa)	$4700\sqrt{f_c}$ [18]	0.10	Lognormal (2 Parameter)
Tensile strength, f_{ct} (MPa)	$0.30f_c^{2/3}$ [8]	0.30	Lognormal (2 Parameter)
Compressive Strength, f_c (MPa)	8.05 EJ-R 9.40 EJ-C	0.15	Lognormal (2 Parameter)
Fracture Energy, G_f (N/m)	$73f_{ct}^{0.18}$ [8]	0.25	Weibull (2 Parameter)
Compressive Strain, ε_{co} (mm/mm)	f_c/E_c [2]	0.15	Lognormal (2 Parameter)
Plastic Displacement, w_d (m)	Linear [19]	0.10	Lognormal (2 Parameter)
	Reinforcing Steel		
Elastic Modulus, E_s (GPa)	190.9	0.07	Lognormal (2 Parameter)
Yield Strength, f_y (MPa)	295.5	0.07	Lognormal (2 Parameter)
Ultimate Strength, f_u (MPa)	437.5	0.07	Lognormal (2 Parameter)
Ultimate Strain, ε_u (mm/mm)	0.21	0.07	Normal
	CFRP		
Elastic Modulus, E_f (GPa)	230	0.08	Lognormal (2 Parameter)
Tensile Strength, f_f (MPa)	4900	0.08	Lognormal (2 Parameter)
Effective thickness, t_f (mm)	0.111	-	Deterministic
	MBT-MBrace® Adesivo (Saturant)		
Elastic Modulus, E_{as} (MPa)	1800	0.10	Lognormal (2 Parameter)
Compressive Strength, f_{cas} (MPa)	80	0.15	Lognormal (2 Parameter)
Tensile strength, f_{ctas} (MPa)	12	0.30	Lognormal (2 Parameter)
Fracture Energy, G_{fas} (N/m)	100 [20]	0.25	Weibull (2 Parameter)
Compressive Strain, ε_{cos} (mm/mm)	f_{cas}/E_{as} [2]	0.15	Lognormal (2 Parameter)
Plastic Displacement, w_d (m)	Linear [2]	0.10	Lognormal (2 Parameter)

Table 2. Correlation coefficients among the random parameters

Concrete and Adesivo (Saturant)					
	E_c	f_c	f_{ct}	G_f	ε_{co}
E_c	1	0.70	0.60	0.40	0.90
f_c		1	0.70	0.50	0.90
f_{ct}	SYM		1	0.80	0.60
G_f				1	0.50
ε_{co}					1

Steel				
	E_s	f_y	f_u	ε_u
E_s	1	0	0	0
f_y		1	0.75	0.45
f_u	SYM		1	0.60
ε_u				1

CFRP		
	E_f	f_f
E_f	1	0.31
f_f	SYM	1

3.2 Random Fields Theory

The response of the structural member is influenced by the uneven distribution of the concrete mechanical properties. For this purpose, the uncertainties in the distribution of the concrete mechanical properties over the specimen were described as random variables. This randomness was considered via the random fields approach [21]. The samples from the statistical analyses were the input parameters

(listed in Table 1) for the nonlinear FE solutions. In the refined numerical models, these input parameters were not distributed evenly, but were established as weaker and stronger regions over the specimen. In other words, the concrete mechanical properties changed with the geometric coordinates, causing variability over the specimen. The random fields for each prominent material parameter were generated in FReET [22]. The deterministic model was then modified in SARA Studio [23], which interfaces the statistical analysis (i.e., FReET results) to FE software, enabling probabilistic nonlinear analyses.

4 CASE I: BEAM TEST

Two different failure modes of RC beam members, which include concrete crushing due to reaching the limit strain of the concrete in compression and excessive shear failure, were examined using experimental and stochastic methods.

4.1 Experimental Program

A series of tests on the shear critical and over-reinforced beams were conducted in cooperation with Structural Mechanics Laboratory, Department of Civil Engineering, Eskişehir Technical University, Turkey. The experimental program consists of a four-point bending test on the shear deficient and over-reinforced substandard RC beam specimens. While the shear critical beam was designed without any transverse reinforcement to achieve excessive shear failure by exceeding the tensile strength of the concrete, the over-reinforced beam was designed with reinforcement detailing, resulting in concrete crushing. The specimens were constructed from low strength concrete. The details of the specimens are depicted in Fig. 4.1a and b, respectively.

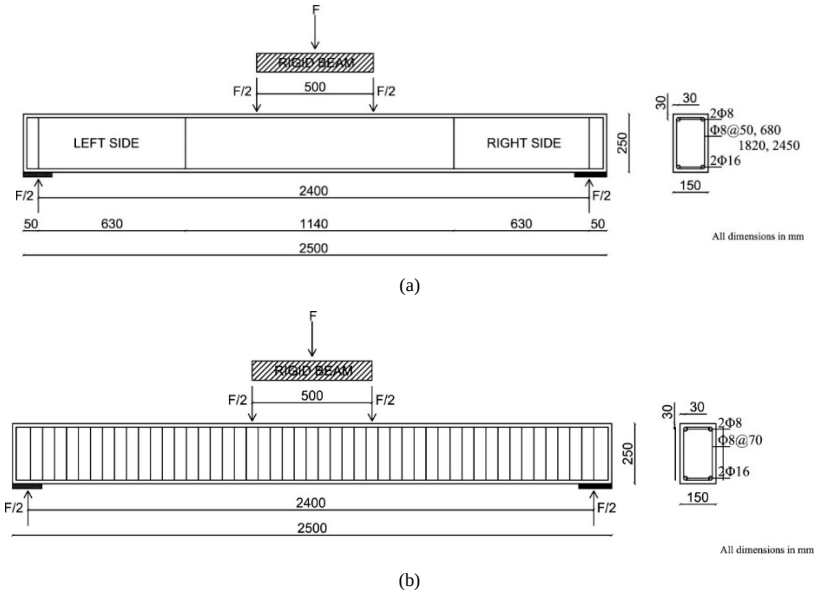

Fig. 4.1 Reinforcement scheme and dimension details (a) shear critical specimen, EB_R (b) over-reinforced specimen, EB_C

The summary of the test specimens is presented in Table 4.1.

Table 4.1 Description of test specimens

	Specimen	
	EB_R	EJ_C
Description	Shear Critical	Over-Reinforced
Reinforcement Scheme	Fig. 4.1a	Fig. 4.1b
Concrete Compressive Strength, f_c (MPa)	15.0	17.1
Elastic Modulus, E_s (GPa)	200	
Yield Strength, f_y (MPa)	460	
Ultimate Strength f_u (MPa)	632	
Ultimate Strain, ε_u (mm/mm)	0.17	
Beam Dimension	150 x 250 x 2500 mm	
Longitudinal Reinforcement	2ϕ16+2ϕ8	4ϕ16+2ϕ8
Transverse Reinforcement	ϕ8@50, 680 1820 and 2450 mm	ϕ8/70
Application of Displacement	Four-Point Bending	
Loading Protocol	Monotonic	
Failure Mode	Shear Failure	Concrete Crushing

4.2 Over-Reinforced Beam

The exhibited performance of the specimen was a brittle type of failure as a result of concrete crushing caused by reaching the limit strain of the concrete in compression (Fig. 4.2a). The stress distribution along the specimen's longitudinal axis and crack pattern are depicted in Fig. 4.2b. The resulting failure mode was predicted well by the numerical assessment. Concrete crushing in the compression zone was in good agreement with the compressive stress distribution obtained from FE analysis. The flexural hairline cracks in the tension zone were also captured by the numerical solution.

(a)

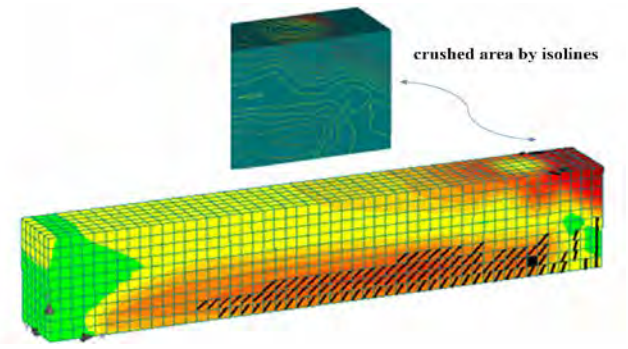

(b)

Fig. 4.2 (a) Concrete crushing in the over-reinforced beam (b) numerical prediction at failure

The deterministic FE model, which was modeled with the average values of the material parameters, matched well with the experimental capacity with an error of 10%. The set of load-displacement curves formed a band around the deterministic model, which was also covered by the experimental results (Fig. 4.3). The stochastic bundle also provided the upper and lower boundaries of the load, corresponding to each displacement level. The scatter was higher in the subsequent displacement due to the effect of different nonlinear mechanisms.

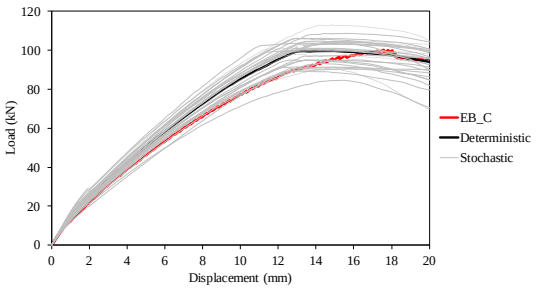

Fig. 4.3 Set of load-displacement curves in over-reinforced beam

4.2.1 Reliability Analysis of Over-Reinforced Beam

The PDF of the load, which corresponds to the critical deflection *L/250* described in EN 1992-1-1 [24], was obtained from the stochastic bundle. After that, the safety margin was obtained by subtracting capacity (i.e., resistance) from demand (i.e., load). Finally, the load corresponding failure probability, related to the irreversible serviceability limit state, was computed as 73.5 kN (Fig. 4.4a). Namely, the values smaller than 73.5 kN are safe according to the reliability concept. The PDF of the ultimate loads is found as well for the over-reinforced beam (Fig. 4.4b). The load corresponding failure probability, related to the irreversible serviceability limit state, was computed as 79.2 kN.

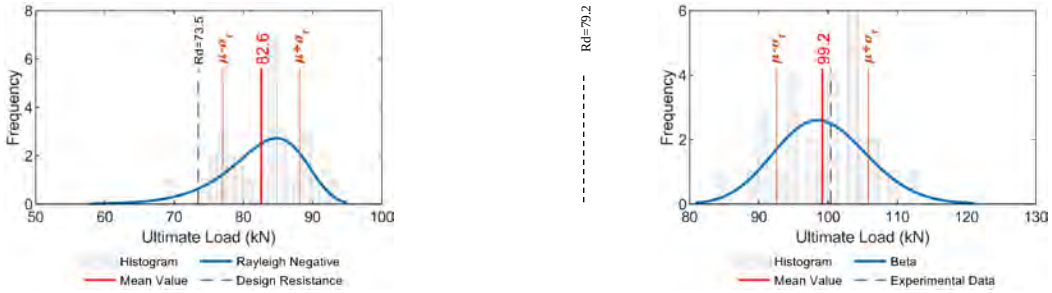

Fig. 4.4 PDF of (a) serviceability limit state (b) ultimate limit state

4.2.1 Sensitivity Analysis of Over-Reinforced Beam

The relative impact of concrete compressive strength f_c was the most considerable among others as it has the highest correlation (Fig. 4.5). Thus, the experimental and numerical responses, which were characterized by concrete crushing due to reaching the limit strain of concrete, were also ascertained by the sensitivity analysis. The tensile strength of concrete f_{ct} influenced the global response remarkably. It is worthy to mention that flexural cracks also appeared during the test. Thus, the tensile strength of concrete f_{ct} became critical up to a certain level of displacement. The sensitivity measures on the remaining materials showed a low correlation coefficient. Thus, their relative impact on the global response was not significant.

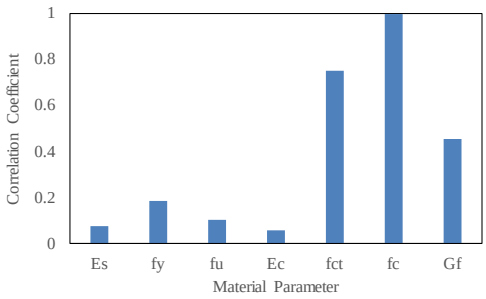

Fig. 4.5 Sensitivity of material properties in EB_C

4.3 Shear Critical Beam

The spatial variability of the concrete mechanical properties along the specimen vitally affects the capacity, initial stiffness, and ultimate displacement of the specimen. These behaviors were clearly identified in the presented stochastic bundle of load–displacement curves. The randomized concrete strength did not influence the linear response of the specimen, but remarkably affected the nonlinear response of the concrete. The shear failure caused severe damage on the left side of the beam (Fig. 4.6a). On the other hand, the crack pattern in the deterministic FE analysis was distributed almost evenly on both sides of the specimen (Fig. 4.6b). The random fields theory accounts for variability in the concrete mechanical properties. The possible crack patterns in some of the selected analyses are presented in Fig. 4.6c. As depicted in the figures, the crack pattern obtained in each analysis considerably depended on the randomness.

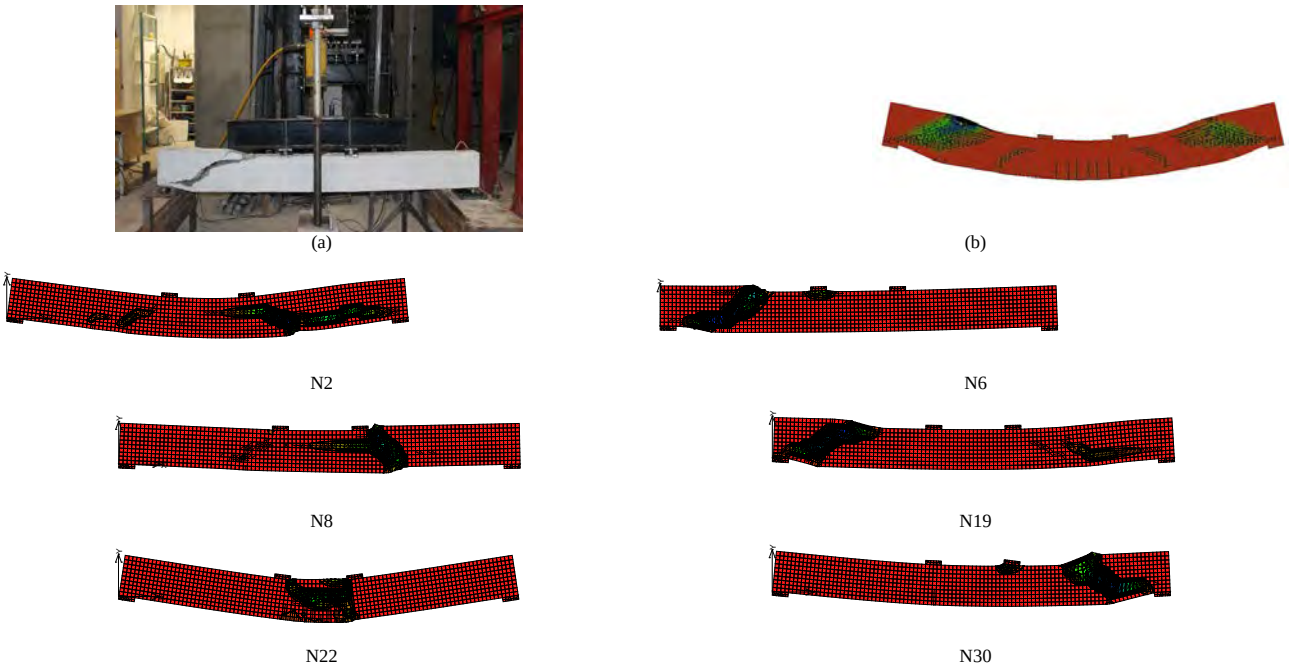

Fig. 4.6 Damage state at failure: (a) experiment (b) deterministic model (c) random fields

Fig. 4.7 shows the range of load-displacement curves for beams with different material properties. The stochastic approach provided the possible ranges of load-displacement curves. As the geometrical position of the weakest spot defines the failure mode and capacity, the load-displacement curves in the stochastic analysis did not form a band around the deterministic model. The important point in such predictions is that the experimental results to be used for the assessment of the member (i.e., the observed initial stiffness, peak load, failure mode, and crack pattern) could be covered by the stochastic model.

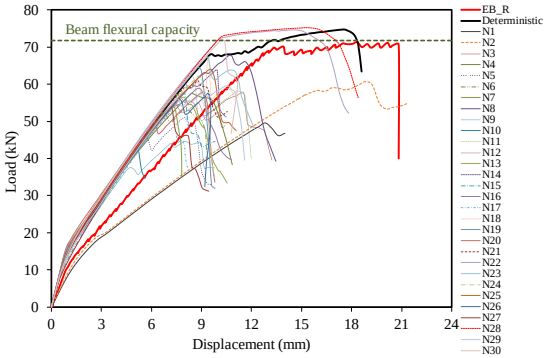

Fig. 4.7 Set of load-displacement curves

5 CASE II: JOINT TEST

The effect of inherent uncertainties in material constitutive models on the response of substandard as-built and CFRP retrofitted RC beam-column joints was investigated through a stochastic study.

5.1 Selected Experimental Tests

The experimental tests used to validate the proposed numerical models collected from two different testing programs previously conducted by the author: Yurdakul [25], Yurdakul and Avşar [26,27], and Yurdakul *et al.* [28]. The full-scale test specimens, which represent the exterior beam-column joint, were constructed by considering the most common deficiencies. Geometrical parameters and material properties were selected in such a way that they would characterize the construction practices of the existing deficient beam-column subassemblies (Fig. 5.1a and b).

5.1.1 Structural Retrofit

The design philosophy in the rehabilitation of specimens is to attain the initial capacity, upgrading the performance of structural members, delaying or eliminating brittle failure modes, and initiating the formation of flexural plastic hinges in the beam to attain a ductile behavior [29]. In dimensioning CFRP sheets, it was assumed that the lateral load causing beam yielding without joint failure will be carried only by the corresponding CFRP sheets (Fig. 5.1c).

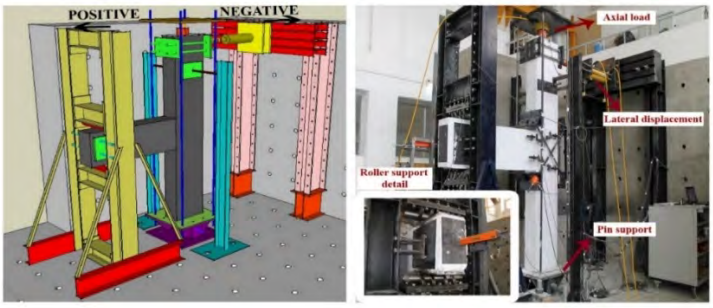

(a)

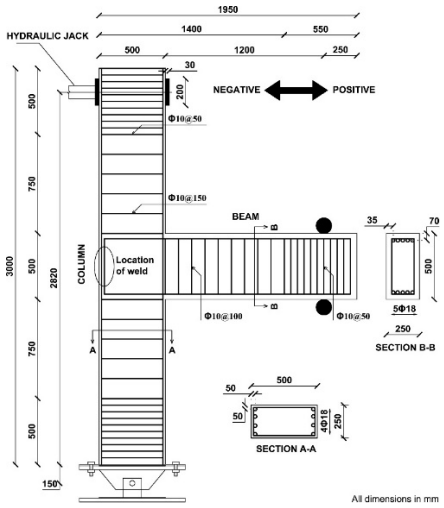

(b)

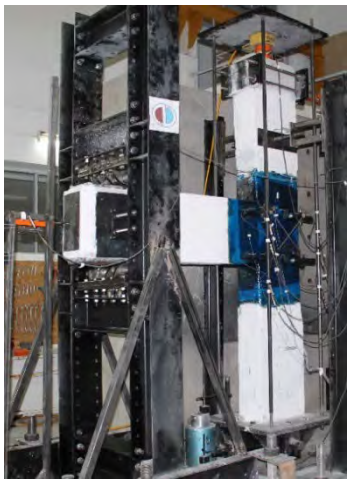

(c)

Fig. 5.1 a) 3D view of the selected specimen (b) dimension and reinforcement details of the subassembly (c) CFRP retrofitted specimen [25,27]

5.2 Hysteric Response

The overall response of the reference specimen representing the as-built subassembly (EJ-R) was dominated by the joint shear failure, which results in premature failure of the RC member. When the deterministic model evolved to the stochastic level, the scatter with the possible range of the load for each drift level can be seen in Fig. 5.2a and b.

(a) (b)

Fig. 5.2 (a) Hysteric response of reference specimen, EJ-R (b) envelope curve of hysteresis loops

The resulting large corner-to-corner cracks in the joint panel and propagated cracks at the joint back were reasonably reproduced by the deterministic numerical assessment of the reference specimen (Fig. 5.3a-c). As the imposed displacement increases, new hairline cracks spread over the whole beam (Fig. 5.3a and b). In the subsequent drift levels, the existing cracks in the joint panel widened while those propagated in the beam almost closed (Fig. 5.3b and c).

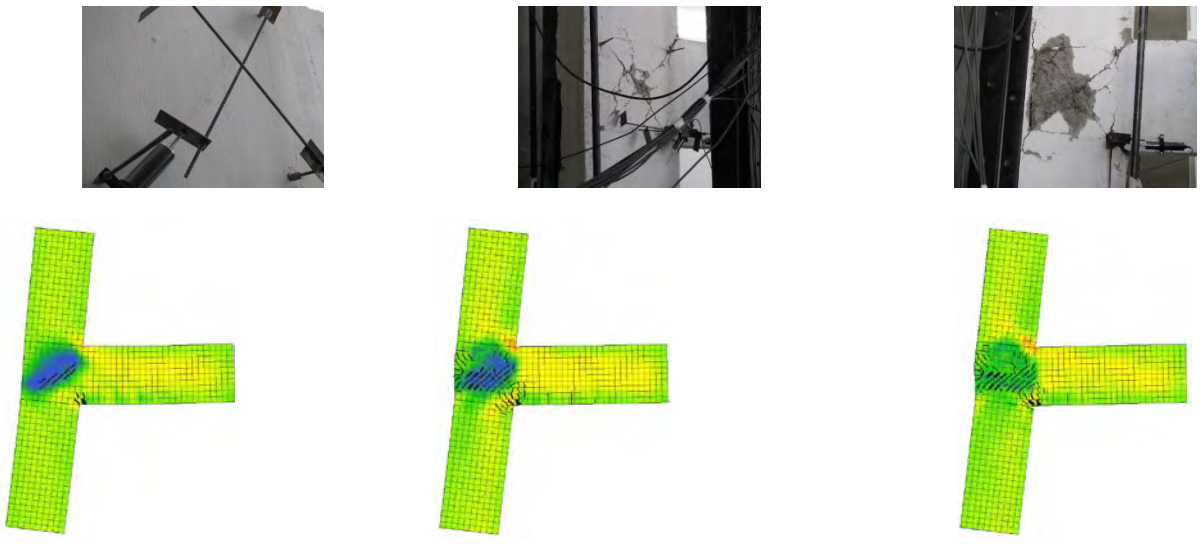

0.2% Drift Ratio (First crack) (a) | 2% Drift Ratio (b) | 4% Drift Ratio (Failure) (c)

Fig. 5.3 Comparison of crack pattern obtained by experimental response and deterministic numerical model for the reference specimen (EJ-R) (a) first joint cracking (b) 2% drift ratio (c) 4% drift ratio

The specimen incorporating the retrofit solution via CFRP wrapped in an X pattern (EJ-C) suffered from diagonal cracks after a certain level of displacement corresponding to CFRP debonding/rupture. Therefore, the specimen displayed a non-ductile behavior together with the distinct strength deterioration and stiffness degradation due to the shear failure of the joint after CFRP rupture. A set of load-displacement curves along with both the experimental response and numerical assessment is depicted in Fig. 5.4a and b for the retrofitted specimen.

(a) (b)

Fig. 5.4 (a) Hysteric response of retrofitted joint, EJ-C (b) envelope curve of hysteresis loops

The deterministic numerical assessment well captured the crack pattern together with the resulting failure mode. The severe joint shear cracks at failure were also monitored in the deterministic model. Moreover, the vertical splitting cracks at the beam-joint interface were closed partially in the beam, which was accurately reproduced in the FE model as well (Fig. 5.5a-c).

4.4.1 Analysis of Results

The ultimate strength of the specimen is one of the important parameters in the cyclic response assessment of specimens. Basic statistical parameters related to the ultimate strength were, therefore, provided in Fig. 5.6a and b. The PDFs of peak strength and their statistical parameters (i.e., mean value and standard deviation) were obtained from the series of data points (i.e., ultimate capacity of each analysis). For the fitted distributions, Chi–square or Kolmogorov–Smirnov tests, which measure the goodness of the fit, are satisfied at the 95% confidence level. Then, the mean value of predicted peak strength was compared with the experimentally obtained capacity.

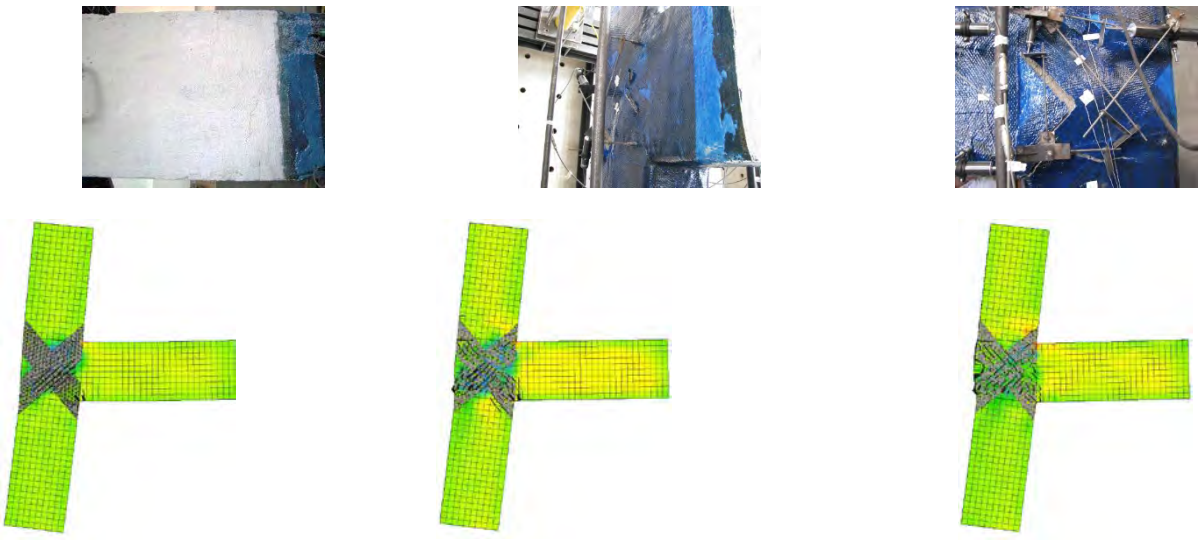

0.2% Drift Ratio (First beam crack) (a) | 2% Drift Ratio (b) | 4% Drift Ratio (Failure) (c)

Fig. 5.5 Comparison of crack pattern obtained by experimental response and deterministic numerical model for the retrofitted specimen (EJ-C) (a) first joint cracking (b) 2% drift ratio (c) 4% drift ratio

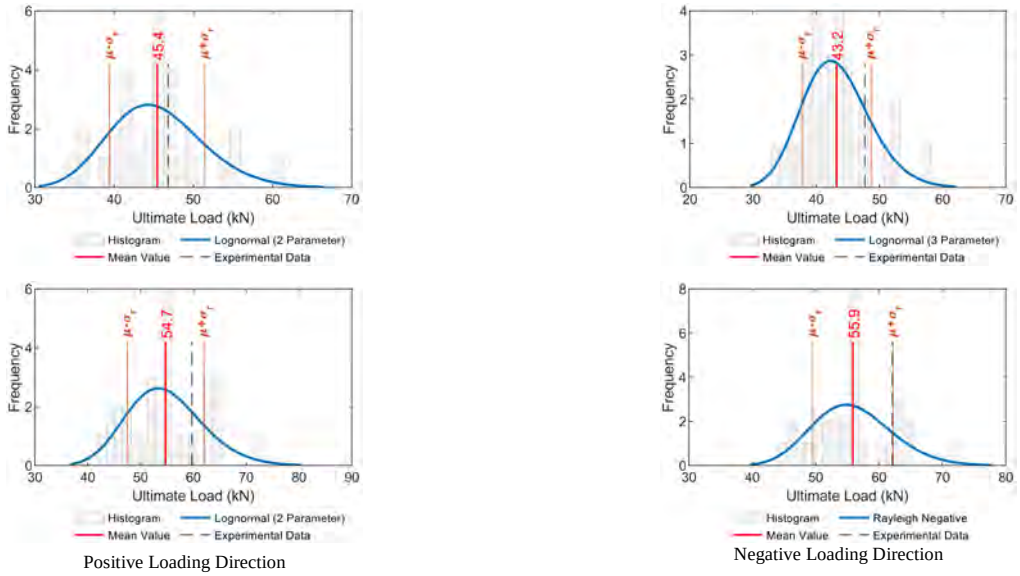

Positive Loading Direction | Negative Loading Direction

Fig. 5.6 (a) PDFs of EJ-R (b) PDFs of EJ-C

5.3 Sensitivity Analysis

The contribution of the concrete tensile strength f_{ct} to the global response was the most significant, because it had the highest correlation coefficient for the positive and negative loading direction of the reference specimen. (Fig. 5.7a and b). The relative impact of the concrete compressive strength f_c on the global response was also considerable. This phenomenon can be attributed to the development of the diagonal compression strut mechanism, which is perpendicular to the tension tie at the joint panel. The remaining material properties had a weak influence on the global response as the correlation coefficients are rather low (in some cases very close to zero).

(a) (b)

Fig. 5.7 Sensitivity analysis in the reference specimen EJ-R (a) positive loading direction (b) negative loading direction

The sensitivity measures resulted in high correlation with three input variables of the retrofitted specimens, which included the tensile strength of concrete f_{ct}, compressive strength of concrete f_c, and tensile strength of epoxy resin f_{ctas} (Fig. 5.8a and b). A gradual increment was observed in the correlation coefficient of the concrete compressive strength f_c.

(a) (b)

Fig. 5.8 Sensitivity analysis in the retrofitted specimen (a) positive loading direction (b) negative loading direction

6 CASE III: BOND TEST

This chapter deals with the exhibited performance of beam-type RILEM bond specimens and their stochastic assessment by computational stochastic mechanics.

6.1 Experimental Program

The principle of the test described in this section is based on RILEM recommendation [30] and EN 10080 [31]. A beam specimen is tested under flexure by a four-point bending test (Fig. 6.1a). The failure criterion is the complete loss of adhesion in one half of the beam or failure of reinforcing steel. The axial stress in the reinforcing bar is transmitted to the surrounding concrete surface through shear stress.

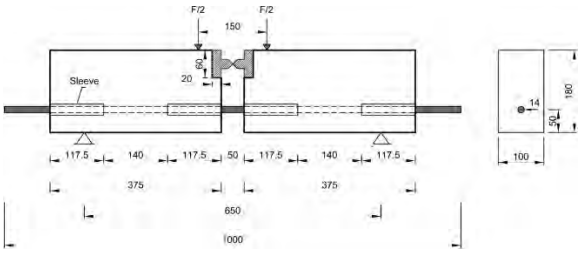

(a)

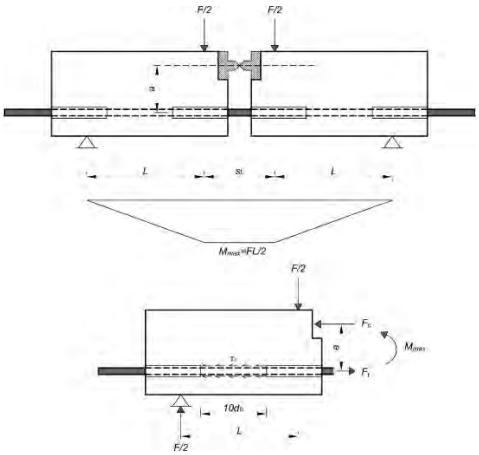

(b)

Fig. 6.1 (a) Beam test specimen detail for d_b=14 mm (b) load transfer mechanism [31]

The experimental program consists of two testing groups (Fig. 6.2). The test samples in both groups were identical in terms of material properties and dimensions but differ in testing methodology. The first test group was exposed to the monotonic loading, while the second one was tested under reverse cyclic loading. Each group was then divided into two testing series. The first test series was constructed without transverse reinforcement. The bond behavior in plain concrete was, therefore, investigated. The second series contains test specimens with transverse reinforcement so that the effect of confinement provided by the shear reinforcement can be revealed.

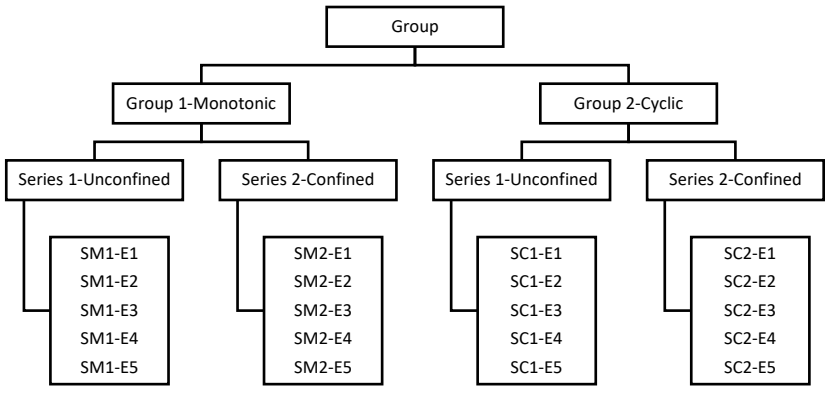

Fig. 6.2 Summary of test specimens

6.1.1 Monotonic Test Setup

The four-point bending test setup with a symmetrical configuration was designed. The specimens were tested under monotonic loading up to failure. The specimens were placed horizontally and then loaded vertically. The displacement was applied at mid-span by a hydraulic jack acting vertically through rigid steel plates. The hydraulic jack was placed to an adjustable steel frame that allows movement in both horizontal and vertical directions. The top-end of the actuator was fixed to the steel frame by a steel plate while a cardan joint was attached to the jack from the bottom-end (Fig. 6.3).

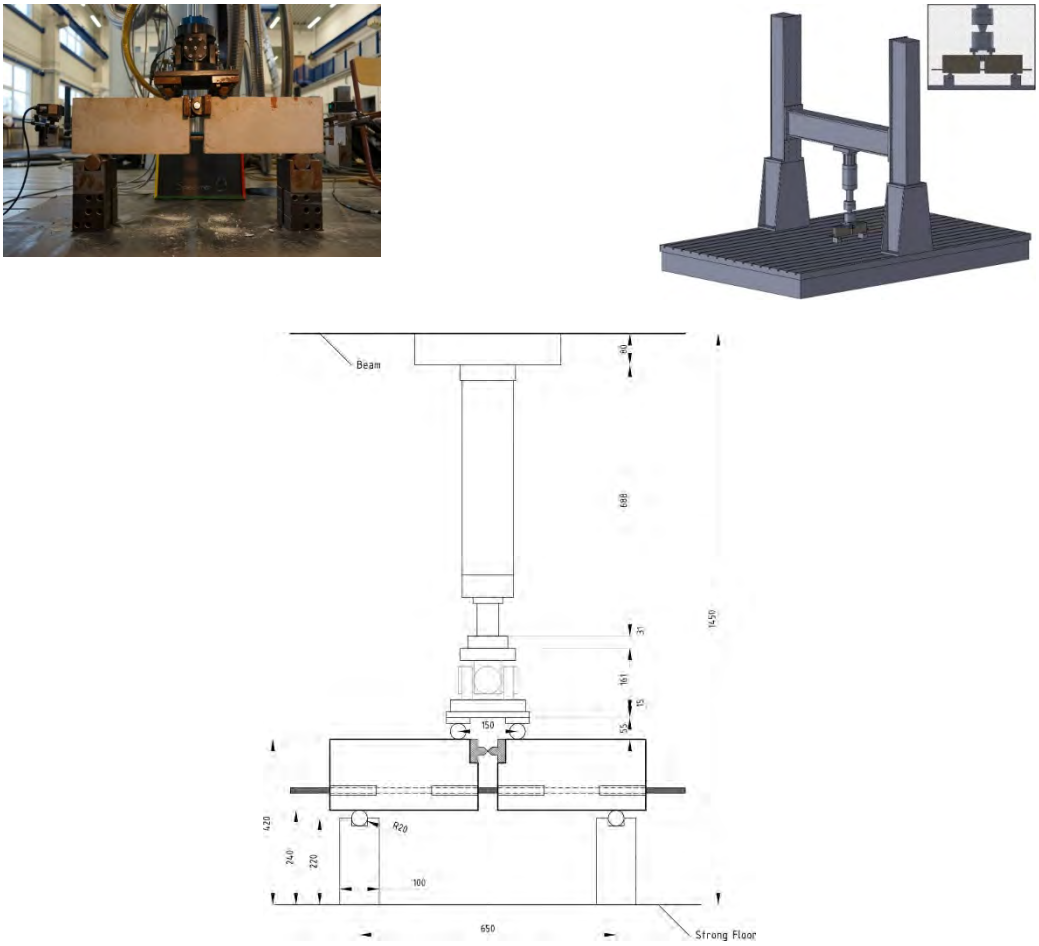

Fig. 6.3 Detail of monotonic test setup

6.1.2 Cyclic Test Setup

The ordinary arrangement of the supports in the monotonic test setup is a pin and roller configuration on each side of the specimen. The loading is provided by two loading rollers placed at an equal distance around the middle of the beam. Then, the specimen sitting on the supports is imposed to load lowered from the above without clamping. This does not bring any indeterminacy in a bent beam since the axial deformations are not restricted. On the other hand, such a test setup configuration results in an instability under reverse cyclic loading since it is not supported during unloading. Thus, the test setup in monotonic cyclic loading is not capable of performing tests under reverse cyclic loading. Therefore, the monotonic four-point bending test setup must be modified for the cyclic tests. Soleymani *et al.* [32] adapted a suitable support-clamping mechanism, which allows one to load and support the specimen under reverse cyclic loading in a stable manner (Fig. 6.4).

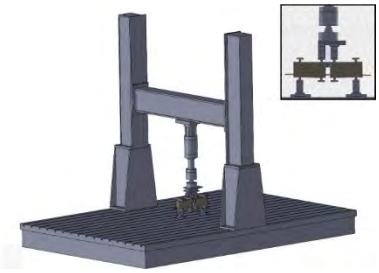

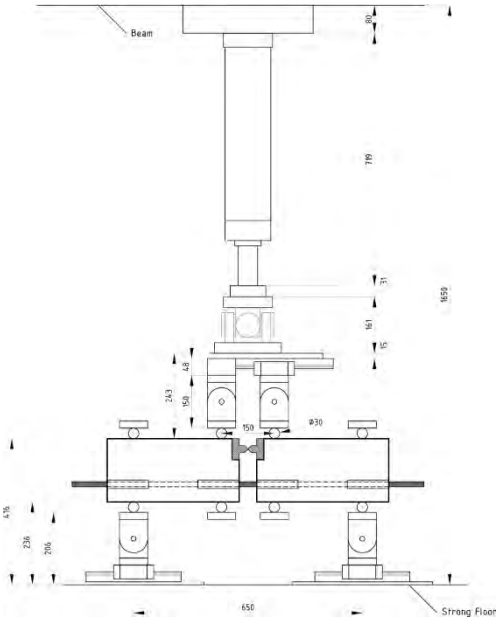

Fig. 6.4 Detail of cyclic test setup

6.2 Bond-Slip Relation for Monotonic Loading

6.2.1 Proposed Bond Model for Unconfined Concrete

Five identical specimens were tested under the same conditions and then the bond strength for each specimen was evaluated. The bond stress was computed as the ratio between axial force in the reinforcing bar and surface area. The analytical relationship (see equations below) was proposed by fitting a curve (i.e., the method of least squares) to the mean experimental data (Fig. 6.5).

$$\tau_u(s) = \begin{cases} \tau_{u1}\left(\dfrac{s}{s_{u1}}\right)^{\alpha} & if\ s < s_{u1} \\ 0.015s^2 - 0.15s + 0.71 & if\ s_{u1} \le s \le s_{u2} \\ \tau_{u2} & otherwise \end{cases} \quad \text{Eq. 6.1}$$

where the variables in the formula defined as follows:

$$\tau_{u1} = 0.63 f_c^{\,1/4} \quad \text{Eq. 6.2}$$

$$\tau_{u2} = 0.53 \times \tau_{u1} \quad \text{Eq. 6.3}$$

$$\alpha = 0.15 \quad \text{Eq. 6.4}$$

$$s_{u1} = \sqrt{\frac{f_c}{40}} \quad s_{u2} = 5.0 \quad \text{Eq. 6.5}$$

Here, τ_{u1} and τ_{u2} are the maximum and residual bond strength values. s_{u1} and s_{u2} are the slip values at the ultimate and residual bond strength, respectively. α is a shape factor.

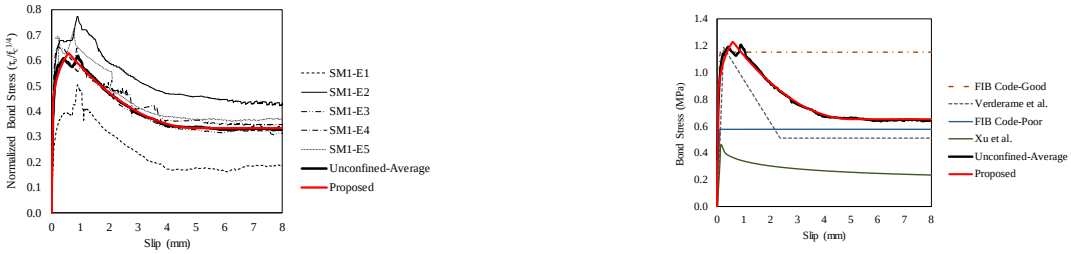

(a) (b)

Fig. 6.5 (a) Proposed bond-slip model for unconfined concrete under monotonic loading (b) comparison with available models

6.2.2 Proposed Bond Model for Confined Concrete

The three-segment curve, which was evaluated by data analysis (i.e., curve fitting to an average of experimental data), was also proposed for the confined concrete (Fig. 6.6).

$$\tau_c(s) = \begin{cases} \beta_c \times \left[\tau_{c1}\left(\frac{s}{s_{c1}}\right)^{\alpha}\right] & if\ s < s_{c1} \\ \beta_c \times [0.01s^2 - 0.11s + 0.782] & if\ s_{c1} \le s \le s_{c2} \\ \beta_c \times \tau_{c2} & otherwise \end{cases} \quad \text{Eq. 6.6}$$

where the variables in the formula defined as follows:

$$\tau_{c1} = 0.69 {f_c}^{1/4} \quad \text{Eq. 6.7}$$

$$\tau_{c2} = 0.70 \times \tau_{c1} \quad \text{Eq. 6.8}$$

$$\alpha = 0.20 \quad \text{Eq. 6.9}$$

$$s_{c1} = \sqrt{\frac{f_c}{12}} \quad s_{c2} = 6.0 \quad \text{Eq. 6.10}$$

$$\beta_c = 0.855 e^{f_e \Big/ f_c^{\frac{2}{3}}} \text{ for } f_e \ge 0.05 \quad \text{Eq. 6.11}$$

Here, τ_{c1} and τ_{c2} are the maximum and residual bond strength values. s_{c1} and s_{c2} are the slip values at the ultimate and residual bond strength, respectively. α is defined as a shape factor. Unlike the bond model proposed for unconfined concrete, two more variables were included in the confined bond-slip relation; those were f_e and β_c, indicating confinement pressure provided by transverse reinforcement and confinement factor, respectively. In this study, the effective lateral confining pressure was computed according to Mander *et al.* [33].

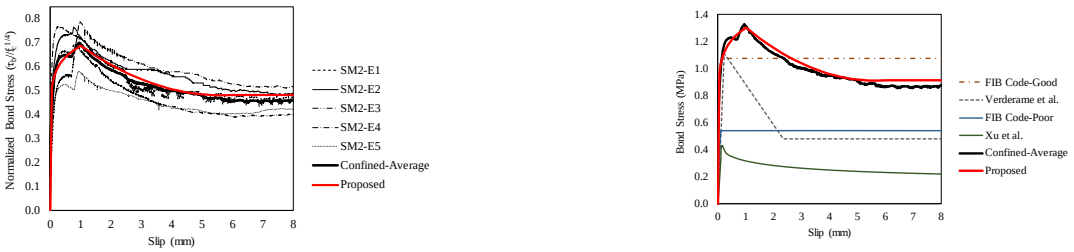

(a) (b)

Fig.6.6 (a) Proposed bond-slip model for confined concrete under monotonic loading (b) comparison with available models

6.3 Bond-Slip Relation for Cyclic Loading

6.3.1 Proposed Bond Model for Unconfined Concrete

Similar to the methodology described in the previous section, the bond-slip relationship under cyclic loading was evaluated from experimental data. The bond stress was computed as the ratio between the axial force in the reinforcing bar and surface area (Fig. 6.7 and Fig. 6.8).

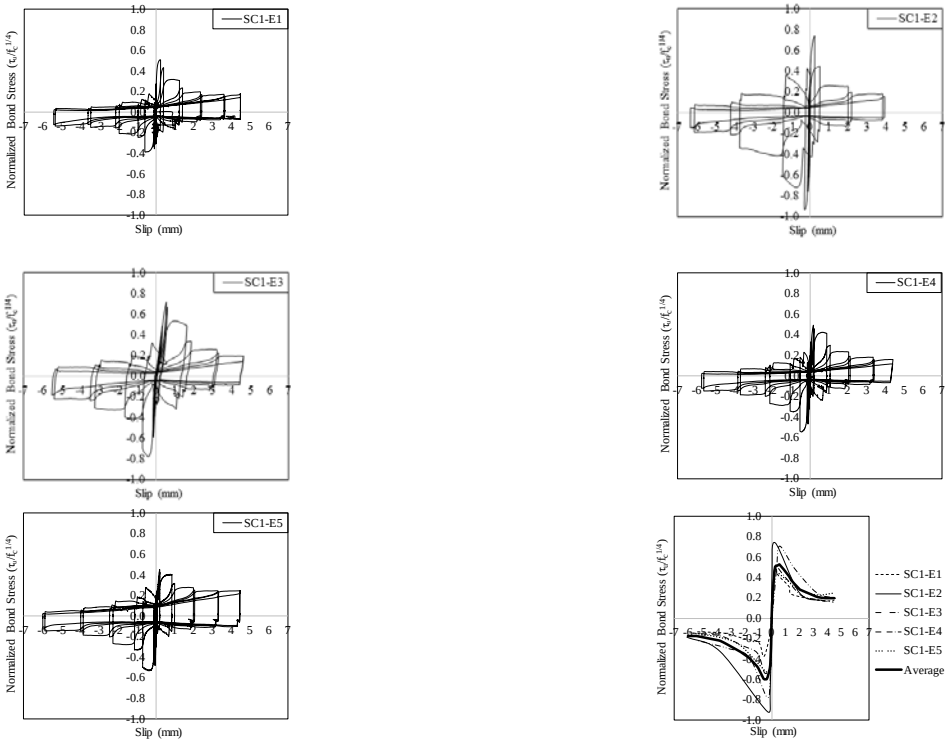

Fig. 6.7 Hysteric bond stress-slip response of unconfined specimens

The bond-slip relationship of the unconfined test specimens under cyclic loading was evaluated from the positive envelope curves, which is as follows:

$$\tau_u(s) = \begin{cases} \tau_{u1}\left(\dfrac{s}{s_{u1}}\right)^{\alpha} & if\ s < s_{u1} \\ 0.027s^2 - 0.23s + 0.65 & if\ s_{u1} \le s \le s_{u2} \\ \tau_{u2} & otherwise \end{cases} \qquad \textbf{Eq. 6.12}$$

where the variables in the formula defined as follows:

$$\tau_{u1} = 0.56 f_c^{\,1/4} \qquad \textbf{Eq. 6.13}$$

$$\tau_{u2} = 0.43 \times \tau_{uc1} \quad \textbf{Eq. 6.14}$$

$$\alpha = 0.42 \quad \textbf{Eq. 6.15}$$

$$s_{u1} = \sqrt{\frac{f_c}{80}} \quad s_{u2} = 2.5 \quad \textbf{Eq. 6.16}$$

Here, τ_{u1} and τ_{u2} are the maximum and residual bond strength values. s_{u1} and s_{u2} are the slip values at the ultimate and residual bond strength, respectively. α is a shape factor.

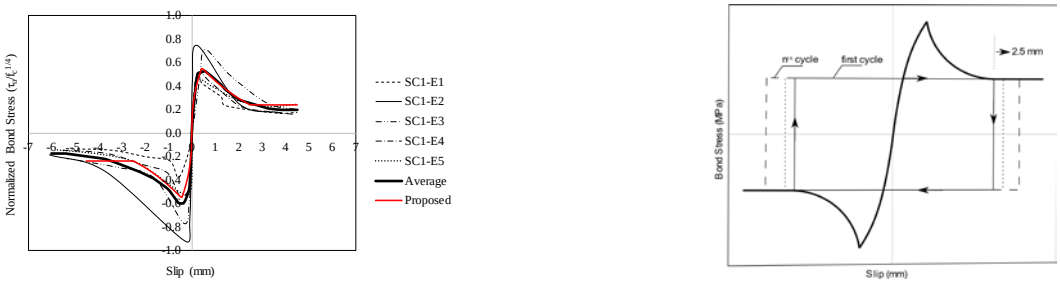

(a) (b)

Fig. 6.8 (a) Proposed bond-slip model for unconfined concrete under cyclic loading (b) schematic representation

6.3.2 Proposed Bond Model for Confined Concrete

The confined specimens under cyclic loading displayed a poor bond performance. The bond strength degraded suddenly and then it remained constant (i.e., residual part). When the load was exerted in the reverse direction, the slip value did not change considerably. On the other hand, the bond stress changed its sign. The semi-circle phenomenon was established under the cyclic action (Fig. 6.9). The proposed relationship was, yet again, obtained only for the positive loading direction. The hysteric bond-slip behavior was considered by the semi-circles' phenomenon in the proposed bond-slip relationship, which can be implemented by *Memory Bond Material* in ATENA [1]. It is assumed that the first critical-inversion slip occurred at 3.0 mm (Fig. 6.10). This value corresponds to the start of the residual bond stress value.

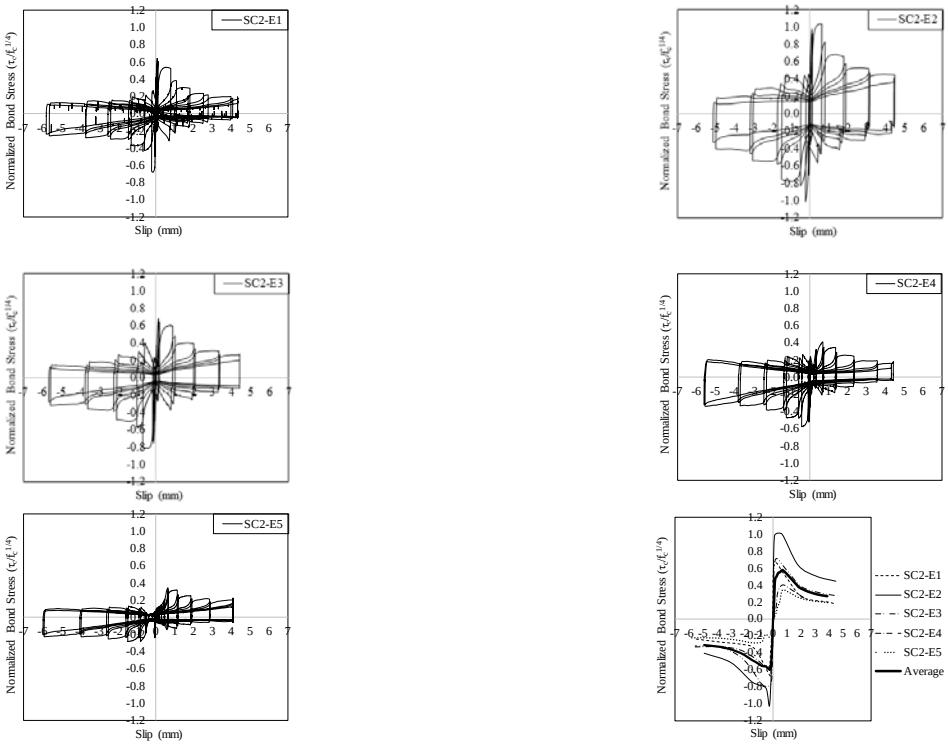

Fig. 6.9 Hysteric bond stress-slip response of confined specimens

The equation of a three-segment curve was provided in Eq. 6.17

$$\tau_c(s) = \begin{cases} \beta_c \times \tau_{c1}\left(\frac{s}{s_{c1}}\right)^{\alpha} & if\ s < s_{c1} \\ \beta_c \times [0.046s^2 - 0.29s + 0.77] & if\ s_{c1} \le s \le s_{c2} \\ \beta_c \times \tau_{c2} & otherwise \end{cases} \quad \text{Eq. 6.17}$$

where the variables in the formula defined as follows:

$$\tau_{c1} = 0.60 {f_c}^{1/4} \quad \text{Eq. 6.18}$$

$$\tau_{c2} = 0.5 \times \tau_{c1} \quad \text{Eq. 4.19}$$

$$\alpha = 0.22 \quad \text{Eq. 6.20}$$

$$s_{c1} = \sqrt{\frac{f_c}{30}} \quad s_{c2} = 3.0 \quad \text{Eq. 6.21}$$

$$\beta_c = 0.855 e^{f_e \Big/ f_c^{\frac{2}{3}}} \ for\ f_e \ge 0.05 \quad \text{Eq. 6.22}$$

Here, τ_{c1} and τ_{c2} are the maximum and residual bond strength values. s_{c1} and s_{c2} are the slip values at the ultimate and residual bond strength, respectively. α is a shape factor. f_e and β_c indicating confinement pressure provided by transverse reinforcement and confinement factor, respectively.

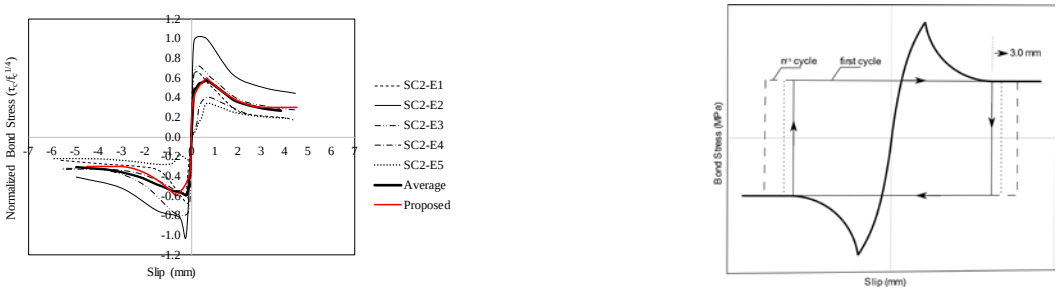

(a) (b)

Fig. 6.10 (a) Proposed bond-slip model for confined concrete under cyclic loading (b) schematic representation

6.4 Effect of Confinement on Bond-Slip Response

The complete loss of adhesion between the plain round bar and surrounding concrete occurred before reaching the tensile strength of the concrete f_{ct}. The microcracks took place in the contact area, which significantly violates the cohesion. Due to lateral confinement provided by the transverse reinforcement, which enhanced the concrete mechanical properties, the microcrack initiation was delayed or somehow minimized, which contributes cohesion in between the reinforcing steel and surrounding concrete. Therefore, a higher ultimate bond strength was computed for the confined concrete (Fig. 6.11a and b). The lateral confinement provided by the transverse reinforcement also changed the post-peak response. The nonlinear descending part of the bond-slip model for the confined concrete diminishes less steeply than the unconfined concrete. The slip corresponding to the bond stresses at transition zones differed as well. The residual bond strength formed at higher values for the confined case.

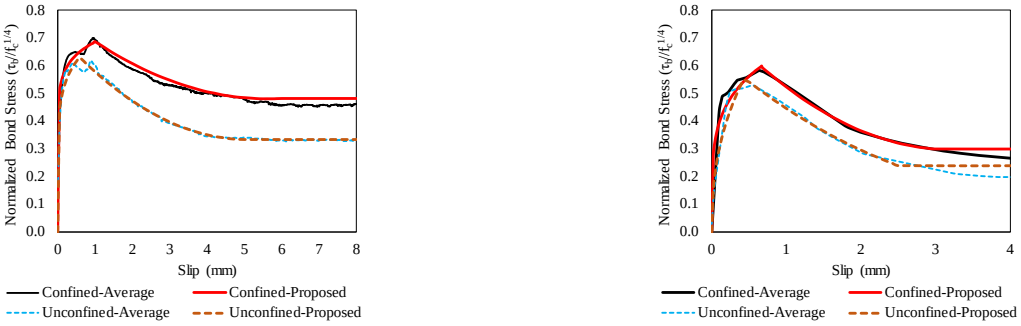

(a) (b)

Fig. 6.11 Comparison of bond-slip models in confined and unconfined cases (a) monotonic loading (b) cyclic loading

6.5 Effect of Loading Scheme

The influence of the loading scheme on the response of the RC structures is essential as the deformation capacity of them differs under cyclic and monotonic loading. This partially violates the interaction between reinforcing steel and the surrounding concrete, which adversely affects the structural integrity. The monotonic and envelope of cyclic curves followed almost the same path in the initial loading stages while the gap widened remarkably at peak response. The significant bond degradation due to the nature of cyclic loading was more pronounced, especially in the post-peak region (Fig. 6.12a and b). The failure came out earlier under cyclic loading.

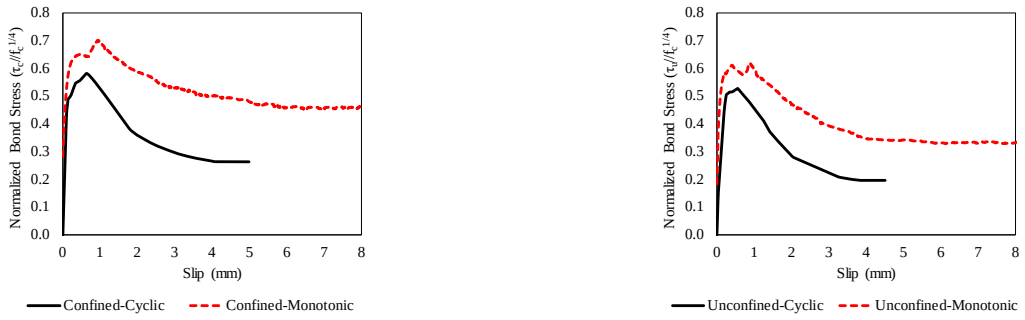

(a) (b)

Fig. 6.12 Effect of loading scheme (a) unconfined concrete (b) confined concrete

6.6 Randomized Behavior under Monotonic Loading

The peak loads observed in the experiments were either at the edges of the bundle or within the upper and lower boundaries of the stochastic assessment (Fig. 6.13a and b). The post-peak response was accurately captured by the stochastic approach in the confined specimen, while the unconfined specimen SM1-E1 imparted a significant strength deterioration. It, therefore, fell out of the stochastic bundle. The remaining samples in the unconfined test series were simulated at an acceptable level.

(a) (b)

Fig. 6.13 Randomized behavior under monotonic loading (a) unconfined case (b) confined case

The PDFs corresponding to the ultimate loads, together with the mean and standard deviation, were determined from the stochastic bundle, which were then compared with the experimentally obtained capacities (Fig. 6.14a and b). The dispersion in the capacity distribution was accurately characterized by the stochastic model.

(a) (b)

Fig. 6.14 PDFs of ultimate load under monotonic loading (a) unconfined case (b) confined case

6.7 Randomized Behavior under Cyclic Loading

The ultimate capacity was satisfactorily captured by the FE solution; on the other hand, the displacement corresponding to the ultimate load was not accurately reproduced. The strength degradation was not characterized as well (Fig. 6.15a and b). The PDFs of the ultimate load were

obtained from the ultimate capacity of each FE solution. Therefore, a good match in the peak response yields an accurate estimation of basic statistical characteristics.

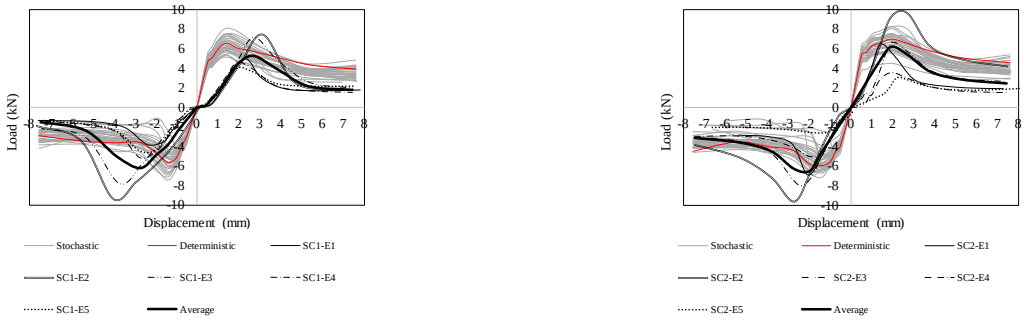

(a) (b)

Fig. 6.15 Randomized behavior under cyclic loading for (a) unconfined case (b) confined case

The PDFs of the ultimate strength were obtained from the stochastic bundle. Experimental capacities were then compared with the stochastic assessment (Fig. 6.16a and b). Note that if n likely specimens were tested n^{th} times under the same conditions, assuming that n is a relatively large number, similar statistical outcomes of the tests (mean, standard deviation, and PDFs) would be expected. Therefore, it is expected that the experimental results would be within the range of the PDF if the scatter was accurately reproduced by the stochastic assessment. On the other hand, some of the test results were not covered by the PDFs.

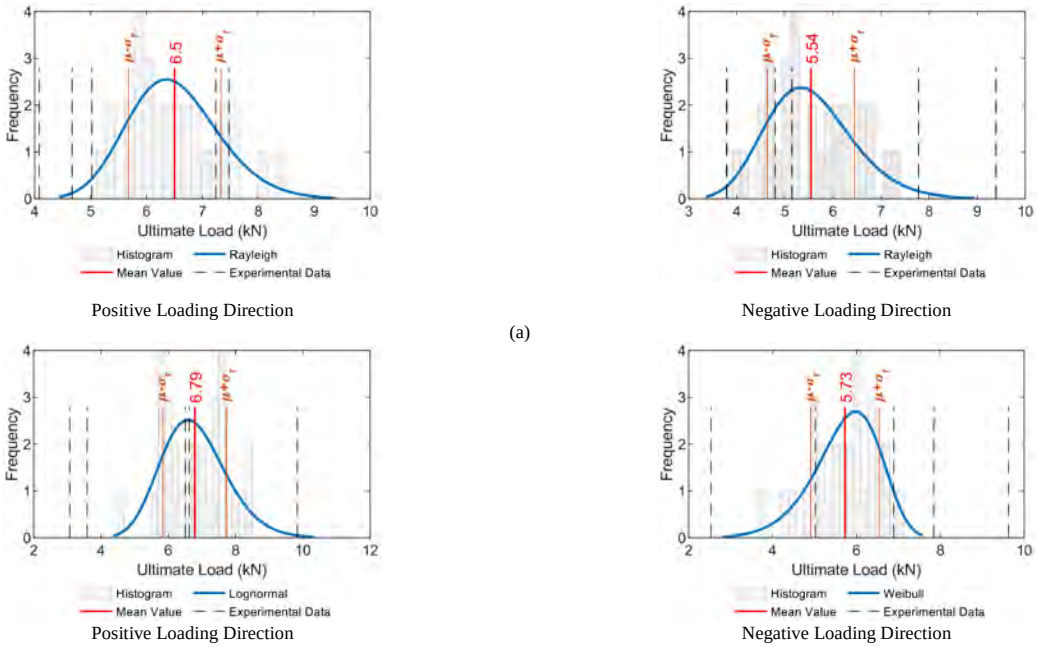

Positive Loading Direction Negative Loading Direction

(a)

Positive Loading Direction Negative Loading Direction

(b)

Fig. 6.16 PDFs of ultimate load under cyclic loading (a) unconfined case (b) confined case

6.8 Sensitivity Analysis

The highest correlation coefficient was computed for the concrete tensile strength f_{ct} in both monotonic and cyclic loading cases (Fig. 6.17a and b). The compressive strength of the concrete f_c contributes to the overall response with a medium impact. The remaining material parameters had little or no influence on the global response as the partial correlation coefficient was nearly zero.

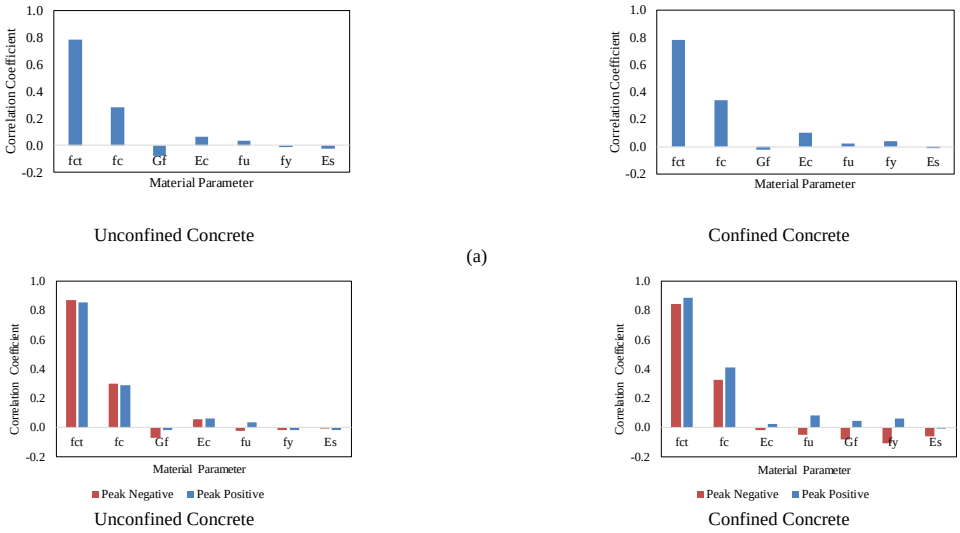

Fig. 6.17 Sensitivity analysis (a) monotonic loading (b) cyclic loading

7 CONCLUSION

This study mainly deals with the assessment of different failure modes in substandard RC members by stochastic approaches. The nonlinear FEM was combined with a suitable stochastic sampling technique for the realistic prediction of the structural response of substandard RC members. The effect of inherent uncertainties on the material mechanical properties was studied using an uncertainty analysis, which also leads to obtaining the basic statistics of response variables. The sensitivity of material properties on the global response was also measured by evaluating the partial correlation coefficient between material parameters (i.e., input variable) and the strength of the member (i.e., response variable). Moreover, the uneven distribution of concrete mechanical properties over the specimen was accurately characterized by random fields theory, which establishes weaker and stronger spots over the specimen.

This research context was organized into seven main chapters. The first three chapters dealt with the motivation for the research, numerical modeling strategy, and stochastic-based analysis methods. The following three chapters introduced the implementation of the advanced assessment strategy on different substandard RC members. Each chapter was identical in terms of the method employed for stochastic assessment, while the test programs and resulting failure modes were different. Note that a section which summarizes the relevant chapter was included at the end of each chapter. The first testing program dealt with the performance of over-reinforced and shear critical beams. The experimental behavior was accurately reproduced in the FE environment. The effect of inherent uncertainties at a material level for over-reinforced and shear critical beam and uneven distribution of concrete mechanical properties over the shear critical beam were handled by a stochastic approach. This led to a more accurate assessment of the results. The shear critical and CFRP retrofitted beam-column joints were analyzed in the following chapter. The experimental performances were closely estimated by the numerical solutions. The relative impact of each material properties on the global response was also provided, which remarked the most critical material parameters. The last testing program focused on the stochastic-based numerical prediction of beam-type RILEM bond specimens. Thus, the proposed bond stress-slip relationship was implemented in the FE

software and then evaluated to the stochastic level. The variability in the identical tests was characterized accurately by the stochastic assessment. The experimental results were covered by the stochastic bundle.

To conclude, owing to the more realistic assessment capability of the stochastic-based nonlinear FE analysis, which is now available in user-friendly computer tools, reproducing the structural response of substandard members by computational stochastic mechanics could yield more accurate results for assessment purposes. Overall, this study showed the efficiency of the advanced modeling strategy in different substandard RC members.

REFERENCES

[1] ATENA Program Documentation, Part 1. Atena theory manual, Cervenka Consulting, http://www.cervenka.cz/. 2014.

[2] Van Mier JGM. Multiaxial strain-softening of concrete, Part I: Fracture. Materials and Structures, RILEM 1986;19.

[3] Vecchio FJ, Collins MP. Modified compression-field theory for reinforced concrete beams subjected to shear. ACI Journal 1986;83:219–31.

[4] Kollegger J, Mehlhorn G. Experimentelle und analytische untersuchungen zur aufstellung eines materialmodels für gerissene stahbetonscheiben. Nr.6 Forschungsbericht, Massivbau, Gesamthochschule Kassel: 1988.

[5] Menetrey Ph, Willam KJ. Triaxial failure criterion for concrete and its generalization. ACI, Structural Journal 1995;92:311–8. doi:10.14359/1132.

[6] Hordijk DA. Local approach to fatigue of concrete. Ph.D. Thesis, Delft University of Technology, Netherlands: 1991.

[7] Bazant Z, Oh B. Crack band theory for fracture of concrete. Materials and Structures 1983;16:155–77.

[8] CEB-FIP Model Code. Comittee Euro-International du Beton, Bulletin d'information. 2010.

[9] Menegotto M, Pinto PE. Method of analysis for cyclically loaded reinforced concrete plane frames including changes in geometry and non-elastic behaviour of elements under combined normal force and bending. International Association of Bridge and Structural Engineering (IABSE), Lisbon, Portugal, vol. 13, 1973, p. 15–22.

[10] ATENA Program Documentation Part 4-9. ATENA Science – GiD Strengthening of concrete structures, Step by step guide for modelling strengthening with ATENA and GiD, http://www.cervenka.cz/. 2016.

[11] Mohr O. Welch umsttinde bedingen die elastizitltsgrenze und den bruch eines materials? Zeitschrift Des Vereins Deutscher Ingenieure 1900;44–45:1524-1530;1572-1577.

[12] Pukl R, Sajdlova T, Routil L, Novák D, Seda P. Case study – Nonlinear reliability analysis of a concrete bridge. Maintenance, Monitoring, Safety, Risk and Resilience of Bridges and Bridge Networks: Proceedings of the 8th International Conference on Bridge Maintenance, Safety and Management (IABMAS2016), 2016.

[13] fib Bulletin No.22. Monitoring and safety evaluation of existing concrete structures. 2003.

[14] Gulbrandsen P. Reliability analysis of the flexural capacity of fiber reinforced polymer bars in concrete beams, M.Sc. Thesis. University of Minnesota, 2005.

[15] Atadero RA, Karbhari VM. Sources of uncertainty and design values for field-manufactured FRP. Composite Structures 2009;89:83–93. doi:10.1016/j.compstruct.2008.07.001.

[16] Baji H, Ronagh HR, Li CQ. Probabilistic design models for ultimate strength and strain of FRP-confined concrete. Journal of Composites for Construction 2016;20:04016051. doi:10.1061/(ASCE)CC.1943-5614.0000704.

[17] Joint Committee on Structural Safety. Probabilistic model code, Part 3: Material properties. http://www.jcss.byg.dtu.dk; 2000.
[18] ACI 318M-11. Building code requirements for structural concrete and commentary (aci 318m-11), USA: American Concrete Institute. 2011.
[19] Duran B, Tunaboyu O, Avşar Ö. Determination of elasticity modulus of low strength concrete and its effect on the risk assessment results by DSVB. Journal of The Faculty of Engineering and Architecture of Gazi University 2017;32:253–64. doi:10.17341/gazimmfd.300617.
[20] Griffiths R, Holloway DG. The fracture energy of some epoxy resin materials. Journal of Materials Science 1970;5:302–307.
[21] Vořechovský M. Interplay of size effects in concrete specimens under tension studied via computational stochastic fracture mechanics. International Journal of Solids and Structures 2007;44:2715–31. doi:10.1016/j.ijsolstr.2006.08.019.
[22] Novák D, Vořechovský M, Rusina R. FReET v.1.5 – program documentation. User´s and Theory Guides. http://www.freet.cz. Brno/Červenka Consulting, Czech Republic: 2015.
[23] SARA Studio. SARA (Structural Analysis and Reliability Assessment) User's Manual. http://www.cervenka.cz/; 2015.
[24] EN 1992-1-1. Eurocode 2: Design of concrete structures - Part 1-1: General rules and rules for buildings. 2004.
[25] Yurdakul Ö. Experimental study on the investigation of strengthening the insufficient reinforced concrete beam-column joints by post-tensioning. M.Sc. Thesis. Civil Engineering Program, Graduate School of Sciences, Anadolu University, 2015.
[26] Yurdakul O, Avsar O. Structural repairing of damaged reinforced concrete beam-column assemblies with CFRPs. Structural Engineering and Mechanics 2015;54:521–43. doi:10.12989/sem.2015.54.3.521.
[27] Yurdakul Ö, Avşar Ö. Strengthening of substandard reinforced concrete beam-column joints by external post-tension rods. Engineering Structures 2016;107:9–22. doi:10.1016/j.engstruct.2015.11.004.
[28] Yurdakul Ö, Tunaboyu O, Avşar Ö. Retrofit of non-seismically designed beam-column joints by post-tensioned superelastic shape memory alloy bars. Bulletin of Earthquake Engineering 2018;16:5279–307. doi:10.1007/s10518-018-0323-y.
[29] El-Amoury T, Ghobarah A. Seismic rehabilitation of beam–column joint using GFRP sheets. Engineering Structures 2002;24:1397–1407.
[30] RILEM TC. RC 5 Bond test for reinforcement steel. 1. Beam test, 1982. RILEM recommendations for the testing and use of constructions materials, E & FN SPON; 1994.
[31] EN 10080. Steel for the reinforcement of concrete - Weldable reinforcing steel - General. 2005.
[32] Soleymani Ashtiani M, Dhakal RP, Scott AN, Bull DK. Cyclic beam bending test for assessment of bond–slip behaviour. Engineering Structures 2013;56:1684–97. doi:10.1016/j.engstruct.2013.08.005.
[33] Mander JB, Priestley MJN, Park R. Theoretical stress-strain model for confined concrete. Journal of Structural Engineering 1988;114:1804–26. doi:10.1061/(ASCE)0733-9445(1988)114:8(1804).

Truncated Conical Shells as Absorbers of Impact Force

Author: Ing. Erdem ÖZYURT

Doctoral study programme:
P3710 Technique and Technology in Transport and Communications

Field of study:
3708V024 Technology and Management in Transport and Telecommunications

Supervisor:
doc. Ing. Petr Tomek, Ph.D.

Supervisor specialist:
Prof. Ing. Petr Pašcenko, Ph.D.

Doctoral thesis has arisen at the supervising:
Department of Mechanics, Materials and Machines Parts

ABSTRACT

In this dissertation, energy absorption capabilities of steel-based truncated conical shells with low base angle and end caps are investigated under axial dynamic loading. The numerical models of absorber were placed between two rigid plates to simulate a crush box around the absorber.

In order to investigate the effect of the design parameters on the energy absorption of the conical shells, three different base conical angle (20◦, 25◦ and 30◦), four different impact velocity (5m/s, 10m/s, 20m/s, 30m/s), four different absorber thick- ness (4mm, 6mm, 8mm, 10mm) and several impact mass val- ues were analyzed. Numerical analyses were performed by FEM software Abaqus.

The simulation results were compared by means of several per- formance parameters such as peak reaction force Fp, mean re- action force Fm, absorbed energy EA specific energy absorption (SEA), crash force efficiency (CFE) and dynamic amplification factor (DAF). In this dissertation, also some guidelines on the design of a truncated conical shell with low base conical angle as an energy absorber are presented.

Keywords

crashworthiness, truncated cone, finite element method, energy absorption

1 INTRODUCTION

1.1 Statement of the Research Problem

With the development of the transport technology, there is a substantial increase in number of vehicles and passengers. This increase led to a demand for developing more powerful and faster vehicles. On the other hand, same demand also led to an increase in undesirable situations such as fatal accidents and injuries. The prevention of collisions may not always be possi- ble despite all collision avoidance systems. So it is of utmost importance to control the possible deformation of the vehicle as a result of the collision. Controlling the deformation basi- cally, means to transfer the impact forces to the appropriate sections selected by the designer. The aim here is to ensure that the collision energy is absorbed by the energy absorbers and to minimize or prevent the possible damage to the struc- tural elements of the vehicle. Thus, the undesired damage to the important sections of the vehicle enclosing occupants can be minimized. Picture 1.1 shows various examples of energy absorbers used in different types of vehicles.

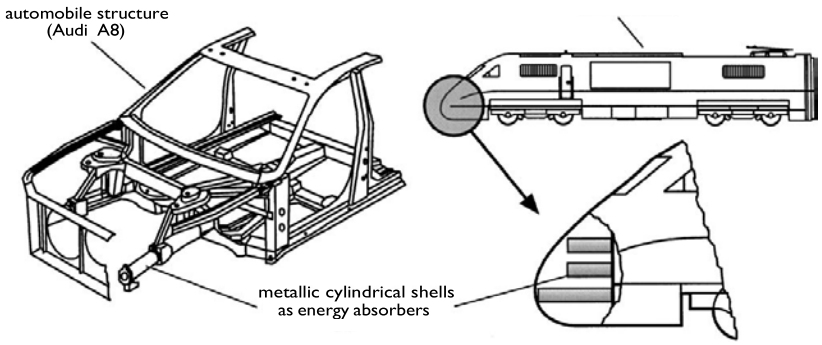

Figure 1.1 Energy absorbers used in various structures. [3]

Another important step of the safety research is to test the developed energy absorbing structure. However, using nu- merous real vehicles to conduct full-scale crash tests can be quite expensive. A virtual testing method using computer sim- ulations become prominent. The finite element method (FEM) is extensively used in crash simulations. The FEM has the abil- ity to solve complex, highly nonlinear problems in many areas with the development of high-performance computers. There- fore, a number of real vehicle tests that need to be performed can be limited and thereby save costs and time.

1.2 Aim of the Doctoral Dissertation

Current doctoral dissertation study is built upon the cur- rent knowledge about the structures used to dissipate impact energy in case of a collision. Current structures being used as impact energy absorbers use mostly the cylindrical tube and rectangular tube geometries more than conical. Thus, most of the studies in the literature are about these type of geometries. On the other hand, there are also too many studies on conically shaped energy absorbers in the literature but most of them have relatively steep conical geometries close to cylindrical tubes.

In this manner, the main aim of this study is to deter- mine the energy absorbing capacity of capped-end truncated cones with relatively low base cone angles and edge ring. Un- like most of the studies, more shallow structures needed to be examined in detail for using as impact

energy absorbers. In this manner it is aimed to investigate conical structures with relatively higher thickness over the thin-walled structures en- countered commonly in the literature.

1.3 Layout of Thesis

The thesis consists of 7 chapters. A brief description of each chapter is presented below.

Chapter 1: Introduces the background of the idea in- cluding the statement of the research problem. Also, introduces the aims of the current study and explanation of the structure of the thesis.

Chapter 2: Involves a detailed information about the crash energy management and energy absorbers. Describes the design requirements and performance parameters which must be considered when designing an energy absorbing structure.

Chapter 3: Includes a summarized literature review about energy absorber structures closely related to the field of this study. Also, a general comparison of the current study with the previous studies in the scopes of the study section takes place.

Chapter 4: Describes the numerical method used in the present study with basic procedures. Numerical difficulties of nonlinearity and time integration methods are presented in de- tail. Also, includes the terminology of the current FEM soft- ware which terms are used in the further chapters of the study.

Chapter 5: Provides a detailed description of numerical simulation techniques performed in this study. This chapter also describes the geometrical parameters, material properties and finite element modeling parameters such as loading condi- tions, boundary conditions and mesh structure of the numerical models.

Chapter 6: Evaluates a detailed investigation of the re- sults obtained from both quasi-static and dynamic simulations in consideration of different performance parameters such as force-displacement curves, absorbed energy, specific energy ab- sorption, and crash force efficiency. The effects of varying load- ing conditions and model geometry are investigated and pre- sented. Also some basic comparisons of the simulation results to the current literature for the effect of the variables on the performance parameters are given.

Chapter 7: Presents a summary of major conclusions and contributions to the current study. Also includes some design guidelines and a brief description of the further works planned to improve the results of the present study.

2 LITERATURE REVIEW

2.1 Literature About the Current Problem

Commonly used geometrical shapes of energy absorbers in most studies are cylindrical tube [18, 19], square tube [20, 21] and truncated conical tube [22] also known as a frustum. In the current literature, there are various terms used for identifying the conical structures which are conical shells, cones, conical tube, frustum and frusta. Although most of the studies are focused on cylindrical and rectangular tubes, crashworthiness of conical structures has been studied by many authors.

Langseth and Hopperstad [23], Mamalis et al. [24], Tai et al. [25], Gupta et al. [28] Alghamdi et al. [30], Azimi and Asgari [34] and more authors have investigated various different

geometries under axial and oblique loading to obtain the energy absorption characteristics of the structures.

2.2 Scope of the Study

With respect to the aims of the dissertation study as men- tioned before, the main scope of the present study is to deter- mine the usability of the conical geometries of low base cone angles as an energy absorbing structure. In this manner, mod- els with various geometric parameters such as the base conical angle and the absorber thickness have been modeled.

A geometry of conical absorbers reversed and connected together was chosen to make the total length of the absorber more adjustable to compare with other absorbers used in the current literature. Based on the aforementioned scope, detailed goals of the study are summarized below.

• To evaluate series of various numerical models for conical structures with different base angle and thickness values in order to simulate the axial impact under various load- ing velocity and mass values by using the Abaqus/Explicit FEM software.

• To perform analysis on the structures modeled as energy absorbers with variable impact velocities, impact masses and geometrical parameters such as the absorber thick- ness and base conical angle.

• To process the data from the numerical results with re- spect to different result parameters to investigate the ef- fectiveness of structures under impact loading to be used as energy absorbers.

• To generate an opinion on the usability of the structure as an energy absorber by taking into consideration of both commonly used structures.

3 BACKGROUND

3.1 Crash Energy Management

Crashworthiness can be defined as the capability of a ve- hicle to withstand a crash and protect its passengers from the effects of an accident. Main crashworthiness goals are to absorb the kinetic energy of a collision with an acceptable deceleration pulse and maintain a survival space to protect passengers.Crash Energy Management (CEM) is the sum of the techniques to im- prove the overall crashworthiness of a vehicle. Possible damages of an accident should be predicted and should be kept under control. With crash energy management systems, damage of a collision is transferred to the parts that designed to absorb the crash energy and protect the main structural elements of the vehicle.

3.2 Energy Absorbers

Energy absorbers absorb energy both in a reversible and irreversible way such as elastic strain energy and plastic defor- mation energy. Collapsible energy absorbers aim to convert the majority of the kinetic energy of impact into plastic deforma- tion in an irreversible manner.[8]

General Design Requirements

In the design phase of an energy absorber, one must consider the specific requirements of the area that absorber is planned to use. In all cases, the main purpose is to scatter crash energy in

a foreordained way. In this manner, some essential requirements are listed and described below.[12]

1. Irreversible Energy Conversion
2. Restricted and Constant Reaction Force
3. Long Stroke
4. Stable and Repeatable Deformation Mode
5. Lightweight and High Specific Energy Absorption
6. Low Cost and Easy Installation

Performance Parameters

Even if the most important parameter of an energy ab- sorber is the amount of dissipated energy, it is not sufficient to estimate the performance of the absorber by considering only the amount of the energy absorbed during the impact. For a reasonable performance estimation, it is needed to define and investigate following parameters:

1. Force-Displacement Curves
2. Energy Absorption
3. Crash Force Efficiency (CFE)
4. Specific Energy Absorption (SEA)
5. Absorbed Energy According to Displacement
6. Stroke Efficiency
7. Dynamic Amplification Factor

4 NUMERICAL MODEL AND SIMULATIONS

The numerical models for the simulations were created using the CAE module of the FEM software Abaqus. [36]

4.1 Model Geometry

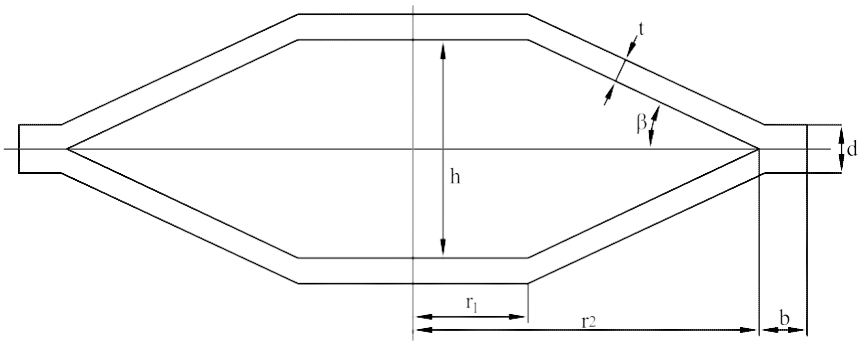

Figure 4.1 Geometry and dimension parameters of the ab- sorber structure.

A basic sketch of the absorber structure is given in Figure 4.1 with dimension parameters. Dimension parameters used to model the structures are, inner diameter r1, outer diameter r2, edge ring width b, edge ring height d, thickness t, cone angle β and deformation length h. The edge ring width b is kept con- stant in all simulations, hence the effect of this parameter on the energy absorbing capability of the structure is not investi- gated in the current study. Values used for all parameters are given in Table 4.1.

Structures were modeled by creating each plate and the absorber as quarter models of real dimensions of structures. The model assembly includes three equally designed rigid plates and a conical absorber. The conical absorber was positioned between two rigid plates (top and bottom plate) to simulate a crush box and also to control the deformation of the struc- ture. Rigid plates were constrained to the absorber using the constraint definitions explained in further sections.

Table 4.1 Dimension values of the absorber structures.

β	h	t	b	d	r_1	r_2
[deg]	[mm]	[mm]	[mm]	[mm]	[mm]	[mm]
20	72.8	10	20	20	50	150
25	93.3	8		16		
30	115.5	6		12		
		4		8		

The third plate (striker plate) is used to simulate the striking mass crushing to the conical absorber. A gap of 1mm between the top plate and the striking plate was modeled to examine the effect of the first contact more conveniently. The general assembly of all parts used in the numerical models are shown in Figure 4.2

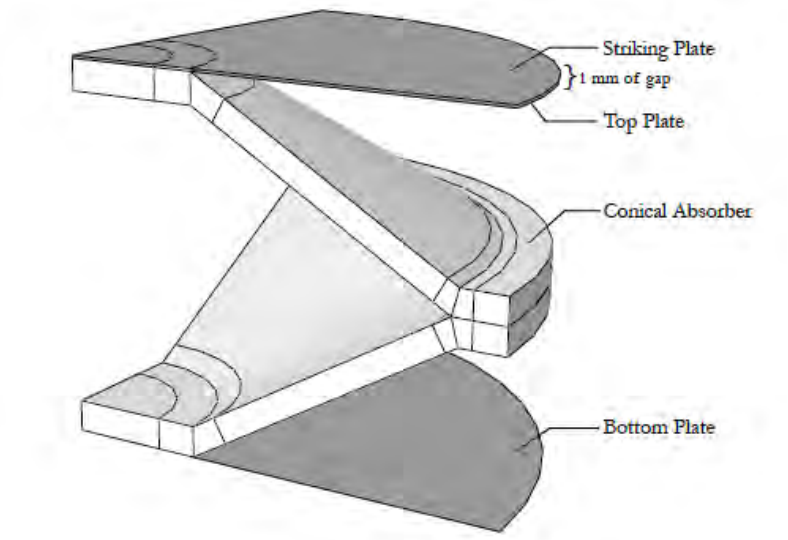

Figure 4.2: Assembly of the absorber and the rigid plates.

4.2 Material Properties

The material used for the simulations were considered to be structural mild steel denominated as S235JR. In numerical analysis, an elastoplastic hardening module was implemented to the material behavior. Mechanical properties of material S235JR are used as; Young's Modulus of 200GPa, Poisson's Ratio of 0.29 Mass Density of 7980kg/m3, Yield Strength of 296.4MPa and Ultimate Tensile Strength of 381MPa.

Material properties are of great importance at crashwor- thiness and impact studies. The plastic flow of some materials is sensitive to loading speed, which is known as material strain- rate sensitivity, or viscoplasticity. The strain rate sensitivity phenomenon can influence the dynamic response of the energy absorbing structures. Previous studies have indicated that S235 steel displays a significant positive strain rate effect on the yield stress of the material. [44, 45] Verleysen et. al. [44] have inves- tigated the influence of the strain rate on the forming properties of three commercial steel grades including S235JR.

The static tensile test results of the present study and the results from the aforementioned article by Verleysen et. al. [44] are compared and they are found to be essentially identical for the S235JR steel. Due to the technical impossibilities and the lack of equipment for SHTB experiments, the Johnson-Cook model in the study of Verleysen et. al. [44] for S235JR steel with strain rate properties are adapted to the numerical models of the present study. Consequently, the Johnson-Cook plasticity model parameters including strain rate used in this study are given in Table 4.2.

Table 4.2 Johnson-Cook plasticity parameters of S235JR. [44]

A	B	n	C	$\dot{\varepsilon}_0$
280 MPa	667 MPa	0.72	0.071	$5.6\text{x}10^{-4}$

4.3 Loading and Boundary Conditions

In quasi-static numerical simulations, the load is applied very slowly that the deformation of the structure is not affected by the strain rate and inertia forces which are very small and

negligible. Loading was applied to the rigid striking plate as a predefined velocity over the longitudinal axis of the model assembly. Quasi-static velocity is selected to be 0.01m/s.

In dynamic simulations, it is planned to apply the load as kinetic energy. The kinetic energy was generated by defining a velocity and a mass to the striking plate. Used mass quanti- ties are calculated to obtain 100kJ of initial kinetic energy for each model. Moreover, mass values of 1000kg and 2000kg were defined for each impact speed to investigate the effect of the impact mass. Four different impact velocities (5m/s, 10m/s, 20m/s and 30m/s) were selected and simulated for each impact mass, base conical angle and absorber thickness combination.

Interactions between parts were defined using self-contact and surface to surface contact algorithms. Self-contact was used to define self-contact of absorber structure with penalty contact definition with a friction coefficient of 0.3 as tangential contact behavior and hard contact as normal contact behavior. To sim- ulate a crush box, the conical energy absorber was coupled to two rigid plates from the top and bottom surfaces. A kinematic coupling definition was used.

Any movement of the bottom plate was restrained using an encastre boundary condition definition. The top plate and striker plate were allowed for translations on the y-axis direction and any other movement of the plates were restrained. Struc- tures were designed as quarter models to reduce the time cost of the simulations. For this purpose, symmetry boundary con- ditions were used for both edges of the absorber. X-symmetry definition for the edge on y-z plate and z-symmetry definition for the edge on x-y plate were made.

5 RESULTS AND DISCUSSION

5.1 Quasi-Static Response of the Conical Absorber

For the quasi-static loading case, the reference model is chosen with respect to the design parameters and response plots. The thickness (t) and the base cone angle (β) for he reference case are selected to be 10mm and 30◦ respectively. The impact velocity for all quasi-static simulations is selected to be 0.01m/s which represents a deformation of 10mm per second.

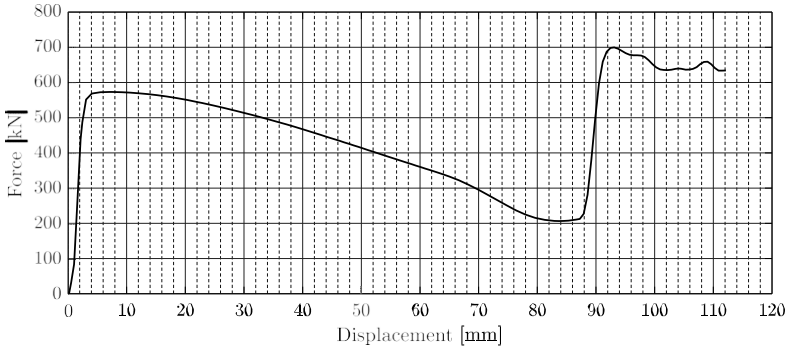

Figure 5.1 Force-Displacement plot of the quasi-static model.

In Figure 5.1, the force-displacement response of the ref- erence case is presented. After 1mm of displacement, the first contact between the striking plate and the absorber occurs. A stable deformation of the structure was observed after the first peak load throughout the simulation. At the displacement value of approximately 90mm, the second contact occurs. Each con- tact between the surfaces in the model assembly causes a peak load in the reaction force response.

Figure 5.2 shows the absorbed energy and the reaction force response of the quasi-static reference model as a function of displacement. Also the deformed shapes of the model are given in Figure 5.2 for selected points to better understand the behavior of the structure under quasi-static axial loading.

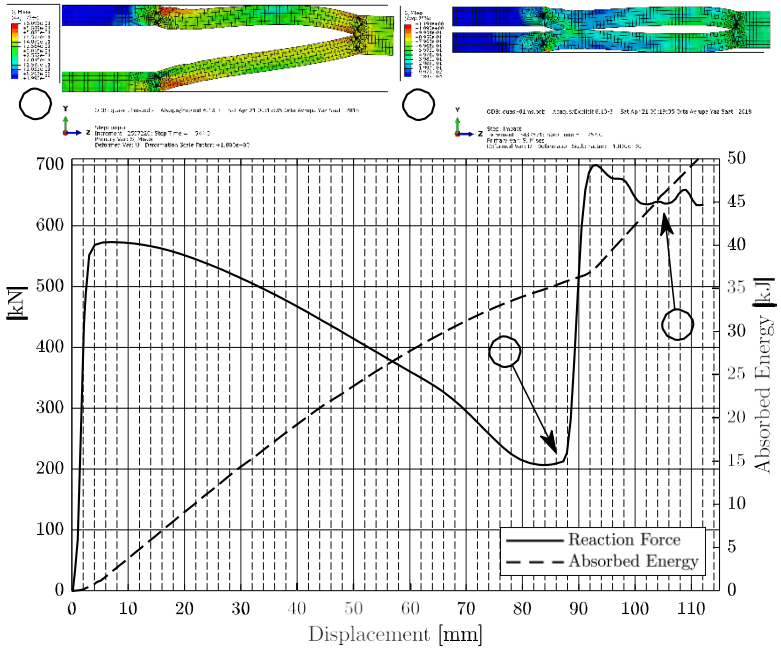

Figure 5.2 Deformation mode for the reference quasi-static case at selected points.

The selected instants for the simulation of the quasi-static reference model are; a) the contact between the conical surface of the absorber and the rigid wall which causes the second peak on the force-displacement response, b) the last contact during the simulation between the conical surface of the absorber and the striking rigid plate. These two instants are selected because at both instants, a sudden change occur on the reaction force response of the structure under quasi-static loading.

5.2 Dynamic Response of the Conical Absorber

The model with a constant impact kinetic energy of 100kJ is chosen for the reference dynamic case with respect to the variations of the design parameters and plots of reaction force and absorbed nergy. The thickness (t) and the base cone angle (β) are chosen as 10mm and 30◦ respectively.

Smoothed force response for the reference case is plotted in Figure 5.3. At 1mm of displacement, the first contact be- tween the striking mass and the absorber structure occurs. As the impact occurs instantaneously, the velocity of the contact surface of the absorber increases immediately. After the first reaction force occurs, the structure exhibits a stable deforma- tion behavior. The reaction force shows a decreasing trend until the next contact between striking plate and the surface of the absorber takes place. This behavior repeats on each contact between surfaces of the absorber and striking plate.

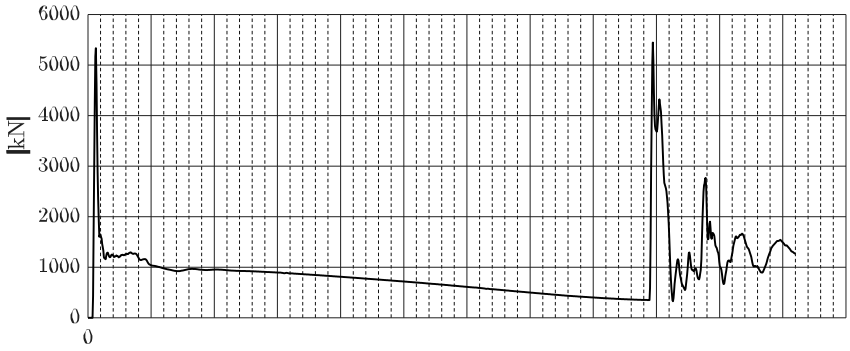

Figure 5.3 Force-Displacement plot of the reference dynamic model.

The dynamic response of the structure by means of the reaction force and the absorbed energy is plotted in Figure 5.4 together. Also pictures of the deformation mode for selected points are shown together to better understand the behavior of the structure.

The selected instants for the reference model are a) the initial contact, and first cone starts bending, b) contact of coni- cal surface to striking plate occurs and second cone starts bend- ing, c) first cone becomes completely flat and contact of the inner surfaces of the cones are achieved.

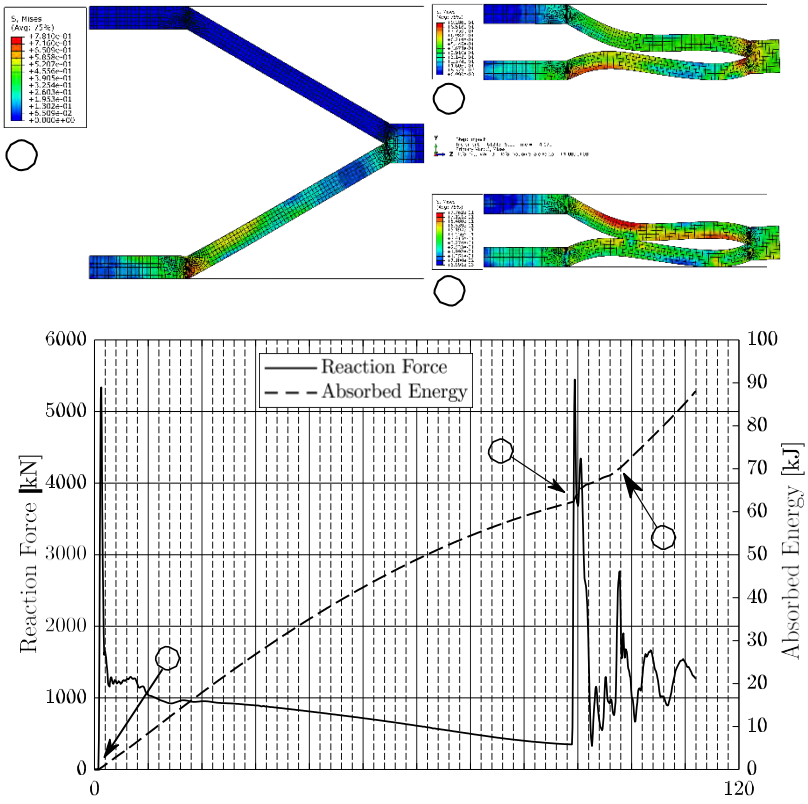

Figure 5.4 Deformation mode for the reference dynamic case at selected points.

5.3 Comparison between Quasi-Static and Dynamic Response

One of the most important performance parameter of an energy absorber is the reaction force. Reaction force response of an energy absorber may change under different conditions such as loading, boundary conditions and material properties. Fig- ure 5.5 shows the comparison of mean dynamic force response of the model with parameters t = 10mm and $\beta = 30^{\circ}$.

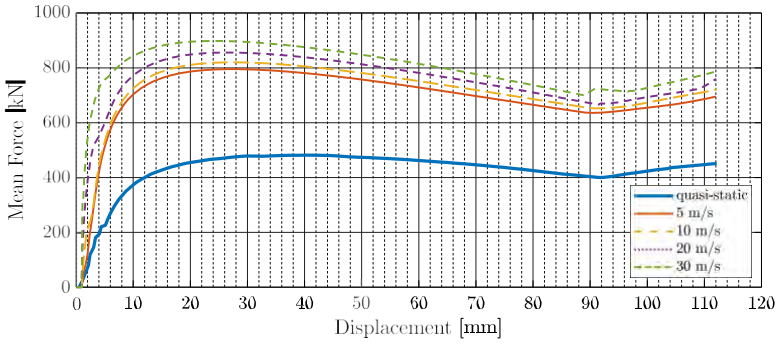

Figure 5.5 Comparison of mean Force-Displacement response of the quasi-static and dynamic models $\beta = 30^{\circ}$ and t = 10mm.

It is observed that there is a significant difference between the quasi-static and dynamic cases in terms of mean reaction force response. This is caused by the strain-rate dependent material model used in this study which changes the structures response under different initial impact velocity conditions.

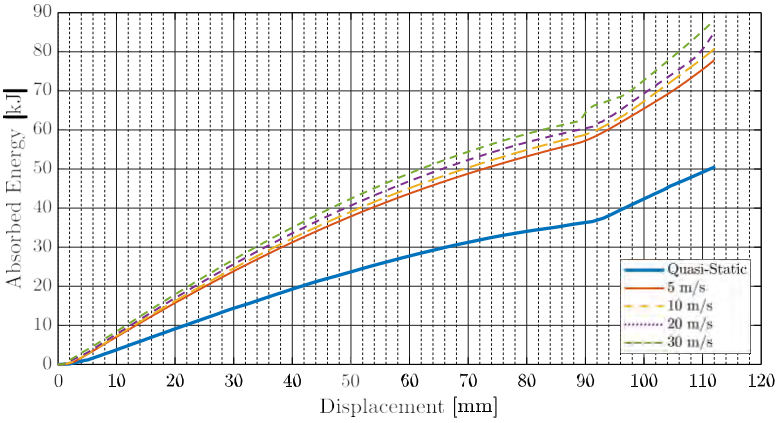

Figure 5.6 Comparison of energy absorption of the model

$\beta = 30^{\circ}$ and t = 10mm.

As the energy absorbing capacity of the structures are strictly related to the reaction force response, the absorbed energy curves conform with the force-displacement plots. The absorbed energy response of the numerical model with $\beta = 30^{\circ}$and t = 10mm is given in Figure 5.6 as a function of displace- ment. The energy absorption capacity of the structures increase with increasing impact velocity. For the impact velocity values of 20m/s and 30m/s, both reaction force and the absorbed en- ergy plots have a slightly different behavior.

5.4 Combined Effects on Performance Parameters

In this section, the performance parameters of an energy absorber are investigated individually for all variable parame- ters. The effect of three different variables (velocity, thickness, base conical angle) are compared for each simulation result out- put, except for the impact mass variable.

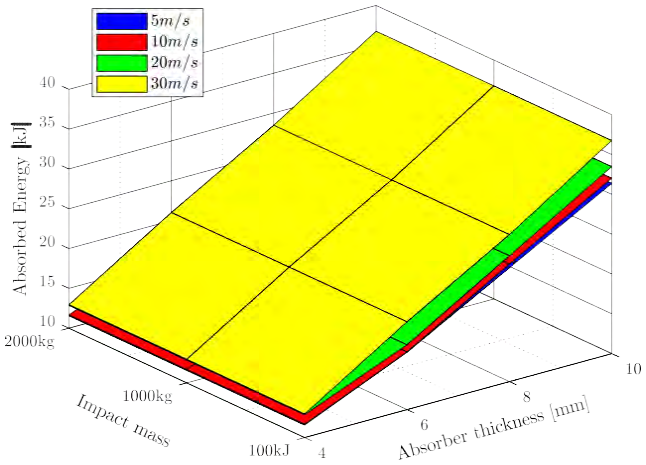

Figure 5.7 Effect of Impact mass, absorber thickness and impact velocity on the amount of absorbed energy.

Figure 5.7 shows the effect of the impact mass, absorber thickness and impact velocity on the absorbed energy. As seen in Figure 5.7, impact mass does not have significant effect on absorbed energy. However, the maximum deformation length is associated with the initial kinetic energy of the system and increases with increasing impact mass. It can be said that the dynamic or non-linear stiffness of the absorber structure is not dependent on the mass of the impactor in the selected mass range. The same result were also observed in the previous studies in the current literature. For this reason, the impact mass parameter is not included to any of the following 3-D plots.

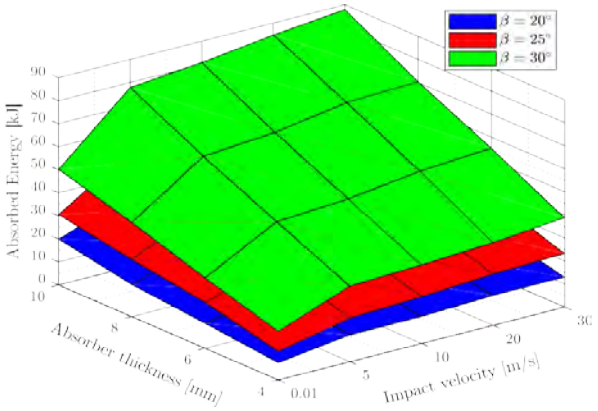

Figure 5.8 Effect of base conical angle, absorber thickness and impact velocity on absorbed energy.

Figure 5.8 shows that the amount of absorbed energy in- creases in all models as the base cone angle β ,absorber thick- ness and impact velocity increases. With increasing β angle, structures exhibit more stiff behavior to the axial loading and also gain more deformation length with constant bottom radius and increasing β angle.

This situation allows the structures with higher β angles to dissipate more kinetic energy at the same impact velocity and absorber thickness. Absorbed energy values also increase with the increasing absorber thickness. The impact velocity has also a non-negligible effect on the energy absorption of the structures due to the inertia effects with increasing impact velocity. When compared together, impact velocity has a less significant effect on the energy absorption capacities of structures.

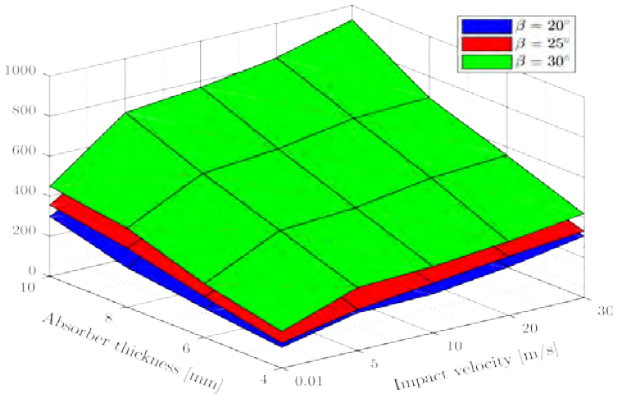

Figure 5.9 Effect of base conical angle, absorber thickness and impact velocity on mean reaction force.

The effect of the impact velocity and the base conical angle on the mean reaction forces are more clearly seen at the higher absorber thickness values. Mean reaction forces have similar behavior with peak reaction forces at different impact velocity, absorber thickness and base conical angle values. The effect of the base conical angle β on the peak reaction forces are more identical at different absorber thicknesses when compared to the mean reaction force. Effects of the variable parameters on mean reaction force values are shown in Figure 5.9.

Crash force efficiency (CFE) values of the structures ex- hibit a significantly decreasing behavior as the impact velocity increases. The complete dataset of the CFE values are plot- ted in Figure 5.10. As the peak reaction force response of the structures increase significantly as the impact velocity increses, the CFE values for higher impact velocities are very low when compared to the quasi-static loading case. Also the the conical angle becomes more effective on the CFE values at relatively lower impact velocity values.

It is found that the absorber thickness has a similar ef- fect on both mean and peak reaction force values. Thus, the CFE values does not change significantly within the range of the absorber thickness values of the present study. Overall, the obtained CFE values of the present study are seem to be compatible with the current literature.

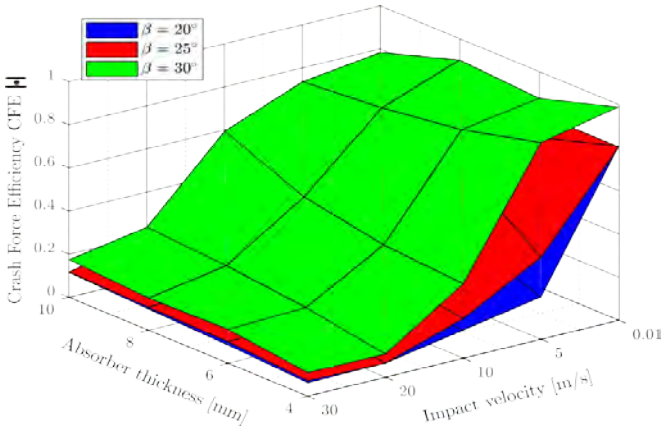

Figure 5.10 Effect of base conical angle, absorber thickness and impact velocity on CFE.

The stroke efficiency is another performance parameter of energy absorbers. It is desired to be as high as possible in order to have a higher maximum deformable length and so the absorbed energy. Calculated values for all models are given in Figure 5.11 by means of base conical angle, impact velocity and the absorber thickness.

Stroke efficiency is directly related to the conical angle β. Besides, the deformation mode has an indirect effect due to the changes in bending shapes of the models. The maximum deformation lengths are seem to be equal for all absorber thickness values due to the selected geometry.

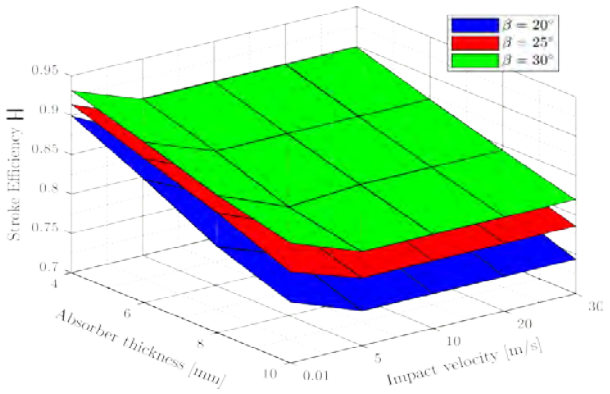

Figure 5.11 Effect of base conical angle, absorber thickness and impact velocity on stroke efficiency.

Under quasi-static loading conditions, stroke efficiency values are obtained to be slightly higher than the dynamic load- ing case, which is caused by the stable deformation of the struc- tures.

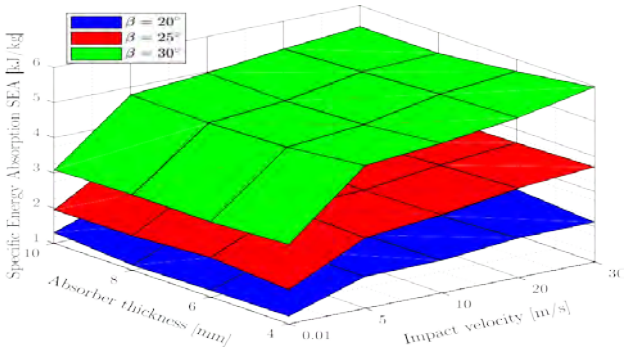

Figure 5.12 Effect of base conical angle, absorber thickness and impact velocity on specific energy absorption SEA.

Specific energy absorption (SEA) values changes signifi- cantly under dynamic loading conditions when compared to the quasi-static case. This is caused by the strain-rate dependency of the material model. The SEA have also a slightly increasing behavior for increasing impact velocity under dynamic loading conditions. The SEA is not seem to be significantly affected from the increasing absorber thickness values. This is caused by the increasing effect of the absorber thickness on both the absorbed energy values and the mass of the structure.

On the other hand, the specific energy absorption values are significantly affected from the base conical angle as seen in Figure 5.12. Although the base conical angle increases the mass of the body, the increase in energy absorption capacity is relatively higher.

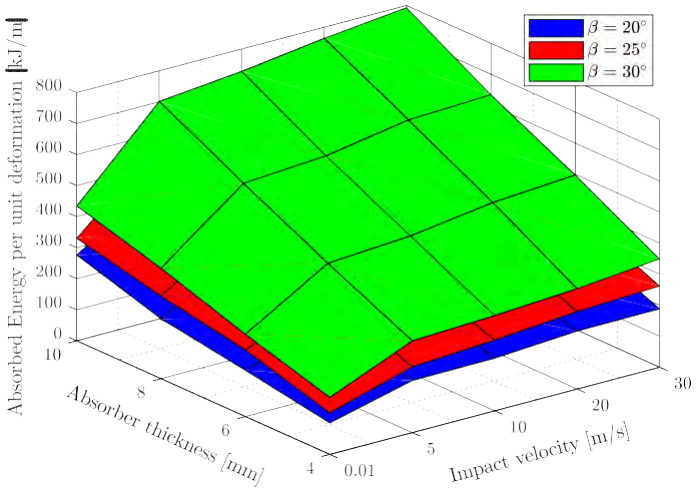

Figure 5.13 Effect of base conical angle, absorber thickness and impact velocity on absorbed energy per unit deformation.

As seen in Figure 5.13, the absorbed energy per unit de- formation is affected from both three parameters. The most effective parameter is the absorber thickness because of the in- crease in the absorbed energy as the thickness increase.

The less effective parameter is the impact velocity be-cause it has the less effect on the energy absorption charac- teristics at a chosen β angle of structure when compared to others under dynamic loading conditions. The effect of the base conical angle is slightly changed by the absorber thickness and impact velocity values. The comparison surfaces of Figure 5.13 are almost parallel although the conical angle changes the maximum deformable length of the structures significantly.

The dynamic amplification factor (DAF) is another useful parameter for comparing the dynamic effects on the absorbed energy of the structures. The calculated DAF values are plotted in Figure 5.14 for the models of selected parameters.

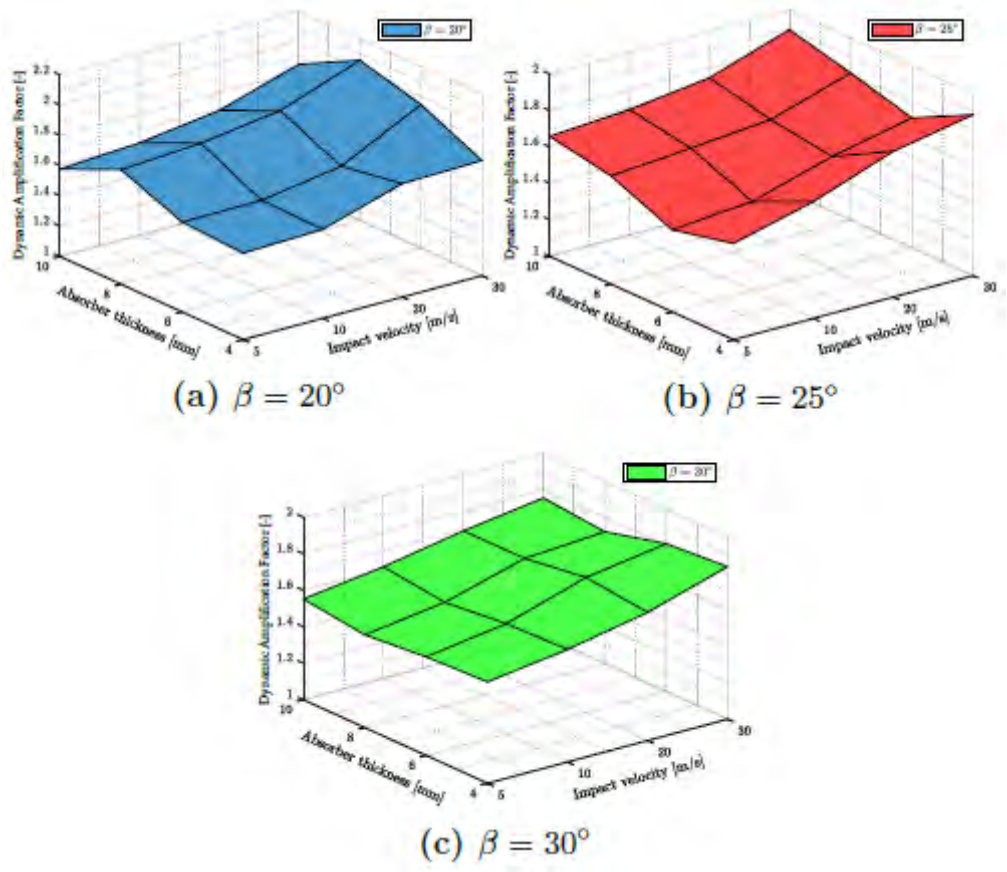

Figure 5.14 Effect of the absorber thickness and the impact velocity on the DAF values.

DAF values slightly increase as the impact velocity in- creases due to the inertia effects. Also the the conical angle becomes more effective on the DAF values with decreasing ab- sorber thickness. The effect of the absorber thickness on the DAF values are more stable at models with higher base conical angle. Due to the lower angle and thickness, the models are more prone to bending. The geometric stiffness of the models are relatively low and the effect of the inertia forces are observed to be higher.

6 CONCLUSION

6.1 Summary and Conclusions

A numerical investigation of the conical energy absorbing structure was examined in this study. In the view of obtained information from the current study, some of the significant con- clusions and some guidelines on the design of a low base conical angle structure are summarized below.

1. The dynamic force-displacement response of the conical structure is affected by the absorber thickness, base coni- cal angle and the impact velocity. However, it is observed that the impact mass of the striker has no effect on the dynamic force response of the structures. The effect of the angle on the force responses become higher as the thickness increases.

2. The energy absorption response of a low angle conical structure under axial dynamic loading is influenced by the absorber thickness, conical angle and impact velocity. However, the conical angle and the absorber thickness are the most effective on the energy absorption of the selected geometry. In other words, structures with higher thickness and angle absorb more energy within a selected crush distance.

3. The CFE values have a decreasing trend as the impact ve- locity increases due to the increasing initial peak reaction force. On the other hand, CFE values do not seem to be affected from the absorber thickness. However, base con- ical angle has an increasing effect on CFE values which is caused by the increasing mean reaction forces due to the bending resistance of the structures with higher β values.

4. The specific energy absorption values are strictly affected from the base conical angle β. Increasing conical angle causes the system to be more resistant to any bending action. However, the absorber thickness does not affect the SEA values significantly.

5. In order to increase the absorbed energy within a given deformation length;

(a) the conical angle can be increased for the same ab- sorber thickness values and/or impact velocity,

(b) absorber thickness can be increased for the same base conical angle and/or impact velocity,

(c) changing the impact mass has no significant effect.

(d) increasing the initial impact velocity also increase the amount of absorbed energy which is caused by the inertia effects and the strain-rate dependency of the material model. However, the effect of the im- pact velocity is quite low when compared to the ef- fect of the thickness and the conical angle.

6.2 Contributions of the Thesis

The primary aim of this thesis is to gain a better under- standing on the impact and energy absorption behavior of trun- cated conical structures with relatively higher thickness values and to investigate their application as an energy absorber.

With respect to the objectives outlined in Chapters 1 and 3, this study has investigated the impact response and energy absorption capabilities of truncated shallow cones under axial impact loading. Studies until current stage has provided a good opportunity to investigate and compare dynamic response of truncated cones by means of some important performance pa- rameters.

The energy absorbing capabilities of the current geome- try, seems to be promising due to it's relatively high thickness and high energy absorption. However, high thickness leads to a more heavy structure which is not preferable as an energy absorber. Also the conical angle has a great influence on the energy absorbing performance of the structure. Structures with higher angle and lower thickness absorbs slightly more energy than the structures with lower angle and higher thickness. How- ever, current stage of the study is still not sufficient to determine the usability of undertaken geometry as an impact absorber. In consideration of parameters compared above and future work explained below, further studies will be more appropriate to resolve the situation of current geometry to be a possible alter- native to the current energy absorber geometry.

6.3 Recommendations for Future Work

In order to obtain sufficient investigation of the geometry undertaken in the current study, amount of the stroke length of an energy absorber is a significant design requirement. It is necessary to have a longer stroke of energy absorbers both to improve the energy dissipation

performance of the structure and to gain a comparable length of geometry with the energy absorbers studied in the literature and used in the industry. In this manner, instead of changing the base cone angle of the structure, it should be investigated to use more than one struc- ture coupled together to obtain sufficient deformation stroke.

BIBLIOGRAPHY

European Railway Agency. Railway safety perfor- mance in the european union. Retrieved from: http://www.era.europa.eu/Document-Register/Documents/SPR2014.pdf , January 2014. [Accessed on Nov. 2015].

Heinz-Peter Bader. Dozens hurt in head-on vienna com- muter train crash. Retrieved from : http://www.reuters. com, January 2013 (Online; Accessed Jan. 2016).

J. Marsolek and H-G Reimerdes. Energy absorption of metallic cylindrical shells with induced non-axisymmetric folding patterns. International Journal of Impact Engi- neering, 30(8):1209–1223, 2004.

MF Horstemeyer, H Li, J Siervogel, L Kwasniewski, J Wekezer, B Christiana, and G Roufa. Material and structural crashworthiness characterization of paratransit buses. International journal of crashworthiness, 12(5):509– 520, 2007.

Xiaochuan Liu, Jun Guo, Chunyu Bai, Xiasheng Sun, and Rangke Mou. Drop test and crash simulation of a civil airplane fuselage section. Chinese Journal of Aeronautics, 28(2):447–456, 2015.

Dellner. Company website. Retrieved from: http: //www.dellner.com/assets/img/slider_1_m.jpg, 2016 (Online; Accessed Jan. 2016). VOITH. Connect and protect:coupler and front end systems. Retrieved from: http://resource.voith.com/vt/publications/downloads/1994_e_g1712en__internet.pdf, 2014 (Online; Accessed Nov. 2015).

A. A A Alghamdi. Collapsible impact energy absorbers: An overview. Thin-Walled Structures, 39(2):189–213, 2001.

VOITH. Voith lightweight components: New energy absorbers made of fibre composite plastics. Retrieved from : http://www.voith.com/en/press/ press-releases-99_58828.html, 2014 (Online; Ac- cessed Nov. 2015).

Dellner. Dellner company brochure. Retrieved from: http://www.dellner.com/assets/Archive/Dellner_ Brochure.pdf, 2014 (Online; Accessed Nov. 2015).

Axtone. Crash components for emu/dmu multiple units. Retrieved from : http://www.axtone.eu/en/ multiple-units--dmu-and-emu-.html, 2015 (Online; Accessed Nov. 2015).

Guoxing Lu and TX Yu. Energy Absorption of Structures and Materials. Woodhead Publishing, 2003.

CEN. Railway applications - crashworthiness require- ments for railway vehicle bodies. Technical Report EN 15227:2008, European Commitee for Standardization, 2008.

Gregory Nagel. Impact and energy absorption of straight and tapered rectangular tubes. Phd thesis, Queensland Uni- versity of Technology, 2005.

Zaini Ahmad. Impact and energy absorption of empty and foam-filled conical tubes. Phd thesis, Queensland Univer- sity of Technology, 2009.

Langseth M. Hanssen, A.G. and O.S. Hopperstad. Static and dynamic crushing of circular aluminium extrusions with aluminium foam filler. International Journal of Im- pact Engineering, 24(5):475–507, 2000.

Langseth M. Hanssen, A.G. and O.S. Hopperstad. Static and dynamic crushing of square aluminium extrusions with aluminium foam filler. International Journal of Impact Engineering, 24(4):347–383, 2000.

JM Alexander. An approximate analysis of the collapse of thin cylindrical shells under axial loading. The Quarterly Journal of Mechanics and Applied Mathematics, 13(1):10– 15, 1960.

AG Mamalis and W Johnson. The quasi-static crum- pling of thin-walled circular cylinders and frusta under ax- ial compression. International Journal of Mechanical Sci- ences, 25(9-10):713–732, 1983.

N. Jones W. Abramowicz. Dynamic axial crushing of square tubes. International Journal of Impact Engineering, 2(2):179–208, 1984.

N. Jones W. Abramowicz. Dynamic progressive buckling of circular and square tubes. International Journal of Impact Engineering, 4(4):243–270, 1986.

AG Mamalis, W Johnson, and GL Viegelahn. The crum- pling of steel thin-walled tubes and frusta under axial compression at elevated strain-rates: some experimental results. International Journal of Mechanical Sciences, 26(11):537–547, 1984.

M Langseth and OS Hopperstad. Static and dynamic ax- ial crushing of square thin-walled aluminium extrusions. International Journal of Impact Engineering, 18(7-8):949– 968, 1996.

AG Mamalis, DE Manolakos, MB Ioannidis, PK Kostazos, and C Dimitriou. Finite element simulation of the axial collapse of metallic thin-walled tubes with octagonal cross- section. Thin-Walled Structures, 41(10):891–900, 2003.

YS Tai, MY Huang, and HT Hu. Axial compression and energy absorption characteristics of high-strength thin- walled cylinders under impact load. Theoretical and ap- plied fracture mechanics, 53(1):1–8, 2010.

F Tarlochan, F Samer, AMS Hamouda, S Ramesh, and Karam Khalid. Design of thin wall structures for energy absorption applications: Enhancement of crashworthiness due to axial and oblique impact forces. Thin-Walled Struc- tures, 71:7–17, 2013.

A Ghafari-Nazari M Fard M Abbasi, S Reddy. Multi- objective crashworthiness optimization of multi-cornered thin-walled sheet metal members. Thin-walled structures, 89:31–41, 2015.

NK Gupta, GL Easwara Prasad, and SK Gupta. Plastic collapse of metallic conical frusta of large semi-apical an- gles. International Journal of Crashworthiness, 2(4):349– 366, 1997.

AAN Aljawi and AAA Alghamdi. Investigation of axially compressed frusta as impact energy absorbers. Compu- tational methods in contact mechanics IV, page 431–443, 1999.

[30] AAA Alghamdi, AAN Aljawi, and TM-N Abu-Mansour. Modes of axial collapse of unconstrained capped frusta. International Journal of Mechanical Sciences, 44(6):1145– 1161, 2002.

GL Easwara Prasad and NK Gupta. An experimental study of deformation modes of domes and large-angled frusta at different rates of compression. International jour- nal of impact engineering, 32(1):400–415, 2005.

NK Gupta et al. Experimental and numerical studies of impact axial compression of thin-walled conical shells. In- ternational journal of impact engineering, 34(4):708–720, 2007.

B. Bayram-B. Gerceker E. Karakaya M. A. Guler, M. E. Cerit. The effect of geometrical parameters on the energy absorption characteristics of thin-walled struc- tures under axial impact loading. International Journal of Crashworthiness, 15(4):377–390, 2010.

M. Asgari M.B. Azimi. A new bi-tubular conical–circular structure for improving crushing behavior under axial and oblique impacts. International Journal of Mechanical Sci- ences, 105:253–265, 2016.

ABAQUS. 6.13, getting started with abaqus interactive edition. Dassault Systemes Simulia Corp., Providence, RI, 2013.

ABAQUS. 6.13, analysis user's manual. Dassault Systemes Simulia Corp., Providence, RI, 2013.

Cook W.H. Johnson, G.R. A constitutive model and data for metals subjected to large strains, high strain rates and high temperatures. In Proceedings of the 7th International Symposium on Ballistics, The Hague, Netherlands, 1983, 1983.

Ali Ghamarian and Hamidreza Zarei. Crashworthiness in- vestigation of conical and cylindrical end-capped tubes un- der quasi-static crash loading. International Journal of Crashworthiness, 17(1):19–28, 2012.

J. S. Lin, X. Wang, and G. Lu. Crushing characteristics of fiber reinforced conical tubes with foam-filler. Composite Structures, 116(1):18–28, 2014.

Alper Tasdemirci, Ali Kara, Kivanc Turan, and Selim Sahin. Dynamic crushing and energy absorption of sand- wich structures with combined geometry shell cores. Thin- Walled Structures, 91:116–128, 2015.

William S Cleveland. Robust locally weighted regression and smoothing scatterplots. Journal of the American sta- tistical association, 74(368):829–836, 1979.

MathWorks. Curve fitting toolbox: for use with MATLABOR user's guide. MathWorks, 2002.

EN ISO. 6892-1. metallic materials-tensile testing-part 1: Method of test at room temperature. International Orga- nization for Standardization, 2009.

Peirs J. Van Slycken-J. Faes K. Duchene L. Verleysen, P. Effect of strain rate on the forming behaviour of sheet metals. Journal of Materials Processing Technology, 211(8):1457–1464, 2011.

Minamoto H. Seifried, R. and P. Eberhard. Viscoplastic effects occurring in impacts of aluminum and steel bodies and their influence on the coefficient of restitution. Journal of Applied Mechanics, 77(4):041008, 2010.

L. Mirfendereski, M. Salimi, and S. Ziaei-Rad. Paramet- ric study and numerical analysis of empty and foam-filled thin-walled tubes under static and dynamic loadings. In- ternational Journal of Mechanical Sciences, 50(6):1042– 1057, 2008.

M. Kathiresan, K. Manisekar, and V. Manikandan. Per- formance analysis of fibre metal laminated thin conical frusta under axial compression. Composite Structures, 94(12):3510–3519, 2012. Norman Jones. Structural impact. Cambridge university press, 2011.

M Langseth, OS Hopperstad, and T Berstad. Crashwor- thiness of aluminium extrusions: validation of numerical simulation, effect of mass ratio and impact velocity. Inter- national Journal of Impact Engineering, 22(9-10): 829–854, 1999.

D Karagiozova and Norman Jones. Dynamic buckling of elastic–plastic square tubes under axial impact—ii: struc- tural response. International Journal of Impact Engineer- ing, 30(2):167–192, 2004.

M Kathiresan and K Manisekar. Low velocity axial col- lapse behavior of e-glass fiber/epoxy composite conical frusta. Composite Structures, 166:1–11, 2017.

D. P. Thambiratnam Z. Ahmad. Dynamic computer sim- ulation and energy absorption of foam-filled conical tubes under axial impact loading. Computers & Structures, 87(3- 4):186–197, 2009.

Lu Wang, Xueming Fan, Hao Chen, and Weiqing Liu. Axial crush behavior and energy absorption capability of foam-filled gfrp tubes under elevated and high tempera- tures. Composite Structures, 149:339–350, 2016.

GM Nagel and DP Thambiratnam. A numerical study on the impact response and energy absorption of tapered thin- walled tubes. International journal of mechanical sciences, 46(2):201–216, 2004.

N.A. Fleck A.R. Akisanya. Plastic collapse of thin- walled frusta and egg-box material under shear and nor- mal loading. International journal of mechanical sciences, 48(7):799–808, 2006.

M Kathiresan and K Manisekar. Axial crush behaviours and energy absorption characteristics of aluminium and e- glass/epoxy over-wrapped aluminium conical frusta under low velocity impact loading. Composite Structures, 136:86– 100, 2016.

Klaus-Jürgen Bathe. Finite element procedures. Klaus- Jurgen Bathe, 2006.

Robert D. Cook, David S. Malkus, Michael E. Plesha, and Robert J. Witt. Concepts and Applications of Finite Ele- ment Analysis, 4th Edition. Wiley, 2001.

James M. Gere and Barry J. Goodno. Mechanics of Ma- terials, 7th Edition. Cengage Learning, 2008.

Crisbon Delfina Joseph. Experimental measurement and finite element simulation of springback in stamping alu- minum alloy sheets for auto-body panel application. Mas- ter's thesis, Mississippi State University, 2003.

European Commission. Eu transport in figures. Statistical pocketbook, 2016.

Publications of the Ph.D. Student

E. Özyurt, H. Yılmaz, P. Pascenko, (2015) An investigation on dynamic response of truncated thick walled cones with edge ring under axial compressive impact load, International Journal of Scientific and Technological Research, Vol 1, No.9, 21-30

H. Yılmaz, E. Özyurt, P. Pascenko, (2015) Elastic buckling of thin conical caps with edge ring constraint under uni-axial com- pression, International Journal of Scientific and Technological Research, Vol 1, No.9, 1-9

H. Yılmaz, E. Özyurt. P. Tomek, (2017) A Comparative study between numerical and analytical approaches to load carry- ing capacity of conical shells under axial loading, International Journal of Engineering Trends and Technology (IJETT), Vol 52, No.1

H. Yılmaz, I. Kocabas, E. Özyurt, (2017) Empirical equations to estimate non-linear collapse of medium-length cylindrical shells with circular cutouts, Thin-Walled Structures, Vol 119, 868-878.

E. Özyurt, H. Yılmaz, P. Tomek, (2018) Prediction of the in- fluence of geometrical imperfection to load carrying capacity of conical shells under axial loading. Sigma Journal of Engineer- ing and Natural Sciences Vol 36, No. 1, 11-20

Experimental Analysis of Special Concrete Exposed to Extreme Thermal Stress

Author: Ing. Vladimír SUCHÁNEK

Doctoral study programme:
P3710 Technique and Technology in Transport and Communications

Field of study:
3706V005 - Transport Means and Infrastructure

Supervisor:
doc. Ing. Jiří Pokorný, CSc.

Supervisor specialist:
Ing. Ladislav Řoutil, Ph.D.

Doctoral thesis has arisen at the supervising:
Department of Transport Structures

INTRODUCTION

High thermal stresses (fires) do not cause only huge material losses, but mean a risk of health danger or death of persons or animals. Even though it is not possible to prevent all fires, there is an effort to eliminate their number and, last but not least, extent of their damage (application of active or passive protection).

It can be noted that concrete structures exposed to the effects of fire "can be assessed" in the same way as when designed according to the (ČSN EN 1992-1-1 ed. 2, 2011). Changes of strength and deformation characteristics are included in the calculation in the form of reduction factors, see (ČSN EN 1992-1-2, 2006). Mathematical model of concrete stress-strain curve in compression at higher temperatures is described by a temperature function of plain concrete in relation with the type of used aggregate (siliceous or limestone). However, it is not valid for light aggregate concrete description. In the author's point of view, this methodology (stipulation of reduction factors for residual properties determination), applied at fire design of concrete structures for simple and particularized methods (ČSN EN 1992-1-2, 2006), does not depict the behaviour of other special types of concrete to a sufficient extent.

1 ANALYSIS OF CURRENT STATE IN THE FIELD OF THE DOCTORAL THESIS

1.1 Structural Fire Design

Fire is an undesirable, unrestrained and uncontrollable burning. It is a process accompanied by chemical and physical effects (ČSN ISO 8421-1, 1996).

Actual progress of burning can be divided into three phases (Procházka et al., 2010) – characteristic periods – start of burning, fully developed fire and burning out.

1.2 Fire Resistance

Fire resistance **is often one of the decisive factors** at structural assessment. Fire resistance of a sample **is given by the time (in minutes), during which corresponding criteria are fulfilled** (ČSN EN 1363-1, 2013).

1.3 Consequence of High Temperature Influence on Concrete

Physicochemical properties of concrete change at extreme thermal stress. There is a significant inner tension caused by different thermal expansion of particular constituents of a concrete element or structure.

Following negative aspects happen:

- increase of permeability and porosity, more at (Bangi et al., 2011, Chan et al., 1999), (influence of compactness breach causes formation of cracks and ruptures, or crumbling),
- explosive spalling of concrete (lasts until the concrete falls apart or the fire calms down),
- concrete falling off (happens primarily in the advanced phase of fire),
- reduction of structural strength and the modulus of elasticity (Khoury, 1992).

Decrease of concrete strength depends primarily on **warming rate, maximum achieved temperature, and concrete humidity** and, from the material base, **primarily on the type of used aggregate.**

1.4 Explosive Spalling of Concrete

Temperature increase influences concrete spalling because of rapid water steam formation and thermal expansion of aggregate. The most important driving mechanisms directly relate **to humidity, microstructure** and transport effects of cement material. The most effective measure against spalling is reduction of inner tension (e.g. by use of polypropylene fibres).

Polypropylene fibres melt down at the temperature of 150–160 °C (Guidance on the Use of Macro-Synthetic-Fibre-Reinforced Concrete, 2007), which enables the water steam to escape without creation of inner pressure. This effect prevents or terminates the explosive spalling.

Procházka et al. (2009) points to a **possible transport of water steam in space between fibres and circumjacent concrete surface** (because of their bad cohesion) **even before the beginning of melting of fibres.**

1.5 Concrete Transformation at Higher Temperatures

In the Tab. 1, principal changes of concrete under the influence of high temperature are summarized.

Table 1 Strength and mineralogical changes of concrete by warming

Temperature [°C]	**Changes caused by warming**	
	Mineralogical changes	**Strength changes**
70–80	Dissociation of ettringite causes its decrease in cement matrix.	
105	Loss of physically bound water in concrete causes increasing capillary porosity and formation of smaller microcracks. The type of concrete influences the water evaporation rate.	Reduction of strength < 10 %
120–163	Dissociation $CaSO_4.2H_2O$	
250–350	The aggregate begins to change colour into pink / red by iron compound oxidation (around 300 °C). Decrease of bound water in cement putty causes degradation that is more significant.	Significant reduction of strength around 300 °C (15–40 %).
450–500	$Ca(OH)_2$ dehydrates. Aggregate coloration into red increases up to the temperature of 600 °C. Siliceous aggregate can change colour into grey or white. Normally isotropic cement putty shows non-homogenously yellow / beige colour in transverse polarized light. Often, it shows even a birefringence at the temperature of 500 °C.	Reduction of strength around 400 °C (> 40 %).

Temperature [°C]	Changes caused by warming	
	Mineralogical changes	**Strength changes**
573	There is a transformation from α into β-silica. Volume of silica is growing about ca 5 %, which causes formation of radial cracks and cracking of aggregate grains.	Concrete ceases to be structurally usable at the temperatures over 550 °C (55–70 %).
600–800	Decarbonation of carbonates. Based on contents of carbonates in concrete, contraction happens because of release of carbon dioxide, which results in formation of a significant amount of microcracks in cement putty. There is a substantial manifestation at limestone aggregate.	
800–1 200	Concrete structure sinters at the temperatures over 800 °C. Complete dissociation of limestone constituents of aggregate and cement matrix because of their dissociation. Concrete changes colour into albescent grey and an extensive net of microcracks is being formed. Limestone aggregate changes colour into white.	Reduction of strength at the temperatures over 800 °C (> 90 %).
1 200	Beginning of concrete meltdown (heat-resistant types of concrete as far as around 1 550 °C).	
1 300–1 400	Complete meltdown of concrete.	

Source: Adapted from (Ingham, 2009; Lee et al., 2010)

1.6 Structural Fire Design of Elements

The standard (ČSN EN 1991-1-2, 2004) offers various ways of fire resistance (reliability) verification – time, load capacity, temperature.

The basic condition of fire resistance compliance:

$$„Required\ FR“ \leq „Actual\ FR“ \qquad (1)$$

1.7 Fire Resistance Testing of Concrete Structures (Experimental Methods)

Experimental methods are the basis of structural fire resistance determination. Unlike theoretical procedures or calculation models, they are, however, **more time-consuming and economically demanding.** Calculations cannot capture e.g. the compactness of areal structure, time development of cracks, layers falling off, etc. The results of calculation models reach less economical solutions. Testing samples are made in real size. If the real size elements do not fit into oven, elements of minimum dimensions according to valid standards have to face the fire at least.

1.7.1 Temperature Curves

Temperature curves are defined by gas temperature in the vicinity of element surface as a function of time (ČSN EN 1991-1-2, 2004). They can be divided into nominal and parametric.

The standard (ČSN EN 1363-2, 2000) defines a standard curve, hydrocarbon curve, outer fire curve, and slow warming curve.

The Standard Curve

The standard (cellulosic) **curve has been derived for fire in underground structures.** It is applied for fire resistance assessment in tunnels, where it is the lowest from the available curves. A fully developed fire is modelled. Start of burning and cooling down is not considered. This curve is described in older literature as ISO 834 (ČSN 73 0851, 1984; Reichel, 1979).

Temperature in Oven

The nominal standard curve is given by equation (ČSN EN 1363-1, 2013):

$$T = 345\ log_{10}(8\,t + 1) + 20 \qquad (2)$$

where:

T … average time in oven (or in particular fire section) [°C]

t … time [min]

The Derived Curves

Derived temperature curves are presented in ZTV-ING regulation.

1.8 Fire Design of Concrete Structures

1.8.1 Mechanical, Temperature and Physical Properties of Concrete under Growing Temperature (Summary)

There are recommending standards and regulations for high temperature / fire design of concrete structures: Eurocodes valid in member states **CEN** (ČSN EN 1992-1-2, 2006), **fib** Model Code 2010 (Model Code 2010, 2012), American Concrete Institute – **ACI** (ACI 216R-89, 1994), recommendation **RILEM** – (RILEM TC 129-MHT; RILEM TC 44-PHT; RILEM TC 74-THT), the National Building Code of Finland (**RakMK** B4, 1991), **ASTM** Standards (ASTM E 119; ASTM E 84) and **CEB** Model Code (Bulletin D´Information, 1991).

Some selected regulations for testing of mechanical properties of concrete including experimentally set properties of concrete under high temperatures are presented further in the text.

1.8.2 Mechanical, Temperature and Physical Properties of Concrete under Growing Temperature (ČSN EN 1992-1-2, 2006)

The standard (ČSN EN 1992-1-2, 2006) presents three options of fire resistance design:

- use of tables,
- simplified design methods,

- general design method for modelling of structural elements or a complete structure.

The fire design code for concrete structures (ČSN EN 1992-1-2, 2006) includes degradation of mechanical, temperature and physical properties under growing temperature as a function of temperature – see the Tab. 2. This approach is described by a simple calculation method – reduction of (characteristic) strength.

Table 2 The values of the main parameters of the stress-strain diagram of traditional concrete at high temperature

Concrete	**Siliceous aggregate**			**Limestone aggregate**		
Temperature [°C] Θ	$f_{c,\Theta}/f_{ck}$	$\varepsilon_{c1,\Theta}$	$\varepsilon_{cu1,\Theta}$	$f_{c,\Theta}/f_{ck}$	$\varepsilon_{c1,\Theta}$	$\varepsilon_{cu1,\Theta}$
20	1.00	0.0025	0.0200	1.0000	0.0025	0.0200
100	1.00	0.0040	0.0225	1.0000	0.0040	0.0225
200	0.95	0.0055	0.0250	0.9700	0.0055	0.0250
300	0.85	0.0070	0.0275	0.9100	0.0070	0.0275
400	0.75	0.0100	0.0300	0.8500	0.0100	0.0300
500	0.60	0.0150	0.0325	0.7400	0.0150	0.0325
600	0.45	0.0250	0.0350	0.6000	0.0250	0.0350
700	0.30	0.0250	0.0375	0.4300	0.0250	0.0375
800	0.15	0.0250	0.0400	0.2700	0.0250	0.0400
900	0.08	0.0250	0.0425	0.1500	0.0250	0.0425
1 000	0.04	0.0250	0.0450	0.0600	0.0250	0.0450
1 100	0.01	0.0250	0.0475	0.0200	0.0250	0.0475
1 200	0.00	-	-	0.0000	-	-

Source: Adapted from (ČSN EN 1992-1-2, 2006)

where:

Θ … temperature [°C]

$f_{c,\Theta}$ … compressive strength at temperature Θ [MPa]

f_{ck} … characteristic value of compressive strength [MPa]

$\varepsilon_{c1,\Theta}$… thermal strain of corresponding compressive strength $f_{c,\Theta}$ [-]

$\varepsilon_{cu1,\Theta}$ … thermal strain of corresponding compressive strength $f_{c,\Theta}$ (limit value) [-]

1.8.3 Mechanical Properties of Concrete under Growing Temperature (ACI 216R-89, 1994)

Experiments performed by the author converge to the "Unstressed Residual" methodology. Residual strength determined by this methodology reach the lowest values [%], as presented in the Fig. 1–2.

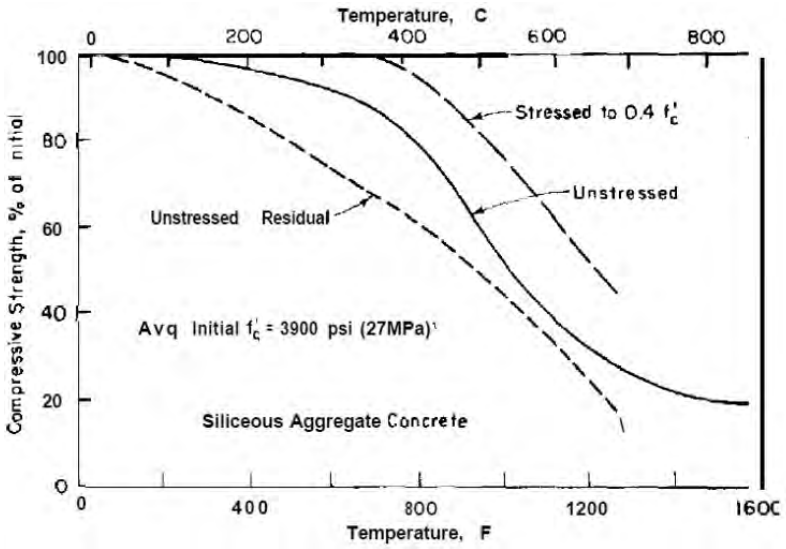

Figure 1 Residual strength (in compression) of siliceous aggregate concrete (ACI 216R-89, 1994)

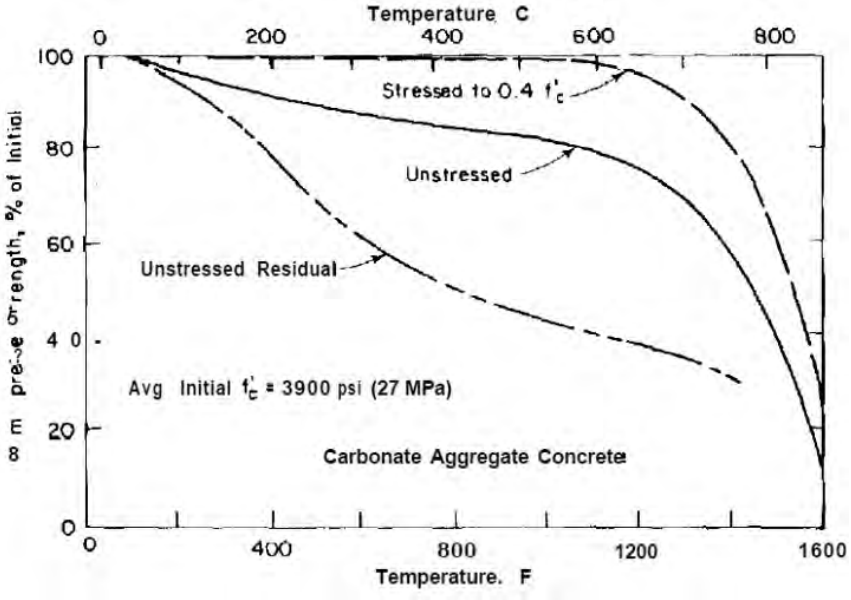

Figure 2 Residual strength (in compression) of limestone aggregate concrete (ACI 216R-89, 1994)

1.9 Description of Concrete Constituents under Higher Temperature

1.9.1 Filler – Aggregate

Concrete with siliceous aggregate shows worse behaviour under high temperature. Better results can be reached **by the use of limestone aggregate**. Concrete with expanded clay aggregate prove the most favourable results.

Siliceous Aggregate

If the temperature exceeds 573 °C, silica (SiO_2) changes from α to β modification with the parallel volume expansion by ca 5 %. Cracks in aggregate grains can appear. Simultaneously, strength of the siliceous aggregate reduces significantly under this temperature.

1.9.2 Binding agent – Cement

If the temperature exceeds 110 °C, physically bound water is expelled and crystal framework of the cement stone is breached, which causes reduction of strength.

If the temperature exceeds 200 °C, cement putty compounds decompose (dehydrates) into compounds without binding abilities.

If the temperature exceeds 500–600 °C, cement stone partly decomposes.

1.9.3 Water

Water transport in pores of concrete is essential as it causes creation of inner tension in the pore vicinity (capillary pressure etc.). Volume change – shrinking or expansion – is the result.

If the temperature exceeds 100 °C, water changes into steam; diffusion is under way. Under higher temperature, **physically bound water** releases from cement hydration products; in the interval of 500–600 °C, it releases from calcium hydroxide.

1.9.4 Limestone

Limestone types of concrete reduce their original strength only by 20 % if the temperature reaches up to 650 °C; see (Collepardi, 2009).

1.10 Special Cement Composite Materials

Considering the fact, that insufficient compaction **is the major cause of deteriorated quality of hardened concrete**, attention focused primarily on self-compacting concrete and its further modification.

1.10.1 Self-Compacting Concrete (SCC)

Definition of SCC – SCC is characterized by higher ratio: cement matrix / aggregate (contrary to ordinary types of concrete); it is able to flow and compact itself by its own weight (significant human factor influence – concrete compaction by external force – is eliminated); better fill in the areas of dense reinforcement and places that are out of reach of vibration is ensured; visible surface is improved; formwork area is well filled out and bled; higher lifetime of forms in the case of prefabrication.

Significant reduction of noise by production, faster process of concrete pouring, increase of concrete (not only surface) quality, use of inorganic fine-grained dust and flour can be determined as **advantages**. On the contrary, **disadvantages** are: higher stress requirements on formwork, possibility to pour concrete up to the slope of ca 3 % (TP 187, 2008), or higher susceptibility to explosive spalling of concrete under high temperatures.

Fresh SCC Testing

Fresh SCC Testing focuses on determination of four key properties: ability to fill out formwork, flow ability, segregation resistance, bleeding resistance.

1.10.2 Lightweight Self-Compacting Concrete (LWSCC)

Advantages of LWSCC are lower density, lower thermal conductivity, better thermal insulation properties, or (based on the type of aggregate) even processing of industrial waste. LWSCC has lower thermal expansion coefficient.

Disadvantages of LWSCC are lower modules of elasticity contrary to ordinary (vibrated) types of concrete (Schutter et al., 2008) and lower ductility. Lightweight aggregate is financially more demanding than ordinary aggregate.

Fresh LWSCC

Fresh LWSCC shows different characteristics (contrary to SCC). Liquidity and "self-compactness" can be reached in a smaller scale (due to insufficient inner kinetic energy). Lightweight aggregate adsorbs part of mixing water and this can lead to an early hardening of LWSCC. Lightweight aggregate "uses" water in pores of the aggregate for additional hydration ("inner self-treatment") and the value of complete shrinking reduces (Hela et al., 2007). If the value of cement paste is higher, lightweight aggregate tends to "float" on the surface of the fresh concrete, because the density of the lightweight aggregate can be lower than the density of the cement paste (tendency to "vice versa" segregation). Determination of air content is not tested according to the standard (ČSN EN 12350-7, 2009), but according to the (ASTM C173, ASTM C 23).

Rugen Aggregate

It excels in processing of high shares of fine inorganic waste materials by keeping the lowest energetic demand (characterized by low production temperature), see Tab. 3.

Table 3 Comparison of technical and technological parameters of lightweight artificial aggregate types available in the Czech Republic

Name	**Fraction [mm]**	**Bulk density [ρ_S]**	**Fragmentation resistance [MPa]**	**Share of waste material [%]**	**Temperature of aggregate production [°C]**
Rugen	4/8	500 - 1200	2 - 20	60 - 100	≥ 5
	8/16	400 - 1000	1 - 12	60 - 100	≥ 5
SioPor	0.1/1	120 - 160	0.08	0	300
	0.63/2.5	60 - 100	0.03	0	300
	2.5/4	60 - 80	0.01	0	300
Poraver	2.4/4.8	145 - 230	1.3	100	900
Liapor	0/2	575	4	0	> 1100

	0/4	450	2.1	0	> 1100
	4/8	450	1.7	0	> 1100
	8/16	275	0.6	0	> 1100

Source: Adapted from (Popis produktu RUGEN, 2013)

1.10.3 Fibre Reinforced Concrete (FRC)

"FRC is a type of concrete with dispersed reinforcement in the shapes of fibres out of suitable material – steel, glass, polymer, carbon, etc. Usually, fibres are dispersed in concrete, but can be oriented, too." (Krátký et al., 1999a).

FRC **excel** by higher resilience, impact resistance and ductility, microcracks development resistance, and resistance against sudden high temperature occurrence. Modification of concrete by PP fibres is considered as one of the options of passive fire protection.

Stress transmission into fibres (in the case of orientation in the direction of stress action) is a function of the length of fibres and slenderness ratio α.

Polymer microfibers serve to reduction and mitigation of microcracks formation (caused due to plastic shrinking). Polymer macrofibres (of irregular shape) serve to improvement of cohesion of cement paste and polymer. Fibres are larger (d_f = ca 10 μm) and terminate growth of macrocracks forming as a result of shrinking by drying out.

Addition of 2 kg of PP fibres into 1 m^3 of concrete prevents explosive spalling ("reach of higher diffusiveness" due to increase of porous system after the meltdown of PP fibres).

1.10.4 Steel Fibre Reinforced Concrete (SFRC)

Advantages of SFRC are the possibility to transmit tensile stress (resilience, ductility, impact resistance) in all directions (prevention of cracks propagation). Reinforcement by steel fibres improves bending, tensile and shear strength, stiffness, impact resistance, and frost resistance.

Steel fibres absorb tensile forces in the area of cement putty – under spatial loading – and reduce fragile character of concrete damage. Lower maintenance requirements are another assumption of SFRC. In some cases, SFRC can substitute ordinary concrete reinforcement.

2 AIMS OF THE DOCTORAL THESIS

The dissertation does not aim to perform standard (code) fire resistance tests on large-dimensional testing bodies, but experimentally perform high thermal loading on the basis of author's warming rate gradient on prepared testing bodies out of special types of concrete (modified by author). Goal of this dissertation is the application of two different experimental methodologies of thermal loading, firstly in electric oven and secondly as a simulation of local (point) fire with the use of propane-butane burner. The direction of research will aim to reach the maximum temperature of 400 °C, further the maximum temperature of 1049 °C (approaching the description of standard curve), 680 / 750 °C (curves of outer fire), and additionally, on prepared cement samples, until the temperatures of 70 and 100 °C.

The desire is to capture the contemporary state of knowledge in the area of selected special types of concrete (SCC, FRSCC, SFRC, PFRC, and LWSCC). Further goal is to apply experimental high thermal loading based on testing samples out of special types of concrete

prepared by author. Attention is focused on determination of one of the most important characteristics of hardened concrete – strength and deformation properties.

Taking into account the fact that modulus of elasticity of concrete and Poisson's ratio are not set in the standards related to concrete (ČSN EN 206+A1, 2018; ČSN P 73 2404, 2016), author's attempt has been to apply two different approaches to the determination of secant modulus of elasticity in compression, firstly the European standard approach and secondly the digital image correlation – in collaboration with Sobriety s. r. o. company. Simultaneously, the Poisson's ratio of special types of concrete has been experimentally determined.

3 LIST OF USED METHODS

Particular methods used in the experimental part of the dissertation are presented in the Chapter 4.

4 PROBLEMS SOLVING – experimental part

4.1 Concrete Production

Motivation of concrete type selection: in view of the fact that the scope of the standard is limited (ČSN EN 1992-1-2, 2006) – (concrete with siliceous or limestone aggregate), production of promising special types of concrete, which are applied (applicable) on real structures (selection of strength classes C 45/55, C 30/37 and LWSC C 25/28), has been chosen. Author has performed its further modification by addition of fibres of various types and weight doses. Selected **key types of concrete** are extensively used in prefabrication (C 45/55 - XF2 (CZ, F1.2) - Cl 0,2 - Dmax16 - SCC (SF2); C 30/37 - XF2 (CZ, F1.2) - Cl 0,2 - D_{max}16 - SCC (SF2); LC 25/28 D1,8 - XC1 (CZ, F.1.1) - Cl 0,2 - Dmax16 - SCC (SF1)). Additional types of concrete add more information about special types of concrete. They have been added in order to determine the modulus of elasticity (in combination with DIC) and Poisson's ratio, in most cases, (C 30/37 - XF4 (F.1.2) - Cl 0,2 - Dmax16 - S3; C 25/30 - XF3 (F.1.2) - Cl 0,2 - Dmax16 - S3; C 25/30 - XC3 - XD1 - XA1 - XF1 (F.1.1) - Cl 0,2 - Dmax16 - S3; alkaline activated material; designed high-strength concrete I, II, III). Author has made self-compacting concrete (SCC), fibre reinforced self-compacting concrete (FRSCC) / steel fibre reinforced self-compacting concrete (SFRSCC), fibre reinforced concrete (FRC) / steel fibre reinforced concrete (SFRC). Author has removed fresh concrete samples from traditional vibrating concrete (TVB) and collected specimens of alkaline activated material (AAM).

Applied fibres were: synthetic microfibers Texiplast – Texzem PPF 370, synthetic large-dimensional fibres Synmix 55, steel wires Dramix 3D 45/50-BL, Dramix 3D 65/35-BG and carbon fabric fibres prepared by author.

4.2 Fresh Concrete Testing

There has been an effort to determine particular characteristics by testing of fresh concrete (consistency / viscosity, density, air content) in the same order and time after mixing / sample removal of fresh concrete.

Maximum effort has been put on performing the tests according to the standards.

4.3 Hardened Concrete Testing

4.3.1 Strength Characteristics

Author has determined density, compressive strength, and flexural strength using reference samples and thermally loaded samples.

4.3.2 Modulus of Elasticity of Concrete in Compression, Poisson's Ratio

Modulus of elasticity is a crucial material parameter describing relation between stress and deformation of concrete. At many structures, it is a determinative characteristic for actual function and bearing capacity (e.g. bridges, pre-stressed structures), because this attribute is applied in the calculation of deformations.

Modulus of elasticity has been set according to the standards (initial and stabilized according to the A Method (ČSN EN 12390-13, 2014) and simultaneously (experimentally) using digital image correlation (in collaboration with Sobriety s. r. o. company).

Selection of methodology (ČSN EN 12390-13, 2014) had been made before the release of the ČBS 05 technical regulations (2016). Upon the release of the regulations, it is possible to specify the concrete type including the required value of the modulus of elasticity.

Poisson's ratio of special types of concrete has been determined using the 3D DIC application.

4.4 Exposure to Thermal Loading (Summary)

Two different experimental methodologies (created by author) based on designed gradient of warming rate have been used by thermal loading. All thermal loadings have been realized on naturally humid concrete samples even though there was a risk of explosive spalling.

Concrete humidity has always been determined using samples free of thermal loading. They have been neither reference samples, nor thermally loaded samples.

4.4.1 Exposure to Thermal Stress in Electric Oven

Experimental non-standard testing of samples has been done in an electric oven (made for ceramics firing – BVD 800/K). Humidity in additional samples from the same mixture had been measured before commencement of any tests.

Natural humidity of samples had been kept and no mechanical stress had been applied on the samples when they were placed into the oven.

Testing conditions in the electric oven have been set on approach to the description of nominal standard curve (max. temperature of 1049 °C), curves of outer fire (max. temperature of 680 °C), and specific loading under the max. temperature of 400 °C designed by author.

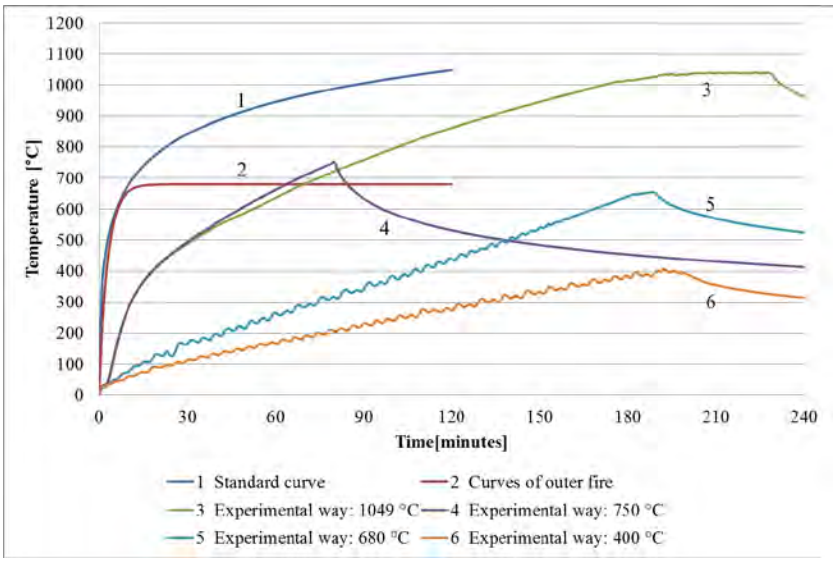

Figure 3 Typical trend of (designed) gradient of loading rate; thermal loading in electric oven

4.4.2 Exposure to Thermal Local (Point) Loading

Local (point) loading has been performed using adjustable propane-butane burner by aiming into the centre of particular loaded prism fragments (note: formerly used by flexural strength test). All heated fragments of samples have been installed between concrete samples that were not mechanically loaded.

Temperature has been detected on the surface exposed to fire on seven exposed spots (0, 0_a, 0_b, 1, 2, 3, 4) – see the Fig. 4). Temperature in the centre of gravity has been measured because of limited measuring range of the contactless thermometer even in points 0_a and 0_b. The far side surface of the samples has been measured on five spots (0, 1, 2, 3, 4 – location identical to the one on the surface exposed to the fire). Thermal share conduction has been represented by temperature progress on the remaining fragment parts (point 5). The values have been noted down every 4 minutes.

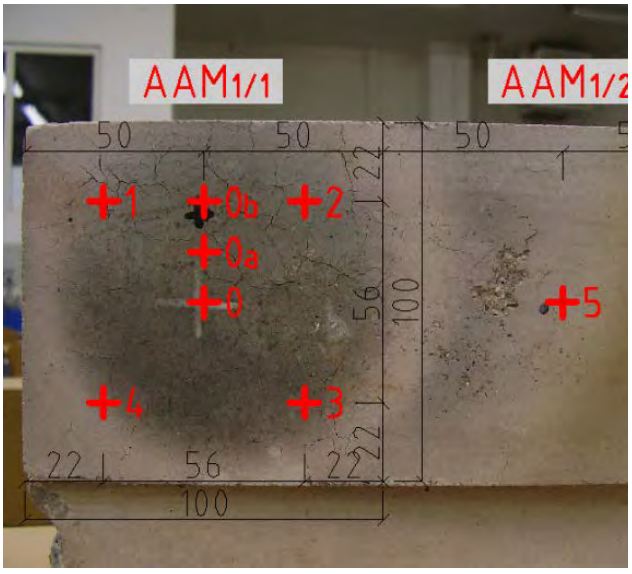

Figure 4 Location of measured points, see Suchánek et al. (2013), sample AAM_annealed_1

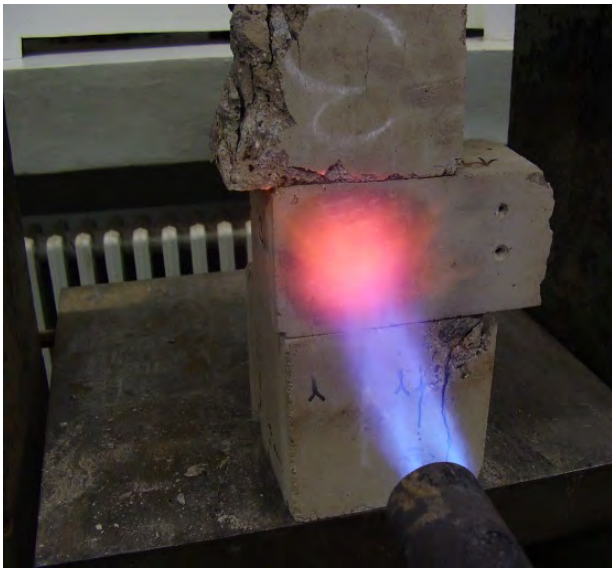

Figure 5 Local fire loading

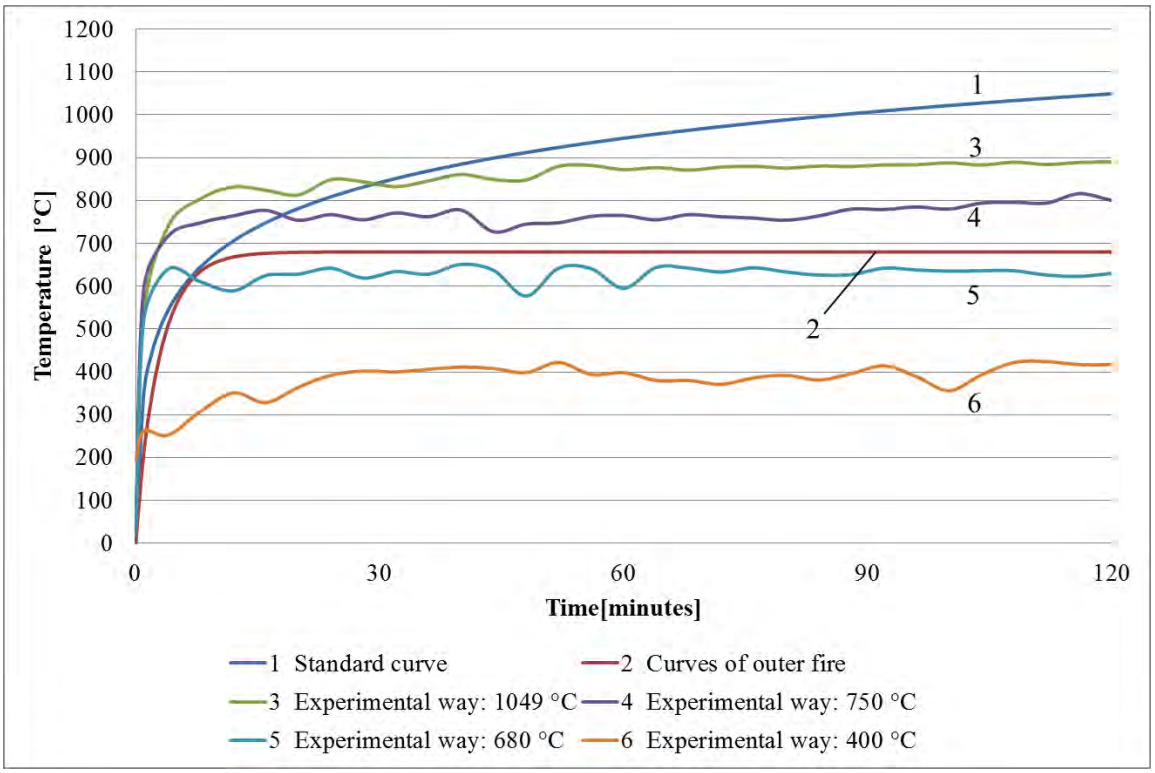

Figure 6 Typical trend of (designed) gradient of warming rate; local (point) loading

5 RESULTS AND DISCUSSION

5.1 Production, Testing of Fresh Concrete – Evaluation

Following Procedure of Dosing of Particular Constituents Proved to be Successful:

1) coarse-grained aggregate (8/16, 4/8) + sand (0/4), 2) addition (limestone), 3) cement, 4) water – ca 2/3 of the dose, 5) / fibres /, 6) super-plasticizing admixture (mixed in ca 1/3 dose of water).

It was proved that the effect of segregation of aggregate to the surface does not arrive by proper selection of artificial porous aggregate.

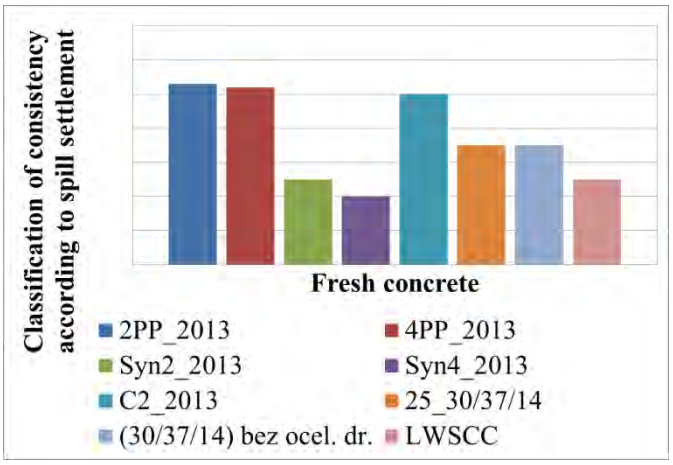

Figure 7 Typical trend of classification of consistency according to spill settlement (SCC, SFRSCC / SFRC)

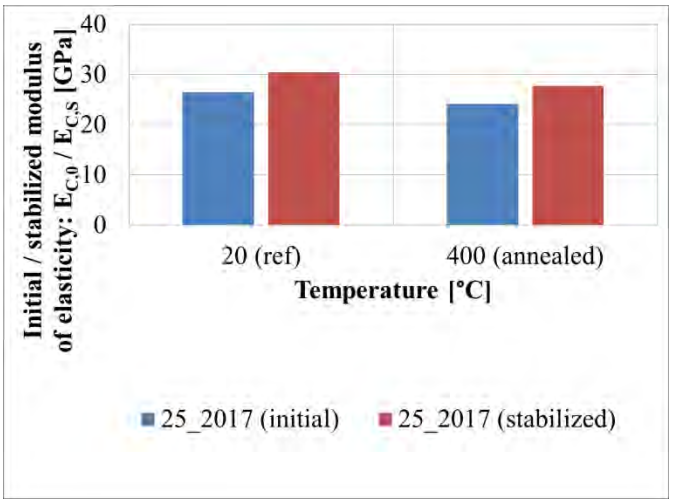

Figure 8 Initial / stabilized secant modulus of elasticity in compression (25_2017), set by standards; loaded on **400 °C** in electrical oven ($age_{ref,\ annealed}$: 1 month)

A type of concrete, which has excellent properties in fresh state, increased architectural surface quality, but lower modulus of elasticity, can be made. Considering the microstructure, spalling of surface layers is easier.

The assumption of the viscosity increase of fresh concrete due to added steel fibres has been confirmed; a typical trend is presented in the Fig. 7.

5.2 Modulus of Elasticity of Concrete in Compression, Poisson's Ratio – Evaluation

Table 4 Comparison of secant modules of elasticity in compression (values determined on set of samples, guide values), SCC, SFRSCC, TVB

SCC45/55ref	**25_2016ref**	**25_2017_ref**	**FRC_ C25/30_2015ref (without fibres)**
According to (ČSN EN 12390-13, 2014), A Method; Stabilized $E_{C,S}$ [GPa], **determined**			
30.3	30.7	30.5	29.5
By means of DIC, Stabilized $E_{C,S,DIC}$ [GPa], vertical dimension 130 mm, **experimentally determined**			
31.2	N/A	31.2	28.6
According to (ČSN EN 1992-1-1 ed. 2, 2011); guide value			
36.0	36.0	36.0	31.0
According to (Model Code 2010, 2012); guide (extrapolated) value			
34.5	34.5	34.5	28.0

Tab. 4 proves reaching of lower values of modules of elasticity of modern types of concrete in comparison to guide values of traditional types of concrete. This is attributed to a higher share of fine constituents and quantity of (super-) plasticizing admixtures.

The assumption of a slight decrease of residual proportional values of modulus of elasticity has been confirmed under the max. temperature of 400 °C, see the Fig. 8.

Poisson's ratio has been determined using 3D DIC. The trend of slightly higher stabilized value in comparison to the initial value of Poisson's ratio has been confirmed. The Poisson's ratio of HSC reaches the average value of 0.19. This lower value is presumably caused by testing of "specific HSC" with the maximum grain size of 16 mm. Application of this coarse fraction in the case of HSC / HPC is very unusual.

5.3 Exposure to Thermal Loading in Electrical Oven - Evaluation

Methodology of experimental determination of residual properties on cooled testing samples approach the methodology of testing according to the "Unstressed Residual"; see the Chap. 1.8.3. It is the most critical approach out of the available ones according to the (ACI 216R-89, 1994).

5.3.1 Loading by the Maximum Temperature of 1049 °C

A negative effect – explosive spalling – has been confirmed due to inner tension and overpressure of steam in naturally humid concrete. Increased fire resistance of SFRC has not been confirmed due to this fact. Selection of steel fibres of different length (shape, diameter) could make different results.

Visible damage by wide cracks (caused by volume changes of concrete structures) has appeared on **LWSCC** and **AAM** samples. Relatively high values of residual compressive and flexural strength have been obtained though the damage was vast and visible (in the case of concrete LWSCC, AAM).

5.3.2 Loading by the Maximum Temperature of 400 °C

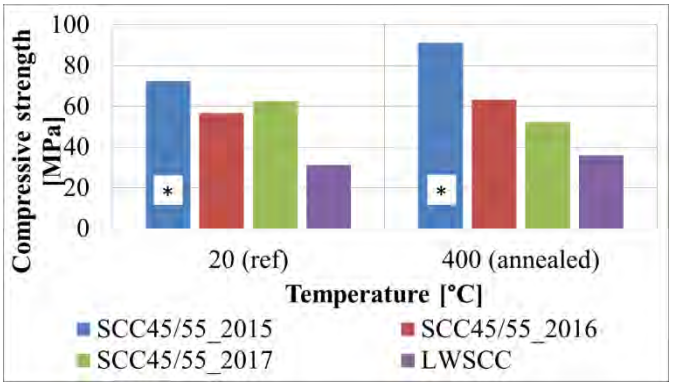

Figure 9 Typical trend of compressive strength of SCC, LWSCC; Thermal Loading in Electrical Oven, loaded on **400 °C**, (age_annealed: SCC: 1 month, LWSCC: 6 months), (* d = 100 mm)

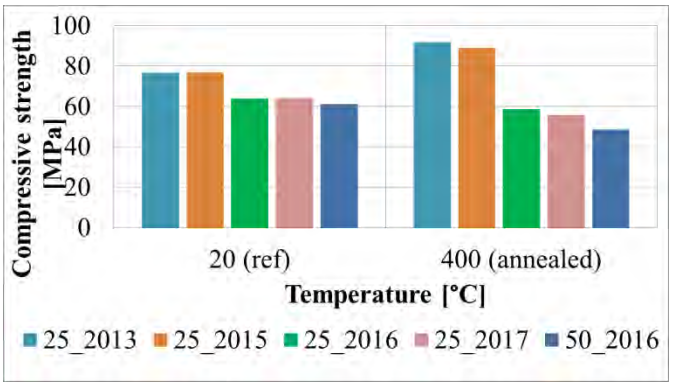

Figure 10 Typical trend of compressive strength of SFRSCC; Thermal Loading in Electrical Oven, loaded on **400 °C** (age_annealed: 25_2013: 3 months, others: 1 month)

5.4 Exposure to Local (Point) Thermal Loading – Evaluation

The effect of synthetic fibres meltdown has been confirmed. Different values of compressive residual strength have been reached in comparison to thermal loading in electric oven. It has been a different way of loading.

Diffusion has appeared. The most significant condensation of water steam has appeared in the case of PFRSCC / PFRC – as soon as in the first minutes of thermal loading.

6 CONCLUSION

Extensive experimental study determines some of the basic characteristics of hardened concrete, strength and deformational properties, using reference and thermally loaded testing samples. Because of the absence of two key sources in the European standards related to concrete – of the modulus of elasticity and the Poisson's ratio – focus has been given on the determination of these important properties.

Exposure to Thermal Loading

Based on two methodologies of thermal loading designed by author, including the concept of warming rate gradient, it can be stated that, under certain conditions and under the maximum temperature of **400 °C**, residual strength characteristics equal or better than reference mechanical properties can be reached. Note: Application of "the most critical methodology" and, at the same time, use of siliceous aggregate concrete has not prevented the increase of residual strength properties.

Exposition to temperature stress – possibilities of further research (~ 400 °C)

Presented experimental methodology of high temperature loading until the maximum temperature of 400 °C is reached could indicate the direction of "modern way of high temperature through-warming" (modern thermal treatment). The determination of the optimum way of temperature loading experimental influence will be a subject of research in the next phase of the experimental work.

Lightweight Self-Compacting Concrete – Further Research Options

Increase of strength of residual mechanical properties of lightweight self-compacting concrete is attributed to chemical processes – in applied type of artificial porous aggregate – caused by

high thermal loading. Follow-up experimental studies will aim into the development of concrete with a particular artificial porous aggregate.

Development of "lightweight high performance / high strength fibre reinforced self-compacting concrete", which excels in advantages arisen from the character of particular special types of concrete, including processing of a significant amount of waste material in aggregate, can be labelled as an eccentric idea. This idea emerged based on a verified fact that residual strength properties can be improved by specific high temperature loading. Density simultaneously decreases in the case of lightweight self-compacting concrete (decrease of nearly 500 $kg \cdot m^{-3}$ was achieved in an experiment). This type of concrete will be resistant to high temperature influence and explosive spalling will be prevented. It will have lower thermal conductivity; therefore, reinforcement will be better protected. In fresh state, it will act like a self-compacting fibre reinforced concrete / steel fibre reinforced concrete. Another research options aim to the improvement of artificial aggregate properties even before the beginning of the concrete production.

Summary of Results

Particular evaluations are the subject of the Chapter 5.

Following Summary Can Be Made for Particular Parts:

Exposure to Thermal Loading of the Maximum Temperature of 1049 °C

Explosive spalling directly relates to microstructure and transport mechanisms. In the case of fibre reinforced concrete with added polymer microfibers, explosive spalling has been prevented. Passive protection has been proved. By this modification of concrete, costs have increased in the minimum extent, but the result has increased passive safety including other advantages emerging from the use of fibre reinforced concrete.

It is known that steel fibre reinforced concrete can, under certain conditions, postpone spalling of concrete. Based on performed experimental work, it can be stated that increased fire resistance of steel fibre reinforced concrete has not been confirmed. Explosive spalling of steel fibre resistance concrete (in comparison to the types of concrete without fibres) has happened. It can be assumed that oxidized steel fibres have caused damage of the samples (popping). The oxidation has caused expansion of particular steel fibres. The effect of growing tensile stress between steel fibres and concrete is attributed to thermal flow transmission into the steel fibres due to high thermal conductivity of steel contrary to concrete. Temperature difference between steel fibres and concrete has caused spalling of concrete.

High thermal loading has caused a change of physicochemical properties. The effect of dominant expansion of aggregate has been confirmed; visible damage in the place of border of phases has happened.

Density of concrete has decreased due to expulsion of free and, later, physically bound water. Due to the decrease of physically bound water, degradation that is more significant has happened. Structural changes of studied special types of concrete are shown using SEM and EDXA.

Modulus of Elasticity of Concrete, Poisson's Ratio

Modulus of elasticity is one of the basic characteristics of hardened concrete. Secant modules of elasticity values of special types of concrete in compression have been determined by standards and by correlation of digital image. Analysis of variance of results has been made by Anova test on the level of significance 0.05. Conclusions could differ in the case of larger statistical data set.

It has been proved, by application of two methods, that "modern types of concrete" have lower values of modules of elasticity. This fact is attributed to the higher share of fine constituents and quantity of (super-) plasticizing admixtures.

It has been proved that modulus of elasticity decreases by high thermal loading more rapidly than strength characteristics.

7 REFERENCES

Bangi, Mugume Rodgers and Takashi Horiguchi, 2011. Pore pressure development in hybrid fibre-reinforced high strength concrete at elevated temperatures. In: *Cement and Concrete Research.* Vol. 41. pp. 1150–1156. DOI.org/10.1016/j.cemconres.2011.07.001

Chan, Y.N., G.F. Peng, and M. Anson, 1999. Residual strength and pore structure of high-strength concrete and normal strength concrete after exposure to high temperatures. In: *Cement and Concrete Composites.* vol. 21, pp. 23–27. DOI 10.1016/S0958-9465(98)00034-1.

COLLEPARDI, Mario, 2009. *Moderní beton*. Praha: Informační centrum ČKAIT. Betonové stavitelství. ISBN 978-80-87093-75-7.

Guidance on the use of Macro-synthetic-fibre-reinforced Concrete: Report of a Concrete Society Working Group, 2007. United Kingdom: The Concrete Society. Technical Report, No. 65. ISBN 1-90-4482-34-1.

HELA, R., HUBERTOVÁ, M, 2007. Ready mixed self compacting concrete. In: *Innovations in Structural Engineering and Construction*. 1. Melbourne, Talylor&Francis London. 2007. p. 477–483. ISBN 978-0-415-45754-5.

INGHAM, Jeremy P., 2009. Application of petrographic examination techniques to the assessment of fire-damaged concrete and masonry structures. *Materials characterization: An International Journal on Materials Structure and Behavior*, Volume 60, Issue 7, s. 700-709. ISSN 1044-5803.

KHOURY, G. A, 1992. Compressive strength of concrete at high temperatures: A reassessment. In: *Magazine of Concrete Research*, Volume 44, Issue 161, s. 291-309. ISSN 0024-9831.

KRÁTKÝ, Jiří, Karel TRTÍK a Jan VODIČKA, 1999a. *Drátkobetonové konstrukce: Úvodní část a příklady použití: Směrnice pro navrhování, provádění, kontrolu výroby a zkoušení drátkobetonových konstrukcí*. Praha: Informační centrum ČKAIT. Betonové stavitelství. ISBN 80-86364-00-3.

LEE, Joongwon, Kwangho CHOI a Kappyo HONG, 2010. The effect of high temperature on color and residual compressive strength of concrete. In: *Fracture Mechanics of Concrete and Concrete Structures: High Performance, Fiber Reinforced Concrete, Special Loadings and*

Structural Applications. Korea: Concrete Institute, s. 1772-1775. FraMCos, 7. ISBN 978-89-5708-182-2. Dostupné z: http://framcos.org/FraMCoS-7/14-11.pdf.

PROCHÁZKA, Jaroslav a Radek ŠTEFAN, 2009. Odštěpování betonu v extrémních teplotních podmínkách. In: *16. Betonářské dny 2009: Sborník ke konferenci*. Hradec Králové: ČBS Servis, s. 431-434. ISBN 978-80-87158-20-3.

PROCHÁZKA, Jaroslav, Radek ŠTEFAN a Jitka VAŠKOVÁ, 2010. *Navrhování betonových a zděných konstrukcí na účinky požáru*. Praha: České vysoké učení technické. ISBN 978-80-01-04613-5.

REICHEL, Vladimír, 1979. *Navrhování požární odolnosti staveb: Díl II*. Praha: Státní nakladatelství technické literatury. SIP-41757/03541-05/91-06-052-79.

SCHUTTER, Geert De, Peter J.M. BARTOS, Peter DOMONE, John GIBBS a Rudolf HELA, 2008. *Samozhutnitelný beton*. Praha: ČBS Servis. ISBN 978-1904445-30-2.

SUCHÁNEK, Vladimír a Jiří POKORNÝ, 2013. Experimentální výzkum odolnosti vybraných nosných kompozitních materiálů při působení požáru. In: *Mosty 2013: 18. mezinárodní sympozium: sborník příspěvků*. Brno: Sekurkon, s. 188-193. ISBN 978-80-86604-60-2.

ACI 216R-89, 1994. *Guide for Determining the Fire Endurance of Concrete Elements*. American Concrete Institute. State of the Art, USA.

ASTM C 173. *Standard Test Method for Air Content of Freshly Mixed Concrete by the Volumetric Method.*

ASTM C 23. *Standard Test Method for Air Content of Freshly Mixed Concrete by the Pressure Method.*

ASTM E 84. *Standard Test Method for Surface Burning Characteristics of Building Materials.*

ASTM E 119. *Standard Test Methods for Fire Tests of Building Construction and Materials*.

Bulletin D´Information, 1991. *No. 208: Fire Design of Concrete Structures*. Comite Euro-International Du Beton (CEB), Lausanne, Switzerland.

ČSN 73 0851, 1984. *Stanovení požární odolnosti stavebních konstrukcí.* Praha: Vydavatelství norem, (zrušená).

ČSN EN 12350-7, 2009. *Zkoušení čerstvého betonu - Část 7: Obsah vzduchu - Tlakové metody*. Praha: Úřad pro technickou normalizaci, metrologii a státní zkušebnictví.

ČSN EN 12390-3, 2009. *Zkoušení ztvrdlého betonu - Část 3: Pevnost v tlaku zkušebních těles*. Praha: Úřad pro technickou normalizaci, metrologii a státní zkušebnictví.

ČSN EN 1363-1, 2013. *Zkoušení požární odolnosti - Část 1: Základní požadavky*. Praha: Úřad pro technickou normalizaci, metrologii a státní zkušebnictví.

ČSN EN 1363-2, 2000. *Zkoušení požární odolnosti - Část 2: Alternativní a doplňkové postupy*. Praha: Český normalizační institut.

ČSN EN 1991-1-2, 2004. *Eurokód 1: Zatížení konstrukcí - Část 1-2: Obecná zatížení - Zatížení konstrukcí vystavených účinkům požáru*. Praha: Český normalizační institut.

ČSN EN 1992-1-1 ed. 2, 2011. *Eurokód 2: Navrhování betonových konstrukcí - Část 1-1: Obecná pravidla a pravidla pro pozemní stavby: ed. 2*. Praha: Úřad pro technickou normalizaci, metrologii a státní zkušebnictví.

ČSN EN 1992-1-2, 2006. *Eurokód 2: Navrhování betonových konstrukcí - Část 1-2: Obecná pravidla - Navrhování konstrukcí na účinky požáru*. Praha: Český normalizační institut.

ČSN EN 206+A1, 2018. *Beton – Specifikace, vlastnosti, výroba a shoda*. Praha: Úřad pro technickou normalizaci, metrologii a státní zkušebnictví.

ČSN ISO 8421-1, 1996. *Požární ochrana - Slovník - Část 1: Obecné termíny a jevy požárů.* Praha: Český normalizační institut.

ČSN P 73 2404, 2016. *Beton – Specifikace, vlastnosti, výroba a shoda – Doplňující informace.* Praha: Úřad pro technickou normalizaci, metrologii a státní zkušebnictví.

Model Code 2010: Final draft: Volume 1, 2012. Germany: Ernst. fib Bulletin, 65. ISBN 978-2-88394-105-2.

Model Code 2010: Final draft: Volume 2, 2012. Germany: Ernst. fib Bulletin, 66. ISBN 978-2-88394-106-9.

Popis produktu RUGEN, 2013. In: *Ekostat, a.s.* [online]. [cit. 2013-02-02]. Dostupné z: http://ekostat.cz/app/downloads/rugen_popis.pdf.

RakMK B4, 1991. *High Strength Concrete Supplementary Rules and Fire Design*. Concrete Association of Finland.

RILEM TC 129-MHT. *Test methods for mechanical properties of concrete at high temperatures.*

RILEM TC 44-PHT. *Properties of materials at high temperatures.*

RILEM TC 74-THT. *Test methods for high temperature properties.*

Technická pravidla ČBS 05: Modul pružnosti betonu. 2016. Praha: Česká betonářská společnost ČSSI. ISBN 978-80-906097-5-4.

TP 187, 2008: Samozhutnitelný beton pro mostní objekty pozemních komunikací. In: *Technické podmínky*. Praha: Ministerstvo dopravy ČR: Odbor infrastruktury.

8 LIST OF AUTHOR'S PUBLICATIONS RELATED TO THE FIELD OF THE DOCTORAL THESIS

SUCHÁNEK, Vladimír, Jiří POKORNÝ a Petr ŠKRÁČEK, 2011. Protihlukové stěny na mostech. In: *Mosty 2011: 16. mezinárodní sympozium: sborník příspěvků*. Brno: Sekurkon, s. 245-250. ISBN 978-80-86604-52-7.

DOLEŽEL, Vladimír, Jiří POKORNÝ a Vladimír SUCHÁNEK, 2012. Posouzení odolnosti ostění podzemních staveb na zmenšeném modelu tunelu při extrémním zatížení - výbuchu. In: *Technologie betonu 2012: 10. konference*. Praha: ČBS Servis – poster.

DOLEŽEL, Vladimír, Jiří POKORNÝ a Vladimír SUCHÁNEK, 2012. Vyhodnocení zkoušek odolnosti ostění podzemních staveb při výbuchu. In: *19. betonářské dny 2012: Sborník příspěvků*. Praha: ČBS Servis, s. 379-385. ISBN 978-80-87158-32-6.

SUCHÁNEK, Vladimír a Jiří POKORNÝ, 2012. *Betonové mosty II* [online]. [cit. 2018-05-04]. Dostupné z: http://vladimirsuchanek.upce.cz/files/Betonove_mosty_2.pdf

DOLEŽEL, Vladimír, Jiří POKORNÝ a Vladimír SUCHÁNEK, 2013. Testing the Model of the Rings of Cement Composites in the Blast. In: *Scientific Papers of the University of Pardubice: Sborník vědeckých prací Univerzity Pardubice*. Pardubice: Univerzita Pardubice, s. 95-104. Series B: Dopravní fakulta Jana Pernera, 18 (2012). ISBN 978-80-7395-684-4 ISSN 1211-6610.

SUCHÁNEK, Vladimír a Jiří POKORNÝ, 2013. Experimentální výzkum odolnosti vybraných nosných kompozitních materiálů při působení požáru. In: *Mosty 2013: 18. mezinárodní sympozium: sborník příspěvků*. Brno: Sekurkon, s. 188-193. ISBN 978-80-86604-60-2.

SUCHÁNEK, Vladimír a Jiří POKORNÝ, 2013. Analýza odolnosti betonových kompozitních materiálů vůči působení vysokých teplot. In: *20. Betonářské dny 2013: Sborník ke konferenci*. Praha: ČBS Servis, s. 167-172. ISBN 978-80-87158-34-0.

SUCHÁNEK, Vladimír a Michal RADOUŠ, 2014. Experimentální analýza navrženého vysokopevnostního betonu. In: *21. Betonářské dny 2014: Sborník ke konferenci*. Praha: Česká betonářská společnost ČSSI. ISBN 978-80-903806-7-7.

SUCHÁNEK, Vladimír a Matěj SLOVÁČEK, 2014. Úprava vlastností čerstvých betonů přimícháním přísad a drátků. In: *21. Betonářské dny 2014: Sborník ke konferenci*. Praha: Česká betonářská společnost ČSSI. ISBN 978-80-903806-7-7.

SUCHÁNEK, Vladimír, 2014. *Analýza vlivu extrémních teplotních namáhání na nosné kompozitní materiály*. Pardubice. Odborná písemná práce. Univerzita Pardubice, Dopravní fakulta Jana Pernera, Katedra dopravního stavitelství. Vedoucí práce Jiří Pokorný.

SUCHÁNEK, Vladimír a Michal RADOUŠ, 2015. Experimental Analysis of the Proposed High-Strength Concrete. In: *Proceedings from 21st Czech Concrete Day 2014*. Vol. 1106. Switzerland: Trans Tech Publications Ltd, pp. 77-80. ISBN 978-0-00003-132-7. ISSN print 1022-6680. ISSN cd 1022-6680. ISSN web 1662-8985. DOI 10.4028/www.scientific.net/AMR.1106.77. Dostupné z: http://www.scientific.net/AMR.1106.77

SUCHÁNEK, Vladimír a Matěj SLOVÁČEK, 2015. Edit the Properties of the Fresh Concrete Admixing Additives and Steel Fibres. In: *Proceedings from 21st Czech Concrete Day 2014*. Vol. 1106. Switzerland: Trans Tech Publications Ltd, pp. 73-76. ISBN 978-0-00003-132-7. ISSN print 1022-6680. ISSN cd 1022-6680. ISSN web 1662-8985. DOI 10.4028/www.scientific.net/AMR.1106.73. Dostupné z: http://www.scientific.net/AMR.1106.73

SUCHÁNEK, Vladimír a Jiří POKORNÝ, 2015. Experimental Investigation of the Properties of the Special Concrete After the Incident – After Fire. In: *6th International Scientific Conference: Conference Proceedings*. Pardubice: Jan Perner Transport Faculty, University of Pardubice, s. 461-474. ISBN 978-80-7395-924-1.

SUCHÁNEK, Vladimír a Kateřina HÁJKOVÁ, 2015. Experimentální analýza vlivu příměsí na trvanlivost betonu. In: *22. Betonářské dny 2015: Sborník ke konferenci*. Praha: Česká betonářská společnost ČSSI. ISBN 978-80-906097-0-9.

SUCHÁNEK, Vladimír, Leoš JIROVSKÝ a Tomáš FRONTZ, 2015. Nedestruktivní vyšetřování vláknobetonů. In: *22. Betonářské dny 2015: Sborník ke konferenci*. Praha: Česká betonářská společnost ČSSI. ISBN 978-80-906097-0-9.

SUCHÁNEK, Vladimír a Kateřina HÁJKOVÁ, 2016. Experimental Analysis of the Impact on the Durability of Concrete Additions. In: *Proceedings from 22nd Czech Concrete Day 2015*. Vol. 249. Switzerland: Solid State Phenomena, pp. 73-78. ISBN 978-3-03835-675-2. ISSN print 1012-0394. ISSN cd 1662-9787. ISSN web 1662-9779. DOI 10.4028/www.scientific.net/SSP.249.73. Dostupné z: http://www.scientific.net/SSP.249.73

SUCHÁNEK, Vladimír a Matěj SLOVÁČEK, 2016. Experimentální analýza navrženého vodonepropustného drátkobetonu. In: *23. Betonářské dny 2016: Sborník ke konferenci*. Praha: Česká betonářská společnost ČSSI. ISBN 978-80-906097-6-1.

SUCHÁNEK, Vladimír a Matěj SLOVÁČEK, 2017. Experimental Analysis of the Proposed Watertight Steel Fibre Reinforced Concrete. In: *23rd Concrete Days 2016*. Vol. 259. Switzerland: Solid State Phenomena, pp. 25-29. ISBN 978-3-0357-1105-9. ISSN print 1012-0394. ISSN cd 1662-9787. ISSN web 1662-9779. DOI 10.4028/www.scientific.net/SSP.259.25. Dostupné z: https://www.scientific.net/SSP.259.25

POKORNÝ, Jiří, Vladimír SUCHÁNEK a Vladimír KŘÍSTEK, 2017. Mostní nosné konstrukce z tyčových prefabrikátů (historie, současnost, návrh koncepce nového prefabrikátu). In: *Mosty 2017: 22. mezinárodní sympozium: sborník příspěvků*. Brno: Sekurkon, s. 253-258. ISBN 978-80-86604-71-8.

SUCHÁNEK, Vladimír, Jiří POKORNÝ a Tomáš BEDNARZ, 2017. Experimentální analýza statického modulu pružnosti speciálních betonů s využitím digitální korelace obrazu (DIC). In: *Technologie 2017: 14. konference: sborník příspěvků*. Praha: Česká betonářská společnost ČSSI. ISBN 978-80-906097-9-2.

SUCHÁNEK, Vladimír, Tomáš BEDNARZ a Tomáš SVOJANOVSKÝ, 2017. Využití korelace digitálního obrazu (DIC) při stanovení modulu pružnosti a Poissonova součinitele speciálních betonů. In: *24. Betonářské dny 2017: Sborník ke konferenci*. Praha: Česká betonářská společnost ČSSI. ISBN 978-80-906759-0-2.

SUCHÁNEK, Vladimír, Tomáš BEDNARZ a Tomáš SVOJANOVSKÝ, 2018. Usage of Digital Image Correlation (DIC) in Determination of Modulus of Elasticity and Poisson's Ratio of Special Concrete. In: *24th Concrete Days 2017*. Vol. 272. Switzerland: Solid State Phenomena, pp. 154-159. ISBN 978-3-0357-1284-1. DOI 10.4028/www.scientific.net/SSP.272.154.Dostupné z: https://www.scientific.net/SSP.272.154.

SUCHÁNEK, Vladimír, Jiří POKORNÝ a Pavel ŠVANDA, 2018. Mechanical, Physical and Chemical Properties of Cementitious Composites Finished by Special Heating, 2018. In: *Juniorstav 2018: 20th International Conference of Doctoral Students: Proceedings*. Brno: Econ publishing, s. 890-899. ISBN 978-80-86433-69-1.

The Formation and Usage of a Regional Public Transport Services Model

Author: Ing. Martin TRPIŠOVSKÝ

Doctoral study programme:
P3710 Technique and Technology in Transport and Communications

Field of study:
3708V024 Technology and Management in Transport and Telecommunications

Supervisor:

doc. Ing. Petr Průša, Ph.D.

Supervisor specialist:

--

Doctoral thesis has arisen at the supervising:

Department of Transport Management, Marketing and Logistics

INTRODUCTION

Human society has very close relationship to transport since ever. Without the existence of quality transport, the historical development would never be possible in its full extent and complexity. It its modes from individual one to the public one transport is the engine and an essential condition of the economic performance of contemporary civilization. To provide public transportation services is one of the basic indicators of the life standard in certain locality, thus public transport services shall be seen as important issue in each region. It is essential to understand local circumstances and transport needs for its proper provision, this is the only way how to achieve the aim of high-quality service offer fulfilling contemporary sustainable mobility requirements.

Public transportation services are natural part of public services provided by the self-governed regions and central government in the Czech Republic as well as former Czechoslovakia, the development of recent years brings up new issues and challenges though. Dynamic development of recent three decades brought extraordinary amount of changes that had to affect the public transport services too. The massive outbreak of individual motorism, growing regional disparities in development and economic efficiency, weakening of local industrial concentration, political and social integration into the structures in politically-western-European area leading to the growth of the standard of living, suburbanization and urban sprawl, cultural and social megatrends, integration of public transport subsystems and cost optimization pressure lead to new requirements.

Public transport services and their provision by public transport contracts are part of complicated multidisciplinary issue. This complex issue has strong impact on the citizens, which very often leads to the fact that the solution are more political compromises (on the local, regional, national as well as international level) than the outcomes of scientific approach.

The evaluation of the public transport services quality level, the influence of certain factors determining its extent and how anticipatively it reacts to the transport needs of local inhabitants with respect to the financial limitations of public budgets are very complicated, it is influenced by many social, political, demographical and economic factors.

The subject of this thesis is to design a methodology of the evaluation of the extent of public transport services in certain municipality units within a region with the usage of a mathematical-statistical model of public transport services connection count prediction. The main aim is accomplished by using appropriate scientific methods based on detailed analysis of present-time knowledge of the issue.

1 ANALYSIS OF CURRENT STATE IN THE FIELD OF THE DOCTORAL THESIS

The first chapter of the thesis covers the analysis of the existing situation in the field of public transportation services. The chapter is based on thorough review of wide variety of domestic and foreign literature. The analysis consists of the topics of public transportation services and their undisputable benefits to contemporary society as it is widely accepted as the only sustainable alternative to individual motorism. The benefits can be recognized in many fields, in particular the benefits in social field are crucial.

Under certain circumstances the public transportation services can bring the economical profit, but in the overwhelming majority of the cases public transportation services aren’t viable in purely economic point of view. The evaluation of the public transportation services shall be

shifted from purely economical to social-economical point and accepted as services provided in public interest. This approach also transforms the economic model, the services are provided not only to meet the demand, but also to meet other needs than a priori demand. Including the social aspects in public transportation services planning and organizing is essential part of sustainable mobility. Public interest is represented by public transport services contracts. The subsidies involved aren't primarily the support to the operator, but the payment for services provided for the region and its inhabitants.

The public transportation services system in the Czech Republic is well known for its long tradition, considerably high quality and high usage by commuting, most of the connections are provided on the base of public transportation contracts. Annual subsidy to the system reaches approximately 20 billion of CZK.

The emphasis was put on public transportation services determining factors, the importance of certain factors varies, but authors of public literature agree on crucial importance of the population. The problem of discontinuity of public transport services quality in different regions is identified, the extent of public transport services varies among regions. Despite this fact no methodology of the evaluation of the extent of public transport services in certain municipality units within a region was found, public transport services standards define only minimum level of service.

Chosen competent authorities (regions, ministry of transport) come up with standard and above-standard extent of public transport services provided and also stronger emphasis on planning and its obligatory character appears recently. These aspects are other reasons to come up with the methodology of the evaluation of the extent of public transport services.

2 AIMS OF THE DOCTORAL THESIS

Based on the detailed literature review of the current state in the field of doctoral thesis in Czech Republic and abroad the aims of the thesis are set. The main aim of this doctoral thesis is to design a methodology of the evaluation of the extent of public transport services in certain municipality units within a region with the usage of a mathematical-statistical model of public transport services connection count prediction.

The model will create predictions of the public transportation services connection count within defined time period in certain municipal units of analyzed regions with high statistical credibility. The starting point for reaching the aim will be the complex analysis of particular factors determining public transportation services in municipal units. The outcome will not be only the count prediction, but also the influence rate of particular factors. The model will cover wide variety of specific aspects determining the final count of public transport service connections serving particular municipal unit, it will allow transparent comparison of the predicted count and reference count. This makes it a useful decision support tool when deciding about public transport services. Also, there is vast potential of wide usage of the whole methodology in order to understand deeper this issue following by the benefits in the sector of education.

The main aim will be reached by accomplishing a serie of sequential sub-aims:

1. To form a mathematical-statistical model predicting the count of public transportation service connections in particular municipal units of a region. The sub-aim is accomplished by using appropriate scientific methods based on detailed analysis of present-time knowledge of the issue. The main requirement to be met by the model is its ability to predict the level of public transport services in assessed municipal units based on factors that are identified as the ones

that determine the extent of public transportation services, the prediction shall be done with high statistical credibility.

2. To form a methodology of the evaluation of the extent of public transport services in certain municipality units with the usage of a model created according to the previous sub-aim.

3. Use the methodology and create the model.

4. To apply the methodology and model created within on certain region, to adjust the model based on the real data from that region and assess its credibility. The outcome should undergo a critical analysis that will be the last step of the methodology.

3 LIST OF USED METHODS

Throughout all the doctoral thesis only methods and techniques based on rational logics in compliance with science methodology are used to reach the aims. The choice of scientific methods originates from the principles of scientific research, the emphasis is put on systematic and organized character. Scientific research is realized in three standard steps – the exploration, the prediction and the explanation (Olecká and Ivanová, 2010):

- The exploration is the introductory part of the scientific research, basic elements of the research scope are identified and characterized.
- The prediction follows, during this phase certain qualitative and quantitative characteristics are identified and links between them are described.
- Final research part is the explanation, during this phase the final information is presented and issue explained.

3.1 Basic Explanatory Methods

The cornerstones are basic explanatory methods that are universally applicable at all steps of scientific research. Among methods used in this thesis literature review, abstraction and concretization, deduction and induction, analysis and synthesis, analogy and comparing and expert estimation.

3.2 Prognostic Methods

Fundamental methods in this thesis are prognostic methods, exact prognostic methods according to Jirsák, Mervart and Vinš (2012) are used. The model created in the methodology is based in regression, that is basic statistical method when exploring links between numerical signs (Blatná, 2008).

3.2.1 Linear regression

Regression function is expected value of the dependent (stochastic; output) variable derived from changeable combinations of independent (deterministic; input) variables, thus regression can be understood in the way presented in the formula (1) according to van Wieringen (2019); Blatná (2008) and Hebák (1998).

$$Y = f(\mathrm{x}, \beta_1, \dots, \beta_k) + \varepsilon = E(Y|x) \quad (1)$$

where:

Y ..... output variable [-],

x ..... input variable [-],

$\beta_1, \dots, \beta_k$ ..... regression parameters [-],

k ..... regression parameters count, $k \geq 1 \wedge k \in \mathbb{N}$ [-],

$f(\mathrm{x}, \beta_1, \ldots, \beta_k)$ ..... regression function [-],

ε ..... error variable caused by the influences not included in the model [-],

$E(Y|\mathrm{x})$ ..... expected value of the output variable Y derived from x [-].

Basic vector view on vector regression based on van Wieringen (2019), Tvrdík (2013), Bremer (2012), Anděl (2005), Zvára (2002), Hebák (1998). Rousseeuw and Yohai (1984), Golub, Heath and Wahba (1979) and Hoerl and Kennard (1970) is presented in formula (2).

$$\mathbf{y} = \mathbf{X}\boldsymbol{\beta} + \boldsymbol{\varepsilon} \tag{2}$$

where:

y..... vector of real empirically found values of dependent variable consisting of n dimensions [-],

X ..... matrix of independent variables of the $(n \times p)$ dimensions [-],

β ..... vector of regression coefficients consisting of p dimensions [-],

ε..... vector of error variable consisting of n dimensions [-].

The linear regression is based on ordinary least squares method introduced by Gauß (1809). The interpretations by Bondell and Stefanski (2013), Bremer (2012) and Franc (2011) are presented in the formula (3).

$$\min_{\widehat{\boldsymbol{\beta}}} \mathbf{e}^{\mathrm{T}}\mathbf{e} = \min_{\widehat{\boldsymbol{\beta}}} \left(\mathbf{y} - \mathbf{X}\widehat{\boldsymbol{\beta}}\right)^{\mathrm{T}} \left(\mathbf{y} - \mathbf{X}\widehat{\boldsymbol{\beta}}\right) = \min_{\widehat{\boldsymbol{\beta}}} \left(\mathbf{y} - \sum_{j=1}^{k} \mathbf{x_j}^{\mathbf{T}}\widehat{\boldsymbol{\beta}}\right)^2 \tag{3}$$

where:

e..... residual vector of differences between real empirically found values of y variable and their predicated estimation consisting of n dimensions [-],

$\widehat{\boldsymbol{\beta}}$ ..... vector of the estimations of the regression coefficient β consisting of p dimensions [-],

y..... vector of real empirically found values of dependent variable consisting of n dimensions [-],

X ..... matrix of independent variables of the $(n \times p)$ dimensions [-],

j ..... identifier of particular input valuable, $j \in \langle 1; k \rangle \wedge j \in \mathbb{N}$ [-],

k ..... regression parameters count, $k \geq 1 \wedge k \in \mathbb{N}$ [-],

$\mathbf{x_j}$ ..... vector of the values of jth independent variable consisting of k dimensions [-].

The outcome of the linear regression model is shown in the formula (4) according to Neubauer (2016), Bremer (2012) and Hebák and Svobodová (2001).

$$\hat{\mathbf{y}} = \mathbf{X}\widehat{\boldsymbol{\beta}} \tag{4}$$

where:

$\hat{\mathbf{y}}$ ..... vector of predicted values of independent variable consisting of n dimensions [-],

$\mathbf{X}$ ..... matrix of independent variables of the $(n \times p)$ dimensions [-],

$\widehat{\boldsymbol{\beta}}$ ..... vector of the estimations of the regression coefficient β consisting of p dimensions [-].

3.2.2 Robust regression using LTS

According to Hebák and Svobodová (2001) any systematic pattern or nonrandomness of the residuals indicates to shortcomings of the regression model. The linear regression model based on the ordinary least squares method is very sensitive to outliers. Robust regression is involved in order to deal with outliers. Based on comparison of different robust regression methods LTS (Least trimmed squares method) is chosen to be used in the model. LTS is based on the iteration principle, it has four main steps (Doornik, 2011):

1. Setting the trimming constant of r.
2. All possible subsets γ consisting of r observations are generated. For each subset γ the regression coefficients β estimations are counted by standard ordinary least squares method.
3. The residuals $e^{m}_{LTS,\gamma}$ are counted for each vector $\widehat{\boldsymbol{\beta}}^{\mathbf{LTS}}_{\boldsymbol{\gamma}}$ and all n observations. Resiudals vector $\mathbf{e}_{\boldsymbol{\gamma}}$ is assembled for each vector $\widehat{\boldsymbol{\beta}}^{\mathbf{LTS}}_{\boldsymbol{\gamma}}$. The dimensions of vector $\mathbf{e}_{\boldsymbol{\gamma}}$ are ordered ordinaly according to the size of the second powers of their residuals.
4. Particular vector $\widehat{\boldsymbol{\beta}}^{\mathbf{LTS}}_{\boldsymbol{\gamma}}$ is chosen, it is the vector that leads to the lowest values of the minimization criterion. The criterion is introduced in the formula (5) (Alfons, Croux and Gelper, 2013).

$$\min_{\gamma} \min_{\widehat{\boldsymbol{\beta}}^{\mathbf{LTS}}_{\boldsymbol{\gamma}}} \mathbf{e}^{*\,2}_{\boldsymbol{\gamma}} = \min_{\gamma} \min_{\widehat{\boldsymbol{\beta}}^{\mathbf{LTS}}_{\boldsymbol{\gamma}}} \left(\mathbf{y}^{*}_{\boldsymbol{\gamma}} - \mathbf{X}^{*}_{\boldsymbol{\gamma}} \widehat{\boldsymbol{\beta}}^{\mathbf{LTS}}_{\boldsymbol{\gamma}}\right)^2 = \min_{\gamma} \min_{\widehat{\beta}_0^{LTS,\gamma}, \widehat{\beta}_j^{LTS,\gamma}} \sum_{[m_\gamma]=1}^{r} e_{\gamma}^{[m_\gamma]^2} =$$

$$= \min_{\gamma} \min_{\widehat{\beta}_0^{LTS,\gamma}, \widehat{\beta}_j^{LTS,\gamma}} \sum_{[m_\gamma]=1}^{r} \left(y^{[m_\gamma]} - \hat{\beta}_0^{LTS,\gamma} - \sum_{j=1}^{k} \hat{\beta}_j^{LTS,\gamma} \times x_j^{[m_\gamma]}\right)^2 \tag{5}$$

where:

γ…….identifier of particular subset consisting of r observations, $\gamma \in \langle 1; \Gamma \rangle \wedge \gamma \in \mathbb{N}$ [-],

$\widehat{\boldsymbol{\beta}}_{\boldsymbol{\gamma}}^{\mathbf{LTS}}$…….vector of the estimations of the regression coefficient β numerated by LTS method for the subset γ consisting of p dimensions [-],

$\mathbf{e}_{\boldsymbol{\gamma}}^{*}$…….residual vector of differences between real empirically found values of y variable and their predicated estimation consisting of r dimensions representing the observations included in subset γ, the order of particular dimensions $e_{\gamma}^{[m_\gamma]}$ is set ordinally according to the size of their second powers [-],

$\mathbf{y}_{\boldsymbol{\gamma}}^{*}$……vector of real empirically found values of dependent variable consisting of r dimensions representing the observations included in subset γ, the order of particular dimenstions $y_{\gamma}^{[m_\gamma]}$ is set ordinally according to the size of the second powers of their residuals $e_{\gamma}^{[m_\gamma]}$ counted for assessed vector $\widehat{\boldsymbol{\beta}}_{\boldsymbol{\gamma}}^{\mathbf{LTS}}$ [-],

$\mathbf{X}_{\boldsymbol{\gamma}}^{*}$……..matrix of independent variables of the $(r \times p)$ dimensions, the order of particular rows $[m_\gamma]$ is set ordinally according to the size of the second powers of their residuals $e_{\gamma}^{[m_\gamma]}$ counted for assessed vector $\widehat{\boldsymbol{\beta}}_{\boldsymbol{\gamma}}^{\mathbf{LTS}}$ [-],

$\hat{\beta}_0^{LTS,\gamma}$……the estimation of the intercept term counted by the LTS method for subset γ [-],

$\hat{\beta}_j^{LTS,\gamma}$……...the estimation of the regression coefficient of jth independent variable counted by the LTS method for subset γ [-],

$[m_\gamma]$……..identifier of particular observation in the adjusted ordinal order according to the size of the second powers of their residuals $e_{\gamma}^{[m_\gamma]}$ counted for asessed vector $\widehat{\boldsymbol{\beta}}_{\boldsymbol{\gamma}}^{\mathbf{LTS}}$, $[m_\gamma] \in \langle 1; n \rangle \wedge [m_\gamma] \in \mathbb{N}$ [-],

r……...trimming constant, the number of observations included in particular subsets γ of the minimization criterion of LTS method, $r \in \langle 1; n \rangle \wedge r \in \mathbb{N}$ [-],

$e_{\gamma}^{[m_\gamma]}$……the residuum of the observation $[m_\gamma]$ counted with the use of assessed estimations of regression coefficients β for subset γ [-],

$y^{[m_\gamma]}$……true empirically identified value of the independent variable for the observation $[m_\gamma]$ [-],

j……identifier of particular input valuable, $j \in \langle 1; k \rangle \wedge j \in \mathbb{N}$ [-],

k……...regression parameters count, $k \geq 1 \wedge k \in \mathbb{N}$ [-],

$x_j^{[m_\gamma]}$…….value of j-th independent variable for the observation $[m_\gamma]$ [-].

3.2.3 Robust regression using LTS

By the multiple regression analysis growing number of variables k leads to a drop in the credibility of the ordinary least squares method, the vectors of input variables aren't orthogonal, the absence of orthogonality means that multicollinearity appears in the model (Bremer, 2012;

Hoerl and Kennard, 1970). Reaching clear orthogonality between all input variables isn't possible in real world. Then multicollinearity leads to the distortion of values of regression coefficients, instability of regression model a very low model credibility (Dorugade, 2018; Buonaccorsi, 1996).

Ridge regression deflects lightly the regression coefficients estimations, the principle is penalization of such regression coefficients β that evince the marks of multicollinearity (NCSS Statistical Software, 2019; Oleszak, 2019; Breheny, 2011; Golub, Heath and Wahba, 1979). The real effect of the ridge regression is strengthening the diagonal of the $\mathbf{X}^{\mathrm{T}}\mathbf{X}$ matrix as described by Zvára (2008). The mathematical form is provided in the formula (6) according to Xiao, Coots and Ye (2017) and Zvára (2008).

$$\hat{\boldsymbol{\beta}}_{\mathbf{RR}} = (\mathbf{X}^{\mathrm{T}}\mathbf{X} + \lambda\mathbf{I}_{\boldsymbol{n}})^{-1}\mathbf{X}^{\mathrm{T}}\mathbf{y}$$

where:

$\hat{\boldsymbol{\beta}}_{\mathbf{RR}}$ .....vector of the estimations of the regression coefficient β numerated by ridge regression for the subset γ consisting of p dimensions [-],

$\mathbf{X}$ .....matrix of independent variables of the $(n \times p)$ dimensions [-],

λ.....ridge regression constant [-],

$\mathbf{I}_{\boldsymbol{n}}$ .....identity matrix of the $(n \times n)$ dimensions [-],

$\mathbf{y}$.....vector of real empirically found values of dependent variable consisting of n dimensions [-].

Van Wieringen (2019) shows that the estimation of vector $\hat{\boldsymbol{\beta}}_{\mathbf{RR}}$ allows the user to compute the final vector of predicted values $\hat{\mathbf{y}}_{\mathbf{HR}}$ as demonstrated in formula (7).

$$\hat{\mathbf{y}}_{\mathbf{RR}} = \mathbf{X}\hat{\boldsymbol{\beta}}_{\mathbf{RR}}$$

where:

$\hat{\mathbf{y}}_{\mathbf{HR}}$.....vector of predicted values of independent variable consisting of n dimensions numerated by ridge regression [-],

$\mathbf{X}$……matrix of independent variables of the $(n \times p)$ dimensions [-],

$\hat{\boldsymbol{\beta}}_{\mathbf{RR}}$……vector of the estimations of the regression coefficient β numerated by ridge regression for the subset γ consisting of p dimensions [-].

4 PROBLEMS SOLVING

This Chapter contains the description of the execution of the subject of the thesis.

4.1 Model inputs

The model quantifies the influence of particular factors, that were identified in the literature review as factors that determine the public transportation services. Each factor is represented by an appropriate input value. The overview of model inputs is introduced in the Table 1.

Table 1. The overview of all potentially entering inputs to the mathematical-statistical model

Input identifier j	Name and description of the factor (always related to the assessed municipality unit)	Binary variable
1	Inhabitants count	no
2	The women share on total inhabitants count	no
3	The share of economically active population on total inhabitants count	no
4	Unemployment rate	no
5	The count of microbusinesses	no
6	The count of little businesses	no
7	The count of middle businesses	no
8	The count of large businesses	no
9	The count of elementary schools	no
10	The count of secondary schools	no
11	The count of tertiary schools and universities	no
12	The count of municipal units with the inhabitant count within the $\langle A; B)$ range remoted no more then defined distance of D	no
13	The count of municipal units with the inhabitant count within the $\langle B;\infty)$ range remoted no more than defined distance of D	no
14	The distance to the regional center, in specific cases of bicentric regions the sum of distances to both centers can be used	no
15	Administrative part of the regional center	yes
16	Regional border remoted no more than defined distance of E	yes
17	National border remoted no more than defined distance of G	yes
18	The existence of important cultural sight or social-cultural facilities	yes
19	The existence of important natural sight or location within the area of natural protected area	yes
20	The location at the road with the transportation density within the $\langle J; K)$ range	yes
21	The location at the road with the transportation density within the $\langle K; \infty)$ range	yes
22	The location by the crossing of important roads both exceeding the transport density of L, or at the railway crossing where both lines are regularly served by passenger transport	yes
23	The existence of a railway station or stop on the track regularly served by passenger transport	yes

24		The altitude higher than the limit of M	yes
25		Specific factor defined in the critical analysis of previous model version	yes /no

Source: author

Particular limit values used in the Table 1 A, B, D, E, G, J, K, L and M shall be defined in more variants and all of them will be tested during the process as limit values ζ.

4.2 Methodology of the evaluation of the extent of public transport services

The methodology of the evaluation of the extent of public transport services in certain municipality units within a region with the usage of a mathematical-statistical model of public transport services connection count prediction is introduced in this chapter. The scientific methods described in chapter 3 are used in order to create the described methodology.

The methodology has 6 steps that will be shortly described in the subchapters.

4.2.1 Initialization – a decision to create the model

There are two basic types of reasons that lead to the decision to create the model:

1. The evaluation of the reference state, which can be present-time situation or potential alternative as s decision support during public transport optimization.
2. Theoretical point of view on this issue as part of scientific research in order to get better understanding of this area.

The decision about the model creation must be followed by exact specification of evaluated region.

4.2.2 Specification of the municipal units and the public transport stops and stations distribution

During the second step of the methodology the municipal units of the region are specified, their area is precisely defined, and the public transport stops and stations are assigned to the units with the emphasis on real importance of these stops and stations for certain municipal units.

When the public transport stops and stations serve more municipal units, it can lead the solver to the respecification of the municipal units structure by merging these municipal units together for the model.

4.2.3 Data collection

Two data spheres are identified and included to the model.

First data needed for the model are the data about reference public transport services within the analyzed region. The most usual type of the analyzed reference public transport services state is the contemporary situation of its provision. The data is structured as the count of public transport service connections in each single municipal unit in defined time unit, typically the amount of public transport service connections within 24 hours of a standard weekday. The difference between public transport service connections of different character aren't considered as all of them lead to the same outcome for analyzed municipal unit, this covers the different transport modes as well as different financial background of the connections (provided by a transport company on a commercial basis or as an obligation given by public transport services contract).

The outcome is structured into a vector y, the vector is described in the formula (8).

$$\mathbf{y} = \begin{pmatrix} y^1 \\ \vdots \\ y^n \end{pmatrix} \tag{8}$$

where:

$\mathbf{y}$ ..... vector of reference values of public transport service connections in all n included municipal units within a defined time unit [-],

y^1 ..... reference value of public transport service connections in the municipal unit $m = 1$ within a defined time unit [-],

y^n ..... reference value of public transport service connections in the municipal unit $m = n$ within a defined time unit [-],

n ..... the count of municipal units included to the model, $n \geq 1 \wedge n \in \mathbb{N}$ [-].

The other data needed are the numerical representations of all the factors that determine public transport service connections count, their overview is in Table 1. The data is structured in an $\mathbf{X_i}$ matrix, its structure is introduced in formula (9). The $\mathbf{X_i}$ matrix has N versions, one for each input combinations i. The input combinations are derived from the limit values introduced in subchapter 4.1.

$$\mathbf{X_i} = \begin{pmatrix} 1 & x_1^1 & \cdots & x_k^1 \\ 1 & \vdots & \ddots & \vdots \\ 1 & x_1^n & \cdots & x_k^n \end{pmatrix} \tag{9}$$

where:

X_i ..... matrix of independent variables of the $(n \times p)$ dimensions for the i −th combination of inputs consisting of n dimensions [-],

i ..... identifier of certain input combination, $i \in \langle 1; N \rangle \wedge i \in \mathbb{N}$ [-],

$x_1^1, \ldots, x_k^n$ ..... particular independent variables [-],

k ..... regression parameters count, $k \geq 1 \wedge k \in \mathbb{N}$ [-],

n ..... the count of municipal units included to the model, $n \geq 1 \wedge n \in \mathbb{N}$ [-].

4.2.4 Model construction

Fundamental step of the methodology is the construction of mathematical-statistical model. The main inputs for the model are vector y and matrices X_i both prepared in the subchapter 4.2.3. The model construction has three phases:

1. Initial construction of the regression model using the multiple linear regression – standard ordinary least squares method.
2. The second phase specifies the prediction from the first phase by implementing the LTS method of robust regression. This method is implemented in order to manage the existence of outlier in the input data (observations).
3. Third phase than deals with the multicollinearity by using ridge regression.

First phase is based on formulas (3) and (4). The output dimensions of vector $\hat{y}$ are used to count the residuals, as shown in formula (10).

$$e_{OLS,i}^{m} = y^{m} - \hat{y}_{OLS,i}^{m} \tag{10}$$

where:

$e_{OLS,i}^{m}$……..the residual in the regression model counted by ordinary least squares regression for the ith combination of inputs for municipal unit m [-],

y^{m}…….reference value of public transport service connections in the municipal unit m within a defined time unit [-],

$\hat{y}_{OLS,i}^{m}$ ……..predicted value of public transport service connection in municipal unit m within defined time unit counted by the ordinary least squares regression for the ith combination of inputs [-].

The next phase is including the robust regression which deals in outliers in data inputs. The robust regression has several methods, the LTS method will be used in this case. The LTS method needs the information about the outlier count in the observation data. This count is represented by the trimming constant r. The outliers count is obtained by testing of studentized residuals of each observation. Afterwards the trimming constant r is set as accrding to the formula (11).

$$r_i = n - \rho_i \tag{11}$$

where:

r_i…….trimming constant, the number of municipal units included in particular subsets γ of the minimization criterion of LTS method for the i th combination of inputs, $r \in \langle 1; n \rangle \wedge r \in \mathbb{N}$ [-],

n…….the count of municipal units included to the model, $n \geq 1 \wedge n \in \mathbb{N}$ [-],

ρ_i …….the count of outliers obtained by the studentized residuals for the i th combination of inputs, $\rho_i \in \langle 1; n-2 \rangle \wedge \rho_i \in \mathbb{N}$ [-].

Afterwards the subsets γ are created for each ith combination of inputs. For each combination of subset γ and input combination i the vector of the estimations of the regression coefficient β is counted according to the formula (12).

$$\widehat{\boldsymbol{\beta}}_{\boldsymbol{\gamma}}^{\boldsymbol{i}} = \left(\mathbf{X}_{\boldsymbol{\gamma}}^{\boldsymbol{i}\,\mathrm{T}}\mathbf{X}_{\boldsymbol{\gamma}}^{\boldsymbol{i}}\right)^{-1}\mathbf{X}_{\boldsymbol{\gamma}}^{\boldsymbol{i}\,\mathrm{T}}\mathbf{y}_{\boldsymbol{\gamma}} \tag{12}$$

where:

$\widehat{\boldsymbol{\beta}}_{\boldsymbol{\gamma}}^{\boldsymbol{i}}$.....vector of the estimations of the regression coefficient β consisting of p dimensions numerated by ridge regression for the subset γ for the i th combination of inputs [-],

$\mathbf{X}_{\boldsymbol{\gamma}}^{\boldsymbol{i}}$.....matrix of independent variables of the $(r_i \times p)$ dimensions for the i th combination of inputs containing only such municipal units m that were included in the subset γ [-],

$\mathbf{y}_{\boldsymbol{\gamma}}$…….vector of reference values of public transport service connections within a defined time unit consisting of r_i dimensions containing only such municipal units m that were included in the subset γ [-].

Based on vector $\widehat{\boldsymbol{\beta}}_{\boldsymbol{\gamma}}^{\boldsymbol{i}}$ the values of $\hat{y}_{\gamma,i}^{m}$ and $e_{\gamma,i}^{m}$ with the usage of analogies to formulas (4) and (10). For each subset γ the ordinal order of second powers of the resiudals $e_{\gamma,i}^{[m_{\gamma}^{i}]}$ for each municipal unit included in such subset γ is set. The order is then used in LTS method as described in the subchapter 3.2.2. Once the optimal subset γ_{opt} is identified, matching vector $\widehat{\boldsymbol{\beta}}_{\boldsymbol{i}}^{\mathbf{LTS}}$ is found and this vector is used to count the vector $\hat{\mathbf{y}}_{\boldsymbol{i}}^{\mathbf{LTS}}$ as described in formula (13).

$$\hat{\mathbf{y}}_{\boldsymbol{i}}^{\mathbf{LTS}} = \mathbf{X}_{\boldsymbol{i}}\widehat{\boldsymbol{\beta}}_{\boldsymbol{i}}^{\mathbf{LTS}} \tag{13}$$

where:

$\hat{\mathbf{y}}_{\boldsymbol{i}}^{\mathbf{LTS}}$…….vector of the predicted values of public transport service connections within defined time unit consisting of n dimensions counted by the LTS method of robust regression for the i −th combination of inputs [-],

$\mathbf{X}_{\boldsymbol{i}}$ ……matrix of independent variables of the $(n \times p)$ dimensions for the i th combination of inputs consisting of n dimensions [-],

$\widehat{\boldsymbol{\beta}}_{\boldsymbol{i}}^{\mathbf{LTS}}$…….vector of the estimations of the regression coefficient β consisting of p dimensions counted by the LTS method of robust regression for the ith combination of inputs [-].

The valuables of $\hat{y}_{LTS,i}^{m}$ and $e_{LTS,i}^{m}$ can be counted afterwards with the usage of analogies to formulas (4) and (10). The calculation follows by calculating the residual sum of squares for each ith combination of inputs as shown in formula (14).

$$RSS_i^{LTS} = \sum_{\substack{m=1 \\ m\in U_i}}^{n} {e_{LTS,i}^{m}}^2 = \sum_{\substack{m=1 \\ m\in U_i}}^{n} \left(y^m - \hat{y}_{LTS,i}^{m}\right)^2 \tag{14}$$

where:

RSS_i^{LTS}…….residual sum of squares for the ith combination of inputs constructed only for such municipal units m that are included in the optimum subset γ_{opt} [-],

m…….identifier of particular municipal unit, $m \in \langle 1; n\rangle \wedge m \in \mathbb{N}$ [-],

U_i……..set of municipal units m that are included in the optimum subset γ_{opt} of the robust regression LTS method for the ith combination of inputs [-],

n……total count of municipal units in the analyzed region, $n \geq 1 \wedge n \in \mathbb{N}$ [-],

$e_{LTS,i}^{m}$……..the residual for the municipal unit m in the model counted only for such municipal units m that were included in the optimum subset γ_{opt} of the robust regression LTS method for the i −th combination of inputs [-],

y^m…….reference value of public transport service connections in the municipal unit m within a defined time unit [-],

$\hat{y}_{LTS,i}^{m}$……..predicted value of public transport service connections in municipal unit m within defined time unit counted by the robust regression LTS method for the ith combination of inputs [-].

Once all the RSS_i^{LTS} counted the minimum value of RSS_i^{LTS} for each set θ_{ζ} can be found. The sets θ_{ζ} are defined for each defined limit value ζ. Finding the ith combination with lowest RSS_i^{LTS} in each set θ_{ζ} allows the user to introduce the final optimum combination of limit values ζ_{opt}. The LTS method is counted once again for the optimum limit values ζ_{opt} that create the matrix $\mathbf{X}_{\boldsymbol{\zeta_{opt}}}$, the outcome of the calculation is new vector $\widehat{\boldsymbol{\beta}}_{\boldsymbol{\zeta_{opt}}}^{\mathbf{LTS}}$.

The statistical t test follows up to identify the variables with statistically significant influence. After carrying out the t tests the set of V that includes v values which represent all the variables that their statistically significant influence wasn't proven. Afterwards new matrix $\mathbf{X^{opt}}$ that replaces the matrix $\mathbf{X_{\zeta_{opt}}}$ in upcoming formulas is created, the rules for $\mathbf{X^{opt}}$ are described clearly in the formula (15).

$$\mathbf{X^{opt}} = \left(x_j^m\right) \text{ for } \forall\, j \in Q \wedge\ j \notin V \wedge \text{for } \forall\, m \tag{15}$$

where:

$\mathbf{X^{opt}}$ …….matrix of the final values of input independent variables with proven statistically significant influence on the final count of the public transport service connections within a defined time unit of the $[n \times (p - v)]$ [-],

x_j^m ……the value of j −th input for the municipal unit m [-],

j ……identifier of particular input independent variable, $j \in \langle 1; k\rangle \wedge j \in \mathbb{N}$ [-],

Q …….....the set of input variables j that are included in the matrix $\mathbf{X_{\zeta_{opt}}}$ that is compliant with optimum limit values ζ_{opt} [-],

V …….....the set of input variables j that were proven to have no statistically significant influence on the final count of the public transport service connections within a defined time unit [-],

m …….....identifier of particular municipal unit, $m \in \langle 1; n\rangle \wedge m \in \mathbb{N}$, where n $(n \geq 1 \wedge n \in \mathbb{N})$ is total count of municipal units in the analyzed region [-].

Analogically to formula (15) the matrix $\mathbf{X_{LTS}^{opt}}$ is created. This matrix has same characteristics, but only $m \in U_{\zeta_{opt}}$ are included. $U_{\zeta_{opt}}$ is the set of municipal units that are included in the optimum subset γ_{opt}.

The ridge regression is included in the third phase. The ridge regression manages the problem of multicollinearity that occurs in the input data vectors. The ridge regression constant λ is counted by the leave-one-out version of generalized cross-validation. The ridge regression is then carried out using the formulas (6) and (7). Final values of the predicted values of public transport service connections in municipal units m within defined time unit is counted according to formula (16).

$$\hat{y}_{RR}^m = \hat{\beta}_0^{RR} + \sum_{\substack{j=1 \\ j \notin V}}^{k} \hat{\beta}_j^{RR} \times x_j^m \tag{16}$$

where:

$\hat{y}_{RR}^m$ ……predicted value of public transport service connections in municipal unit m within defined time unit counted by the ridge regression [-],

$\hat{\beta}_0^{RR}$ ……the estimation of the intercept term counted by the ridge regression [-],

j ……identifier of particular input independent variable, $j \in \langle 1; k\rangle \wedge j \in \mathbb{N}$ [-],

V ……the set of input variables j that were proven to have no statistically significant influence on the final count of the public transport service connections within a defined time unit [-],

k …….regression parameters count, $k \geq 1 \wedge k \in \mathbb{N}$ [-],

$\hat{\beta}_j^{RR}$…….the estimation of the regression coefficient of jth independent variable counted by the ridge regression [-],

x_j^m……..the value of jth input for the municipal unit m [-].

The value $\hat{y}_{RR}^m$ as the result of formula (16) represents the main outcome from the model. The residual e_{RR}^m shall be counted afterwards by using the analogy of formula (10).

The model optimization is based on the multiply linear regression and ordinary least squares method, however it is adapted to the need to reflect the real state of different factors that determine public transportation services in analyzed region. The model is robust enough to prevent outliers from spoiling the outcome data and ridge regression removes ominous influence of the unavoidable multicollinearity.

4.2.5 Model assessment

The statistical model is subject to tests of statistical credibility afterwards, the adjusted index of determination is counted as well as t tests and F test are carried out.

The second phase of this step is critical assessment of the model and models comparison with the assumptions and experience. The critical assessment may lead to identification of new factor that was omitted when the first set of public transport determining factors were firstly set.

In case that statistical verification is negative or the logical assessment leads to such discrepancies that cause serious doubts about the models credibility it can lead to rejecting all the models outcome.

4.2.6 Outcomes interpretation

Final part of the methodology is the outcomes interpretation, the verbal explanation of values from the model leads to understanding the real importance of the outcomes and also it sketches the logical bonds in the model. The degree of influence of each factor can be counted for each municipal unit. Also, the residuals shall be discussed, and the larger residuals explained.

4.2.7 Methodology scheme

The schematic representation of the methodology of the evaluation of the extent of public transport services in certain municipality units within a region with the usage of a mathematical-statistical model of public transport services connection count prediction is provided in the Figure 1. The scheme shows basic structure of the methodology, it doesn't cover all the details, only main steps. The scheme includes the connection to the subchapters that describe particular step of the methodology in wider details.

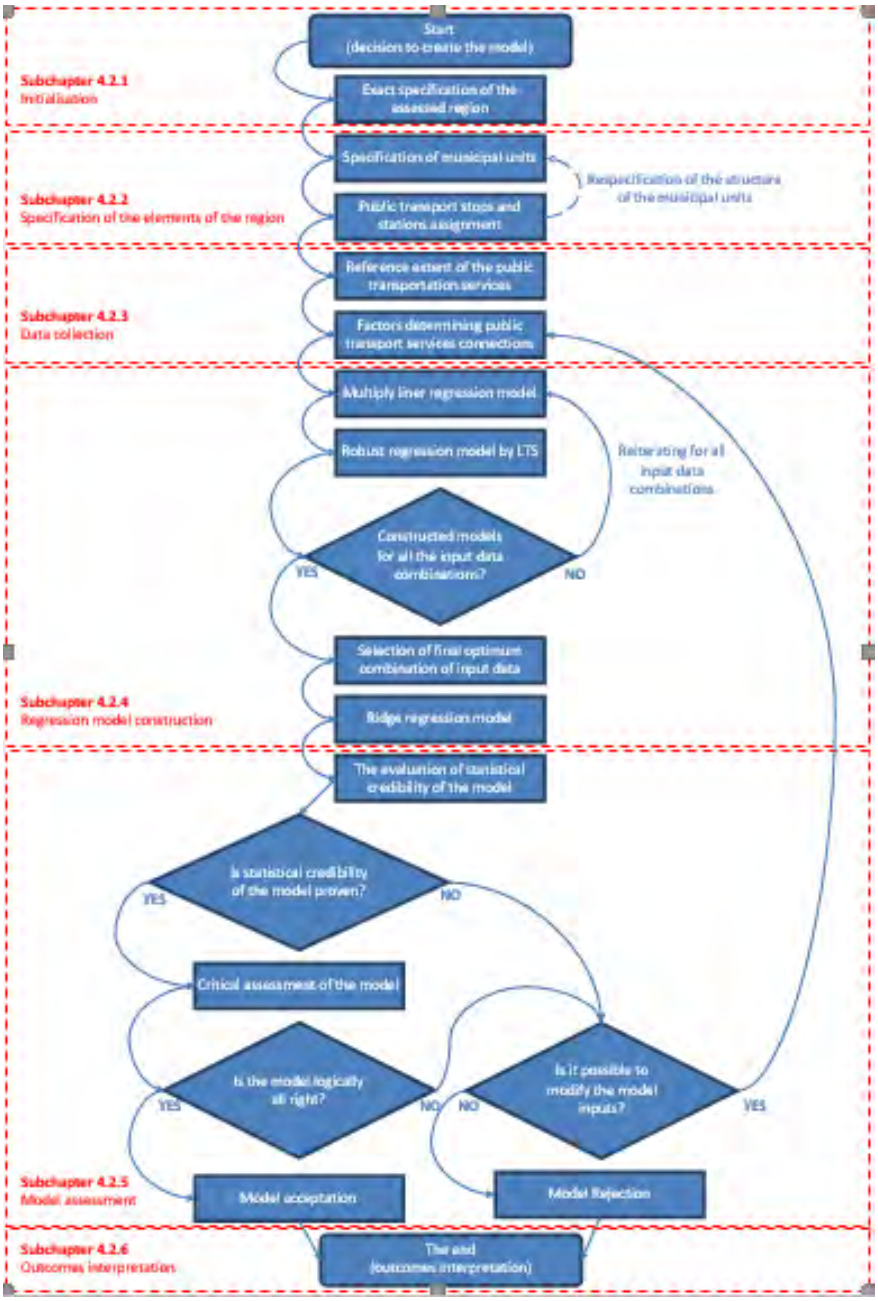

Figure 1 Schematic representation of the methodology (author)

4.3 Methodology application

Within the scope of the doctoral thesis the methodology was applied on a real data from chosen region of the Czech Republic. The application was carried out on the data from the district of Ústí nad Labem in northwest part of the Czech Republic in the Ústecký region. The methodology used the data updated to 1 August 2019. The acceptable walking distance was set to 1 km. According to Czech Statistical Office 207 basic municipal units were identified, out of them 97 were parts of the regional center of Ústí nad Labem. After the analysis 95 municipal units enter the model. Out of the 95 municipal units, the outcomes for 15 chosen municipal units is presented in Table 2.

Table 2 Final estimations of the public transport services connection counts in chosen municipal units m and the residuald of these estimations including the comparison with reference state

m	**Municipal unit**	**Reference count of public transport services connection** y^m	**The estimation of the public transport services connection count** $\hat{y}_{RR}^m$	**The residual** e_{RR}^m
2	Arnultovice	25,0	22,54	2,46
9	Čeřeniště	5,0	22,42	-17,42
11	Český Újezd	130,0	108,67	21,33
12	Dolní Zálezly	46,0	33,63	12,37
14	Dubice	18,0	27,00	-9,00
26	Knínice	42,0	37,04	4,96
32	Libouchec	113,0	75,60	37,40
37	Lysá	4,0	7,50	-3,50
52	Ostrov	0,0	7,54	-7,54
53	Petrovice	40,0	37,53	2,47
66	Řehlovice	44,0	53,29	-9,29
67	Řetouň	12,0	7,85	4,15
68	Sebuzín	68,0	83,48	-15,48
80	Telnice	29,0	24,39	4,61
84	Ústí nad Labem	2.498,4	2.374,14	124,26

Source: Dopravní podnik města Ústí nad Labem (2019), CHAPS and Ministerstvo dopravy ČR (2019), SŽDC (2019), author

The adjusted determination index reaches the value of 88,71 %, that is acceptable. Statistical tests approve the credibility of the model.

5 RESULTS AND DISCUSSION

In this thesis a methodology of the evaluation of the extent of public transport services in certain municipality units within a region with the usage of a mathematical-statistical model of public transport services connection count prediction has been proposed. This methodology has been proposed based on the results of the analysis of the current situation in the researched area in the Czech Republic and abroad in compliance with the findings of the analysis. Public transport services are essential for contemporary society, they bring crucial benefits especially in the social area and at the same time it's the only competitive alternative to individual motorism that is widely understood as environmentally friendly. Its importance increases in suburb and rural areas, where often it is the only possibility to access civic amenities. Public transport services aren't viable on commercial basis in most cases, they have to subsidized through public service obligations contracts. The system has long history and in general it's rather quality system, the problem is its regional inconsistency. The issue of the thesis is very actual.

There are three general areas of usage of the proposed methodology. The first one is the practical application on particular regions according to the needs of the competent authorities managing public transport services, especially the organizers of integrated transport systems and transport responsible at the regions. The usage of such methodology can be very good decision supporting tool when deciding about public transport services and their extent. Also, it can be useful when defining standard and above-standard level of public transport services.

The second are of usage is the field of theoretical transport research for science, it is first tool that can help to understand which factors really influence the final extent of public transport services. The third area is strongly connected to the second one, it's the field of education.

The overview of pros and cons of the methodology follows in the Table 3.

Table 3 Pros and cons of the methodology

Pros	Cons
High statistical credibility of the prediction	Limits given by the regression function
Stability and logical integrity of the prediction	The necessity to discard fully linearly dependent input variables
Models modularity	Extreme computation demanding
Universal applicability	Model can't include all the existing factors, such as political ones
Simplicity of the construction	The accessibility and recency of input data

Source: author

Several ways of future development of the model are to be mentioned:

1. First area is the implementation of detailed characteristics of included public transport connections. This could cover their routing (towards the regional center, from the regional center, round connection) as well as more accurate time description (peak/off-peak hour).
2. The second area leads to transforming the model into the normative one. The universal descriptive model can be easily transformed into normative one that would enable the competent authorities to model easily public transport services structure. Normative parameters would have to be introduced and implemented.
3. The third area covers the implementation of socio-economical characteristics that would enable the weighted comparison of particular regions based on their economical productivity.

In compliance with these three areas of future development there is still vast potential to implement new factors to the model and to find mathematical ways of quantification to include the factors that are known to determine the public transport service, but there is no known way how to transform them into values that could be used as inputs in the model. Also, minor simplifications can be done in the model after wider user experience, when it's obvious that certain changes can lead to reducing the complicative manners of the model with only weak influence on the results if any influence at all.

6 AUTHOR'S OWN CONTRIBUTION

The doctoral thesis brings three major areas of author's own contribution. First of them is the thorough and detailed literature review analyzing both on Czech and foreign literature sources. The literature review focuses on public transportation services and their position in context of transport in general. The emphasis is put on the importance of public transport services in contemporary society, especially from the point of view of social aspects. The stronger accent is kept on the area of factors determining public transport services, that is cornerstone of the literature review. Also transport policy and the actual political situation in the Czech Republic is covered. The literature review is widely used as a base for other research in this scientific field.

Second major area of author's contribution is the analysis and choice of particular prognostic methods derived from basic liner regression. During the process of methodology creation several scientific methods based on regression were tested on particular regions. As the result of this analysis author introduces the issue of linear regression, it's mathematical formulas and systematics and its application into practical problem. Considering the characteristic of input data the higher penetration of outliers would spoil the outcomes and also refuse the essential condition of normal statistical distribution of the residuals, thus robust regression is implemented. Several robust regression methods were analyzed and finally the LTS method was chosen. The outliers were followed by another problematic issue, the multicollinearity. Few methods were tested, among Partial Least Squares, Least Absolute Shrinkage and Selection Operator, Best Subset Regression and Ridge Regression the ridge regression was chosen because of higher fidelity and credibility, but still ability to interpret the influence of particular factors.
Third major area of author's contribution is crucial one from the point of view of this doctoral thesis and it is designing a methodology of the evaluation of the extent of public transport services in certain municipality units within a region with the usage of a mathematical-statistical model of public transport services connection count prediction. The methodology leads to designing a model, that predicts the estimations of public transport service connection counts in particular municipality units in the analyzed region within defined time unit, with high credibility. Several control mechanisms are included in the methodology too, these mechanisms focus not only on mathematically correct way, but also on the logical connections and critical analysis of the outcome. The model is universal decision supporting tool for all public transport services organizers.

7 CONCLUSION

The public transport in the Czech Republic haven't fully adapted yet to the complex major changes that happened in last 30 years in the structure of national economy and political and social life, however dynamical development is already setting new challenges of the social-cultural as well as economical kind. Its character as social service is emphasized recently, it leads to the essential mobility, whole this point is gaining more importance in the future prospect in compliance with society aging, living standard growth and paradigm change in the relationship to the environment and its harming by the society.

The aim of this doctoral thesis was designing a methodology of the evaluation of the extent of public transport services in certain municipality units within a region with the usage of a mathematical-statistical model of public transport services connection count prediction. The methodology was designed by the author, described in very detailed way and applied on real data from the Ústí nad Labem district. The model which is an outcome from the methodology reaches high statistical credibility and it is universally usable. The aim was thoroughly fulfilled.

Introduced methodology is widely usable as a decision supporting tool for the competent authorities responsible for public transport services in each region. At the same time constructed model brings valuable information for the theoretical research in the area of transport sciences. The scientific work can focus on further development of the model.

Authors ambition is to use this doctoral thesis as a starting point for wider discussion about the importance of public transport services provided in regions of the Czech Republic and complex point of view on transport in general, regional disparities and reasons that lead to them, extent of public transport services in particular regions and general purpose of public transport services supply and its priorities in future development.

8 REFERENCES

ALFONS, Andreas, Christophe CROUX and Sarah GELPER, 2013. Sparse least trimmed squares regression for analyzing high-dimensional large data sets. *The Annals of Applied Statistics*. Vol. 7, no. 1, s. 226-248. ISSN 1932-6157.

ANDĚL, Jiří, 2005. *Základy matematické statistiky*. Praha: Matfyzpress. ISBN 80-86732-40-1.

BLATNÁ, Dagmar, 2008. Metody statistické analýzy. Vyd. 3. Praha: Bankovní institut vysoká škola. ISBN 978-80-7265-129-0.

BONDELL, Howard D. and Leonard A. STEFANSKI, 2013. Efficient Robust Regression via Two-Stage Generalized Empirical Likelihood. *Journal of the American Statistical Association*. Vol. 108, no. 502, s. 644-655. ISSN 0162-1459.

BREHENY, Patrick, 2011. Ridge Regression. *College of Arts & Science – University of Kentucky* [online]. [citováno 2016-12-15]. Dostupné z: http://web.as.uky.edu/statistics/users/pbreheny/764-f11/notes/9-1.pdf

BREMER, Martina, 2012. Multiple Linear Regression. *Jason Mezey Lab – Cornel University* [online]. [citováno 2017-06-22]. Dostupné z: http://mezeylab.cb.bscb.cornell.edu/labmembers/documents/supplement%205%20-%20multiple%20regression.pdf

BUONACCORSI, John P., 1996. A modified estimating equation approach to correcting for measurement error in regression. *Biometrika*. Vol. 83, no. 2, s. 433-440. ISSN 0006-3444.

DOORNIK, Jurgen A., 2011. Robust Estimation Using Least Trimmed Squares. *Department of Economics and Business Economics, School of Business and Social Sciences | Aarhus University* [online]. [citováno 2018-11-03]. Dostupné z: http://econ.au.dk/fileadmin/site_files/filer_oekonomi/subsites/creates/Seminar_Papers/2011/ELTS.pdf

DOPRAVNÍ PODNIK MĚSTA ÚSTÍ NAD LABEM, 2019. Jízdní řády. *Dopravní podnik města Ústí nad Labem* [online]. [citováno 2019-08-02]. Dostupné z: https://dpmul.cz/?page=jizdni-rady

DORUGADE, Ashok Vithoba, 2018. New ridge parameters for ridge regression. *Journal of the Association of Arab Universities for Basic and Applied Sciences.* Vol. 15, no. 1, s. 94-99. ISSN 1815-3852.

FRANC, Jiří, 2011. Robust regression - Robust estimation of regression coefficients in linear regression model when orthogonality condition is breaking. *Univerzita Karlova* [online]. [citováno 2017-06-20]. Dostupné z: http://ai.ms.mff.cuni.cz/~sui/franc.pdf

GAUß, Carl Friedrich, 1809. Theoria motus corporum coelestium in sectionibus conicis solem ambientium. *ETH Bibliothek Zürich* [online]. [citováno 2016-05-11]. Dostupné z: https://www.e-rara.ch/zut/doi/10.3931/e-rara-522

GOLUB, Gene H., Michael HEATH and Grace WAHBA, 1979. Generalized Cross-Validation as a Method for Choosing a Good Ridge Parameter. *Technometrics.* Vol. 21, no. 2, s. 215-223. ISSN 0040-1706.

HEBÁK, Petr, 1998. *Regrese. Část 1*. Praha: Vysoká škola ekonomická v Praze. ISBN 80-7079-909-9.

HEBÁK, Petr and Alžběta SVOBODOVÁ, 2001. *Regrese - II. část*. Praha: Vysoká škola ekonomická. ISBN 80-245-0134-1.

HOERL, Arthur E. and Robert W. KENNARD, 1970. Ridge Regression: Biased Estimation for Nonorthogonal Problems. *Technometrics.* Vol. 12, no. 1, s. 55-67. ISSN 0040-1706.

CHAPS and MINISTERSTVO DOPRAVY ČR, 2019. Celostátní informační systém o jízdních řádech. *CHAPS spol. s r.o. – Portál CIS JŘ* [online]. [citováno 2019-06-12]. Dostupné z: http://portal.cisjr.cz

JIRSÁK, Petr, Michal MERVART and Marek VINŠ, 2012. *Logistika pro ekonomy: vstupní logistika.* Praha: Wolters Kluwer ČR. ISBN 978-80-7357-958-6.

NCSS STATISTICAL SOFTWARE, 2019. Chapter 335: Ridge Regression. *NCSS Statistical Software* [online]. [citováno 2019-04-10]. Dostupné z: https://ncss-wpengine.netdna-ssl.com/wp-content/themes/ncss/pdf/Procedures/NCSS/Ridge_Regression.pdf
NEUBAUER, Jiří, 2016. Lineární modely | Ekonometrie. *Katedra ekonometrie FVL UO Brno* [online]. [citováno 2018-10-21]. Dostupné z: https://k101.unob.cz/~neubauer/pdf/ekon_linearni_modely.pdf
OLECKÁ, Ivana and Kateřina IVANOVÁ, 2010. *Metodologie vědecko-výzkumné činnosti*. Olomouc: Moravská vysoká škola Olomouc. ISBN 978-80-87240-33-5.
OLESZAK, Michał, 2019. A Comparison of Shrinkage and Selection Methods for Linear Regression. *Towards Data Science* [online]. [citováno 2019-06-07]. Dostupné z: https://towardsdatascience.com/a-comparison-of-shrinkage-and-selection-methods-for-linear-regression-ee4dd3a71f16
ROUSSEEUW, Peter J. and Victor J. YOHAI, 1984. Robust Regression by Means of S-Estimators. In: FRANKE, Jürgen, Wolfgang HÄRDLE a Douglas MARTIN, eds. *Robust and Nonlinear Time Series Analysis.* New York, NY: Springer US, s. 256-272. ISBN 978-0-387-96102-6.
SŽDC, 2019. Jízdní řád. *Správa železniční dopravní cesty* [online]. [citováno 2019-08-03]. Dostupné z: https://www.szdc.cz/cestujici/jizdni-rad
TVRDÍK, Josef, 2013. Analýza vícerozměrných dat. *Ostravská univerzita v Ostravě* [online]. [citováno 2017-10-30]. Dostupné z: http://www1.osu.cz/~bujok/files/avdat.pdf
VAN WIERINGEN, Wessel N., 2019. Lecture notes on ridge regression. *Cornell University* [online]. [citováno 2019-08-05]. Dostupné z: https://arxiv.org/pdf/1509.09169;Lecture
XIAO, Ruikun, Reed COOTS and Yuzhe YE, 2017. Ridge Regression | R. *JB Hender* [online]. [citováno 2019-04-12]. Dostupné z: https://jbhender.github.io/Stats506/F17/Projects/G13/R.html
ZVÁRA, Karel, 2002. Regrese. *Univerzita Karlova* [online]. [citováno 2017-06-20]. Dostupné z: http://www.karlin.mff.cuni.cz/~zvara/regrese/PREDN01.pdf
ZVÁRA, Karel, 2008. *Regrese*. Praha: Matfyzpress. ISBN 978-80-7378-041-8.

9 LIST OF AUTHOR'S PUBLICATIONS RELATED TO THE FIELD OF THE DOCTORAL THESIS

TRPIŠOVSKÝ, Martin and Petr PRŮŠA, 2012. Užití CBA pro hodnocení investic do dopravy. In: *LOGI 2012 – Conference Proceeding*. Brno: Tribun EU, s. 340-350. ISBN 978-80-263-0336-7.

ČÁP, Jiří, Jindřich JEŽEK and Martin TRPIŠOVSKÝ, 2013. Plány dopravní obslužnosti krajů ČR. In: *Horizons of Railway Transport 2013*. Žilina: EDIS - vydavateľstvo Žilinskej univerzity, s. 93-102. ISBN 978-80-554-0764-7.

TRPIŠOVSKÝ, Martin, Jan CHOCHOLÁČ, Jindřich JEŽEK and Petr PRŮŠA, 2013. Rovnoběžné trasy MHD obsluhující sídliště. In: *Current trends in transport and economy in 2013 (Aktuální trendy v dopravě a ekonomice 2013)*. Pardubice: Univerzita Pardubice, s. 203-217. ISBN 978-80-86530-90-1.

TRPIŠOVSKÝ, Martin, Jindřich JEŽEK and Petr PRŮŠA, 2013. Faktory determinující dopravní obslužnost v městské zástavbě. In: *Current trends in transport and economy in 2013 (Aktuální trendy v dopravě a ekonomice 2013)*. Pardubice: Univerzita Pardubice, s. 47-56. ISBN 978-80-86530-90-1.

TRPIŠOVSKÝ, Martin, Radhika JADE and Petr PRŮŠA, 2013. Public transport services in the Czech Republic. *Focus: The International Journal of Management Digest*. Vol. 9, no. 2, s. 6-14. ISSN 0973-9165.

TRPIŠOVSKÝ, Martin, Tomáš RÝC a Petr PRŮŠA, 2013. Modelování dopravní obslužnosti obcí. In: *Sborník příspěvků z mezinárodní Masarykovy konference pro doktorandy a mladé vědecké pracovníky 2013*. Hradec Králové: MAGNANIMITAS, s. 765-774. ISBN 978-80-87952-00-9.

TRPIŠOVSKÝ, Martin, Jan CHOCHOLÁČ and Darko BABIĆ, 2013. City public transport infrastructure investments determining factors. In: *ZIRP 2013*. Zagreb: University of Zagreb, s. 111-122. ISBN 978-953-243-064-6.

TRPIŠOVSKÝ, Martin, Jan CHOCHOLÁČ and Petr PRŮŠA, 2013. Plány dopravní obslužnosti krajů ČR. In: *Dopravní obslužnost měst a krajů*. Praha: B.I.D. services, s. 17-35. ISBN 978-80-87534-51-9.

GĄSKA, Damian, Martin TRPIŠOVSKÝ and Maria CIEŚLA, 2013. Comparison of public transport services organization in the Prague and Warsaw metropolitan regions. In: *II International Symposium of Young Researchers TRANSPORT PROBLEMS 2013*. Katowice: Silesian University of Technology, s. 87-96. ISBN 978-83-935232-1-4.

TRPIŠOVSKÝ, Martin and Petr PRŮŠA, 2014. Regional Public Transportation Services Modelling. *Naše more: Journal of Marine Science*. Vol. 61, no. 3-4, s. 77-82. ISSN 0469-6255.

HUSÁK, Jiří, Dalibor GOTTWALD and Martin TRPIŠOVSKÝ, 2014. Rozvoj dopravní infrastruktury ve vybraných regionech České republiky. In: *Sborník příspěvků Mezinárodní Masarykovy konference pro doktorandy a mladé vědecké pracovníky 2014*. Hradec Králové: MAGNANIMITAS, s. 1213-1222. ISBN 978-80-87952-07-8.

GĄSKA, Damian, Martin TRPIŠOVSKÝ and Maria CIEŚLA, 2015. Comparison of public transport services organization in the Prague and Warsaw metropolitan regions. *Zeszyty Naukowe Politechniki Śląskiej: Transport*. Vol. 86, no. 1, s. 21-32. ISSN 0209-3324.

TRPIŠOVSKÝ, Martin, 2015. Public transportation services determining factors in the urban areas. In: *ZIRP 2015*. Zagreb: University of Zagreb, s. 219-224. ISBN 978-953-243-073-8.

CHOCHOLÁČ, Jan, Martin TRPIŠOVSKÝ and Dana SOMMERAUEROVÁ, 2016. Komparace marketingového mixu železničních dopravců v souvislosti s dopravní obslužností na trase Praha - Ostravsko v souladu s principy udržitelného rozvoje. In: *Aktuální trendy v dopravě a ekonomice.* Pardubice: Univerzita Pardubice, s. 246-251. ISBN 978-80-8653-095-6.

CHOCHOLÁČ, Jan, Martin TRPIŠOVSKÝ and Nina KUDLÁČKOVÁ, 2018. The evaluation of the service quality performed by the rail passenger transport carriers on the Prague – Ostrava region route: primary marketing research. In: *Transport Means: proceedings of the international scientific conference.* Kaunas: Kaunas University of Technology., s. 91-106. ISSN 1822-296X.

Anti-slip Control of Traction Motor of Rail Vehicles

Author: Ing. Abdulkadir ZIREK

Doctoral study programme:
P3710 Technique and Technology in Transport and Communications

Field of study:
3706V005 - Transport Means and Infrastructure

Supervisor:
doc. Ing. Michael Lata, Ph.D.

Supervisor specialist:
Prof. Ing. Jaroslav Novák, CSc.

Doctoral thesis has arisen at the supervising:
Department of Transport Means and Infrastructure

ABSTRACT

This work deals with the use of anti-slip control methods for rail vehicles. Initially, to give readers a general picture of the research covered in the thesis, the adhesion and slip mechanism are explained. Furthermore, the slip detection methods and slip control methods based on the literature review are introduced. To verify the validity of the anti-slip control schemes, a numerical model of a tram wheel roller rig that includes nonlinear effects caused by time delay and disturbances to match the values of the experimental test setup has been generated using MATLAB editor. Five wheel slip control strategies -wheel slip control based on single threshold (WSCST), wheel slip control based on multiple thresholds (WSCMT), wheel slip control based on angular acceleration of wheel (WSCAA), PI wheel slip control (PI-WSC), and sliding mode wheel slip control (SM-WSC)- are suggested. In addition to the simulation calculations, this work includes an experimental part in which extensive experiments are carried out on laboratory test equipment where the anti-slip algorithms are implemented and tested. The validity of the developed numerical model is proven with the comparison of the simulation and experimental results. The performances of all the wheel slip control methods are evaluated by the mathematical model and experimental setup. The influences of different roller speeds and control parameters are analysed via validated numeric model.

KEYWORDS

adhesion, wheel slip, anti-slip, acceleration, roller rig, control, PMSM, sliding mode.

1 INTRODUCTION

Due to the demand and emerging technologies in the railway sector, more powerful rail vehicles have been recently produced. The current development in the power capacity of the vehicles drive systems enables them reaching high torques in a short time. The tractive effort of vehicle is transferred to the rail in a small contact area that provides the vehicle with an advantage due to the lower power losses caused by friction in wheel-rail contact [1]. On the other hand, the traction ability of these vehicles is limited to environmental conditions (i.e. rain, snow, leaves and mud) and human influences. Besides, the adhesion between wheel and rail decreases with the increase of the running speed under contaminated surface conditions [2]. All these factors lead the slip of the wheel, which occurs when tractive effort exceeds the available adhesion, whereas sliding occurs when the braking effort exceeds the available adhesion. If the slip/slide reaches the high value, it causes severe wear of wheel and rail surfaces, increasing mechanical stress in the system and affects stability. The presence of high wheel slip is an undesired situation resulting in a reduction in the safety, traction performance and wheel-rail lifetime.

Due to requirements anti-slip, control systems have been developed. In the early age of railway transportation, the vehicles were equipped with the sander which improves the adhesion conditions. However, the sanding increases 10 to 100 times the wheel and rail wear [1], [3]. Thus, new strategies were sought out to be used for rail vehicles. In the late 70s, thanks to the rapid development of automatic control strategies and electronic technologies, the microprocessors with online processing were used for the detection of wheel slip and torque adjustment [4]. The first developed wheel slip control methods are the re-adhesion controller. The conventional re-adhesion control methods use the wheel slip speed or acceleration criterions to detect wheel slip. The methods do not require exact information of the wheel-rail contact condition for wheel slip detection and compensation of poor adhesion [4]. However, such strategies do not stop the wheel slip formation but suppress it. Due to the requirements of the trains hauled by locomotives, more advanced wheel slip control strategies are developed. The methods aim to stabilise the wheel slip at the peak of the slip curve to establish the optimum utilisation of the adhesion characteristic. Although there is a vast amount of literature on both re-adhesion and wheel slip control strategies, there is still a need for further investigations.

1.1 Purpose of the thesis

The basic premises of this study are summarised as follows:

(i) Summarising a large number of published studies on the wheel slip, adhesion and slip control methods.

(ii) Reproducing a numerical model of the tram wheel roller rig in MATLAB environment that can be used for performance evaluation of the wheel slip control strategies.

(iii) Proposing algorithms to control the wheel slip mechanism and establishing optimum utilisation of adhesion.

(iv) Validation of reproduced numeric model.

(v) Verifying the functionality of proposed wheel slip control algorithms by either the validated numerical model or experimentally obtained results from the tram wheel roller rig.

(vi) Performance evaluation of the proposed wheel slip control algorithms with different speeds and control parameters.

2 THEORETICAL BACKGROUND

2.1 Adhesion Phenomenon

The coefficient of the adhesion is usually represented by the ratio of the traction force (T) and the normal force (N). The free body diagram of a driven wheel is presented in Figure 1, while the coefficient of the adhesion can be calculated using Eq. 1.

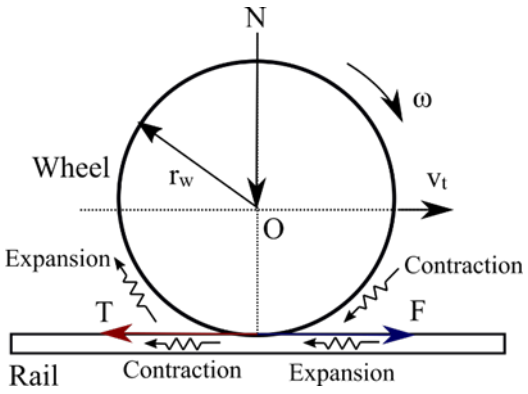

Figure 1. The forces and velocities acting on a driven wheel.

$$\mu = \frac{T}{N} \qquad \textit{Eq. 1}$$

where T is traction force, N is normal load force, and μ is the coefficient of adhesion. The loss of adhesion between wheel and rail can adversely influence the traction and braking effort of the vehicles. As it is mentioned below, poor adhesion causes wheel slip during the traction process and leads to the damage of wheel and rail [5]. Recently, various approaches have been proposed to outline the reasons for the loss of the adhesion [2], [6]–[9]. Overall, these studies show that the loss of adhesion may occur due to the presence of water (rain, snow, dew), oil, and leaf contaminants. Moreover, the temperature is another factor which influences the adhesion.

2.2 Slip Phenomena

The most common definition of the wheel slip in the railway area is the normalised difference of the angular and longitudinal velocities of the vehicle. The wheel slip occurs when the tractive effort of the vehicle exceeds the adhesion force, whereas sliding occurs when the braking force exceeds the adhesion force.

The adhesion is defined as a function of the slip at the contact point of the wheel and rail [10]. The slip velocity and relative slip (hereinafter is referred to as wheel slip) can be calculated using the Eq. 2 and Eq. 3 as given below.

$$w_s = \omega \cdot r_w - v_t \qquad \textit{Eq. 2}$$

$$s = \frac{\omega \cdot r_w - v_t}{v_t} \qquad \textit{Eq. 3}$$

where w_s is slip speed, v_t is the vehicle longitudinal speed, ω is the wheel rotational speed, r_w is wheel radius, and s is the wheel slip.

2.2.1 Problem formulation

A certain amount of wheel slip is required to transfer the tractive effort from the wheel to the rail. As it is illustrated in Figure 2, the slip curve has a nonlinear characteristic. The area on the left side of the peak of the slip curve is called adhesion zone while the one on the right side of the peak is the slip zone. The adhesion zone is stable, and adhesion proportionally increases with the wheel slip. On the other hand, the slip zone is nonstable part of the curve, and adhesion decreases when the wheel slip increases. Most of the wheel slip control methods aim to keep the slip in the stable part of the curve. While the main goals of the optimisation methods are to control the slip toward the peak of the curve where the maximum traction effort is achieved at [11]. Therefore, in this study, conventional and novel wheel slip control strategies are implemented to control the wheel slip toward the peak of the slip curve. The operation zone of the controllers is limited with the stable and the unstable parts of the slip curve near the maximum point [1].

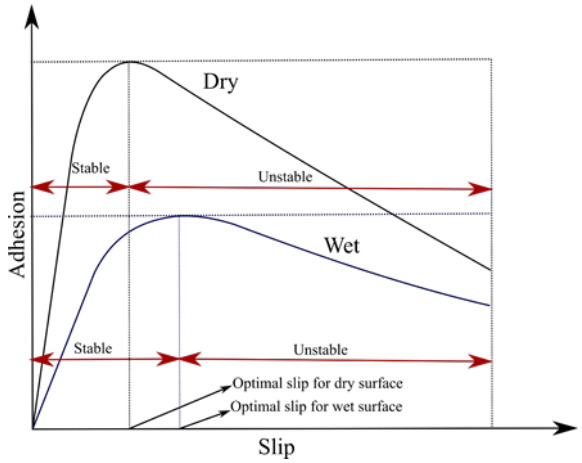

Figure 2. Slip-adhesion curve illustrating the characteristic of CoA under dry and wet contact conditions.

2.3 Wheel Slip Identification Methods

The most common wheel slip identification methods are summarised as follows:

- Current-based wheel slip detection of the all-wheel driving vehicle [12]
- Using the speed difference of driven and non-driven wheels [13].
- Method based time-frequency analysis [14]
- Linear, nonlinear and Kalman filters [15], [16].
- Nonlinear observers [17], [18].
- Using global positioning Systems (GPS) [19].
- Use of the optical-based sensor [20].

2.4 Wheel Slip Control Methods

Recently, various wheel slip control methods have been put forward to solve the issue of high slip between the wheel and rail. Pichlík [13] classified the wheel slip control method in two categories which are used for the electric multiple units (EMU) and the locomotives. According to Pichlík, the wheel slip control methods that are used in EMU aim to prevent the high value

of slip velocity; thus, these methods reduce the power loses and wear of the vehicle wheels and rails. The wheel slip control methods for locomotive aim to achieve maximum adhesion rather than preventing the wheel slip [13]. Kondo explains the reason for this classification due to axle loads of the EMU and locomotive [21]. Since the axle loads of the EMU is lower than the locomotive, the adhesive region is too narrow to control the adhesion at the peak of the slip curve precisely. The wheel slip control methods for EMU and locomotives are the main interest of this work. Therefore, the current work deals with wheel slip control algorithms in general. Frylmark and Johnsson have summarised the most common wheel slip control methods, as indicated in Figure 3 [11]:

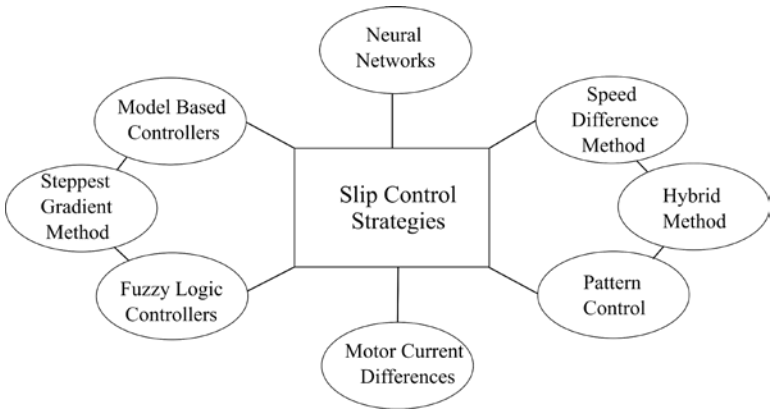

Figure 3. The wheel slip control strategies [11].

Besides the strategies mentioned above, angular acceleration-based control methods and PID (proportional, integral and derivative) control methods are some of the other control strategies used for the slip control. The basic principles of the mentioned methods are described in the following sections. The further details are available in the thesis.

3 METHODS AND METHODOLOGY

Performing on-track tests of railway vehicles are challenging, time-consuming and less cost effective. In keeping with the purpose of the study, the whole vehicle can be reduced to one powered bogie or a single wheelset [22]. Since the dynamics of the drive system are the main interest, a full-scale tram wheel roller rig is used for validation of the control algorithms. For experimental tests, the vehicle is replaced by a tram wheel that is connected to a permanent magnet synchronous motor with the rail being replaced by a roller connected to an asynchronous motor. These substitutions differ from the actual case. More detailed information about the replacements and their effects are presented by Voltr [23] and Gerlici et al. [24].

In this thesis, the performances of the wheel slip control algorithms are investigated using a full-scale tram wheel roller rig and its numerical model that is generated in MATLAB editor.

3.1 Experimental setup

The experiments are performed on the tram wheel roller rig, which was constructed by VÚKV (Výzkum, Vývoj a Zkušebnictví Kolejových Vozidel) and was renewed by the Faculty of Transport Engineering for further research. The tram wheel roller rig is composed of three main parts; a tram wheel, a roller, and a mainframe. The roller, which is manufactured from a railway wagon wheel, represents the rotating rail [25]. The roller is connected to the AM, which keeps the system at a constant speed by providing opposing torque. A schematic view and photos of the full-scale tram wheel roller rig are presented in Figure 4 and Figure 5, respectively. The details about the experimental test stand are provided in the thesis.

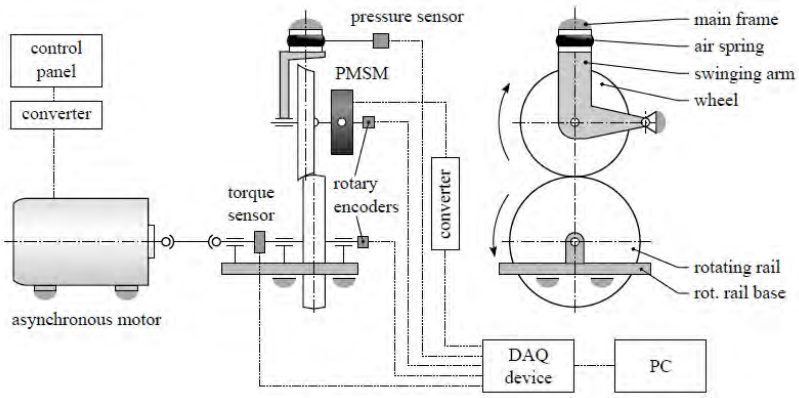

Figure 4. Schematic view of full-scale tram wheel roller rig measurement configuration [26].

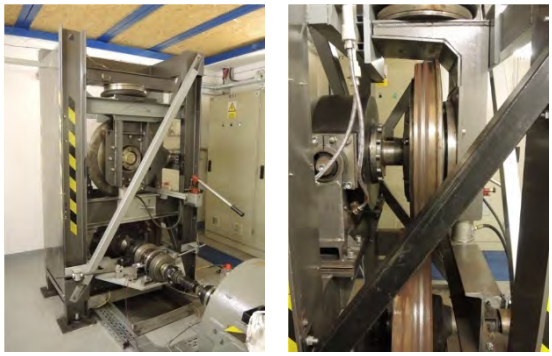

Figure 5. The full-scale tram wheel roller rig [22],[27].

3.2 The Numerical Model of Tram Wheel Roller Rig

In order to evaluate the performance of the developed wheel slip control methods, a numerical model representing the tram wheel roller rig has been generated in the MATLAB environment. The numerical model consists of five main components: the mechanical model of the torsional system, the dynamic model of the PMSM, dynamic model of the AM, the Freibauer/Polach adhesion force model, and the anti-slip control model. All the components of the numerical model are explained in detail in the thesis. The finite difference method is used for the calculation of the dynamic equations. The step time of integration is selected as $20\ \mu s$ to guarantee the accuracy of the calculations. However, the control action of the anti-slip control model is limited to the period of $0.04\ ms$ to simulate the control action of the controller in the real tram wheel roller rig. The complete structure of the developed numerical model tram wheel roller rig is depicted in Figure 6.

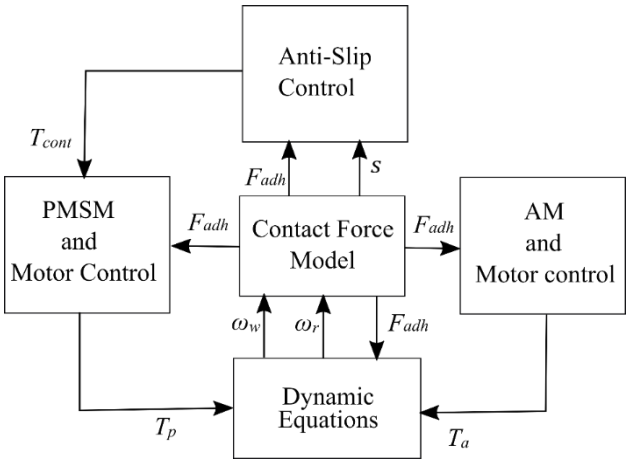

Figure 6. Complete structure of developed numerical model of tram wheel roller rig.

4 DEVELOPED WHEEL SLIP CONTROL METHODS

4.1 Wheel slip control based on a Single Treshold

The wheel slip control based on a single threshold (WSCST) is a conventional method. The principle of the method is illustrated graphically in Figure 7. The actual value of wheel slip is compared with a constant threshold value. If actual wheel slip exceeds the threshold value, the controller regulates the applied torque according to Eq.4. The block diagram of the controller is depicted in Figure 8. The output of the torque regulator is limited to prevent excessive torque increase. The output torque request of the limiter is compared with the driver torque request. The smaller torque request is selected as control torque.

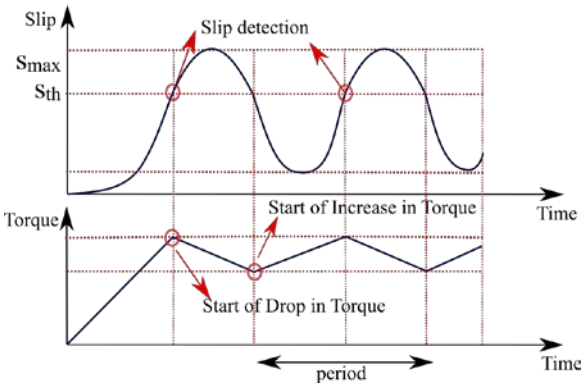

Figure 7. Wheel slip detection and torque regulation for WSCST.

$$T^*_{ref} = \begin{cases} T_{cont}\,(1 - \frac{dt}{A_{dec}}), & s_{act} \geq s_{th} \\ T_{cont}\,(1 + \frac{dt}{A_{inc}}), & s_{act} < s_{th} \end{cases} \qquad \textit{Eq. 4}$$

where T_{ref}^* is the reference torque output of the controller, T_{cont} is the final output torque request, dt is the resolution time of speed sensor, A_{dec} is the control parameter which determines the deceleration rate of torque, A_{inc} is the control parameter which determines the increment rate of the torque, s_{th} is the slip threshold value, and s_{act} is the actual wheel slip occurs between the wheel and the roller.

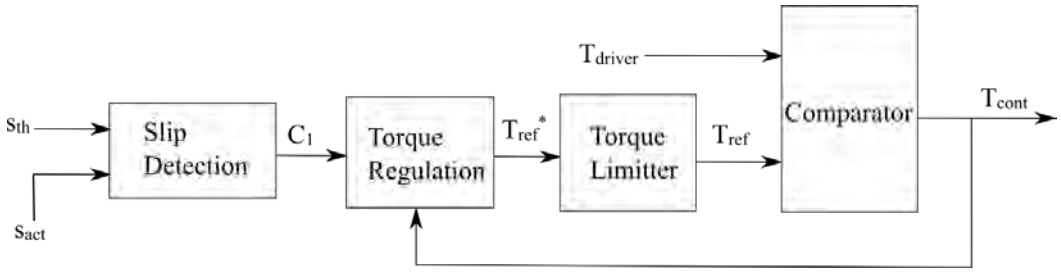

Figure 8. Block diagram of WSCST.

3.2 Wheel Slip Control Based on Multiple Thresholds

Wheel slip control based on multiple thresholds (WSCMT) is an improved version of the abovementioned method (WSCST). To prevent extreme torque drop and increase, two threshold values are employed. Both threshold values are assigned in the stable part of the slip curve. The control action of the developed control is illustrated graphically in Figure 9. The torque regulation of the motor is provided by Eq. 5. The WSCMT is expected to provide less wheel slip and better adhesion utilisation than the WSCST.

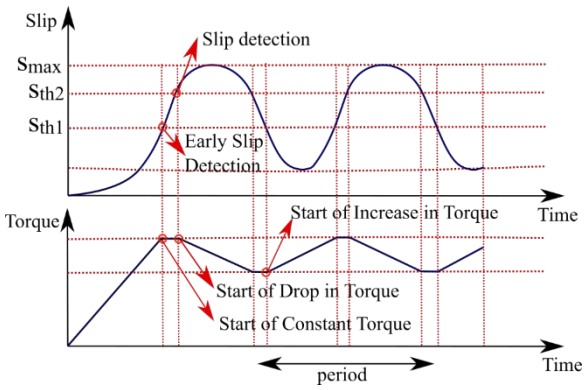

Figure 9. Wheel slip detection and torque regulation with multiple threshold values.

$$T_{ref}^{*} = \begin{cases} T_{cont}\,(1-\frac{dt}{A_{dec}}), & s_{act} \geq s_{th2} \\ T_{cont}\,, & s_{th1} \leq s_{act} \leq s_{th2} \\ T_{cont}\,(1+\frac{dt}{A_{inc}}), & s_{act} < s_{th1} \end{cases} \qquad Eq.5$$

where s_{th1} is the first threshold value, and s_{th2} is the second threshold value.

4.3 Wheel Slip Control Based on Angular Acceleration of Wheel

The wheel slip control based on the angular acceleration of wheel (WSCAA) is a conventional method. It is based on the principle that the angular acceleration of a vehicle wheel, provided that it rolls without slip, is equal to linear acceleration of the vehicle divided by the wheel radius. The acceleration of the vehicle is limited by the inertia of the vehicle and the traction force. If the wheel shows higher angular acceleration than what corresponds to this limit, it means that it accelerates independently of the vehicle motion – in other words, it slips.

The control action WSCAA is summarised in Figure 10. The wheel slip is detected through comparison of actual angular acceleration and the threshold value of the acceleration. When the actual value of acceleration exceeds the threshold value, the controller reduces toque request according to Eq.6 until it becomes lower than the threshold. Then,

the torque request rises again. The action of the controller takes place periodically until the bad contact conditions disappear.

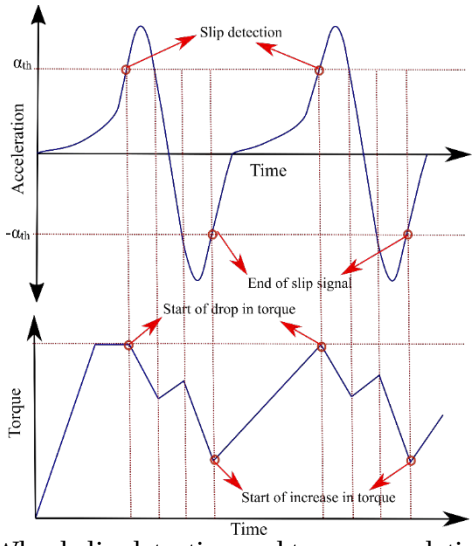

Figure 10. Wheel slip detection and torque regulation of WSCAA

$$T^*_{ref} = \begin{cases} T_{cont}\,(1 - \frac{dt}{A_{dec}}), & \alpha_{act} \geq \alpha_{th} \,||\, \alpha_{act} \leq -\alpha_{th} \\ T_{cont}\,(1 + \frac{dt}{A_{inc}}), & \alpha_{act} < \alpha_{th} \,||\, \alpha_{act} \geq -\alpha_{th} \end{cases} \qquad \text{Eq. 6}$$

where α_{act} is the actual angular acceleration of the wheel and α_{th} is the threshold value of angular acceleration for the wheel slip detection.

4.4 PI Wheel Slip Control

The PI control strategy is widely used for industrial applications. The PI controller can be used for the rail vehicles to control wheel slip and improve their traction performance. For effective control, a reference slip value that is close to the peak of the slip curve can be chosen as a control signal. It is also essential that the selected reference wheel slip value is on the stable side of the slip curve.

The discrete time form of a PI controller is expressed as in Eq. 7.

$$u(k) = u(k-1) + K_p\big(e(k) - e(k-1)\big) + K_i e(k) \qquad \textit{Eq. 7}$$

where u is the output torque of the controller, K_p is the proportional gain of the controller, K_i is the integral gain of the controller, k is the iterative step, e is the error between the actual wheel slip and desired wheel slip. The error is calculated, as shown in Eq. 8.

$$e(k) = s_d - s_{act}(k) \qquad \textit{Eq. 8}$$

where s_d is the desired wheel slip value, and s_{act} is the actual wheel slip value.

The block diagram of the PI wheel slip control method (PI-WSC) is provided in Figure 11. The difference between the desired wheel slip and actual wheel slip (error) is calculated first and then sent to the PI torque regulator as an input signal. The PI torque controller regulates the torque applied to wheel according to the error signal.

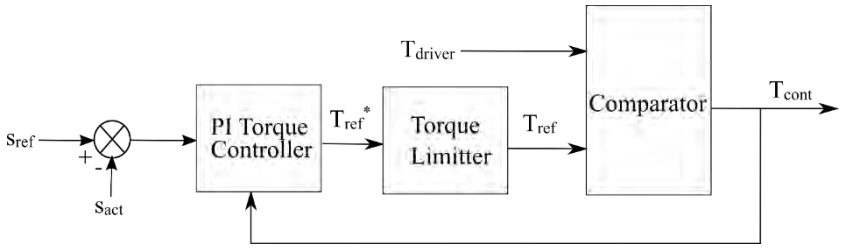

Figure 11. Block diagram for PI-WSC.

4.5 Sliding Mode Wheel Slip Control

The sliding mode controller (SMC) has been widely-studied for vehicle control systems because of certain advantages [33]–[35]. The controller is an attractive robust control method with effective properties to stabilise nonlinear and uncertain systems. The controller keeps the systems insensitive to uncertainties on a sliding surface. Moreover, the SMC has good and rapid transient performance [36].

The sliding mode wheel slip controller (SM-WSC) is designed in two steps. In the first step, the sliding surface is defined to obtain specific desired characteristics along the sliding surface trajectories. Next, the controller is designed to lead the system to the desired system trajectories within a finite time.

The sliding surface *S(t)* for the design of the adaptive sliding mode torque control systems is defined as follows:

$$S(t) = s - s_d \qquad \textit{Eq. 9}$$

The main objective of Eq. 9 is to track the desired wheel slip ratio (s_d) that is given as an input to the system, based on experience from previous experimental measurements. In order to satisfy the reachability conditions directing the system trajectories toward a sliding surface where they remain, the derivative of the sliding surface is selected as Eq. 10 [37], [38]:

$$\dot{S} = -DS - K \cdot sgn(S) = -D(s - s_d) - K \cdot sgn(s - s_d) \qquad \textit{Eq. 10}$$

where the proportional term-DS forces the system state to approach the sliding surface faster when the sliding surface has a significant value [33]. The parameters D and K are positive definite design parameters. D determines the convergence rate of the tracking error, while K is adjusted in compliance with the number of uncertainties and the disturbance in the system.

The sgn function in Eq. 10 results in a chattering issue because of undesired noise and delays in the actuator. For this reason, the sgn function is replaced with a saturation function [39]. Nevertheless, a lowpass filter is implemented to overcome the high-frequency chattering problem in the system, which is basically to stabilise the algorithm.

The sliding mode control law is designed in the following steps, according to Eq. 10.

The wheel slip dynamics during acceleration obtained by taking the time derivative of Eq.3.

$$\dot{s} = r_w \frac{\dot{\omega_w}}{r_r |\omega_r|} - r_w \frac{\omega_w |\dot{\omega_r}|}{r_r \omega_r^2} \qquad \textit{Eq. 11}$$

The relationship between the wheel slip dynamic and forces at the contact point is shown in Eq. *11*.

$$\dot{s} = r_w \frac{-T_w - r_w F_{adh}}{J_w r_r |\omega_r|} - r_w \frac{\omega_w |\dot{\omega_r}|}{r_r \omega_r^2} + d \qquad \textit{Eq. 12}$$

where d is disturbance due to vibration in the system, driving resistances and parameter uncertainties.

By taking the time difference of the sliding surface in Eq. 9, and substituting Eq. 10 and Eq. 12, the following sliding law control torque can be achieved:

$$T_{p,con} = -r_w F_{adh} - \frac{J_w \omega_w |\dot{\omega_r}|}{|\omega_r|} - \frac{J_w r_r |\omega_r| (-D(s - s_d) - K \cdot sgn(s - s_d))}{r_w} - \frac{J_w r_r |\omega_r| \dot{s_d}}{r_w} \qquad \textit{Eq. 13}$$

Since the time derivative of s_d constant is zero and the acceleration value of the roller is neglected for the tram wheel roller rig, the sliding mode control law torque is modified to the following equation:

$$T_{p,con} = -r_w F_{adh} - \frac{J_w r_r |\omega_r| D(s - s_d)}{r_w} - \frac{J_w r_r |\omega_r| K \cdot sgn(s - s_d)}{r_w} \qquad \textit{Eq. 14}$$

Asymptotical stability of the sliding mode control law can be proven for closed-loop control by employing a Lyapunov function [33], [39].

5 RESULTS AND DISCUSSION

5.1 Validation of Numerical Model

In order to use the developed numerical model of the tram wheel roller rig for the performance evaluation of the implemented wheel slip control strategies, the validity of the model has to be proven. Hence, the numerical model is tested without any wheel slip controller. Figure 12 shows the comparison of the simulation and experimental results carried out under water contaminated conditions. The tests are performed for the same PMSM torque request (Figure 12(a)). The resultant wheel slips are in good agreement which can be seen in Figure 12(b). Besides, the slip curves of simulation and experiment are presented in Figure 12(c). The slender clockwise loops observed in experiment results are closely simulated by the numeric model. Furthermore, slight differences between the simulation and experimental wheel speed results are displayed in Figure 12(d).

Even though the simulated performance characterised the experimental response satisfactorily, differences established between experimental and numerical results (Figure 12). The pre-assumed simplifications in the model which does not include all mechanical details and imperfections of the real experimental device and testing conditions yield the first group of factors causing mentioned differences. Other factors are related to the measurement procedure including parasitic signals (mainly electromagnetic noise), resolution of sensors, as well as processing the simulation results – filtering which impacts the signals particularly when wheel slip is suddenly terminated.

Despite the effects of mentioned factors, it is seen that the results obtained from the developed numerical model are consistent with the experimental results. This fact proves the validity of the developed numerical model.

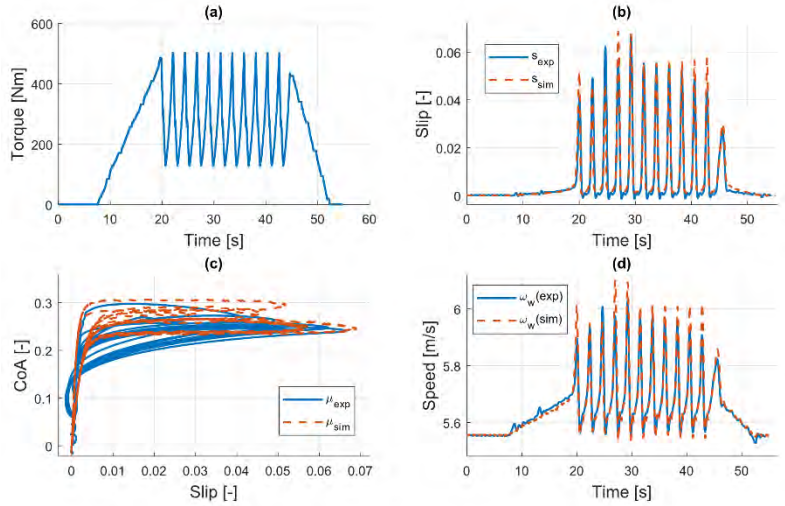

Figure 12. The comparison of the simulation and experimental results.

5.2 Simulation Results

The step time of the integrations is selected as *20 μs* to guarantee the accuracy of calculations. However, the control action of the anti-slip control models is limited to the period of *0.04 ms* to simulate the control action of the controller in the real tram wheel roller rig. The initial peripheral speed of the roller is selected as *5.56 m/s*, which corresponds to *20 km/h* for a tram vehicle, in the simulations. To be able to observe wheel slip in low torque value, the normal force is assigned relatively small. Hence, the normal force is provided to the simulation as an average value of *4250 N*.

5.2.1 Wheel Slip Control Based on a Single Threshold

The initial test for WSCST is carried out under the assumption of continuous water contaminated test conditions. The control parameters are selected as; $s_{th}=0.01$, $A_{inc}=1$ and $A_{dec}=0.5$. The minimum torque (T_{min}) generated by the WSCST controller is set as *15%* of the nominal torque of PMSM. It is assumed that the water is continuously supplied to the contact area. The simulation results are illustrated in Figure 13. It can be seen in Figure 13(c), wheel slip is controlled cyclically. However, the amplitude and the frequency of the cycles are not constant due to the nonlinearity, and numerical errors. The response of the controller is sufficient since the maximum wheel slip ever to occur is merely *7.4%.*

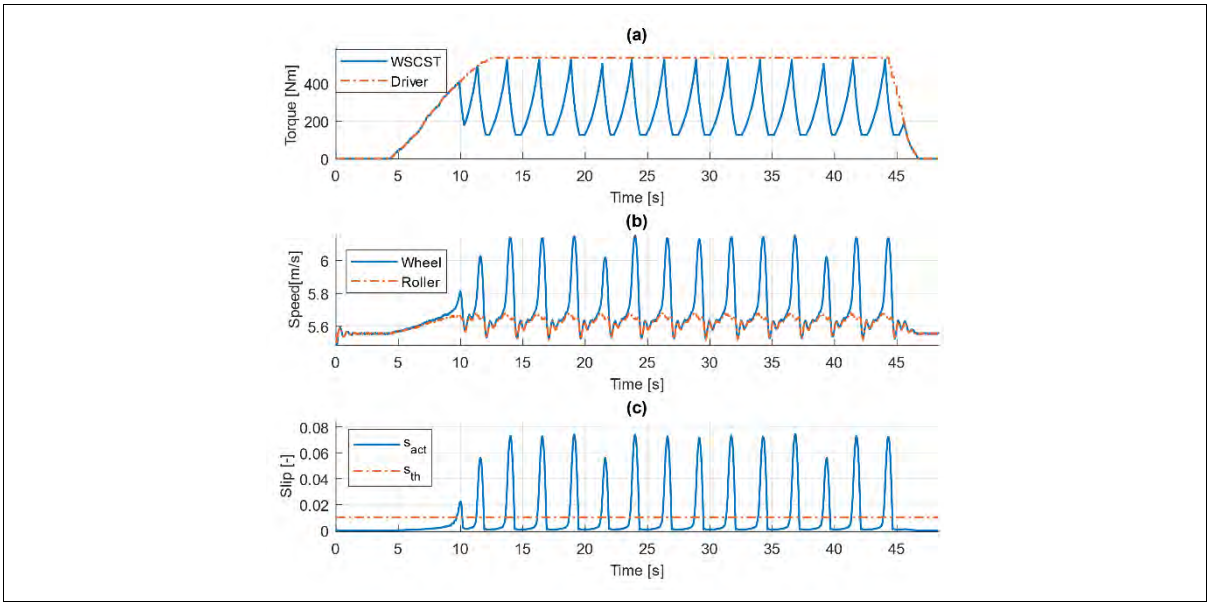

Figure 13. Simulation result of WSCST performed under the assumption of water contaminated test condition.

The second simulation is carried out to investigate the performance of WSCST under the assumption of steady grease contaminated test condition. The control parameters are set as; $s_{th}=0.015$, $A_{inc}=2$ and $A_{dec}=1$. T_{min} is selected 1% of the nominal torque of PMSM. The results are presented in Figure 29 of the thesis. Similar to the previous simulation, the wheel slip is controlled cyclically. The dynamic behaviour (non-periodic response, irregular cycles, i.e.) of the wheel slip observed are caused by the uncertainties and numerical errors. The WSCST achieves a successful control within *4.1%* maximum wheel slip.

5.2.2 Wheel Slip Control Based on Multiple Thresholds

The performance of the controller is initially tested under the assumption of the continuous water existing between the wheel and roller. The control parameters are set as; $s_{th2}=0.006$, $s_{th1}=0.008$, $A_{inc}=4$ and $A_{dec}=1$. The minimum torque (T_{min}) generated by the WSCMT is set as *15%* of the nominal torque of PMSM. When Figure 14(c) is analysed, it can be seen that the maximum wheel slip of *2.3%* is observed during the simulation. Moreover, it is found in Figure 14 (a) that the minimum torque the output of WSCMT is *224 N.m*. Overall, the controller provides an improvement in the traction characteristic of the wheel.

The performance of the controller is tested under the assumption of steady grease contaminant existing between the wheel and the roller. The results are presented in Figure 31 of the thesis. Maximum wheel slip of *4%* occurs. When the output of the controller is examined, it is noticed that the minimum torque is *62 N.m*. From the results, it is possible to claim that the controller prevents the wheel from the severe slip effectively. Furthermore, the controller reduces the amount of torque drop slightly.

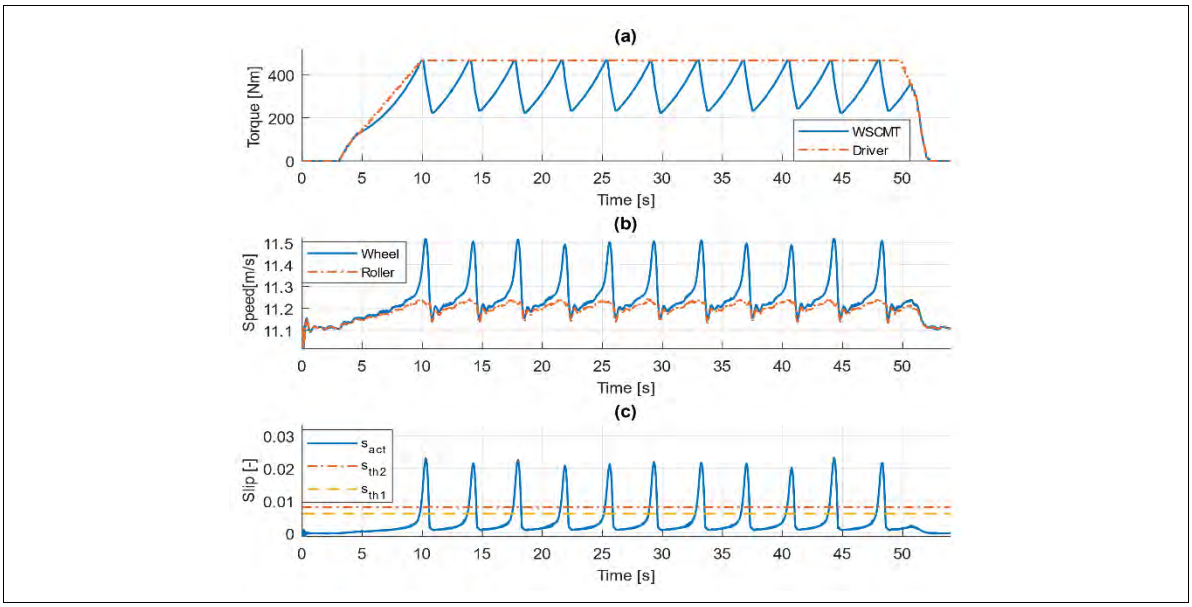

Figure 14. Simulation result of WSCMT performed under the assumption of water contaminated test condition.

5.2.3 Wheel Slip Control Based on Angular Acceleration of Wheel

To confirm the operation verification of the WSCAA method, we conduct the first simulation under the assumption of water contaminated test condition. The control parameters are selected as; $\alpha_{th}=1$, $A_{inc}=1$ and $A_{dec}=0.5$. The simulation is conducted for two different cases of wheel-roller surface conditions which are half-dry and wet. The resultant wheel slip is depicted in Figure 15(b). During the first cycle, the wheel slip raises to *8.6%* on the other hand, in the next cycles, the peaks of the wheel slip are noticed around *5.9%.* The results have proved that WSCAA can avoid severe wheel slip when the sudden changes occur in adhesion condition.

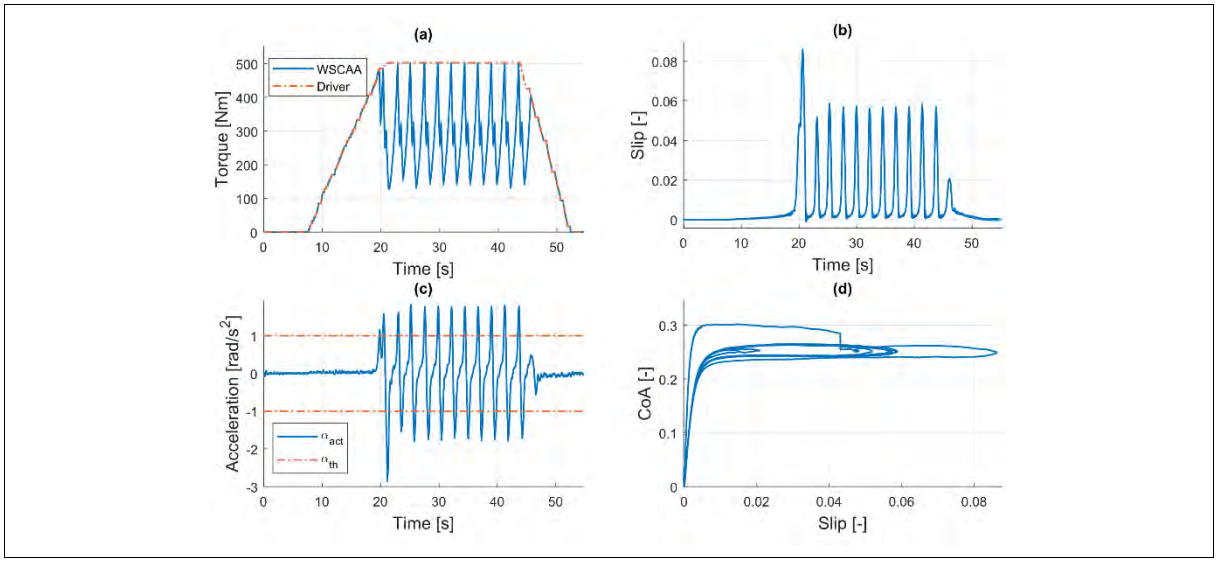

Figure 15. Simulation result of WSCAA performed under the assumption of water contaminated test condition.

Another simulation is carried out under the assumption of grease contaminated test condition. The results are depicted in Figure 33 of the thesis. It is noticed that during the first cycle; the wheel slip raises to *9.9%*. In the next cycles, the peaks are observed at *7%*. It is seen that the WSCAA provides a successful wheel slip control during the low adhesion condition.

5.2.4 PI Wheel Slip Control

The initial test is conducted under the assumption of the continuous water contaminant existing between the wheel and roller. The control parameters are set as; $s_d=0.01$, $K_p=500$ and $K_i=2000$. The response of the controller is presented in Figure 16. The desired wheel slip ($s_d=0.01$) is reached successfully, as illustrated in Figure 16(b). Moreover, the desired wheel slip corresponds to the peak of the slip curve, as depicted in Figure 16(c). When the path of the wheel slip is analysed, no significant overshoot is observed.

The second simulation is carried out to test the reaction of the PI-WSC method toward the sudden change of the friction condition. The presented results (see Figure 35 for further information in the thesis) show that the controller stabilises the wheel slip at *1%* in a short time. Because of the sudden change of the friction condition, the wheel slip increases up to *11.5%.*

The last simulation is conducted with the assumption of the steady grease contaminated test conditions. It is observed that the controller effectively stabilises the wheel slip at the desired level with a slight overshoot. Furthermore, the desired level corresponds to the peak of the slip curve. The results are presented in Figure 36 of the thesis.

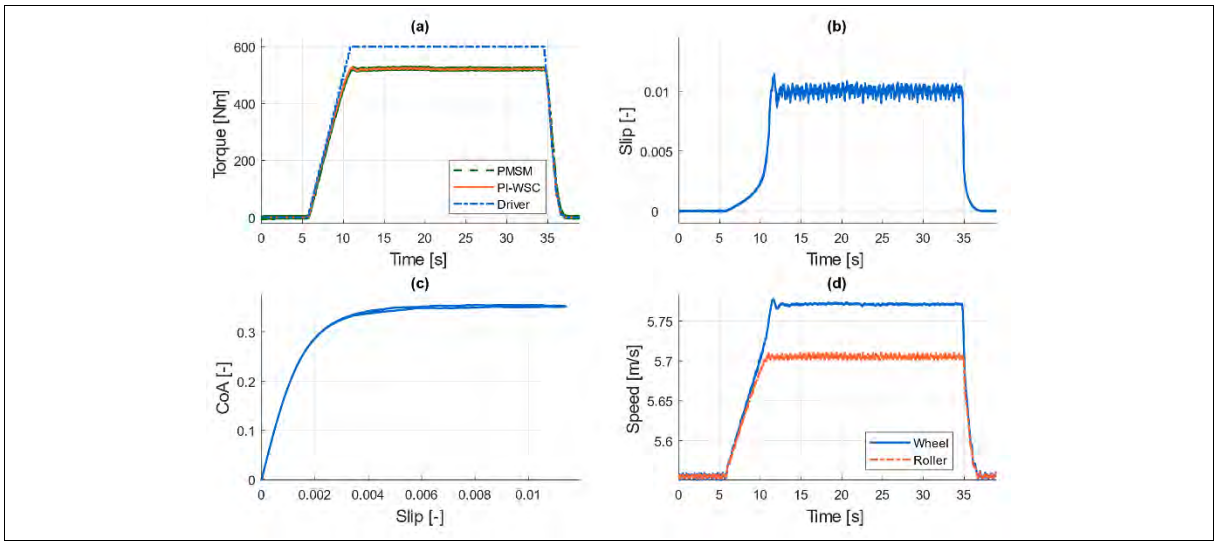

Figure 16. Simulation results of PI-WSC performed under the assumption of water contaminated test condition.

5.2.5 Sliding Mode Wheel Slip Control

To verify the effectiveness of the developed control method, we performed the initial tests using the validated numeric model. The following values are selected for the control parameters; *D=10, K=1 and* $s_d=0.02$.

The simulation results of SM-WSC performed under the assumption of water contaminated test condition can be seen in Figure 17. Two phases of the adhesion scenario are selected for the simulation of water contamination (Half-dry and wet). The controller effectively stabilises the wheel slip at *2%,* as seen in Figure 17(b). The maximum overshoot displayed in the wheel slip is about *5.1%,* which has a relatively low value. Moreover, the indicated results demonstrate the effective performance of the proposed strategy since the wheel slip is stabilised almost at the peak of the slip curve (see Figure 17c).

Similar performances observed for the simulation which is carried out under the assumption of steady grease contaminant. The results are available in Figure 38 of the thesis. The presented results confirm the functionality of the controller.

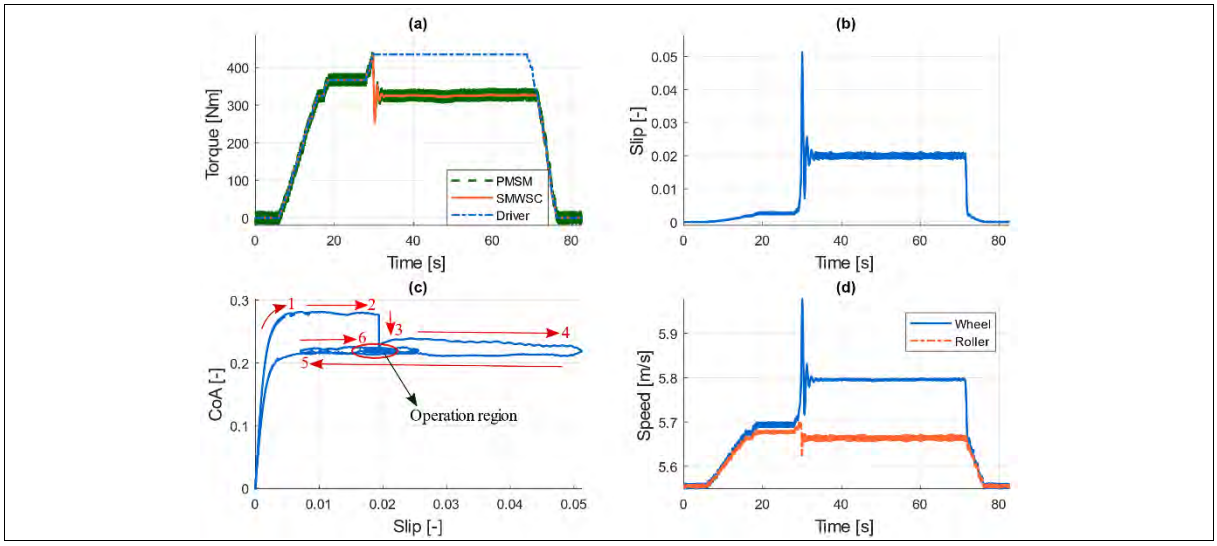

Figure 17. Simulation results of SM-WSC performed under the assumption of water contaminated test condition.

5.3 Experimental Results

The sampling rate of data logger that is connected to the test stand is *200 Hz*. However, the control action of the anti-slip algorithm is limited with *25 Hz* to gain time for data processing. The initial peripheral speed of the roller is selected as *5.56 m/s*, which corresponds to *20 km/h* for a tram vehicle. The air spring provides no air pressure to obtain the higher wheel slip with lower traction torque. On the other hand, the average of the normal force is measured as *4250 N*, due to self-weights of the wheel, air spring and swinging arm.

5.3.1 Wheel Slip Control Based on a Single Threshold

Figure 18 shows the experimental results of WSCST performed under water contaminated test condition. The resultant wheel slip is provided in Figure 18(c). The controller prevents the severe wheel slip effectively where maximum wheel slip of *8.1%* is seen.

The experimental test results of WSCST under the steady grease contaminated test condition are presented in Figure 40 of the thesis. The results are quite similar to findings under the water contaminated condition. The wheel slip is suppressed successfully with a maximum of *4%*.

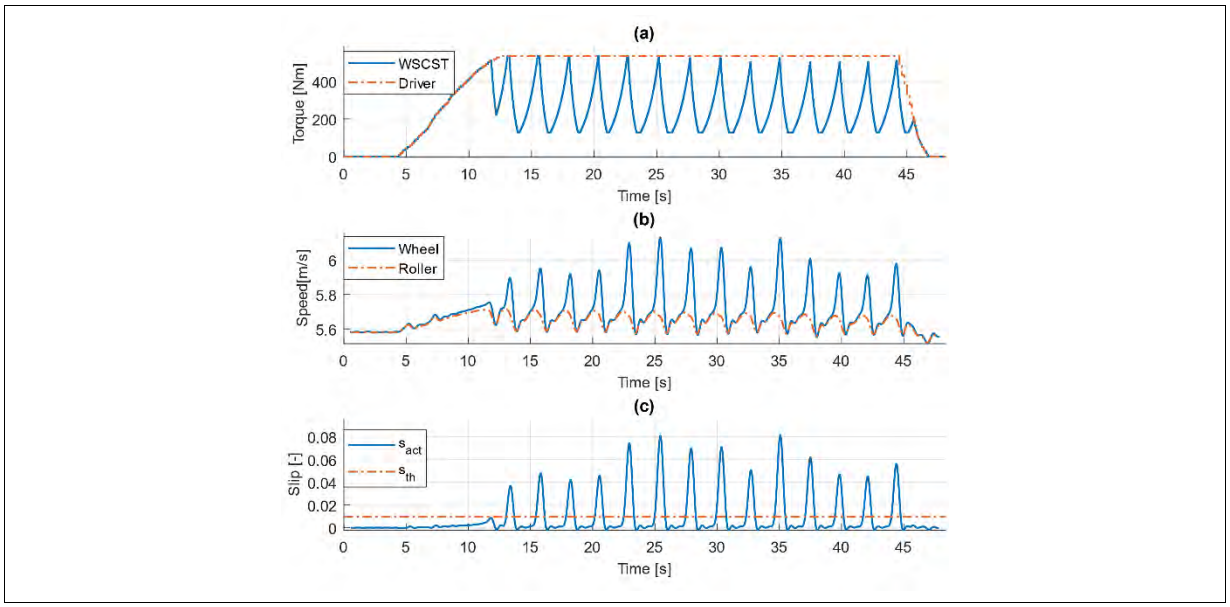

Figure 18. Experimental result of WSCST performed under water contaminated test condition.

5.3.2 Wheel Slip Control Based on Multiple Thresholds

The performance of the WSCMT is verified with the help of the experimental tram wheel roller rig. The initial roller speed is set as *11.2 m/s* that approximately corresponds to *40 km/h* for a tram vehicle.

Figure 19 shows the response of the WSCMT carried out under the continuous water contaminated test condition. The proposed algorithm appears to deliver a satisfactory performance since the strategy provides a cyclic control of wheel slip where the peaks are noticed between *1.3-2%.* Besides, the controller prevents the wheel from the excessive torque drops, which reduce traction performance.

The results of the experiment which are conducted under the steady grease contaminated test condition are provided in Figure 42 of the thesis. When the presented results are analysed, the controller suppresses the severe wheel slip effectively since the peaks of the cycles are found to be around *4.4%.*

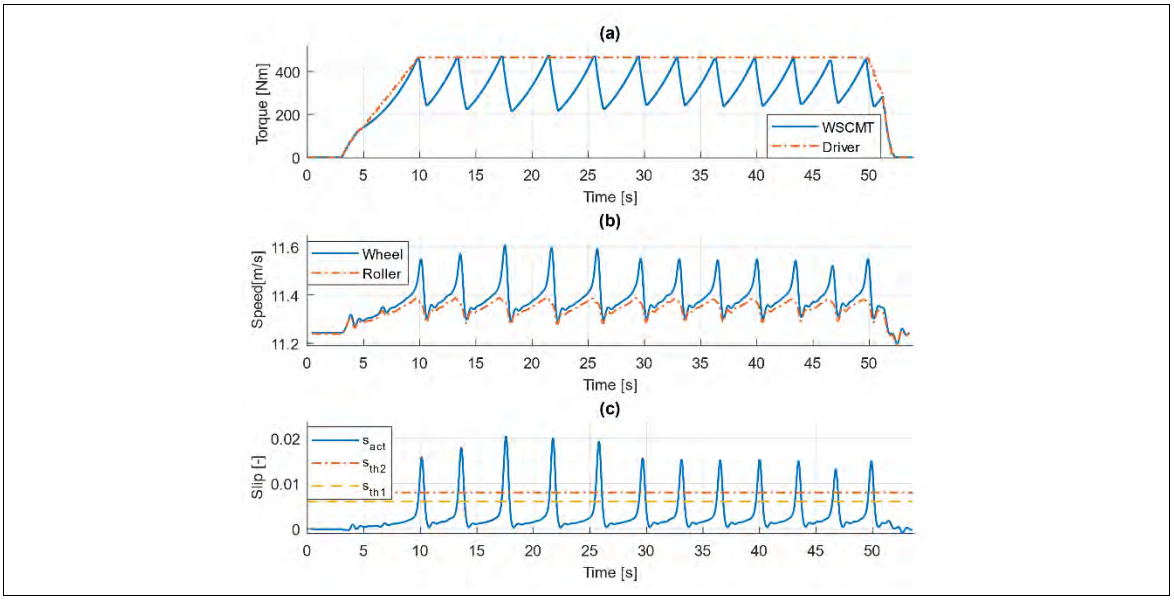

Figure 19. The experiment result of WSCMT performed under water contaminated test condition.

5.3.3 Wheel Slip Control Based on Angular Acceleration of Wheel

To confirm the operation of the WSCAA, we conducted the first experimental test under water contaminated test condition (half-dry and wet). The wheel slip control performance of WSCAA is depicted in Figure 20(b). During the first five cycles of the control process, the magnitude of the peak of the wheel slip tends to increase while the magnitude of the peak of wheel slip reduces gradually in the subsequent cycles. A maximum wheel slip of *6.7%* is observed during the test.

Similar performances are observed for the steady grease contaminated wheel-roller surface conditions which are presented in Figure 46 of the thesis. Due to the system delay, a sudden wheel slip occurs at the first cycle, and then, the controller reduces the wheel slip to lower values in the next cycles. The peaks of the wheel slip cycles are observed around *5.9%.*

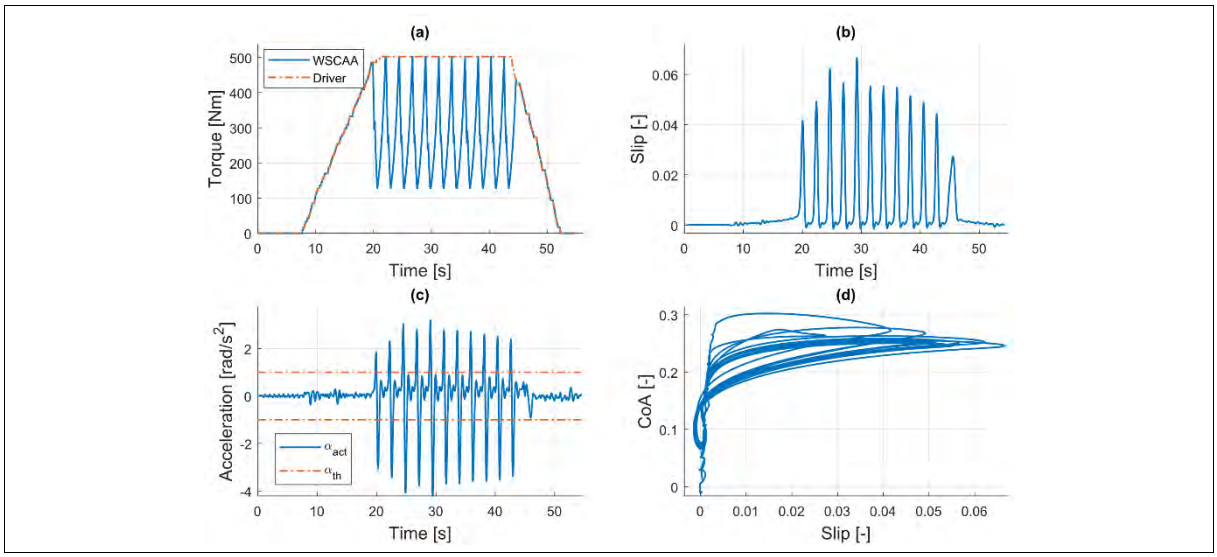

Figure 20. Experimental result of WSCAA performed under water contaminated test condition.

5.3.4 PI Wheel Slip Control

The operation of the PI-WSC is verified initially under the continuous water contaminated test conditions. The controller stabilises the desired wheel slip, as given in Figure 21(b). Closer inspection to Figure 21(c) shows that the controller operates at the peak of the slip curve. Surprisingly, a constant difference between the wheel and roller speeds is observed in Figure 21(d), even at free rolling. This difference causes an offset in the calculated wheel slip value.

Another experimental test is carried out to examine the dynamic response of the controller to the sudden decrease in the friction condition (half-dry to wet). The results are provided in Figure 48 of the thesis. The controller provides a successful control since the recovery from the unstable side of the slip curve to the stable side of the slip curve takes in an instant. The PI-WSC stabilises the wheel slip at *1%* (for both conditions of adhesion) which corresponds to the peak of the slip curve for the water contaminated test condition.

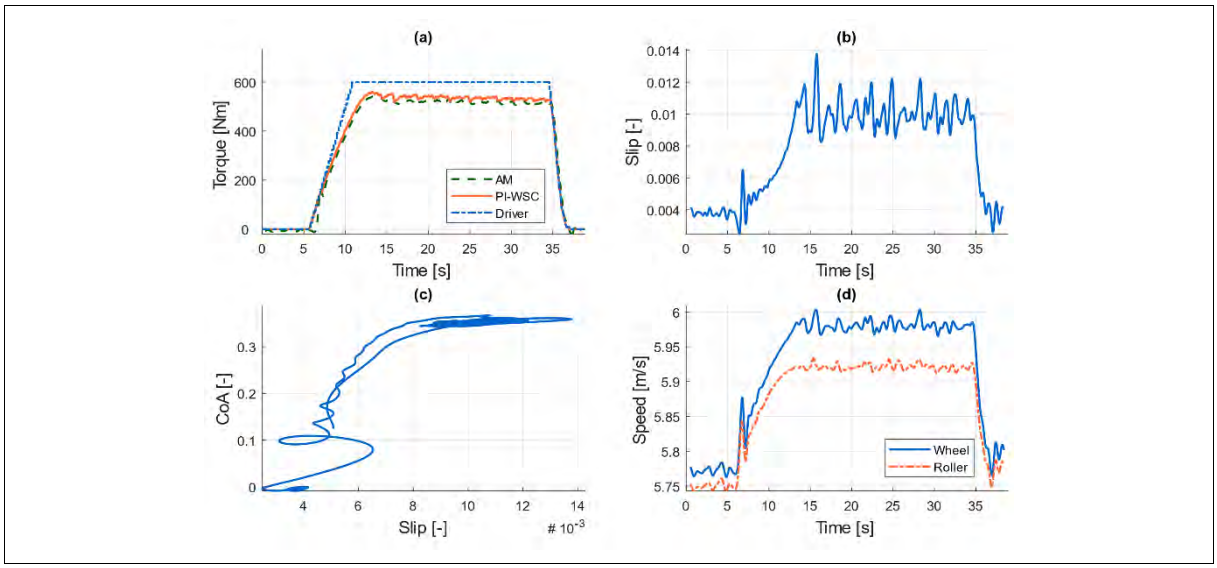

Figure 21. Experimental results of PI-WSC performed under water contaminated test condition.

5.3.5 Sliding Mode Wheel Slip Control

The experimental results of the proposed algorithm performed under water contaminated wheel-roller surface conditions are presented in depth in Figure 22. The resultant wheel slip is provided in Figure 22(b). The SM-WSC is activated right after the wheel slip value reaches beyond the desired amount (*2%*). The controller reduces the motor torque, as indicated in Figure 22(a), and the wheel slip is stabilised at *2%.* A maximum wheel slip of *7%* is observed during this test.

The performance of the controller under the steady grease contaminated test condition is very effective where the wheel slip on *2%* level is successfully established, as indicated in Figure 50 of the thesis. Moreover, it is seen that *2%* of wheel slip corresponds to a point where the maximum adhesion is seen.

One of the interesting results is observed during the test with grease and water&grease contaminated conditions. When the water is sprayed on to the grease contaminated surface, the available adhesion drops severely. Furthermore, the water particles removed from the contact surface when the application of water is stopped. It is seen that the SM-WSC stabilises the wheel slip at *2%* within all case of the adhesion conditions. Here, it must be noted that *2%* of the wheel slip corresponds to the point where the peaks of the slip curves are observed. Hence, the controller achieves the maximum utilisation of the adhesion in all cases. The test results are available in Figure 51 of the thesis.

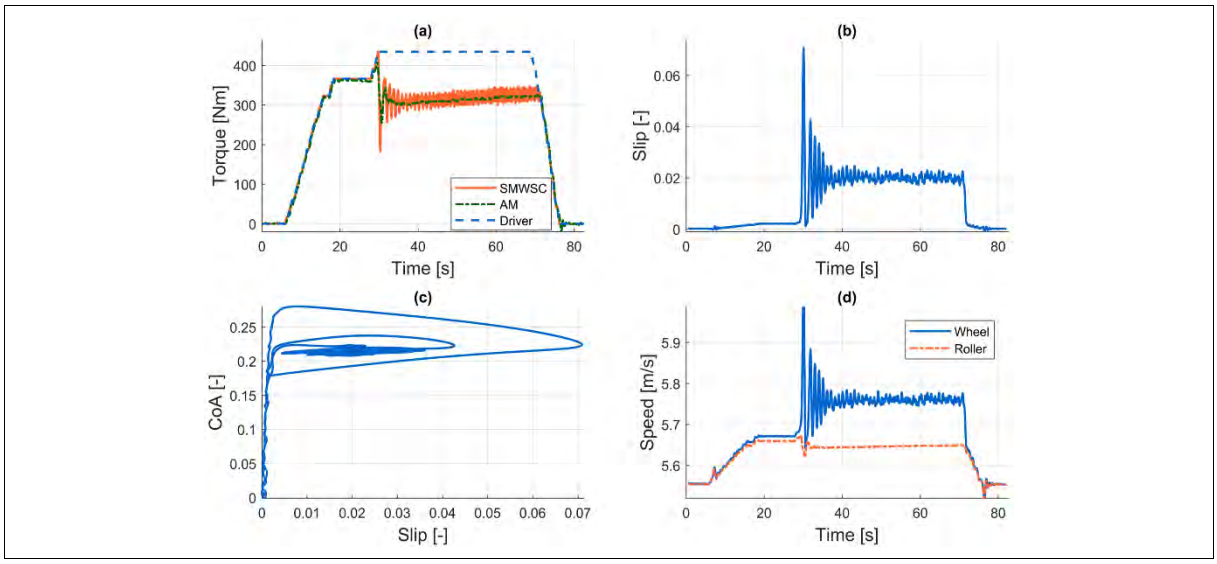

Figure 22. Experimental results of SM-WSC performed under water contaminated test condition.

5.4 Analysis of Results

The performances of the control methods are evaluated via experiments on a roller rig and simulations on its numerical model. The conditions of the simulations and experiments are employed identically to provide a comparative discussion.

When the simulation and experimental results for each method under the same test conditions are compared, it is obvious that both results are in good agreement.

Moreover, it is observed that the WSCST and WSCMT suppress the wheel slip slightly better than the WSCAA. On the other hand, the experimental tests summarised in Table 7 of the thesis show that WSCAA improves traction performance better than the WSCST and WSCMT. Consequently, the WSCAA strategy is primarily recommended to be used on EMUs due to its advantages (see section 4.3 of the thesis) over the other methods.

The performance evaluation of control strategies with different roller speeds, threshold values, deceleration rates and increment rates are conducted through the validated numerical model. Findings from the validated numerical model for the re-adhesion methods can be summarised as depicted in Table 1:

Table 1: Effect of increasing the control parameter on wheel slip

	WSCST	**WSCMT**	**WSCAA**
s_{th} / α_{th}	Increase	Increase	Increase
v_r	Decrease	Decrease	Decrease
A_{dec}	Increase	Increase	Increase
A_{inc}	Decrease	Decrease	Decrease

The assignment of threshold values (s_{th} and α_t) is very critical for the control process. When it is set higher, severe wheel slip is observed while lower values caused insufficient adhesion utilisation. Furthermore, A_{dec} is a vital control parameter which directly affects the convergence rate of the actual wheel slip. Selecting a high value for A_{dec} results in an excessive drop in the motor torque. If A_{dec} is set to a low entity, the wheel slip reaches very high levels. The control

parameter A_{inc} determines the torque increase rate of the controller. Adjustment a small value for A_{inc} causes a slow torque recovery; nevertheless, selecting a higher value results in unstable wheel slip control.

The impact of each parameter on the control behaviour the PI-WSC and SM-WSC are summarised as follows:

PI-WSC method:

- The controller exhibits good wheel slip tracking performance with all roller speeds and all contact conditions. However, low amplitude vibrations are noticed at lower roller speeds.
- The controller provides successful performance under the water and grease contaminated test conditions when the desired wheel slip is set on the stable part of the slip curve. On the other hand, adjustment of the desired wheel slip to the unstable part of the slip curve brings the risk of control quality deterioration.
- Higher overshoot is observed with the lower proportional gain parameter (K_p) independent from the contact conditions. Moreover, the controller is capable of stabilising the wheel slip under grease contaminated case for lower K_p
- The integral gain parameter (K_i) influences the rise time to the desired set point. When K_i sets to a lower value, the higher rise time is observed.

SM-WSC method:

- The wheel slip overshoot increases slightly at higher roller speeds; however, the amplitude of vibrations reduces.
- The controller is able to stabilise wheel slip even on the unstable part of the slip curve.
- The convergence rate parameter (D) influences the damping of the wheel slip. The higher value of the convergence rate parameter causes higher overshoot and longer settling time.
- The uncertainties parameter (K) has no significant influence on the results.

The presented results show that both controllers are able to stabilise the wheel slip effectively when the desired wheel slip is set on the stable part of the slip curve. However, the performance of the PI-WSC deteriorates when the desired wheel slip is set on the unstable part of the slip curve. On the other hand, SM-WSC is able to stabilise wheel slip even on the unstable part. Hence, the application of the SM-WSC on electric locomotives is advised.

6 CONCLUSION

The work presented in the thesis is aimed to determine effective and viable solutions to wheel slip problem. Hence, Five wheel slip control strategies -wheel slip control based on single threshold (WSCST), wheel slip control based on multiple thresholds (WSCMT), wheel slip control based on angular acceleration of wheel (WSCAA), PI wheel slip control (PI-WSC), and sliding mode wheel slip control (SM-WSC)- are suggested. Initially, the validity of the developed numerical model is proven through the comparison of the numerical and experimental results. Then, the performances of the control methods are evaluated through experiments on a roller rig and simulation tests on the validated numerical model. Moreover, the influence of different roller speeds and control parameters are investigated through the validated numerical model since it provides an advantage by allowing us to set the identical test condition for each case.

It is observed that wheel slip control strategies based on the threshold value (WSCST, WSCMT and WSCAA) suppress the severe wheel slip effectively. Due to its advantages over the other methods, the WSCAA strategy is primarily recommended to be used on EMUs. The PI-WSC

and SM-WSC successfully stabilise the wheel slip at a defined reference slip value. Furthermore, the PI-WSC and SM-WSC algorithms do not only stabilise the wheel slip but also help to establish optimum utilisation of the adhesion characteristic regardless of the severity of contaminants between the wheel and the roller when the optimal reference wheel slip is introduced. The SM-WSC has an advantage over the PI-WSC due to its useful properties in the stabilisation of nonlinear and uncertain systems. Hence, it is appropriate to use the SM-WSC on electric locomotives.

6.1 Completed Objectives of Doctoral Thesis

The completed objectives of the thesis are as follows:

(i) **Summarising a large number of published studies on the wheel slip, adhesion and slip control methods:** the gathered information about the adhesion, slip mechanism, wheel slip detection methods and wheel slip control methods are included in section 2, to give the reader a general overview of the research covered in the thesis.

(ii) **Reproducing a numerical model of the tram wheel roller rig in MATLAB environment that can be used for performance evaluation of the wheel slip control strategies:** In section 0, the numerical model of tram wheel roller rig, that is introduced in section 3.1, is reproduced in MATLAB environment.

(iii) **Proposing algorithms to control the wheel slip mechanism and establishing optimum utilisation of adhesion**: In section 4, the developed wheel slip control strategies are introduced. Strategies in sections 4.1, 4.2 and 4.3 are designed to be used on EMU while the strategies in sections 4.4. and 4.5 are designed to be used on electric locomotives.

(iv) **Validation of reproduced numeric model:**In section5.1, the validity of the developed numerical model (see section 3.2)is proven by comparing simulation results with experimental results.

(v) **Verifying the functionality of proposed wheel slip control algorithms by either the validated numerical model or experimentally obtained results from the tram wheel roller rig:** In section 5.2, the functionality of the proposed wheel slip control algorithms is verified by the validated numerical model (under the assumption of several surface conditions). In section 5.3, the functionality of the controllers is proven with the experimental setup under several test conditions.

(vi) **Performance evaluation of the proposed wheel slip control algorithms with different speeds and control parameters:** The validated numerical model is used for the further performance evaluation of the wheel slip control algorithms with different speeds and control parameters. The simulation results are presented in the Appendices of the thesis. The summaries of the simulations are presented in section 5.4.

6.2 Scientific Contributions of Doctoral Thesis

An advanced numerical model of a tram wheel roller rig that includes nonlinear effects caused by time delay and disturbances to match the values of the experimental test setup is developed so that other researchers can easily simulate the dynamic responses of wheel slip and electric motor control strategies.

Three different re-adhesion (WSCST, WSCMT and WSCAA) are suggested for the use on the EMUs. The WSCST and WSCAA are conventional re-adhesion strategies. Employing WSCMT on wheel slip control is unique and proposed by the author. It aims to provide an improvement to the utilisation of the adhesion.

Two more different strategies (PI-WSC and SM-WSC) for the use of electric locomotive are also proposed in this thesis. It is known that the PI-WSC method is widely used for industrial applications. However, the wheel slip control stability cannot be guaranteed with the PI controllers due to their linear characteristics [11]. On the other hand, SM-WSC is an attractive robust control method which has effective properties to stabilise the nonlinear and uncertain systems. The author has modified and applied a control strategy which is presented for a personal electric vehicle in the previous literature [33]. According to the author's knowledge, SM-WSC is an original control strategy in the related literature which aims to stabilise the wheel slip for a roller rig.

The dynamic responses of the implemented anti-slip control strategies are evaluated under different surface conditions (half-dry, wet, greasy and wet&greasy) on both experimental tram wheel roller rig and its numeric model. Furthermore, the performance of the control strategies with different speeds, threshold values, deceleration and increment rates are evaluated on the validated numerical model. The carried-out simulations and experiments bring considerable knowledge in the scientific field.

6.3 Future Works

The purpose of the slip control methods is to prevent the wheel from severe slip and improve the traction effort of the vehicle. Furthermore, the development of such systems is very critical for the safety of the vehicles. Hence, we have presented five of the wheel slip control strategies. Tests carried out on the experimental roller rig and its numerical model verify the presented strategies. The further verification of the developed strategies can be carried on the real locomotive in future. Another future work can be the development of optimal reference slip ratio seeking algorithm. In this work, the reference value of the wheel slip is obtained from the experimental measurements (predefined reference value). However, it is possible to obtain the reference using the characteristic slip curve. Hence, it is planned to adopt the recursive least square with the steepest gradient method (RLS-SGM) to determine the optimal wheel slip ratio online for the presented control strategies.

References

[1] P. Pichlík, “Strategy of Railway Traction Vehicles Wheel Slip Control,” CZECH TECHNICAL UNIVERSITY, Prague, 2018.

[2] H. Chen, T. Ban, M. Ishida, and T. Nakahara, “Experimental investigation of influential factors on adhesion between wheel and rail under wet conditions,” *Wear*, vol. 265, no. 9–10, pp. 1504–1511, Oct. 2008.

[3] C. W. Jenks, “Improved Methods for Increasing Wheel/Rail Adhesion in the Presence of Natural Contaminants,” Transit Co-operative Research Program, Research Results Diges, 17, 1997.

[4] J. Yu, “Re-adhesion control for railway traction systems,” The University of Leeds, Leeds, 2007.

[5] W. J. Wang, H. F. Zhang, H. Y. Wang, Q. Y. Liu, and M. H. Zhu, “Study on the adhesion behavior of wheel/rail under oil, water and sanding conditions,” *Wear*, vol. 271, no. 9–10, pp. 2693–2698, Jul. 2011.

[6] H. Chen, T. Ban, M. Ishida, and T. Nakahara, “Adhesion between rail/wheel under water lubricated contact,” *Wear*, vol. 253, no. 1–2, pp. 75–81, Jul. 2002.

[7] E. A. Gallardo-Hernandez and R. Lewis, “Twin disc assessment of wheel/rail adhesion,” *Wear*, vol. 265, no. 9–10, pp. 1309–1316, Oct. 2008.

[8] R. Lewis, R. S. Dwyer-Joyce, S. R. Lewis, C. Hardwick, and E. A. Gallardo-Hernandez, "Tribology of the Wheel-Rail Contact: The Effect of Third Body Materials," *Int. J. Railw. Technol.*, vol. 1, no. 1, pp. 167–194, Apr. 2012.
[9] Z. Li, O. Arias-Cuevas, R. Lewis, and E. A. Gallardo-Hernández, "Rolling–Sliding Laboratory Tests of Friction Modifiers in Leaf Contaminated Wheel–Rail Contacts," *Tribol. Lett.*, vol. 33, no. 2, pp. 97–109, Feb. 2009.
[10] M. Malvezzi, L. Pugi, S. Papini, A. Rindi, and P. Toni, "Identification of a wheel–rail adhesion coefficient from experimental data during braking tests," *Proc. Inst. Mech. Eng. Part F J. Rail Rapid Transit*, vol. 227, no. 2, pp. 128–139, Mar. 2013.
[11] D. Frylmark and S. Johnsson, "Automatic Slip Control for Railway Vehicles," Linköpings Universitet, Linköpings, 2003.
[12] Z. Zhu, K. Yuan, W. Zou, and H. Hu, "Current-based wheel slip detection of all-wheel driving vehicle," in *2009 International Conference on Information and Automation*, Zhuhai, Macau, China, 2009, pp. 495–499.
[13] P. Pichlík, "Overview of Slip Control Methods Used in Locomotives," *Trans. Electr. Eng.*, vol. 3, no. 2, pp. 38–43, 2014.
[14] J. Huang, J. Xiao, D. Zhao, and S. Wang, "A wheel slip detection method of electric locomotive based on time-frequency analysis," in *International Conference on Intelligent Transportation Systems*, Qingdao, China, 2014, pp. 1221–1225.
[15] M. Amiri and B. Moaveni, "Vehicle velocity estimation based on data fusion by Kalman filtering for ABS," in *20th Iranian Conference on Electrical Engineering (ICEE2012)*, Tehran, Iran, 2012, pp. 1495–1500.
[16] B. Moaveni, M. Khosravi Roqaye Abad, and S. Nasiri, "Vehicle longitudinal velocity estimation during the braking process using unknown input Kalman filter," *Veh. Syst. Dyn.*, vol. 53, no. 10, pp. 1373–1392, Oct. 2015.
[17] L. Imsland, T. A. Johansen, T. I. Fossen, H. Fjær Grip, J. C. Kalkkuhl, and A. Suissa, "Vehicle velocity estimation using nonlinear observers," *Automatica*, vol. 42, no. 12, pp. 2091–2103, Dec. 2006.
[18] L. Imsland, T. A. Johansen, T. I. Fossen, J. C. Kalkkuhl, and A. Suissa, "Vehicle Velocity Estimation using Modular Nonlinear Observers," in *Proceedings of the 44th IEEE Conference on Decision and Control*, Seville, Spain, 2005, pp. 6728–6733.
[19] D. M. Bevly, J. C. Gerdes, and C. Wilson, "The Use of GPS Based Velocity Measurements for Measurement of Sideslip and Wheel Slip," *Veh. Syst. Dyn.*, vol. 38, no. 2, pp. 127–147, Feb. 2003.
[20] M. Joos, J. Ziegler, and C. Stiller, "Low-cost sensors for image based measurement of 2D velocity and yaw rate," in *IEEE Intelligent Vehicles Symposium*, San Diego, CA, USA, 2010, pp. 658–662.
[21] K. Kondo, "Anti-slip control technologies for the railway vehicle traction," in *2012 IEEE Vehicle Power and Propulsion Conference*, Seoul, South Korea, 2012, pp. 1306–1311.
[22] P. Voltr and M. Lata, "Transient wheel–rail adhesion characteristics under the cleaning effect of sliding," *Veh. Syst. Dyn.*, vol. 53, no. 5, pp. 605–618, May 2015.
[23] P. Voltr, "Simulation of wheel-rail contact conditions on experimental equipment," *Railw. Transp. Logist.*, vol. 11, pp. 77–82, 2015.
[24] J. Gerlici, M. Gorbunov, K. Kravchenko, O. Nozhenko, and T. Lack, "Experimental rigs for wheel/rail contact research," *Manuf. Technol.*, vol. 16, no. 5, pp. 909–916, 2016.
[25] P. Voltr, M. Lata, and O. Cerny, "Measuring of wheel-rail adhesion characteristics at a test stand," in *18th International Conference Engineering Mechanics*, Svratka, Czech Republic, 2012, pp. 1543–1553.

[26] A. Onat, P. Voltr, and M. Lata, “An unscented Kalman filter-based rolling radius estimation methodology for railway vehicles with traction,” *Proc. Inst. Mech. Eng. Part F J. Rail Rapid Transit*, vol. 232, no. 6, pp. 1686–1702, 2017.
[27] A. Onat, A. Zirek, and P. Voltr, “Dynamic Modelling and Numerical Simulation of a Tram Wheel Test Stand,” in *3rd International Symposium on Electrical Railway Transportation Systems, ERUSIS 2017, Eskisehir, Turkey*, 2017.
[28] A. Apte, R. Walambe, V. Joshi, K. Rathod, and J. Kolhe, “Simulation of a permanent magnet synchronous motor using matlab-simulink,” in *2014 Annual IEEE India Conference (INDICON)*, Pune, India, 2014, pp. 1–5.
[29] J. Simanek, J. Novak, O. Cerny, and R. Dolecek, “FOC and flux weakening for traction drive with permanent magnet synchronous motor,” in *2008 IEEE International Symposium on Industrial Electronics*, Cambridge, UK, 2008, pp. 753–758.
[30] A. W. Leedy, “Simulink/MATLAB dynamic induction motor model for use as a teaching and research tool,” *Int. J. Soft Comput. Eng.*, vol. 3, no. 4, pp. 102–107, 2013.
[31] J. Simanek, J. Novak, R. Dolecek, and O. Cerny, “Control Algorithms for Permanent Magnet Synchronous Traction Motor,” in *The International Conference on “Computer as a Tool,”* Warsaw, Poland, 2007, pp. 1839–1844.
[32] O. Polach, “Creep forces in simulations of traction vehicles running on adhesion limit,” *Wear*, vol. 258, no. 7–8, pp. 992–1000, Mar. 2005.
[33] K. Nam, Y. Hori, and C. Lee, “Wheel Slip Control for Improving Traction-Ability and Energy Efficiency of a Personal Electric Vehicle,” *Energies*, vol. 8, no. 7, pp. 6820–6840, Jul. 2015.
[34] D. Caporale, P. Colaneri, and A. Astolfi, “Adaptive nonlinear control of braking in railway vehicles,” in *52nd IEEE Conference on Decision and Control*, Florence, Italy, 2013, pp. 6892–6897.
[35] L. Jin and Y. Liu, “Study on Adaptive Slid Mode Controller for Improving Handling Stability of Motorized Electric Vehicles,” *Math. Probl. Eng.*, vol. 2014, pp. 1–10, 2014.
[36] J. J. E. Slotine and W. Li, *Applied Nonlinear Control*. NJ, USA,: Prentice-Hall: Englewood Cliffs, 1991.
[37] J. S. Kim, S. H. Park, J. J. Choi, and H. Yamazaki, “Adaptive Sliding Mode Control of Adhesion Force in Railway Rolling Stocks,” in *Sliding Mode Control*, Rijeka, Croatia: InTech, 2011, pp. 385–408.
[38] W. Gao and J. C. Hung, “Variable structure control of nonlinear systems: A new approach,” *IEEE Trans. Ind. Electron.*, vol. 40, no. 1, pp. 45–55, 1993.
[39] K. Nam, H. Fujimoto, and Y. Hori, “Design of an adaptive sliding mode controller for robust yaw stabilisation of in–wheel–motor–driven electric vehicles,” *Int. J. Veh. Des.*, vol. 67, no. 1, pp. 98–113, 2014.

PUBLICATIONS OF STUDENT

A. Zirek, P. Voltr, M. Lata, and J. Novák, "An adaptive sliding mode control to stabilize wheel slip and improve traction performance," *Proceedings of the Institution of Mechanical Engineers, Part F: Journal of Rail and Rapid Transit*, vol. 232, no. 10, pp. 2392–2405, May 2018.

A. Onat, **A. Zirek**, and P. Voltr, "Dynamic Modelling and Numerical Simulation of a Tram Wheel Test Stand," in *3rd International Symposium on Electrical Railway Transportation Systems, ERUSIS 2017,* Eskisehir, Turkey, 2017.

P. Voltr, **A. Zirek**, and B. T. Kayaalp, "New Experience and Results from Experimental Measurement of Adhesion on a Roller Rig," in *23rd International Conference on Current Problems in Rail Vehicles,* Ceska Trebova, Czech Republic, 2017, pp. 423-432

A. Zirek and B. T. Kayaalp, "The Slip Control of a Tram-Wheel Test Stand Model with Single Neuron PID Control Method," in *VII. International Scientific Conference of the Faculty of Transport Engineering*, Pardubice, Czech Republic, 2018, pp. 268-275

Title	Scientific Papers – University of Pardubice – Faculty of Transport Engineering Collection of Academic Precis
Publisher	University of Pardubice Faculty of Transport Engineering Studentská 95, 532 10 Pardubice Czech Republic
Edition	First
Year of issue	2020
Printed by	Printing Centre of the University of Pardubice

ISBN 978-80-7560-273-2

ISBN 978-80-7560-273-2